Reconceptualizing the Periaqueductal Grey: Fear, Anxiety and Motivational Systems in an Ancient Structure

by

Carlos Eduardo Barroso Silva

A thesis submitted for the degree of

Doctor of Philosophy

at the University of Otago, Dunedin

New Zealand

September 2018

Thesis Supervisor: Neil McNaughton

Abstract

The periaqueductal grey (PAG) is classically seen as a region responsible for the control of defensive reactions. This thesis provides a detailed review of anatomical and functional data on the different parts of the PAG together with the dorsal raphe. Based on anatomical features, this thesis proposes a new subdivision of the PAG that accounts for the distinct characteristics of the area. I provide a comprehensive functional view of the PAG, going beyond simple panic and escape to integrate data on fear, anxiety, and depression. Importantly, I conclude that this periaqueductal cluster of nuclei is broadly involved in motivated behavior controlling not only aversive but also appetitive behavior and with some involvement in more complex motivational processes such as approach-avoidance conflict resolution. To test some of these hypotheses, I present experimental evidence showing that the PAG can produce an anxiety-like signal in the forebrain, and compare it to the signal evoked by reticular stimulant. Furthermore, I explore the effect of pharmacological interventions in tegmental areas and how these impact PAG- and RPO-evoked responses. In sum, I propose that the PAG is a highly conserved region surrounding the aqueduct and it appears to be the simplest, foundational, element of controlling integrated motivated goal-directed behaviors of all types.

Acknowledgements

Acknowledgment and gratitude are due first of all to my supervisor, Professor Neil McNaughton. Neil was actively involved in the past 3+ years to make sure that I was kept on track in this project. His counseling and advice with the more instrumental aspects of a research project were fundamental for my progress and my formation as a young researcher.

But Neil's contributions were not only limited to advice on how to run experiments properly or on how to effectively organize my files (sorry Neil, I've been doing my best but my files are still a mess). Neil was also very intellectually open, receiving and generous. It was surprising to me how such a senior academic would make an unexperienced student feel like his ideas, no matter how improbable they were sometimes, would be actually not that bad after all. The core of this thesis, the review produced for Chapter 2, is perhaps the best example of this. Prompted by Neil to produce an "exhaustive *and* exhausting" review of my topic of research made me go beyond of what I expected that I could or would. After getting a better understanding on my subject, I would very excitedly come back to Neil with a pile of malformed ideas and crazy theories. Then Neil would drag me back to planet Earth again, point me to the right direction and back I would go to think more about the meaning of all that gathered evidence. While I anticipate that a good part of the ideas presented in this thesis are not endorsed by Neil – after all, there is only so much convincing that a supervisor can do to avoid a student bastardizing his ideas – his fingerprints are all over my academic worldview and my way of thinking. It has been said that science advances one funeral at a time: when the older generation retires, the ideas of the new academics can finally be accepted. academic progress is possible because a new generation stands on the shoulder of giants. After 3+ years under the supervision of Neil McNaughton I can say this is absolutely true and I could not have been more privileged to have had him as the giant whose shoulder I stood on.

Many special thanks are also due to Dr Calvin Young, who acted as a *de-facto* co-supervisor. Calvin's technical knowledge in electrophysiology, data processing and signal analysis were paramount to much of the experimental work done here. Long conversations with Calvin, spanning topics from research techniques, scientific publishing and the culture of science in general made me better understand not only the techniques that I was using for my project, but also broadened my view of science and academia. Calvin also dedicated many hours to adapt and customize Matlab routines for my use, and then spent another set of countless hours correcting all my mistakes while using his code. While it is pretty daunting to handle huge datasets in a complete unknown programing environment (or in my case, any programing environment at all), Calvin was there for all the times I hit that proverbial brick wall.

I would also like to acknowledge the staff of the psychology department at the University of Otago, who make the show run seamlessly and make it look all too easy for the students and faculty. Special thanks are due to the technical staff, headed by Jeremy Anderson. Big shout out to animal technicians Saralee Illingworth, Natasha O'Docherty and Sophie French for looking after us all (rodents and students). Another set of special thanks to Lindsay Robertson for supplying technical advice and support for our electrophysiology gear, and to Richard Hamelink for helping us out with electrical stimulator troubleshooting and maintenance.

Also many thanks to the students and researchers in the McNaughton Lab other labs in the department who helped out in big and small ways: Dr Shabah Shadli and Dr Ming Ruan (for showing the lay of the land in the department and the lab), Dr Thom Elston (for isoflurane and surgical suggestions), Dr Owen Jones and Regina Hegemann (for lending their lab gear), Dr Kristin Hillman and Professor David Bilkey (for data discussion), Ashik Banstola and Paul Buchannan (for helping with early electrode design and manufacturing) and Anne Kim (for assistance in conducting histology).

Finally, the biggest thanks of all to my wife, Lisa Silva. It is impossible to describe in words Lisa's role in my life during the three years while this thesis was being produced. She reviewed my writing, made suggestions about content and helped me out when the limits of my second language were reached when trying to convey ideas. Although she is on her way to also complete her PhD, of course her contributions were not only academic. Her partnership and support allowed me to remain sane and happy in a country (that no matter how beautiful and welcoming) is very different and very distant from my own home located more than 10,000 kms away. Thanks to Lisa I can now say that my home is here, and anywhere else that I go with her. Also many thanks for the warmth in which her parents, Leta and Willem Labuschagne received me, and the many delicious meals and drinks that they provided. Having spent a lifetime in academia, the last thing that the now retired Professor Willem Labuschagne would like to do in his spare time is answering questions from his intrusive son-in-law about philosophy, the nature of the mind and academic life. But alas, this is exactly what he did, and I couldn't be more grateful to be able to pick his brain.

Table of Contents

Chapter 1. Introduction 1

1.1. Basic problem: what's so special about the PAG and the mind? 2

1.2. Defensive systems 4

1.2.1. The question of movement 4

1.2.2. Trying to predict the future: not-so-clear and not-so-present danger 5

1.2.3. Could rudimentary structures have some form of sophistication? 9

1.3. Wrapping up – establishing some of the questions and deciding on a plan 10

1.3.1. Thesis outline 11

Chapter 2. The periaqueductal grey and the dorsal raphe: a locus of control for aversive and appetitive states 13

2.1. Introduction 13

2.2. Anatomy of the periaqueductal complex 13

2.2.1. Phylogeny of the PAG 13

2.2.2. The division of nuclei surrounding the aqueduct 15

2.2.3. Intra-periaqueductal connections 17

2.2.4. Afferent connections 18

2.2.5. Efferent connections 30

2.2.6. A new parcellation of the PAG: internal and external columns 41

2.2.7. Neurochemical profile 43

2.3. Functions within the PAG 65

2.4. The dorsal-ventral axis 67

2.5. The anterior-posterior axis 70

2.6. The interior-exterior axis 73

2.7. Summary 80

Chapter 3. General methods 81

3.1. Animal housing, handling 81

3.2. Electrodes 82

3.2.1. Multipolar arrays 82
3.2.2. Bipolar recording 84
3.2.3. Ground, reference and stimulating electrodes 84
3.3. Surgical methods 85
3.4. Behavioral apparatus 88
3.5. Electrical stimulation response thresholds 88
3.6. Data acquisition and processing 89
3.6.1. Spectral analysis 90
3.6.2. Pairwise phase consistency analysis 90
3.6.3. Partial directed coherence analysis 90
3.7. Statistical analysis 90
3.8. Histological methods 92
Chapter 4. Cortico-hippocampal oscillations and interactions during PAG-generated freezing 94
4.1. Introduction 94
4.2. Methods 98
4.2.1. Behavioral apparatus 98
4.2.2. Electrical stimulation response thresholds 98
4.2.3. Recording sessions 99
4.2.4. Data processing 100
4.3. PAG-induced responses vs. RPO-induced responses 101
4.3.1. Histology 101
4.3.2. Results 104
4.4. Anterior PAG vs. Mid PAG 115
4.4.1. Histology 115
4.4.2. Results 117
4.5. Summary and data discussion 126

Chapter 5. Pharmacological manipulation of a region in the theta-generating system: how anxiolytic drugs in the nucleus incertus affect PAG-evoked responses 130

5.1. Introduction 130

5.2. Methods 132

5.2.1. Intracerebral microinjections 132

5.2.2. Experimental session and design 133

5.2.3. Data processing 133

5.2.4. Histology 134

5.3. Results 136

5.3.1. CDP and buspirone 136

5.3.2. RXFP3-A2 and R2B(1-22)R 142

5.4. Summary and data discussion 147

Chapter 6. Discussion 155

6.1. Reconceptualizing the PAG/DR complex 156

6.2. Approach, avoidance and conflict: a new perspective of the PAG 158

6.3. Negative and positive goals: the dorsal PAG as a motivational driver 159

6.4. Motivational conflicts: the DLPAG and VLPAG 162

6.5. Acute and chronic unresolvable goals and conflicts: the VLPAG and DR as general inhibitors of behavior and neuronal activity 168

6.6. Final remarks 174

7. Postscript 210

List of Tables

Table 2.1. Projections from the Medial Aspect of All PAG/DR Divisions to the Anterior, Medial and Posterior Aspect of All Other Divisions 18

Table 2.2. Projections from the Cingulate Cortex to the PAG/DR at Anterior, Medial and Caudal Levels 19

Table 2.3. Projections from the Medial Prefrontal Cortex to the PAG/DR at Anterior, Medial and Caudal Levels 20

Table 2.4. Projections from the Orbito-Insular Cortices to the PAG/DR at Anterior, Medial and Caudal Levels 22

Table 2.5. Projections from the Amygdaloid Complex to the PAG/DR at Anterior, Medial and Caudal Levels 23

Table 2.6. Projections from the Hippocampal Formation to the PAG/DR at Anterior, Medial and Caudal Levels 24

Table 2.7. Projections from the Hypothalamus to the PAG/DR at Anterior, Medial and Caudal Levels 25

Table 2.8. Projections from the Tectum to the PAG/DR at Anterior, Medial and Caudal Levels 27

Table 2.9. Projections from the Midbrain, Basal Ganglia and Pons to the PAG/DR at Anterior, Medial and Caudal Levels 28

Table 2.10. Projections from the Medulla and Spinal Cord to the PAG/DR at Anterior, Medial and Caudal Levels 29

Table 2.11. Projections Targeting the Frontal Cortices from the PAG/DR at Anterior, Medial and Caudal Levels 31

Table 2.12. Projections Targeting the Amygdaloid Complex from the PAG/DR at Anterior, Medial and Caudal Levels 32

Table 2.13. Projections Targeting the Hippocampal Formation from the PAG/DR at Anterior, Medial and Caudal Levels 34

Table 2.14. Projections Targeting the Hypothalamus from the PAG/DR at Anterior, Medial and Caudal Levels 36

Table 2.15. Projections Targeting the Tectum from the PAG/DR at Anterior, Medial and Caudal Levels 37

Table 2.16. Projections Targeting the Midbrain, Basal Ganglia and Pons from the PAG/DR at Anterior, Medial and Caudal Levels 39

Table 2.17. Projections Targeting the Medulla and Spinal Cord from the PAG/DR at Anterior, Medial and Caudal Levels 40

Table 2.18. Afferents to the internal and external divisions of the DLPAG and LPAG 42

Table 2.19. Concentrations of GABAergic Cell Bodies, Axonic Processes and Receptors in the PAG/DR Region, at Anterior, Medial and Caudal Levels 44

Table 2.20.Concentration of Nitric Oxide Cell Bodies and Axonic Processes in the PAG/DR Region, at Anterior, Medial and Caudal Levels 45

Table 2.21. Concentrations of Glutamatergic Cell Bodies, Axonic Processes and Receptors in the PAG/DR Region, at Anterior, Medial and Caudal Levels 46

Table 2.22. Concentrations of Cholinergic Cell Bodies, Axonic Processes and Receptors in the PAG/DR Region, at Anterior, Medial and Caudal Levels 48

Table 2.23. Concentrations of Catecholaminergic Cell Bodies, Axonic Processes and Receptors in the PAG/DR Region, at Anterior, Medial and Caudal Levels 50

Table 2.24. Concentrations of Histaminergic Cell Bodies, Axonic Processes and Receptors in the PAG/DR Region, at Anterior, Medial and Caudal Levels 51

Table 2.25. Concentrations of Substance P Cell Bodies, Axonic Processes and Receptors in the PAG/DR Region, at Anterior, Medial and Caudal Levels 53

Table 2.26. Concentrations of Serotonergic Cell Bodies, Axonic Processes and Receptors in the PAG/DR Region, at Anterior, Medial and Caudal Levels 54

Table 2.27. Concentrations of Endogenous Opioid Cell Bodies, Axonic Processes and Receptors in the PAG/DR Region, at Anterior, Medial and Caudal Levels 56

Table 2.28. Concentrations of Orexin Cell Bodies, Axonic Processes and Receptors in the PAG/DR Region, at Anterior, Medial and Caudal Levels 57

Table 2.29. Concentrations of Endocannabinoid Receptors in the PAG/DR Region, at Anterior, Medial and Caudal Levels 59

Table 2.30. Concentrations of CCK Cell Bodies and Axonic Processes in the PAG/DR Region, at Anterior, Medial and Caudal Levels 60

Table 2.31. Concentrations of Glycine Cell Bodies, Axonic Processes and Receptors in the PAG/DR Region, at Anterior, Medial and Caudal Levels 61

Table 2.32. Concentrations of Corticotropin Releasing Factor (CRF) Cell Bodies and Axonic Processes in the PAG/DR Region, at Anterior, Medial and Caudal Levels 62

Table 2.33. Concentrations of Neurotensin Cell Bodies, Axonic Processes and Receptors in the PAG/DR Region, at Anterior, Medial and Caudal Levels 63

Table 2.34. Concentrations of Relaxinergic Axonic Processes and Receptors in the PAG/DR Region, at Anterior, Medial and Caudal Levels 64

Table 2.35. Functions of the Dorsal and Ventral Extremes of the PAG/DR 69

Table 2.36. Functions of the Anterior and Posterior Extremes of the PAG/DR. 72

Table 2.37. Functions of the Columns of the Dorsal PAG. 76

Table 2.38. Features and Functions of the Internal and External Subdivisions of the DLPAG. 77

Table 2.39. Features and Functions of the Internal and External Subdivisions of the LPAG 78

Table 3.1. Coordinates for stereotaxic implantations. 86

Table 5.1. Summary of results from CDP and Buspirone analysis in this Chapter. 149

Table 5.2. Summary of results from RXFP3-A2 (ago) and R3B(1-22)R (ant) analysis in this Chapter. 150

Table 6.1. Internal Representations of Acute and Resolvable and Unresolvable Goals in the Rat's PAG, the Actions Produced by the Structures Involved, and Analogous Human Pathological Manifestations 168

Table 6.2. Internal Representations of Chronic, Unresolvable Goals in the Rat's PAG, the Actions Produced by the Structures Involved, and Analogous Human Pathological Manifestations 173

List of Figures

Figure 1.1.The hierarchical organization of avoidance and approach (McNaughton et al., 2016). Original model proposed by McNaughton and Corr (2004) 11

Figure 2.1. PAG (yellow) in different vertebrates, as determined by similar local mRNA or protein expression. Adapted with permission from O'Connell and Hofmann (2012). 15

Figure 2.2. Columnar division of the PAG through the anterior posterior axis. Approximate bregma coordinates for the rat brain from the atlas of Paxinos and Watson (1998). DM: dorsomedial PAG; DL: dorsolateral PAG; L: lateral PAG; VL: ventrolateral PAG; DR: dorsal raphe nucleus; Cb: cerebellar lobule. 17

Figure 2.3. The predominant, contrasting functions of the dorsal and ventral PAG. 67

Figure 2.4. The predominant functions of the anterior and posterior PAG. 70

Figure 2.5. The predominant and unique functions and characteristics of the DMPAG and the proposed internal and external subdivisions of the DLPAG and LPAG. 74

Figure 3.1. Sheets of plastic punctured at different distances for array building. Punctures were made at either 500µ or 200µ distances for prefrontal and hippocampal arrays, respectively. The two hippocampal sheets were the same as each other. 83

Figure 3.2. A: Nichrome wires threaded through the punctured plastic sheet, and then twisted. B: Finalized PrL array including tungsten rod used to maintain rigidity during implantation. 84

Figure 3.3. Schematic top view of rat's skull during implantation surgery. Placement of structural and reference screws (grey) are displayed, along with craniotomy holes (black) for electrode and cannula implantation. The posterior-most right side screw served as a reference electrode, and the posterior-most right side screw was used to secure the uninsulated silver ground wire. 87

Figure 4.1. Timeline of experiment. A: time interval between stimulations. RPO and PAG stimulation trains are presented each 30 seconds, alternating between the two. B: view of a single minute of the experimental session. PAG trains last 8 seconds, and RPO ones 1 second. 100

Figure 4.2. EEG segmentation from original RPO (A) and PAG (B) stimulation periods, demarcated by vertical red lines. Two 1-second segments of data before and after the onset of stimulation (0 second on X-axis) were used as "sham stimulation" and "real stimulation" epochs for analysis, respectively. 101

Figure 4.3. Histological placements of recording electrodes for the left PrL. Black dots in panel A show the centerpoint between the two pairs of electrodes in each rat that were used for analysis. A-P coordinates from bregma are indicated. Panel B is a representative photomicrograph showing the electrode trace through the medial wall of the prefrontal cortex. 102

Figure 4.4. Histological placements of recording electrodes for the left and right HPC. Black dots in panel A show the centerpoint between the two pairs of electrodes in each rat that were used for analysis. A-P coordinates from bregma are indicated. Panel B is a representative photomicrograph showing the electrode trace through the right hippocampus. 103

Figure 4.5. Histological placements of stimulating electrodes for the PAG. . Black dots in panel A indicate location of the anode of the two stimulating tips in each rat.

A-P coordinates from bregma are indicated. Panel B is a representative photomicrograph showing the electrode trace through the left PAG..... 103

Figure 4.6. Histological placements of stimulating electrodes for the RPO. Black dots in panel A indicate location of the anode of the two stimulating tips in each rat. A-P coordinates from bregma are indicated. Panel B is a representative photomicrograph showing the electrode trace through the right hemisphere..... 104

Figure 4.7. LFP activity under PAG stimulation for a representative rat. Event epochs are comprised of a total of 24 seconds including 8 second periods before, during and after stimulation. A: Each panel presents raw LFP of ten individual trials of PAG stimulation, with stimulation periods indicated by black dashed lines at the center. Top: Left HPC; bottom: left PrL. Panel B shows spectrograms for relative power (averaged trials). From top to bottom: Left HPC, left PrL and right HPC spectrograms, with PAG-stimulation periods delimited by white dashed lines at the center. 107

Figure 4.8. Theta power during real and sham stimulations of PAG and RPO (n=7). Panel A shows the overall effects of stimulation, with the activity of the regions averaged. PAG stimulation promotes a significant decrease in LFP power, and RPO promotes a non-significant increase in LFP power. Panel B shows a non-significant increase in hippocampal power during RPO stimulation. Panel C shows a detailed view of LFP power in all regions, with their quadratic curves fitted. Power was significantly decreased during PAG stimulation at both the hippocampal sites and the left PrL. RPO stimulation promotes a non-significant change in the quadratic relationship between left PrL and the HPC sites. Solid lines indicate statistically significant differences, and dashed lines indicate non-significant differences..... 108

Figure 4.9. Frequency changes during sham and real stimulations of the PAG and RPO (n=7). Both PAG (panel A) and RPO (panel B) stimulations promote a general decrease in frequency from baseline across regions. Panel C shows the effects of stimulation in each region separately. The reductions in frequency coming from PAG stimulation are mostly due to decreases in left PrL, with hippocampal sites remaining mostly unchanged. The image shows the quadratic curve and the changes promoted by stimulation. Solid lines indicate statistically significant differences, and dashed lines indicate non-significant differences. 111

Figure 4.10. Pairwise Phase Consistency (PPC) and coherence for PAG and RPO stimulation (n=7). Panel A shows the average PPC between regions, averaged across sham and real types of both stimulation. Panel B and C show the detailed view for each state, respectively for PPC and coherence. Solid lines indicate statistically significant differences, and dashed lines indicate non-significant differences. 112

Figure 4.11. PDC during PAG stimulation (A) and RPO stimulation (B). The same results are also shown in bar graph form, and with more detailed explanation, in Figure 4.12..... 113

Figure 4.12. Statistical results for PDC. Panel A shows PDC activity averaged across PAG, RPO, Sham and Real states for L-HPC → left PrL, L-HPC → R-HPC and R-HPC → left PrL, along with linear and quadratic relationships. Panel B shows PDC activity averaged across PAG, RPO, Sham and Real states for left PrL → L-HPC, R-HPC → L-HPC and left PrL → R-HPC along with linear and quadratic relationships. Panels C and D show detailed effects of stimulation on

the same pairs in A and B, respectively. Solid lines indicate statically significant differences, and dashed lines indicate non-significant differences (NS = non-significant). 114

Figure 4.13. Histological placements of recording electrodes for the left PrL. Black dots show the centerpoint between the two pairs of electrodes in each rat in the mPAG group. Grey dots show the centerpoint between the two pairs of electrodes in each rat in the aPAG group. A-P coordinates from bregma are indicated. 115

Figure 4.14. Histological placements of recording electrodes for the left and right HPC. Black dots show the centerpoint between the two pairs of electrodes in each rat for the mPAG group. Grey dots show the centerpoint between the two pairs of electrodes in each rat for the aPAG group. A-P coordinates from bregma are indicated. 116

Figure 4.15. Histological reconstruction of PAG stimulating electrode placements. Black dots in panel A indicate location of the anode of the two stimulating tips in the animals in the mPAG group. Panel B shows the location of the anode of the two stimulating tips in animals in the aPAG. On the right, the concentration of the stimulating regions for each group is indicated in the anterior-posterior axis of the PAG. 117

Figure 4.16. LFP activity under stimulation of the medial PAG (left column) and anterior PAG (right column) of one representative rat in each group (10 individual trials averaged). Event epochs are comprised of a total of 24 seconds including 8 second periods before, during and after stimulation. 119

Figure 4.17. Theta power during real and sham stimulations of medial PAG (n=7) and anterior PAG (n=5). Panel A presents the changes promoted by mPAG and aPAG stimulations on the general activity of the regions, averaged. mPAG stimulation promotes a significant decrease in power, while aPAG promotes a marginally non-significant global increase. Panel B shows results per individual channels. mPAG promotes equal decreases in HPC and left PrL power. aPAG stimulation produces an increase in left PrL and right HPC power, which is significantly reflected on their quadratic curves. Panel C shows post-hoc tests comparing sham and stimulation effects on left PrL and right HPC. Solid lines indicate statically significant differences, and dashed lines indicate non-significant differences. 121

Figure 4.18. Frequency changes during real and sham stimulations of the mPAG (n=7) and aPAG (n=5). mPAG induces significant decreases in left PrL frequency, but aPAG effects are non-significant. Solid lines indicate statically significant differences, and dashed lines indicate non-significant differences (NS = non-significant). 122

Figure 4.19. Pairwise Phase Consistency (panel A) and coherence (panel B) for mPAG (n=7) and aPAG (n=5). 124

Figure 4.20. PDC activity during sham and stimulation states of mPAG and aPAG. Panel A shows L-HPC → left PrL, L-HPC → R-HPC and R-HPC → left PrL, and panel B shows left PrL → L-HPC, R-HPC → L-HPC and left PrL → R-HPC. Dashed lines indicate statically non-significant differences (NS = non-significant). 125

Figure 5.1. Components of the experimental session. Each session lasted approximately 20 minutes. Data from the baseline period (a block of 5 minutes previous to the

start of drug injection), from post injection 1 (a block of 5 minutes immediately following end of injection) and post injection 2 (a blocks of 5 minutes following post injection 1) were used for analysis in this experiment. Each 5 minute block contains 5 samples of the three types of stimulation (PAG, RPO and Sham). 133

Figure 5.2. Histological reconstruction of sites of injection. Panel A shows the location of the tips of the injector cannula, along with the estimated diffusion of the compounds. Panel B shows the cannula tract in the brain of a representative rat. 135

Figure 5.4. Summary of LFP power data in the significant contrast of Stim x Drug x Region x Time (linear, linear, linear, quadratic) in the NI injection group. Panel A: PAG stimulation. Panel B: RPO group. NS = non-significant; * = significant. 137

Figure 5.6. Summary of LFP frequency data in the significant contrast of Stim x Drug x Region x Time x Injection (linear, quadratic, quadratic, linear) in the OS injection group (N=2). Panel A: The quadratic effect a factor of time under both PAG and RPO stimulations. Panel B: Effect of drugs over time during PAG stimulation. Panel C: Effect of drugs over time during RPO stimulation. NS = non-significant; * = significant. 140

Figure 5.8. Summary of coherence data in the significant contrast of Stim x Drug x Region x Time (linear, quadratic, linear quadratic) with injection groups pooled (N=6). Panel A: The quadratic effect as a factor of time under both PAG and RPO stimulations. Panel A: Effect of drugs over time during PAG stimulation. Panel B: Effect of drugs over time during RPO stimulation. NS = non-significant; * = significant. 141

Figure 5.10. Summary of PPC data in the contrast of Stim x Drug x Region x Time (linear, linear, linear, linear), with both groups shown (NI, N=3; OS N=3). NS = non-significant. 142

Figure 5.12. Summary of LFP power data in the significant contrast of Stim x Drug x Region x Time (linear, quadratic, linear, quadratic) in the NI injection group (N=3). Panel A: The quadratic effect as a factor of time under both PAG and RPO stimulations. Panel B: Effect of drugs over time during PAG and RPO stimulation. 145

Figure 5.14. Summary of LFP frequency data in the significant contrast of Drug x Region x Time (linear, linear, quadratic) in the OS injection group during RPO stimulation (N=3). Panel A: The quadratic effect as a factor of time under RPO stimulation. Panel B: Effect of drugs over time during RPO stimulation. NS = non-significant. * = significant. 147

Figure 6.1. Approach, withdrawal and conflict systems in the brain. Adapted and updated from Figure 7 in McNaughton et al. (2016) 159

Figure 6.2. Above: DMPAG neurons at intermediate and posterior sites of the PAG initiate behaviors to deal with an aversive stimulus. Below: internal PAG neurons at more anterior sites initiate behaviors to deal with an appetitive stimulus. 161

Figure 6.3. Projections from the anterior cingulate cortex to the PAG/DR. Cingulate projections target the DL column exclusively, not projecting to any of the other

subdivisions in significant volumes. Line thickness indicates volume of terminals sent to the area. 163

Figure 6.4. Projections from the Central Nuclei of the amygdala to the PAG/DR. Amygdalar projections intensely target all PAG/DR subdivisions, with the exception of the DL column to which it has fewer terminals. Line thickness indicates volume of terminals sent to the area. 164

Figure 6.5. Unique inputs from sensory and cortical areas reaching the DLPAGe might help detect and solve conflicts. Upon detection of a conflict, DLPAGe neurons at intermediate and posterior sites of the PAG signal VLPAG and DR neurons to stop motor action until the conflict is resolved. 165

Figure 6.6. Intra-PAG/DR connections. From left to right: projections from the DMPAG, DLPAG, LPAG, VLPAG and DR to other subdivisions. The DLPAG is the only subdivision that does not receive projections from its ventral counterparts. Line thickness indicates volume of terminals sent to the area. 166

Figure 6.7. Repeated unresolvable scenarios cause long-term changes in serotonergic patterns in the DR, which in turn promote general inhibition in the dorsal PAG and its roles in aversive and appetitive motivation. Concurrently, descending signals from the VLPAG promote general inhibitions in motor, nociceptive and sympathetic activity. 170

Figure P5.3. The effect of CDP and buspirone over LFP power in the hippocampus and PrL during PAG, sham and RPO stimulations over three time periods. Panel A: NI injected animals (N=3). Panel B: OS injected animals (N=3). 211

Figure P5.5. The effect of CDP and buspirone over LFP frequency in the hippocampus and PrL during PAG, sham and RPO stimulations over three time periods. Panel A: NI injected animals (N=3). Panel B: OS injected animals (N=3). 212

Figure P5.7. The effect of CDP and buspirone over theta coherence in the hippocampus and PrL during PAG, sham and RPO stimulations over three time periods. This figure shows the pooled data from the two groups (N=6). 213

Figure P5.9. The effect of CDP and buspirone over PPC in the hippocampus and PrL during PAG, sham and RPO stimulations over three time periods. Panel A: NI injected animals (N=3). Panel B: OS injected animals (N=3). 214

Figure P5.11. The effect of RXFP3-A2 and R3B(1-22)R over LFP power in the hippocampus and PrL during PAG, sham and RPO stimulations over three time periods. Panel A: NI injected animals (N=3). Panel B: OS injected animals (N=3). 215

Figure P5.13. The effect of RXFP3-A2 and R3B(1-22)R over LFP frequency in the hippocampus and PrL during PAG, sham and RPO stimulations over three time periods. Panel A: NI injected animals (N=3). Panel B: OS injected animals (N=3). 216

Figure P5.15. The effect of RXFP3-A2 and R3B(1-22)R over theta coherence in the hippocampus and PrL during PAG, sham and RPO stimulations over three time periods. Panel A: NI injected animals (N=3). Panel B: OS injected animals (N=3). 217

Figure P5.16. The effect of RXFP3-A2 and R3B(1-22)R over PPC in the hippocampus and PrL during PAG, sham and RPO stimulations over three time periods. Panel A: NI injected animals (N=3). Panel B: OS injected animals (N=3). 218

Figure P5.17. A comparison of the effects of RXFP3-A2 and R2B(1-22)R in the NI (N=3) and OS (N=3) groups under PAG, Sham and RPO stimulations, capturing the two significant trends (linear, linear, linear, quadratic and quadratic, linear, linear, quadratic). 219

List of Abbreviations and Symbols

µA	microamperes
µL	microliter
µm	micrometer
µV	microvolt
5-HT	5-hydroxytryptamine, serotonin
5-HT_{1A}	serotonin receptor, subtype 1A
A1	adrenaline receptor, type 1
A2	adrenaline receptor, type 2
ACC	anterior cingulate cortex
Ach	acetylcholine
AID	agranular insular cortex, dorsal part
AIV	agranular insular cortex, ventral part
AMPA	α-amino-3-hydroxy-5-methyl-4-isoxazolepropionic
ANOVA	analysis of variance
A-P	anterior-posterior
aPAG	anterior PAG
C	celcius
CA1	Cornu Ammonis field 1 of the hippocampus
CA2	Cornu Ammonis field 2 of the hippocampus
CA3	Cornu Ammonis field 3 of the hippocampus
Cb	cerebellar lobule
CB1	cannabinoid receptor, type 1
CB2	cannabinoid receptor, type 2

CCK	cholecystokinin
CDP	chlordiazepoxide
CG1	cingulate cortex, area 1
CG2	cingulate cortex, area 1
cm	centimeter
CNA	central nucleus of the amygdala
CO_2	carbon dioxide
CRF	corticotropin release factor
CRF1	corticotropin release factor receptor, type 1
D1	dopamine receptor, type 1
D2	dopamine receptor, type 2
DG	dentate gyrus
DLO	dorso-lateral orbital cortex
DLPAG	dorsolateral PAG
DLPAGe	dorsolateral PAG, external part
DLPAGi	dorsolateral PAG, internal part
DMPAG	dorsomedial PAG
DP	dorsopenducular cortex
dPAG	dorsal PAG
DR	dorsal raphe
D-V	dorso-ventral
EAA	excitatory aminoacids
EEG	electroencephalogram
EPM	elevated plus maze
ETM	elevated T maze

fMRI	functional magnetic resonance imaging
GABA	γ-aminobutyric acid
H1	histamine receptor, type 1
H2	histamine receptor, type 2
H3	histamine receptor, type 3
HPC	hippocampus
Hz	hertz
IC	inferior colliculus
IL	infralimbic cortex
i.p.	intraperitoneal
i.v.	intravenous
KA	kainic acid
kg	kilogram
LDTg	laterodorsal tegmental nucleus
LFP	local field potential
L-HPC	left hippocampus
LO	lateral orbital cortex
LPAG	lateral PAG
LPAGe	lateral PAG, external part
LPAGi	lateral PAG, interior part
m2	muscarinic receptor, type 2
m3	muscarinic receptor, type 2
mg	miligram
mGluR	metabotropic glutamate receptors
min	minute

M-L	meso-lateral
ml	mililiter
mm	milimiter
MO	medial orbital cortex
mPAG	medial PAG
mPFC	medial prefrontal cortex
mRNA	messenger RNA
ms	millisecond
NaCl	sodium chloride
NADPH-d	dihydronicotinamide adenine dinucleotide phosphate diaphorase
NI	nucleus incertus
NMDA	N-methyl-D-aspartate
NO	nitric oxide
NS	non-significant
OS	outside NI
OX1	orexin receptor, type 1
OX2	orexin receptor, type 2
PAG	periaqueductal grey
PDC	partial directed coherence
PFA	perfluoroalkoxy
PFC	prefrontal cortex
PMd	dorsal premmamilary nucleus
PPC	pairwise phase consistency
PrL	prelimbic cortex
R-HPC	right hippocampus

RPO	reticularis pontis oralis
RXFP-3	relaxin receptor, type 3
s	second
S.E.M.	standard error of the mean
s.c.	subcutaneous
SC	superior colliculus
SN	substantia nigra
V	volts
VLPAG	ventrolateral PAG
VO	ventral orbital cortex
vPAG	ventral PAG

Dedication

Esta tese é dedicada às duas pessoas que me fizeram chegar até aqui: meus pais, Maria de Fátima e José Carlos.

Chapter 1. Introduction

The need to survive by reacting appropriately to external threats is one of the strongest drives in biology. Many animals, from the simplest marine vertebrates to neurologically complex primates, have nervous systems dedicated to producing appropriate reactions to perceived threats. It is generally believed that many mental disorders arise from dysfunction of these defense systems. For example, a human panic attack is recognized as a homologue of the defensive reactions animals make to threats that are close, imminent and life-threatening. While panic can be adaptive in the face of actual danger, it becomes a 'disorder' if it occurs unexpectedly when no danger exists, or if the response is otherwise inappropriate or excessive given the actual threat.

Panic disorder is among the most expensive of the psychiatric disorders, at both the individual and societal level (Smit et al., 2006). In Europe, panic disorder has an annual cost of ~€14,000 per person diagnosed (Batelaan et al., 2007). Furthermore, comorbidity is common and half the patients diagnosed with panic disorder also suffer from depression and/or agoraphobia (Baldwin, 1998), making diagnosis and treatment even more challenging and costly.

Both adaptive and dysfunctional panic are controlled by the midbrain's periaqueductal grey (PAG), which is the lowest structure in a neural hierarchy controlling defense and aggression. The PAG is thus implicated in a range of mental disorders and is best known for its involvement in panic and anxiety. However, the nuclei of the PAG have quite a complex structure and a broader functional scope than usually attributed to them (which I will argue can be treated as including the dorsal raphe). In Chapter 2, I review the structure and function of the different parts of the PAG; argue that the dorsal raphe (DR) constitute a vital part of this complex; and present a novel picture of these nuclei as the most caudal integrative control centers of not only defensive responses but also appetitive ones. Necessarily, I also discuss the systems that resolve goal conflict between these two types of responses.

The PAG's involvement in disorders of emotion was first demonstrated via stimulation experiments with cats, where electrical stimulation of the PAG directly elicits aggressive-defensive behavior, despite the absence of any threatening stimulus (Fernandez De Molina & Hunsperger, 1962; Hunsperger, 1956). Although a very similar set of responses is evoked from electrical stimulation of the central nucleus of the amygdala and from an area that the authors dubbed the "hissing zone" of the hypothalamus, destruction of the cat PAG renders stimulation of these other areas ineffective, while the opposite is not true: PAG stimulation still elicits

aversive reactions even after hypothalamic and amygdalar lesions (Schreiner & Kling, 1953). PAG is therefore considered fundamental and necessary as the lowest structure in the hierarchical top-down control of defensive and aggressive strategies in the brain.

Human case studies show similar results. Patients with Urbach-Wiethe disease, a rare genetic disorder that causes calcification of parts of the brain (Koen et al., 2016), show some dysfunction in emotional memory and negative facial expression recognition if their amygdala has been affected, but are still largely emotionally and autonomically responsive to other fear- and anxiety-inducing cues (Adolphs, Tranel, Damasio, & Damasio, 1994; Bach, Hurlemann, & Dolan, 2013; Becker et al., 2012; Hurlemann et al., 2007; Lindquist, Wager, Kober, Bliss-Moreau, & Barrett, 2012; Markowitsch et al., 1994; Terburg et al., 2012).

1.1. Basic problem: what's so special about the PAG and the mind?

The PAG stands as a misunderstood structure in the current neuropsychological research landscape. A lot is known about its properties, functions and involvement with pathologies, and yet this information has not been drawn together to make a coherent picture. Take for instance the most common conceptualization of the PAG as a crucial node in the defense and emotional system. This is in fact correct: the PAG is the lowest level in the brain hierarchy that produces unified, intense aversive reactions in any animal that has an identifiable PAG. Although other parts of the brain are also capable of producing intense emotional reactions, if the PAG is removed from the system (pharmacologically or through lesioning) then these responses cease, indicating that the PAG is of fundamental importance. With more than 50 years of research into the midbrain and its roles in emotion, the image of the PAG as the seat of negative emotions has dominated the field.

However, as early as the 1980s, the PAG was also shown to be fundamental to something a lot more pleasant than fearful experiences of terror: the initiation of sexual behavior. It is true that sexual behaviors can be generated from regions other than the PAG, such as certain divisions of the hypothalamus. However, just as it is the case with fear evocation, lesions of the PAG eliminate sexual behaviors evoked by the hypothalamus (Chapter 2).

The PAG's influence on positive behaviors does not stop only at sexual initiation: it is also part of the circuit involved in speech generation. In fact, its role in vocalizations is so deep that animals can be rendered mute by lesions of the PAG. Certainly, there are important differences between animal vocalizations and human speech. The first and most obvious difference is that

animal vocalizations are devoid of complex semantic content. Although several mammalian species are endowed with the ability to produce distinct vocalizations that are understood by conspecifics to convey different messages, these clearly pale in comparison with the complexity of human speech. Secondly, animal sounds are frequently the result of an emotional response to environmental pressures and not something that appears to be under volitional control, as seen during threat or conflict, sexual courting, or when distressed pups seek maternal attention. Speech in humans, on the other hand, is a more measured affair, where individuals tend to engage in controlled, voluntary exchanges instead of involuntary emotional utterances. With that in mind, can we claim that the PAG is fundamentally involved in human speech? Evidence is mounting that it is. At least three reported cases of human PAG lesions have resulted in mutism (Esposito, Demeurisse, Alberti, & Fabbro, 1999), and, in fMRI studies where participants are instructed to produce voluntary speech, the PAG is shown to be active both during proper speech, and also during whispered, non-vocalized speech (Schulz, Varga, Jeffires, Ludlow, & Braun, 2005).

How can a region that is capable of producing intense fear and aggressive defensive reactions also produce states that are at the other end of the emotional spectrum? A search on the Web of Science database for the keyword "periaqueductal" plus "panic" or "fear" yields 95,561 research papers. In comparison, "periaqueductal" plus "sex" or "lordosis" (the prominent female sexual behavior in rodents) only returns 5,367 articles. Furthermore, the PAG's involvement in sex and speech are not the only overlooked functions of this region: the rodent PAG has clear involvement in maternal behavior and is part of the brain networks controlling social interactions as well.

The inconsistencies about what kind of structure the PAG is exist even in its most widely accepted role as a defensive region of the brain. For example, the dorsolateral division of the PAG has been described as "an important site for the organization of fear responses to predators" (Gross & Canteras, 2012). However, responding to the presence of a predator was a role also ascribed to a different part of the PAG, the dorsomedial column: "[which] could contribute to the overall pattern of somatomotor and autonomic responses expressed by animals facing natural threats" (Borelli & Brandao, 2008). The dorsomedial and dorsolateral are two distinct parts of the PAG, with different connections and receptors. It is unlikely that structurally different regions would have the same function. As another example of inconsistencies regarding the PAG, it has been said that "the lateral PAG column (and its associated circuit) is activated preferentially by 'escapable' physical stressors to which an active defensive reaction(s) is the primary response" (Keay & Bandler, 2015), while at the same

time it has been said that "(…) the lateral PAG can influence motivational drive to seek appetitive reward" (Motta, Carobrez, & Canteras, 2017). Once again, it is inconceivable, at least at face value, that activation of a single specific region of the brain would provoke *escape* (the act of moving away from physical stressors) and at the same time drive *approach* (the act of moving closer to appetitive rewards).

And beyond this functional inconsistency, how can the PAG be conceptualized in models and theories of the mind as this ancient region for negative reactions, if it also regulates aspects that are so diametrically different? Theoretical frameworks, which are used to guide further research and insights into the nature of the human mind, have an incomplete view of the PAG. The main objective of this thesis is to attempt to correct how the PAG is conceptualized.

1.2. Defensive systems

1.2.1. The question of movement

"If you root yourself to the ground, you can afford to be stupid."
(Churchland, 1986)

In order to discuss the functions of the PAG, we first need to discuss the dynamics that were responsible for the development of the PAG itself – and the rest of the nervous system, for that matter. The evolution of the neuron, one of the fundamental units in the nervous system and one of the main targets of scientific enquiry into the human mind, gives insight into what these forces might be. Sedentary multicellular organisms, like for instance the sponges in the phylum *Porifera*, lack neurons – i.e. cells capable of transmitting signals, electrical and/or chemical, among themselves. Despite possessing many features that would indicate otherwise, such as receptor genes and neurotransmitters, no animal in this phylum is endowed with a neuronal network similar to mammals (Conaco et al., 2012).

The phylum *Ctenophora* is considered to be the earliest example of animals possessing a nervous system serving molecular functions similar to mammals. Jellyfish in the *Cnidaria* group are also endowed with a diffuse nerve network, which is capable of signaling to produce a motor response if mechanical stimulation to the organism is detected. But the nature of the responses produced are crude; cells in the jellyfish orchestrate motor responses that are not guided in any particular orientation in relation to the detected stimulus (Bucher & Anderson, 2015). In other words, a jellyfish reacts to a threat, even if such reaction involves moving *in the direction* of the threat. Clearly animals that are capable of coordinating the direction of their responses to environmental stimuli would be at an evolutionary advantage. Indeed, the comb

jellies in the phylum *Ctenophora* are greatly differentiated from the cnidarians by the defining presence of small filaments over their bodies called cilia. It has been shown that organisms in the *Ctenophora* group are capable of producing directed escape *away* from physical stimulation (Mackie, Mills, & Singla, 1992) Also, the same cilia are also used to direct the animal *towards* food (Tamm, 2014).

Looking to these rudimentary organisms for inspiration and extrapolating the simple dynamics of these early neurons to the more complex mammalian nervous system, a reasonable theory would be that humans are at the end of an evolutionary road that pressured organisms to produce increasingly sophisticated responses to guide them toward or away from certain discrete positive or negative stimuli. Although sedentary sponges have virtually the same genes coding for the expression of receptors and neurotransmitters found in higher order animals, it may have been the necessity to move and control the direction of that movement that transformed these cells into recognizable neural networks.

1.2.2. Trying to predict the future: not-so-clear and not-so-present danger

As new and ever more complex nervous systems started to develop, the strategies employed to deal with environmental pressures grew more sophisticated. Whereas the early sea ctenophores and cnidarians could only move away from danger once it was close enough for physical contact, humans, as other vertebrates, are capable of foreshadowing future events with some degree of precision, allowing them to act long before physical contact with the threat is established.

The influential work of Caroline and Robert Blanchard (1988) highlights the arsenal of distinct behaviors employed by rats depending on the imminence of the threat. They demonstrated that the array of behaviors shown by rats is dependent both on the *distance* between the rat and the perceived threat, as well as the rat's perception of the *likelihood* of escape.

At the lowest level of the defense hierarchy is the phenomenon of *thanatosis*, or tonic immobility. When prey perceives that it is cornered or captured by a predator, it can cease movement and become unresponsive to physical stimuli, even painful ones. In rare controlled lab experiments that studied this tonic immobility, it was shown that the behavior increases survival of the prey by serving as a distraction to predators (R. K. R. Thompson et al., 1981). Once the prey was captured and started displaying tonic immobility, the predator, probably assuming that their prey is dead, would release it and engage in hunting other nearby targets. However, as soon as the predator removed itself from the location, the prey would return to its

active state and make its escape. As a very crude means of survival, tonic immobility is present across a wide range of land vertebrates such as mammals, birds, reptiles and amphibians, and also in fish. Beyond vertebrates, it has also been reported in invertebrates such as crustaceans, and even insects and arachnids. As it does not require distinct anatomical appendages or specialized behavior to develop (in fact, this strategy relies solely on *not having* any overt behaviors), tonic immobility is a suitable mechanism of defense even among the simplest of organisms (Humphreys & Ruxton, 2018). Despite being a very cunning method of self-defense, tonic immobility is very rudimentary as it is employed not to avoid threat, but to try and solve it after attack has commenced.

On the next level of the defense hierarchy is *attack*. When an animal is cornered and perceives no available escape route, but has yet to be captured, it may display signs of aggression, such as threatening vocalizations and body postures. In rats, if these strategies are not sufficient to thwart predator approach, then the animals might attack the predator at close-quarters distances, usually in the face area, and then attempt to escape. Although this behavior is observable in wild rats, the behavior is virtually abolished in laboratory strains of rats (D. C. Blanchard, Griebel, & Blanchard, 2003), making the study of this behavior difficult in domesticated strains.

However, if predator presence is detected but attack is perceived as not being imminent, the prey will most likely engage in freezing. Also, it is thought that animals might display freezing under scenarios of uncertainty, when predator presence is not well established. Freezing behavior works by mostly reducing detection by a predator, and it also provides the prey with time to assess the situation and gather more evidence as to whether or not it should escape the location or attack the predator. Although freezing is perhaps the most studied defensive behavior in animals, it is also extremely misunderstood in relation to its functions. For instance, freezing behavior not only occurs as a pre-emptive measure *before* a physical confrontation, but it also frequently happens *after* an aversive physical event (Fanselow & Lester, 1988). At this point it should be noted that, at a superficial level, although pre-encounter freezing, post-encounter freezing and tonic immobility all resemble one another, they are very distinct strategies of defense that are heavily dependent on context and situation. Also, these behaviors are sensitive to different classes of drugs, and are reliant on different brain networks.

Whenever a predator's presence is at all uncertain, rodents and other animals will also engage in *risk assessment behaviors*, which is the next level of the defense hierarchy. In the Blanchard's Visible Burrow System (R. J. Blanchard & Blanchard, 1989), an artificial system of subterranean tunnels was built in a lab setting, and animals were allowed to live in it as a

colony. When a cat was placed on the surface level of the system, the rats would quickly escape into the burrows below (one of the first, more basic defensive responses described above). When the cat was subsequently removed from the area by the experimenters, the rats would eventually move gradually back up towards the surface, displaying risk assessment behaviors. These would include stretching from the inside of the burrow to the opening outside, sniffing and head poking. The Blanchards noted that these risk assessment behaviors were long-lasting, and the colony would engage in them for 20 hours or more after the cat had been removed, while also suppressing other social activities (R. J. Blanchard & Blanchard, 1989). Another type of risk assessment strategy, when threat is perceived to be even less imminent or even more ambiguous than in the example above, is rearing behavior. Many mammals will rear on their hind legs when presented to novel stimuli or environments. This behavior, much like the stretching and sniffing of the Blanchard's experiments, is thought to serve the purpose of gathering information about the environment and possible threats (Lever, Burton, & O'Keefe, 2006). However, as the body posture of rearing leaves animals considerably exposed and vulnerable, it is reasonable to expect that it is only displayed when the animals assume that threat is not certain, and therefore is a behavior more toward the safe end of the defensive distance gradient.

Now, let us pause for a moment and assume that the defensive hierarchy described above is more or less correct – and this is somewhat of a hard concession, as in the case of the confusion regarding the freezing behaviors described above, this is not a topic that the research community can readily agree on. But, considering momentarily that this hierarchy is an acceptable one, we can readily see that strategies at the close-proximity end of the spectrum (tonic immobility, fighting, escaping) are present in a big range of animal taxa, from creatures with simpler nervous systems such as insects and crustaceans to animals with complex ones, such as mammals. As we move towards the more elaborate end of defensive strategies that rely on information gathering and short- and long-term memory systems (stretching, sniffing, rearing), these behaviors start to be limited to selected mammals only (Lever et al., 2006).

Leaving aside selective pressures (defensive behaviors are probably more acute in prey animals than predators, for instance) it seems evident that throughout the road of evolution animals gradually developed responses not only to clear and present danger, but also to not-so-clear and not-so-present ones – or 'imagined' threats, in a sense. Perhaps no better example of reacting to imagined threats exists than humans. While rats can react cautiously for up to 20 hours after they last had evidence that something dangerous was in the area, humans can react cautiously for a lifetime, even when the danger was never experienced first-hand. As

exemplified by Sapolsky (1998) book title, zebras indeed don't get ulcers, because zebras are not spending their days in the savannah worrying about crime that they heard about in the news but were never victims of. Zebras have to deal with acute, immediate problems like a lion sprinting towards them, and then producing an according response, like escaping. Humans, like zebras, also have to deal with acute immediate dangers, and are well equipped to do so. However, unlike zebras, humans are also equipped to deal with future, anticipated problems that zebras cannot even fathom. In Woody Allen's 1977 movie Annie Hall, a flashback scene to the main character's childhood reveals that once as a young boy he ended up in the psychiatrist office with depression:

***Dr. Flicker**: Why are you depressed, Alvy?*

***Alvy Singer**: The universe is expanding.*

***Dr. Flicker**: The universe is expanding?*

***Alvy Singer**: Well, the universe is everything, and if it's expanding, someday it will break apart, and that will be the end of everything.*

***Mrs. Singer**: What has the universe got to do with it? You're here, in Brooklyn. Brooklyn is not expanding!*

***

In the same way that brains are capable of reacting to *aversive* stimuli that can either be close or distant (be it physically or temporally), they are equally capable of reacting to close and distant *appetitive* stimuli as well. Hungry rats, for instance, can easily learn to press levers in order to receive a food reward. Given enough training, rats can even be convinced to engage in a little bit of future planning: press lever number one, and get a small reward; or press lever number two, wait a few seconds, and get a larger reward. With some tinkering, experimenters can adjust the ratios of delay, so if animals initially choose the sooner and smaller reward, the time delay of the larger reward would be decreased so it would be more seductive in the next trial. If then the animal chooses the delayed reward, its time delay would be increased, and so on. After a lot of micro-adjustments to these delay times (or the same can be done with reward sizes, to the same effect), animals eventually reach a stage of indifference to preference where they essentially choose the immediate reward in 50% of the trials and the delayed reward in the other 50%. At this point, the smaller immediate reward is taken to represent the subjective value that the rat gives to the larger future reward; in other words, if a rat's point of indifference is between 1 pellet of food delivered now and 5 pellets of food delivered after 5 seconds, it would

be implied that both rewards have the same subjective value to the animal. As the value of the delayed reward is established as a function of the immediate reward, common delays to both the immediate and delayed rewarded can be added (i.e. in the case of the example above, now the 1 pellet of food comes after 2 seconds or the 5 pellets come after 7 seconds). As the common delay to both rewards starts to be gradually increased, animals gradually switch their preference and start to become future planners: the more delayed reward would be valued more highly. In humans, these patterns of valuing are remarkably similar to the ones in animals, with one single difference: the magnitude of the scale of the time that organisms are willing to wait for their rewards. As shown in figure 8 of Vanderveldt, Oliveira, and Green (2016), pigeons and humans show the same pattern of valuation of delayed rewards, but with many orders of magnitudes of difference in the time scale: a 20-second delay of food reward in the pigeon follows the same discounting pattern to a 10-year delay in monetary reward in humans. This could be taken as empirical evidence that pigeons, unlike young Alvy in Annie Hall, are probably not endowed with brain systems that allow them to worry about the consequences of the universe expanding.

1.2.3. Could rudimentary structures have some form of sophistication?

During vertebrate evolution (or at least during *gnathostomes* evolution), Nature promoted the creation of ever-increasing cerebral complexity not by scrapping previous ones and starting again from scratch, but by subtly modifying existing brain or, more usually, adding new brain on top of old, unchanging brain. Although some subcortical structures altered their shape due to other hypertrophied regions (for example, the superior colliculus of birds is relatively larger than the one in mammals, distorting the borders of the periaqueductal grey located ventrally), the more phylogenetically old brain regions remained largely preserved across species. The behaviors employed by vertebrates to deal with immediate threats and rewards are largely commanded by ancient, well preserved, midbrain, pontine and medullary regions. Aggressive reactions, the likes of which would be seen in animals reacting to close-quarter threats, are solely dependent on the PAG to the point that a cat that had most of its brain anterior of the hypothalamus removed would still produce defensive responses – albeit it in a more exacerbated, uncontrolled manner (Kaada, 1967). The PAG, by the way, is anatomically and biochemically similar across mammals, and has analogous regions in birds and fish as well. As another example, the basal ganglia in birds, reptiles and mammals is extremely well preserved, with similar cell populations, neurotransmitters and functions (Reiner, Brauth, & Karten, 1984). On the other hand, when it comes to cortical regions, in particular the neocortex, the differentiation among species is enormous even within primates (Kaas, 2012).

We could assume at this point that simplistic nervous systems give rise to blunt defensive reactions related to present and clear stimuli, while on the other end of evolutionary spectrum, complex brains developed the capacity to deal not only with certain and present stimuli, but that are also capable of predicting and committing to future, uncertain ones.

1.3. Wrapping up – establishing some of the questions and deciding on a plan

With the scenario presented in this Chapter so far, I would like to return to the first question poised at the beginning about the PAG: how can an ancient region that is capable of producing intense fear and aggressive defensive reactions, also be capable of producing states and functions that are completely opposite in the emotional and evolutionary spectrum?

In a two-dimensional system of defense proposed by McNaughton and Corr (2004), an anatomical hierarchy is described for the control of defensive reactions in the brain, related to distance to the threat (figure 3 in that publication). In this model, fear-related states (defensive avoidance) and anxiety-related ones (defensive approach) are placed in parallel on the defensive-distance continuum. For each level, it was hypothesized that each structure would possess anatomical subdivisions that command both avoidance and approach. Essentially, the avoidance column represents responses that are produced to threats perceived to be certain, while the approach column represents responses to threats perceived to be uncertain. An updated version of the scheme was proposed later (McNaughton, DeYoung, & Corr, 2016), with the addition of a third parallel column, indicating non-defensive approach systems – that is, brain structures concerned with commanding behavior and states to unambiguous appetitive stimuli at different distances from the organism. This image is reproduced here in Figure 1.1.

As is clear in the figure, both phylogenetically old and new structures possess the ability to generate strategies that are rudimentary and sophisticated, respectively, to solve the problems of avoidance, approach and conflict. At the bottom of the image, however, we see an untidy scenario: where we might expect there to be approach properties assigned to the PAG, there is nothing.

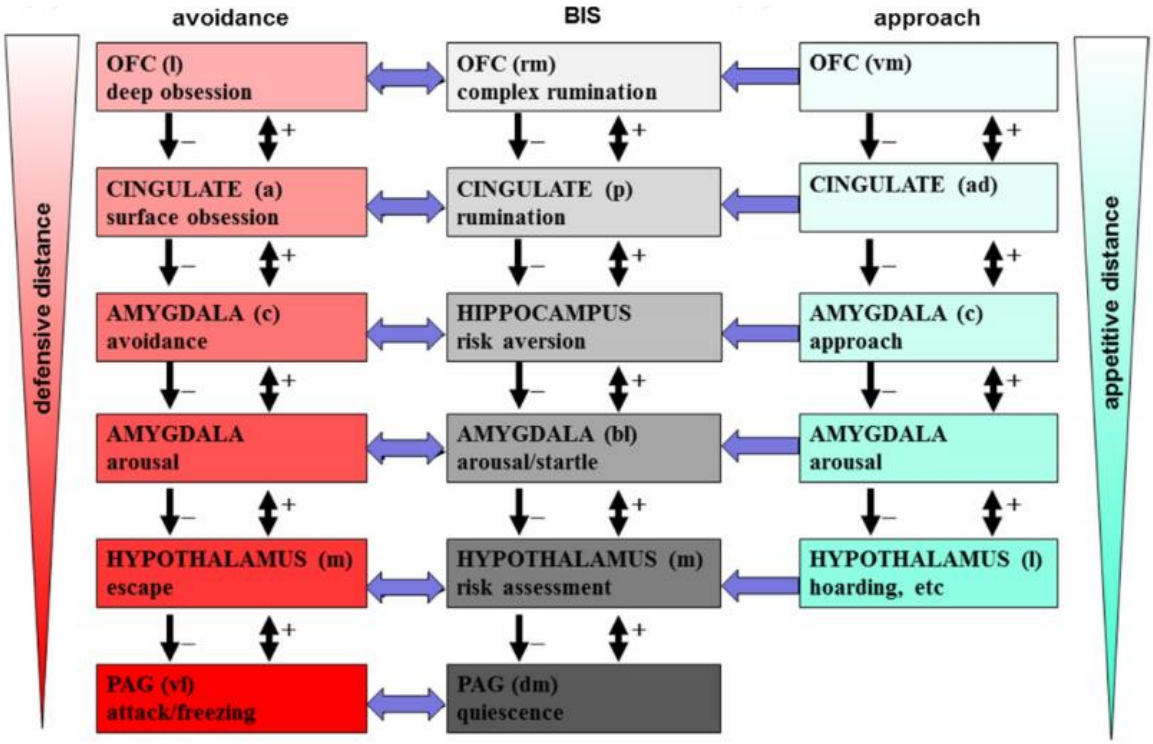

Figure 1.1.The hierarchical organization of avoidance and approach (McNaughton et al., 2016). Original model proposed by McNaughton and Corr (2004)

The scenario presented in this Chapter – where approach and avoidance have primitive origins that are conserved and overlaid by later systems – suggests that the approach slot at the bottom right of the image should rightfully be occupied by the PAG. Simple approach is surely as primitive as simple avoidance. But which subdivision of the PAG would that be? And, if approach and avoidance are represented in PAG, would it not be reasonable to expect primitive mechanisms of approach-avoidance conflict resolution to have some presence there also? Is the existing evidence strong enough to justify altering the model? Do we have novel experimental evidence to support this change? This thesis will address these questions and go toward re-conceptualizing the place of the PAG in the vertebrate motivational landscape.

1.3.1. Thesis outline

What is the PAG?

In Chapter 2, I present an extensive review of the PAG's anatomy and functions, in order to: 1) solve the inconsistencies about which part commands fear reactions; 2) propose a region that controls conflict; 3) propose a new subdivision of the PAG to accommodate evidence of its involvement in appetitive states; and 4) present a functional view of the PAG and dorsal raphe in relation to repeated conflict and the pathogenesis of depression.

Can the PAG produce conflict?

In Chapter 4, I test the hypothesis that the PAG is able to generate conflict-like activity in the forebrain. By recording local electrical activity from the prefrontal cortex and hippocampus of rats, I show that freezing behavior from electrical stimulation of the PAG generates cortical and hippocampal theta, an estimated index of conflict and anxiety. I also demonstrate that different regions of the PAG in the anterior-posterior axis produce opposing cortico-hippocampal responses, while generating the same behavior of freezing.

Can the nucleus incertus influence PAG-generated states?

In Chapter 5, I investigate how manipulating the nucleus incertus (one of the nodes in the theta-generating circuits of the brain) impacts the cortical and hippocampal theta produced by the PAG. The nucleus incertus has been shown to influence the generation of theta and also to heavily project to the PAG. I test the administration of both a classical and a novel anxiolytic into the nucleus incertus, as well as an agonist and an antagonist of the local nucleus incertus receptor, relaxin.

Chapter 2. The periaqueductal grey and the dorsal raphe: a locus of control for aversive and appetitive states

2.1. Introduction

In this review, I describe the topography and biochemistry of the PAG complex, and delve into three of its functional domains: the regulation of appetitive and aversive states; motivation and decision-making during conflict; and its involvement in the behavioral traits and symptomology of depression.

First, I summarize evidence that the dorsal PAG plays a major role in appetitive behaviors and states. While its role in positive affect is seldom emphasized in the literature, I highlight the dorsal PAG's involvement in sexual and social approach, and propose two new anatomical divisions that account for this functional specificity, supported by anatomical and biochemical evidence.

Second, I aim to demonstrate that the dorsal and ventral parts of the PAG compete and self-regulate. The interactions of the parts of the PAG influence not only states and processes related to motivation but also decision-making during conflict.

Third, I argue that, although the PAG's hallmark function is the control of defensive reactions, the ventral PAG and DR evoke quiescent, recuperative states, and are involved in the long-term reduction of behavioral and autonomic activity seen in animal models of depression. By extension, I propose that a similar mechanism occurs in humans.

2.2. Anatomy of the periaqueductal complex

2.2.1. Phylogeny of the PAG

The PAG is a heterogeneous region. It has varying densities of cells and neuron-to-glia ratios throughout its extension, and also has distinct somatic shapes and dendritic arborization patterns that show no particular orientation (Behbehani, 1995). Despite this lack of uniformity, the whole length of the PAG shows a stable trend of increasing cell body size when moving radially from the aqueduct to the periphery.

While early Nissl and Golgi staining methods failed to show partitions in the periaqueductal complex, later investigations employing cluster analysis of neuron groupings asserted that the PAG can be divided into dorsal and ventral portions (see F. Conti, Barbaresi, and Fabri (1988), for an overview).

Later immunohistochemical and retrograde tracing established that there were distinct columns within the PAG, using NADPH-d labeling (Carrive & Paxinos, 1994; Gonzalez-Hernandez, Conde-Sendin, & Meyer, 1992; Johnson & Ma, 1993; Leigh, Connick, & Stone, 1990), nitrous oxide synthase (Onstott, Mayer, & Beitz, 1993), cytochrome oxidase (F. Conti et al., 1988), substance P (Barbaresi, 1998), and localized autoradiography binding sites for cholecystokinin (H. Liu, Chandler, Beitz, Shipley, & Behbehani, 1994) and excitatory amino acids (Albin et al., 1990). Columnar divisions are also seen in the patterns of medullar, cortical and subcortical topographical to PAG (discussed below), and through functional experiments demonstrating how separate loci within the PAG control and integrate defensive and autonomic functions (see Section 2.3).

As seen in Figure 2.1, the organization of the cells surrounding the brain aqueduct is generally stable across diverse species. The set of nuclei that form the PAG are present in a similar form in all mammals; generally sharing the same functions and basic organization (Kingsbury, Kelly, Schrock, & Goodson, 2011). For example, the PAG retains its overall shape, morphology, density and relative volume across non-human primates, felines and rodents (Mantyh, 1982b). Recently, certain midbrain structures in other vertebrates were described as being homologues of the mammalian periaqueductal complex as well. Although the PAG and its homologues retain the same general function and properties across different classes of animals, the cell distribution differs somewhat among fish, amphibians, reptiles and birds. In birds, the PAG homologue is shifted laterally because of a hypertrophied tectum, but the cell organization is the same as that in mammals (Dubbeldam & den Boer-Visser, 2002; Kingsbury et al., 2011). In teleost fish, the equivalent of the mammalian PAG is located opposite the nucleus torus semicircularis, a homologue for the inferior colliculus, making its location similar to that in mammals (Bass, Rose, & Pritz, 2005). In fish, this PAG homologue exerts control over the vocalizations made during mating and social scenarios (Bass, 2008; Bass & McKibben, 2003); both features of the mammalian PAG (see Section 2.3). Furthermore, the PAG of the plainfin midshipman (*Porichthys notatus*) projects to cortical, thalamic and hindbrain regions as it does in mammals (Kittelberger & Bass, 2013).

Overall, this suggests that the PAG has been highly conserved during evolution and is common across tetrapods in general (Bass et al., 2005). Indeed, analogues of the PAG across different vertebrates have similar mRNA and protein expression patterns, indicating similar genetic origin (O'Connell & Hofmann, 2012).

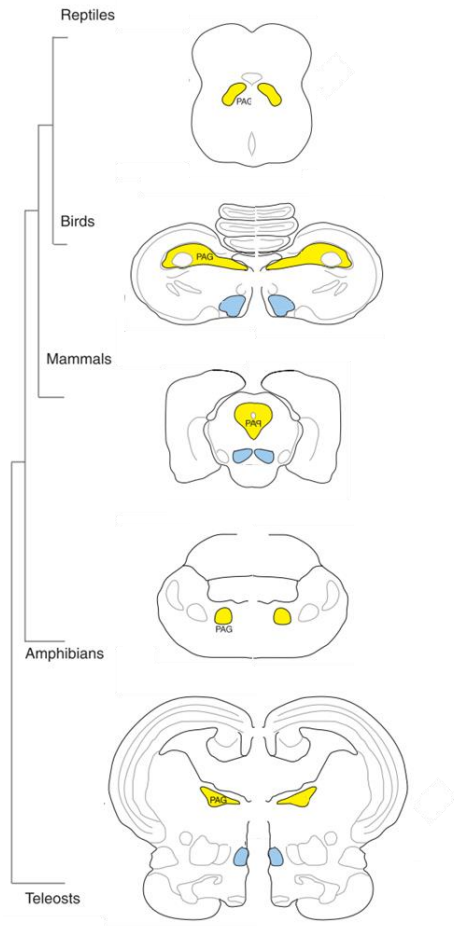

Figure 2.1. PAG (yellow) in different vertebrates, as determined by similar local mRNA or protein expression. Adapted with permission from O'Connell and Hofmann (2012).

2.2.2. The division of nuclei surrounding the aqueduct

Here I review the mammalian PAG, as conventionally labeled, together with the dorsal raphe nucleus (DR), which together with the PAG forms a simple 'O' of grey matter around the aqueduct. The traditional columnar division of the PAG and DR through the anterior posterior axis is presented in Figure 2.2.

The DR, located ventrally to the PAG, is the most rostrally positioned of the raphe nuclei: clusters of cell populations mostly located in the midline between hemispheres, whose defining characteristic is the high density of serotonin-producing cells that innervate most of the forebrain and hindbrain. The DR is not a homogenous structure, and is by convention separated into dorsal and ventral divisions, as well as lateral wings that extend ventrally to the ventral PAG. According to Descarries, Watkins, Garcia, and Beaudet (1982), the DR can easily be distinguished from the PAG by the dense packing of cells in the region, while the cell body

diameter is less different between the two structures, with the PAG averaging a diameter of 13.6µm against the DR average of 15.5µm.

Although the DR has distinct features that separate it from the PAG hodologically, chemically and functionally, I argue in this review that the DR shares common functions and anatomical features with the PAG and should be viewed as a crucial component of the PAG complex, without which most of the functions, evoked behaviors, or adaptive roles of the latter would not be possible.

As discovered by Beitz (1985), the neuron-to-glia density in the PAG varies in its rostral-caudal axis, with the highest density of neurons found in the more rostral portion, while this density gradually decreases towards the more caudal part. Similarly, the extreme dorsal portion has a higher density of cells than the more ventral aspect. The shape of the perikarya also varies in the rostro-caudal axis: *cell bodies on the caudal portion are more elongated and cells in the rostral part are more circular. Similarly, a slightly higher proportion of rostral cells than caudal cells are oriented in parallel to the aqueduct.* Meanwhile, the average size (length, width, axial ratio and area) of periaqueductal cells are consistent throughout.

The tissue immediately surrounding the aqueduct constitutes a ring of low neuron-to-glia cell density in comparison to the rest of the PAG, as shown through Golgi staining (Beitz & Shepard, 1985; Hamilton, 1973a, 1973b; Mantyh, 1982b) and observed clearly in Nissl- and Cresyl violet-stained sections (Beitz, 1985; Gioia, Bianchi, & Tredici, 1984; Paxinos & Watson, 1998).

Radially, PAG cells cluster in regard to their size and population density. The dorsal part has the highest density of neurons, followed by the dorsolateral and lateral, the ventrolateral, and finally the more sparsely populated medial ring. This cytological pattern disappears once I move to the caudal extreme of the PAG, where subdivisions can no longer be distinguished by density alone, and Beitz collectively refers to these cells simply as PAG. While the average soma size of PAG cells is constant across subdivisions, the medial ring has slightly smaller cells, a finding reported in the rat, cat and monkey (Hamilton, 1973a; Mantyh, 1982b)

Based on these anatomical findings, and further functional and biochemical data, the PAG is conventionally divided into dorsomedial (DMPAG), dorsolateral (DLPAG), lateral (LPAG) and ventrolateral (VLPAG) columns (Bandler, Carrive, & Depaulis, 1991), as shown in Figure 2.2. Given their common shared properties, the DM and DL are sometimes collectively referred as simply “dorsal PAG” (DPAG), as for example in W. Zhang, Hayward, and Davenport (2007) and Roncon et al. (2015).

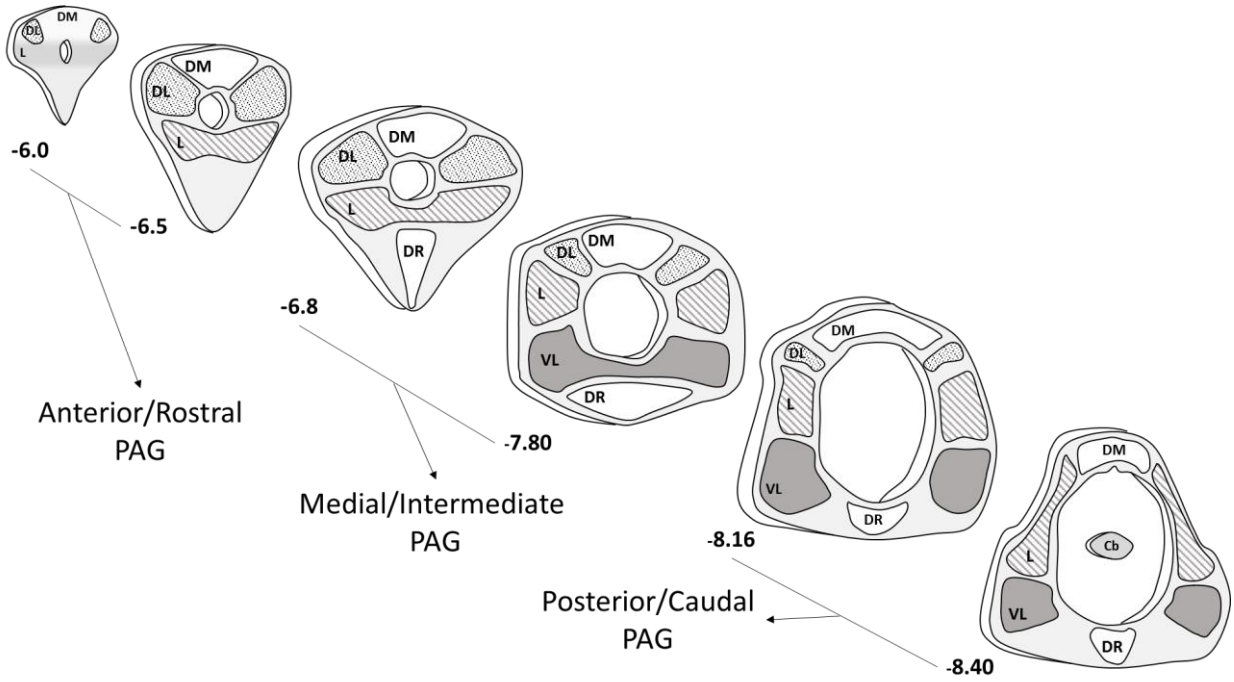

Figure 2.2. Columnar division of the PAG through the anterior posterior axis. Approximate bregma coordinates for the rat brain from the atlas of Paxinos and Watson (1998). DM: dorsomedial PAG; DL: dorsolateral PAG; L: lateral PAG; VL: ventrolateral PAG; DR: dorsal raphe nucleus; Cb: cerebellar lobule.

There are no general synaptic distinctions between the different columns of the PAG at the caudal end (Moss & Basbaum, 1983a). Most connections of the caudal PAG are symmetrical, with axodendritic synapses amounting to 97% of the observed connections in the region. Of note, the ventral PAG is completely absent of axosomatic connections, a type of synapse seen in the dorsal regions, albeit in small numbers.

2.2.3. Intra-periaqueductal connections

The nuclei of the PAG are strongly interconnected (see Table 2.1). All parts receive projections from the other subdivisions, with the exception of the DLPAG column, which only receives projections from the DMPAG (Jansen, Farkas, Mac Sams, & Loewy, 1998; Canteras & Goto, 1999; Vertes, 1991).

The subdivisions of the PAG also project to *themselves* at more anterior and posterior levels. For example, cells in the intermediate level of the DMPAG send axons to the anterior and posterior levels of DMPAG; a trend also seen in the other divisions. This organization could

indicate that extremes of the PAG that contain unique afferents could receive information from different sources and relay the signal to other parts of itself in the anterior-posterior axis.

Table 2.1. Projections from the Medial Aspect of All PAG/DR Divisions to the Anterior, Medial and Posterior Aspect of All Other Divisions

			mDM	mDL	mL	mVL	mDR	References
PROJECTING TO	DM	A	+++	+++	++	+	+	Jansen, Farkas, Mac Sams, & Loewy, 1998; Canteras & Goto, 1999; Vertes, 1991
		M	■	+++	++	+	+	
		P	+++	++	++	+	.	
	DL	A	+++	+++	.	.	.	
		M	+	■	.	.	.	
		P	++	++	.	.	.	
	L	A	++	.	++	++	+++	
		M	++	+	■	++	++	
		P	++	+	++	++	+	
	VL	M	+	.	++	■	++	
		P	+++	+	+	+	++	
	DR	M	++	+	+	++	■	
		P	++	+	.	+		

Note: ■ = site of injection; . = negligible projections; + = weak or small projections; ++ = medium projections; +++ = strong or large projection. A = anterior/rostral; M = medial/intermediate; P = posterior/caudal.

Strong connective patterns include the DM sending heavy terminals to itself and the DL, both caudally and rostrally; this is reciprocated by the DL also connecting to the DM. The DM also displays strong connections ventrally, having synaptic terminals and fibers scattered on the L, VL and DR. On the other hand, the L, VL and DR send weaker projections to the dorsal aspect of the PAG, and none at all to the DLPAG, suggesting a biased relationship between the dorsal and ventral PAG.

2.2.4. Afferent connections

The afferent connections to the PAG do not show particularly strong localizations in the rostro-caudal or dorso-ventral aspects of the region (see Tables 2.2-2.10). The clear exception to this rule that might prove to be functionally relevant is the DL column. In some instances this column is the preferred site of incoming projections, such as the ones from the anterior

cingulate cortex (Table 2.2). In other respects, the DL is completely devoid of terminal fields when compared to neighboring areas, as in the case of fibers arriving from the amygdala (Table 2.5) and ventrolateral medulla (Table 2.10).

Frontal cortex. Remarkably, both the CG1 and CG2 subdivisions of the anterior cingulate cortex (ACC) exclusively and consistently target the DLPAG throughout its dorso-caudal extent, with no significant efferents to other divisions of the PAG/DR at any level (Beckstead, 1979; Floyd, Price, Ferry, Keay, & Bandler, 2000; Meller & Dennis, 1986; Wyss & Sripanidkulchai, 1984). This information is summarized in Table 2.2. The majority of the cingulate cells that target the DLPAG are glutamate- and aspartate-positive in nature (Beart, Summers, Stephenson, Cook, & Christie, 1990; Beitz, 1989).

Table 2.2. Projections from the Cingulate Cortex to the PAG/DR at Anterior, Medial and Caudal Levels

			DM	DL	L	VL	DR	References
CINGULATE CORTEX	Anterior CG1	A	.	++	.	■	■	(Beckstead, 1979; Floyd et al., 2000; Meller & Dennis, 1986; Wyss & Sripanidkulchai, 1984)
		M	.	++	.	.	.	
		P	.	++	.	.	.	
	Anterior CG2	A	.	+++	.	■	■	(Floyd et al., 2000; Wyss & Sripanidkulchai, 1984)
		M	.	++	.	.	.	
		P	.	++	.	.	.	

Note. ■ *= anatomical division is non-existent at this level; . = negligible projections; + = weak or small projections; ++ = medium projections; +++ = strong or large projections; A = anterior/rostral; M = medial/intermediate; P = posterior/caudal.*

Meanwhile, the subdivisions of the medial prefrontal cortex (mPFC) show distinct patterns of connections with the PAG, as summarized in Table 2.3.

Table 2.3. Projections from the Medial Prefrontal Cortex to the PAG/DR at Anterior, Medial and Caudal Levels

			DM	DL	L	VL	DR	References
MEDIAL PREFRONTAL CORTEX	Posterior Prelimbic Cortex	A	++	+++	+			(Floyd et al., 2000; Meller & Dennis, 1986; Sesack, Deutch, Roth, & Bunney, 1989; Wyss & Sripanidkulchai, 1984)
		M	++	+++	+	+	.	
		P	+	+++	+	++	+	
	Anterior Prelimbic Cortex	A	.	.	+	■	■	(Floyd et al., 2000)
		M	.	.	++	+++	+++	
		P	.	.	+	+++	+++	
	Infralimbic Cortex	A	.	.	.	■	■	(Hurley, Herbert, Moga, & Saper, 1991; Sesack et al., 1989; Takagishi & Chiba, 1991; Wyss & Sripanidkulchai, 1984)
		M	.	.	.	++	+	
		P	.	+	+	+++	+++	
	Dorsal Peduncular Cortex	A	.	.	+	■	■	(Floyd et al., 2000; Hurley et al., 1991)
		M	.	.	.	+++	++	
		P	.	.	.	+++	++	

Note. ■ *= anatomical division is non-existent at this level; . = negligible projections; + = weak or small projections; ++ = medium projections; +++ = strong or large projections; A = anterior/rostral; M = medial/intermediate; P = posterior/caudal.*

The prelimbic cortex (PrL), an extensive cortical subdivision on the medial wall of the prefrontal cortex (PFC) that extends from the olfactory bulb to the genu of the corpus callosum in the rat (Paxinos & Watson, 1998), projects heavily to the PAG/DR. Despite being treated by the Paxinos atlas as a single homogenous region, the anterior and posterior parts of the PrL project differently to the PAG.

Subdividing the PrL is necessary due to both anatomy and function. For example, projections from the parahippocampal cortices to the PrL show distinct anterior-posterior patterns, with denser projections at rostral PrL levels, but this parcelation is not seen in other prefrontal areas like the orbital or insular cortices (Delatour & Witter, 2002). Furthermore, PrL projections to the thalamus are more concentrated in the anterior than the caudal part (S. Li & Kirouac, 2012), and the anterior and posterior parts of the PrL differentially connect to subdivisions of the hypothalamus (Floyd, Price, Ferry, Keay, & Bandler, 2001). In rats exposed

to a rewarding conditioned stimulus, the anterior and posterior portions of the PrL display different levels of c-Fos expression (Schroeder, Binzak, & Kelley, 2001).

Connections from the PrL to the PAG/DR also display distinct anterior-posterior characteristics. The more anterior half of the PrL has been shown to preferentially target ventral periaqueductal regions, particularly the VLPAG and DR, although a few scattered processes can be found in the LPAG (Floyd et al., 2000). Cells in the posterior half of the PrL, however, tend to intensely target the DMPAG and DLPAG, with a few scattered fibers in the LPAG, VLPAG and DR (Floyd et al., 2000; Meller & Dennis, 1986; Sesack et al., 1989; Wyss & Sripanidkulchai, 1984). A recent study investigating the nature of these medial PFC (mPFC) projections to the PAG found that most PrL axons originate from pyramidal cells on Layer 5 of the medial wall, and are glutamatergic in nature (Franklin et al., 2017)

The infralimbic cortex (IL), located ventrally to the PrL in the medial wall, preferentially targets the VLPAG and DR, with more dense fiber distribution at the caudal levels (Hurley et al., 1991; Sesack et al., 1989; Takagishi & Chiba, 1991; Wyss & Sripanidkulchai, 1984).

Located ventrally to the IL is the DP cortex. This segment of the mPFC shows a similar pattern of projections to those of the IL, and targets mostly the ventral parts of the PAG (Floyd et al., 2000; Hurley et al., 1991).

As shown in Table 2.4, the projections from the orbital and insular cortices are mostly concentrated in the ventral PAG, with a few exceptions. The few terminals originating from the very anterior dorso-lateral orbital cortex (DLO) preferentially target the VLPAG and DR, with only a few processes in the LPAG at intermediate levels (Floyd et al., 2000), and the more posterior lateral orbital cortex (LO) also projects exclusively to the ventral parts of the PAG/DR (Beckstead, 1979). Projections originating from the medial orbital cortex (MO) are quite intense in the VLPAG and DLPAG at intermediate and caudal levels, and a few scattered terminals also selectively innervate the DLPAG at the more extreme posterior region (Floyd et al., 2000). This distribution is also witnessed with projections from the ventral orbital cortex (VO) cells, albeit at a smaller volume (Hoover & Vertes, 2011).

Table 2.4. Projections from the Orbito-Insular Cortices to the PAG/DR at Anterior, Medial and Caudal Levels

			DM	DL	L	VL	DR	References
ORBITO-INSULAR CORTICES	Orbital Cortex	A	.	++	+	■	■	(Beckstead, 1979; Floyd et al., 2000; Hoover & Vertes, 2011)
		M	.	.	+	+++	+++	
		P	.	.	.	+++	+++	
	Insular Cortex	A	.	.	.	■	■	(Beckstead, 1979; Floyd et al., 2000; Neafsey, Hurley-Gius, & Arvanitis, 1986; Reep & Winans, 1982)
		M	.	.	.	++		
		P	.	.	.	++	++	

Note. ■ *= anatomical division is non-existent at this level; . = negligible projections; + = weak or small projections; ++ = medium projections; +++ = strong or large projections; A = anterior/rostral; M = medial/intermediate; P = posterior/caudal.*

As with orbital projections, cells from the insular cortices terminate strongly in the VLPAG and DR, with no registered projections aimed at the dorsal parts of the PAG (Beckstead, 1979; Floyd et al., 2000; Neafsey et al., 1986; Reep & Winans, 1982). Both the dorsal and ventral divisions of the agranular insular cortex (AIV, AID) project to the PAG/DR.

Temporal Areas. The central nucleus of the amygdala (CNA) is the only region in the amygdaloid complex projecting to the PAG (Krettek & Price, 1978; Pardo-Bellver, Cadiz-Moretti, Novejarque, Martinez-Garcia, & Lanuza, 2012; Petrovich, Risold, & Swanson, 1996). It targets mostly the LPAG, VLPAG and DR, although some processes are found in the DMPAG (Hopkins & Holstege, 1978; Price & Amaral, 1981; Rizvi, Ennis, Behbehani, & Shipley, 1991). As shown in Table 2.5, no amygdalar afferents reach the DLPAG at any point in the rostro-caudal axis, making it the only PAG/DR division not innervated by the amygdala.

Table 2.5. Projections from the Amygdaloid Complex to the PAG/DR at Anterior, Medial and Caudal Levels

			DM	DL	L	VL	DR	References
AMYGDALA	Central Nuclei	A	++	.	+++	■	■	(Hopkins & Holstege, 1978; Price & Amaral, 1981; Rizvi et al., 1991)
		M	++	.	+++	++	++	
		P	+	.	+	+++	+++	
	Basolateral Nucleus	A	.	.	.	■	■	(Krettek & Price, 1978)
		M	.	.	.	.	.	
		P						
	Basomedial Nucleus	A	.	.	.	■	■	(Petrovich et al., 1996)
		M						
		P						
	Medial Nuclei	A	.	.	.	.	.	(Pardo-Bellver et al., 2012)
		M	.	.	.	.	.	
		P	.	.	.	.	.	

Note. ■ *= anatomical division is non-existent at this level; . = negligible projections; + = weak or small projections; ++ = medium projections; +++ = strong or large projections; A = anterior/rostral; M = medial/intermediate; P = posterior/caudal.*

The PAG/DR complex does not receive direct projections from the hippocampus or the septum (Marchand & Hagino, 1983; Meibach & Siegel, 1977; Raisman, Cowan, & Powell, 1966; Staiger & Nurnberger, 1991; L. W. Swanson & Cowan, 1977; van Groen & Wyss, 1990), but other structures related to the hippocampus do project to the PAG/DR (see Table 2.6). The lateral habenula sends direct projections to the VLPAG and DR (Canteras & Swanson, 1992; Herkenham & Nauta, 1979; Neckers, Schwartz, Wyatt, & Speciale, 1979; Pasquier, Anderson, Forbes, & Morgane, 1976), while the medial part does not (Herkenham & Nauta, 1979; Pasquier et al., 1976). Meanwhile, the perirhinal and entorhinal cortices target mostly the dorsal PAG, with no evidence of projections reaching the VPAG or DR (Witter & Groenewegen, 1986a, 1986b).

Table 2.6. Projections from the Hippocampal Formation to the PAG/DR at Anterior, Medial and Caudal Levels

			DM	DL	L	VL	DR	References
HIPPOCAMPAL FORMATION	Lateral Septal Nucleus	A				■	■	(Powell, 1963; Staiger & Nurnberger, 1991)
		M	.	.	.	.	.	
		P	.	.	.	.	.	
	Medial Septum	A	.	.	.	■	■	(Marchand & Hagino, 1983; Powell, 1963)
		M	.	.	.	.	.	
		P	.	.	.	.	.	
	CA1	A	.	.	.	■	■	(Marchand & Hagino, 1983; Meibach & Siegel, 1977; Raisman et al., 1966; L. W. Swanson & Cowan, 1977; van Groen & Wyss, 1990)
		M	.	.	.	.	.	
		P	.	.	.	.	.	
	CA2	A	.	.	.	■	■	(Marchand & Hagino, 1983; Raisman et al., 1966; L. W. Swanson & Cowan, 1977)
		M	.	.	.	.	.	
		P	.	.	.	.	.	
	CA3	A	.	.	.	■	■	(Marchand & Hagino, 1983; Meibach & Siegel, 1977; Raisman et al., 1966; L. W. Swanson & Cowan, 1977)
		M	.	.	.	.	.	
		P	.	.	.	.	.	
	DG	A	.	.	.	■	■	(Marchand & Hagino, 1983; Meibach & Siegel, 1977; Raisman et al., 1966; L. W. Swanson & Cowan, 1977)
		M	.	.	.	.	.	
		P	.	.	.	.	.	
	Medial Habenula	A	.	.	.	■	■	(Herkenham & Nauta, 1979; Pasquier et al., 1976)
		M	.	.	.	.	.	
		P	.	.	.	.	.	
	Lateral Habenula	A	.	.	.	■	■	(Araki, McGeer, & Kimura, 1988; Herkenham & Nauta, 1979; Neckers et al., 1979; Pasquier et al., 1976)
		M	.	.	.	++	+	
		P	.	.	.	++	+	
	Perirhinal and Entorhinal Cortices	A	++	+	.	■	■	(McIntyre, Kelly, & Staines, 1996; Witter & Groenewegen, 1986a, 1986b)
		M	+	+	++	.	.	
		P	.	.	+	.	.	

Note. ■ *= anatomical division is non-existent at this level; . = negligible projections; + = weak or small projections; ++ = medium projections; +++ = strong or large projections; A = anterior/rostral; M = medial/intermediate; P = posterior/caudal.*

Hypothalamus. Diencephalic regions are the densest source of projections to the periaqueductal area, with hypothalamic areas being the largest contributors (Marchand & Hagino, 1983). This is summarized in Table 2.7.

Table 2.7. Projections from the Hypothalamus to the PAG/DR at Anterior, Medial and Caudal Levels

			DM	DL	L	VL	DR	References
HYPOTHALAMUS	Medial Preoptic Area	A	++	++	+++			(Rizvi, Ennis, & Shipley, 1992)
		M	++	+	+++	+++	+	
		P	+	+	+++	+++	+	
	Dorsal Pre-mammillary Body	A	+	+++	+			(Canteras & Swanson, 1992)
		M						
		P	+	+++	+	.	.	
	Ventromedial Hypothalamic Nucleus	A	++	++	++			(Shimogawa, Sakuma, & Yamanouchi, 2015; Veening et al., 1991)
		M	++	++	+++	++	+	
		P	++	+	++	+++	+	
	Posterior Hypothalamic Area	A	+++	+++	+++			(Vertes & Crane, 1996)
		M	+++	+++	+++	+++	++	
		P	+	+	++	+++	++	
	Anterior Hypothalamic Area	A	+	+	++			(Conrad & Pfaff, 1976; Saper, Swanson, & Cowan, 1978)
		M	+	+	++	++	+	
		P	+	+	++	++	+	
	Supramammillary Area, Medial Part	A	+	+	++			(Vertes, 1992)
		M	.	.	+	++	+++	
		P						
	Lateral Hypothalamic Area	A	.	.	+++			(Nauta, 1958; Roeling et al., 1994; Veening et al., 1991)
		M	.	.	+	+++	++	
		P	.	.	+	++	+++	

Table continued on following page.

(Table 2.7 continued)

			DM	DL	L	VL	DR	References
HYPOTHALAMUS	Dorsomedial Hypothalamic Nucleus	A	.	+	++	■	■	(R. H. Thompson, Canteras, & Swanson, 1996; Veening et al., 1991)
		M	.	+	+++	++	+	
		P	+	+	+++	++	++	
	Ventral Pre-mammillary Body	A				■	■	(Canteras, Simerly, & Swanson, 1992)
		M	.	.	.	++	+	
		P	.	.	+	++	+	
	Supramammillary Area, Lateral Part	A	.	.	++			(Vertes, 1992)
		M			++	+		
		P						

Note. ■ *= anatomical division is non-existent at this level; . = negligible projections; + = weak or small projections; ++ = medium projections; +++ = strong or large projections; A = anterior/rostral; M = medial/intermediate; P = posterior/caudal.*

Regions like the anterior hypothalamic area (Conrad & Pfaff, 1976; Saper et al., 1978), ventromedial hypothalamus (Shimogawa et al., 2015; Veening et al., 1991), and posterior hypothalamic area (Vertes & Crane, 1996) target all parts of the PAG/DR, whereas a dorsal-ventral trend can be seen in projections from other hypothalamic regions. For instance, the VLPAG and DR are the exclusive destination of fibers arising from the lateral hypothalamic area (Nauta, 1958; Roeling et al., 1994; Veening et al., 1991) and most of the supramammillary region (Vertes, 1992).

While the dorsal aspects of the PAG, particularly the DLPAG, are specifically targeted by the dorsal pre-mammillary body (Canteras & Swanson, 1992), the ventral pre-mammillary body predominately projects to the VLPAG and DR (Canteras et al., 1992).

Tectum, midbrain, pons, medulla and spinal cord. Projections from the tectum to the PAG/DR are shown in Table 2.8. While there are no projections from the inferior colliculus to the PAG/DR area (Mantyh, 1982a; Moore & Goldberg, 1966; Peyron, Luppi, Fort, Rampon, & Jouvet, 1996), the superior colliculus (SC), targets the antero-dorsal aspect of the PAG, and fibers originating mostly from the deep layers of the SC reach the DL column, as well as parts of the LPAG (An, Bandler, Ongur, & Price, 1998; Graham, 1977; Mantyh, 1982a).

Table 2.8. Projections from the Tectum to the PAG/DR at Anterior, Medial and Caudal Levels

			DM	DL	L	VL	DR	References
TECTUM	Superior Colliculus	A	+	++	++	■	■	(An et al., 1998; Graham, 1977; Mantyh, 1982a)
		M	.	+++	++	.	.	
		P	.		.	.	.	
	Inferior Colliculus	A	.	.	.	■	■	(Mantyh, 1982a; Moore & Goldberg, 1966; Peyron et al., 1996)
		M	.	.	.	.		
		P	.	.	.	.	.	

Note. ■ *= anatomical division is non-existent at this level; . = negligible projections; + = weak or small projections; ++ = medium projections; +++ = strong or large projections; A = anterior/rostral; M = medial/intermediate; P = posterior/caudal.*

Projections from the midbrain, basal ganglia and pons to the PAG/DR are summarized in Table 2.9. Numerous structures in the midbrain and pons send projections to the PAG/DR, although a distinctive topography is not always present. Interestingly, while the raphe magnus targets both the dorsal and ventral PAG (Levine & Jacobs, 1992; Mantyh, 1982a), the median raphe only sends connections to the ventral parts, not targeting the DLPAG or DMPAG (Azmitia & Segal, 1978a; Vertes, Fortin, & Crane, 1999).

Nuclei that express modulatory neurotransmitters send projections widely to the PAG. These include the locus coeruleus (Jones & Moore, 1977; Jones & Yang, 1985; Kim, Lee, Lee, & Waterhouse, 2004; Mantyh, 1982a) and nucleus incertus (Goto, Swanson, & Canteras, 2001; Olucha-Bordonau et al., 2003). Other modulatory regions, however, exclusively target the ventral PAG. For example, the substantia nigra (Gerfen, Staines, Arbuthnott, & Fibiger, 1982; Hopkins & Niessen, 1976) and ventral tegmental area (Beckstead, Domesick, & Nauta, 1979; Simon, Le Moal, & Calas, 1979) predominantly target the VLPAG and DR.

Table 2.9. Projections from the Midbrain, Basal Ganglia and Pons to the PAG/DR at Anterior, Medial and Caudal Levels

			DM	DL	L	VL	DR	References
MIDBRAIN, BASAL GANGLIA AND PONS	Cuneiform Nucleus	A	++	++	+++	■	■	(Edwards & de Olmos, 1976; Mantyh, 1982a; Steeves & Jordan, 1984)
		M	+	++	++	+++		
		P						
	Locus Coeruleus	A	+	+	+++	■	■	(Jones & Moore, 1977; Jones & Yang, 1985; Kim et al., 2004; Mantyh, 1982a)
		M	+	++		++	++	
		P					+++	
	Magnus Raphe	A				■	■	(Mantyh, 1982a; Peyron et al., 1996)
		M	+++	+++		+++		
		P					++	
	A5 Noradrenaline Cell Group	A	++	++	++	■	■	(Byrum & Guyenet, 1987)
		M						
		P						
	Reticulus Pontis Oralis	A				■	■	(Mantyh, 1982a)
		M	++	++		++		
		P						
	Nucleus Incertus	A	.	++	+	■	■	(Goto et al., 2001; Olucha-Bordonau et al., 2003)
		M	.	++	.	++	++	
		P	+	+	.	+++	+++	
	Zona Incerta	A	+	+	+++	■	■	(Ricardo, 1981)
		M	.	.	+++	++	+	
		P	.	.	++	++	.	
	Median Raphe	A	.	.	++	■	■	(Azmitia & Segal, 1978a; Vertes et al., 1999)
		M	.	.	.	++	++	
		P	.	.	+	++	+++	
	Substantia Nigra	A	.	.	+	■	■	(Gerfen et al., 1982; Hopkins & Niessen, 1976)
		M	.	.	.	++	++	
		P	.	.	.	++	+	
	Ventral Tegmental Area	A	.	.	++	■	■	(Beckstead et al., 1979; Simon et al., 1979)
		M	.	.	+	++	++	
		P	.	.	.	++	++	

Note. ■ *= anatomical division is non-existent at this level; . = negligible projections; + = weak or small projections; ++ = medium projections; +++ = strong or large projections; A = anterior/rostral; M = medial/intermediate; P = posterior/caudal.*

Projections from the medulla and spinal cord to the PAG/DR are presented in Table 2.10. Perhaps the most notable feature about the projections originating from the medulla to the PAG/DR is that they appear to target all subdivisions while selectively ignoring the DL column (Blomqvist & Craig, 1991; Herbert & Saper, 1992b; Mantyh, 1982a; Rinaman, 2010). The ventrolateral medulla, for instance, sends heavy projections to the DMPAG and LPAG, while the DLPAG located between the two receives no projections (Bjorkeland & Boivie, 1984; Herbert & Saper, 1992b).

Neither the cervical nor lumbar parts of the spinal cord send afferents to the DMPAG and the DR, while both heavily target the LPAG (Bjorkeland & Boivie, 1984; Blomqvist & Craig, 1991; Keay, Feil, Gordon, Herbert, & Bandler, 1997; Wiberg & Blomqvist, 1984).

Table 2.10. Projections from the Medulla and Spinal Cord to the PAG/DR at Anterior, Medial and Caudal Levels

			DM	DL	L	VL	DR	References
MEDULLA AND SPINAL CORD	Ventrolateral Medulla	A	+++	.	+++	■	■	(Bjorkeland & Boivie, 1984; Herbert & Saper, 1992b)
		M	+++	.	+++	++	.	
		P	+++	.	++	++	.	
	Nucleus Tractus Solitarius	A	.	.	+	■	■	(Herbert & Saper, 1992b; Rinaman, 2010)
		M	.	.	+	++	+	
		P	.	.	+	+++	++	
	Spinal Trigeminal Nucleus	A	.	.	++	■	■	(Blomqvist & Craig, 1991; Mantyh, 1982a)
		M	.	+	++	+	.	
		P	.	.	.	.	.	
	Cervical Spinal Cord	A	.	+	+++	■	■	(Bjorkeland & Boivie, 1984; Blomqvist & Craig, 1991; Keay et al., 1997; Wiberg & Blomqvist, 1984)
		M	.	+	+++	+	.	
		P	.	.	++	+	.	
	Lumbar Spinal Cord	A	.	+	+	■	■	(Bjorkeland & Boivie, 1984; Blomqvist & Craig, 1991; Wiberg & Blomqvist, 1984)
		M	.	++	+++	++	.	
		P	.	+++	++	+++	.	

Note. ■ *= anatomical division is non-existent at this level; . = negligible projections; + = weak or small projections; ++ = medium projections; +++ = strong or large projections; A = anterior/rostral; M = medial/intermediate; P = posterior/caudal.*

2.2.5. Efferent connections

In general terms, outgoing projections from the PAG complex retain their columnar pattern at different rostro-caudal levels. However, the nature of these projections is very different between the dorsal (DM, DL and L) and ventral (VL and DR) divisions (see Tables 2.11-2.17).

The dorsal portions only send significant ascending projections as far as the thalamus through the periventricular bundle. In contrast, the ventral portions innervate the thalamus, hypothalamus, hippocampal formation and frontal cortices through two different nerve pathways: the first goes to the thalamus through the periventricular bundle and then ventrally to the hypothalamus, while the second departs the PAG ventrally, synapses collaterals in the hypothalamus, and continues from there to terminate in forebrain structures.

Fibers descending from the dorsal PAG to the medulla target a limited number of hindbrain and pontine structures, like the cuneiform nucleus and the magnus and median raphe nuclei. Axons from the ventral regions, on the other hand, are directed to a larger variety of regions in the pons and on the floor of the 4th ventricle: descending fibers from the VLPAG and DR split into two bundles, one traveling more dorsally and connecting to locations on the 4th ventricle like the nucleus incertus, dorsal tegmental nucleus and locus coeruleus, and the second bundle diverting ventrally and innervating different points of the reticular formation and other pontine structures on its way towards the medulla.

Frontal cortex. Table 2.11 summarizes PAG/DR projections to the frontal cortices. The ventral portions of the PAG, especially at the caudal extreme, project to the frontal cortices (Herrero, Insausti, & Gonzalo, 1991). Sparse projections from the VLPAG reach the PrL and IL cortices, but most of the efferent connections to these areas depart from the DR (Conde, Maire-Lepoivre, Audinat, & Crepel, 1995; Hoover & Vertes, 2007; Meller & Dennis, 1991). The dorsal aspect of the PAG, on the other hand, does not project to the medial PFC in any significant amount.

As with the medial PFC, the ACC receives projections originating mostly from cells in the DR (Conde et al., 1995; Hoover & Vertes, 2007). Although a few scattered cells in the lateral portion of the PAG at the more rostral level are found to project to the orbital cortex, most of the efferents to this region follow the same pattern as the other cortical targets in the area, and are limited to the DR at more caudal portions (Azmitia & Segal, 1978a; Coffield, Bowen, & Miletic, 1992).

The DR innervates the rostral DLO, LO, VO and MO subdivisions of the orbital cortex. The agranular subdivisions of the insular cortex are also preferentially targeted by DR neurons,

with no cells from the dorsal PAG known to project to this cortical region (Jasmin, Burkey, Granato, & Ohara, 2004).

The raphe cells reaching the PFC are mostly of non-serotonergic nature, and originate from a population located at the midline level that is distinct from cells that project to other areas (Vanbockstaele, Biswas, & Pickel, 1993).

Table 2.11. Projections Targeting the Frontal Cortices from the PAG/DR at Anterior, Medial and Caudal Levels

			DM	DL	L	VL	DR	References
CINGULATE CORTEX	Anterior CG1	A	.	.	.	■	■	(Conde et al., 1995; Hoover & Vertes, 2007)
		M	.	.	.	.	++	
		P	.	.	.	.	++	
	Anterior CG2	A				■	■	
		M						
		P						
MEDIAL PREFRONTAL CORTEX	Posterior Prelimbic Cortex	A				■	■	(Herrero et al., 1991; Meller & Dennis, 1991.5)
		M	.	.	.	.	++	
		P	.	.	.	.	++	
	Anterior Prelimbic Cortex	A	.	.	.	■	■	(Conde et al., 1995; Hoover & Vertes, 2007; Meller & Dennis, 1991.5)
		M	.	.	.	.	++	
		P	.	.	.	+	++	
	Infralimbic Cortex	A	.	.	.	■	■	(Conde et al., 1995; Hoover & Vertes, 2007; Meller & Dennis, 1991.5)
		M	.	.	.	.	++	
		P	.	.	.	+	++	
	Dorsal Peduncular Cortex	A				■	■	(Meller & Dennis, 1991.5)
		M				.		
		P						
ORBITO-INSULAR CORTICES	Orbital Cortex	A	.	.	+	■	■	(Azmitia & Segal, 1978a; Coffield et al., 1992.8; Craig, Wiegand, & Price, 1982)
		M	.	.	.	+	++	
		P	.	.	.	.	+++	
	Insular Cortex	A	.	.		■	■	(Jasmin et al., 2004; Saper, 1982)
		M	.	.	.	++	+++	
		P						

Note. ■ *= anatomical division is non-existent at this level; . = negligible projections; + = weak or small projections; ++ = medium projections; +++ = strong or large projections; A = anterior/rostral; M = medial/intermediate; P = posterior/caudal.*

Temporal areas. Most amygdalar subdivisions are targeted by VLPAG and DR cells, apart from the central nuclei (CNA), which receives some fibers originating from the LPAG at rostral and intermediate levels (see Table 2.12). There is no reported innervation from the DMPAG and DLPAG to the amygdala (Bobillier et al., 1976; Ottersen, 1981; Reichling & Basbaum, 1991). The CNA receives input from cells that are highly concentrated in the DR and VLPAG at the caudal level, and a moderate number of cells grouped at the caudal extreme of the LPAG (Rizvi et al., 1991). Furthermore, the caudal DR consistently projects to the basolateral, medial and basomedial amygdala, with some cells in the VLPAG also projecting to the basomedial nucleus (Ottersen, 1981).

The axons originating in the ventral PAG/DR and targeting the central amygdala are at least partly dopaminergic (Hasue & Shammah-Lagnado, 2002), despite few dopaminergic cell bodies in the PAG and DR (Shimada, Ishikawa, & Tanaka, 1976; L. W. Swanson, 1988).

Table 2.12. Projections Targeting the Amygdaloid Complex from the PAG/DR at Anterior, Medial and Caudal Levels

			DM	DL	L	VL	DR	References
AMYGDALA	Central Nuclei	A	.	.	++	■	■	(Bobillier et al., 1976; Reichling & Basbaum, 1991.2; Rizvi et al., 1991)
		M	.	.	+	++	+++	
		P	.	.	.	+++	+++	
	Basolateral Nucleus	A	.	.	.	■	■	(Meller & Dennis, 1991.5; Ottersen, 1981; Reichling & Basbaum, 1991.2)
		M	.	.	.	.	++	
		P	.	.	.	.	++	
	Basomedial Nucleus	A	.	.	.	■	■	(Meller & Dennis, 1991.5; Ottersen, 1981; Reichling & Basbaum, 1991.2)
		M	.	.	.	++	++	
		P	.	.	.	++	++	
	Medial Nuclei	A	.	.	.	■	■	(Meller & Dennis, 1991.5; Ottersen, 1981; Reichling & Basbaum, 1991.2)
		M	.	.	.	.	+	
		P	.	.	.	.	+	

Note. ■ *= anatomical division is non-existent at this level; . = negligible projections; + = weak or small projections; ++ = medium projections; +++ = strong or large projections; A = anterior/rostral; M = medial/intermediate; P = posterior/caudal.*

Table 2.13 shows PAG/DR projections targeting the hippocampal formation. As with the rest of the forebrain, most periaqueductal efferents to the hippocampal formation originate in the VLPAG and the DR, with the exception of the entorhinal area in mammals, which receives sparse axons from the rostral DMPAG and DLPAG (Insausti, Amaral, & Cowan, 1987; Kohler & Steinbusch, 1982; Segal, 1977).

The DR projects significantly not only to the parahippocampal cortices (Insausti et al., 1987; Kohler & Steinbusch, 1982; Room & Groenewegen, 1986; Segal, 1977; Vertes, 1991.5), but also to the medial septum (Bobillier, Petitjean, Salvert, Ligier, & Seguin, 1975; McKenna & Vertes, 2001; Pasquier & Reinoso-Suarez, 1978) and lateral septum (Waselus, Galvez, Valentino, & Van Bockstaele, 2006), and dorsal CA1 (McKenna & Vertes, 2001; Wyss, Swanson, & Cowan, 1979). The lateral septum is also considerably targeted by VLPAG neurons (Wyss et al., 1979), although they are not serotonergic in nature (Kohler & Steinbusch, 1982). The dorsal columns, however, do not connect directly to the hippocampal region (Amaral & Cowan, 1980; Azmitia & Segal, 1978b; Herkenham & Nauta, 1977; Krout & Loewy, 2000; Meller & Dennis, 1991.5; Olucha-Bordonau et al., 2003.; Pasquier & Reinoso-Suarez, 1977; Segal & Landis, 1974; Waselus et al., 2006).

Table 2.13. Projections Targeting the Hippocampal Formation from the PAG/DR at Anterior, Medial and Caudal Levels

			DM	DL	L	VL	DR	References
HIPPOCAMPAL FORMATION	Parahippocampal Cortices	A	+	+	.	■	■	(Insausti et al., 1987; Kohler & Steinbusch, 1982; Room & Groenewegen, 1986; Segal, 1977; Vertes, 1991.5)
		M	.	.	.	+	+++	
		P	.	.	.	+	+++	
	Lateral Septal Nucleus	A	.	.	.	■	■	(Meller & Dennis, 1991.5; Pasquier & Reinoso-Suarez, 1978; Waselus et al., 2006)
		M	.	.	.	.	++	
		P	.	.	.	.	+++	
	Medial Septum	A	.	.	.	■	■	(Bobillier et al., 1975; McKenna & Vertes, 2001; Pasquier & Reinoso-Suarez, 1978)
		M	.	.	.	.	+	
		P	.	.	.	.	++	
	CA1	A	.	.	.	■	■	(Amaral & Cowan, 1980; Kohler & Steinbusch, 1982; McKenna & Vertes, 2001; Olucha-Bordonau et al., 2003.; Pasquier & Reinoso-Suarez, 1977; Segal & Landis, 1974; Wyss et al., 1979)
		M	.	.	.	++	++	
		P	.	.	.	++	+++	
	CA2	A	.	.	.	■	■	(Amaral & Cowan, 1980; Pasquier & Reinoso-Suarez, 1977, 1978; Segal & Landis, 1974)
		M	.	.	.	.	.	
		P	.	.	.	.	.	
	CA3	A	.	.	.	■	■	(Amaral & Cowan, 1980; Pasquier & Reinoso-Suarez, 1977, 1978; Segal & Landis, 1974)
		M	.	.	.	.	.	
		P	.	.	.	.	.	
	DG	A	.	.	.	■	■	(Amaral & Cowan, 1980; Azmitia & Segal, 1978b; Kohler & Steinbusch, 1982; McKenna & Vertes, 2001; Olucha-Bordonau et al., 2003.; Pasquier & Reinoso-Suarez, 1977, 1978)
		M	.	.	.	.	.	
		P	.	.	.	.	++	
	Medial Habenula	A			.	■	■	(Herkenham & Nauta, 1977; Krout & Loewy, 2000)
		M	.	.		.	.	
		P				.		
	Lateral Habenula	A			.	■	■	(Herkenham & Nauta, 1977; Krout & Loewy, 2000)
		M	.	.		.	.	
		P				+		

Note. ■ *= anatomical division is non-existent at this level; . = negligible projections; + = weak or small projections; ++ = medium projections; +++ = strong or large projections; A = anterior/rostral; M = medial/intermediate; P = posterior/caudal.*

Hypothalamus.

Projections from the PAG/DR to the hypothalamus are described in Table 2.14. Several parts of the hypothalamus receive projections from the dorsal PAG, including the medial preoptic area (Simerly & Swanson, 1986), anterior hypothalamic area (Meller & Dennis, 1991), dorsomedial hypothalamus (Meller & Dennis, 1991; R. H. Thompson & Swanson, 1998) and posterior hypothalamic area (Abrahamson & Moore, 2001; Bobillier et al., 1976; Meller & Dennis, 1991). This is in contrast with cortical and other forebrain regions which are only targeted by the ventral PAG (see above sections).

The other hypothalamic regions, however, are more preferentially targeted by the ventral parts of the PAG. The lateral hypothalamus receives strong projections from the DR (Bobillier et al., 1976; Reichling & Basbaum, 1991), and so does the medial part of the supramammillary nucleus (Hayakawa, Ito, & Zyo, 1993).

Table 2.14. Projections Targeting the Hypothalamus from the PAG/DR at Anterior, Medial and Caudal Levels

			DM	DL	L	VL	DR	References
HYPOTHALAMUS	Medial Preoptic Area	A	++	+	+	■	■	(Simerly & Swanson, 1986)
		M	+	+	+	+	+	
		P						
	Dorsomedial Hypothalamic Nucleus	A				■	■	(Meller & Dennis, 1991.5; R. H. Thompson & Swanson, 1998)
		M	+	+	+	+		
		P	+	+	+	++	+	
	Anterior Hypothalamic Area	A				■	■	(Meller & Dennis, 1991.5)
		M		++		+++		
		P						
	Posterior Hypothalamic Area	A	.	++	+++	■	■	(Abrahamson & Moore, 2001; Bobillier et al., 1976; Meller & Dennis, 1991.5)
		M	.	+	+++	+	++	
		P	.	.	+	+	+	
	Lateral Hypothalamic Area	A				■	■	(Bobillier et al., 1976; Reichling & Basbaum, 1991.2)
		M	.	.	.	.	+++	
		P	.	.	.	+	+++	
	Ventromedial Hypothalamic Nucleus	A	.	.	++	■	■	(Shimogawa et al., 2015)
		M	.	.	.	++	+	
		P	.	.	.	+	+	
	Dorsal Pre-mammillary Body	A	.	.	.	■	■	(Comoli, Ribeiro-Barbosa, & Canteras, 2000; Meller & Dennis, 1991.5)
		M	.	.	.	.	.	
		P	.	.	.	.	.	
	Ventral Pre-mammillary Body	A				■	■	(Meller & Dennis, 1991.5)
		M		.				
		P						
	Supramammillary Area, Medial Part	A	.	.	.	■	■	(Hayakawa et al., 1993)
		M	.	.	.	.	++	
		P	.	.	.	.	++	
	Supramammillary Area, Lateral Part	A	.	.	.	■	■	(Gonzaloruiz, Alonso, Sanz, & Llinas, 1992)
		M						
		P						

Note. ■ *= anatomical division is non-existent at this level; . = negligible projections; + = weak or small projections; ++ = medium projections; +++ = strong or large projections; A = anterior/rostral; M = medial/intermediate; P = posterior/caudal.*

Tectum, midbrain, pons, medulla and spinal cord. Table 2.15 summarizes projections from the PAG/DR to the tectum. The superior colliculus (SC) and inferior colliculus (IC) have consistently been reported to receive little-to-no projections from the PAG/DR (Appell & Behan, 1990; Beyerl, 1978; Bobillier et al., 1976; Brunso-Bechtold, Thompson, & Masterton, 1981; Coleman & Clerici, 1987; Mantyh, 1983). Of note, fiber tracts exiting the PAG formation towards both the forebrain and hindbrain pass through both the SC and IC without synapsing locally (Meller & Dennis, 1991).

However, as discussed previously in this review (see Section 2.4.4), the SC does have efferent projections to the PAG, and it contributes to the PAG/DR processing of environmental threats (Brandao, Anseloni, Pandossio, De Araujo, & Castilho, 1999; Brandao, Cardoso, Melo, Motta, & Coimbra, 1994; Redgrave & Dean, 1991). This collicular-periaqueductal relationship, however, as shown by anatomical and functional data, appears to be one way, top-down only.

Table 2.15. Projections Targeting the Tectum from the PAG/DR at Anterior, Medial and Caudal Levels

			DM	DL	L	VL	DR	References
TECTUM	Superior Colliculus	A	.	.	.	■	■	(Appell & Behan, 1990; Bobillier et al., 1976; Mantyh, 1983; Waterhouse, Border, Wahl, & Mihailoff, 1993)
		M	.	.	.	+	.	
		P	.	.	.	.	+	
	Inferior Colliculus	A	.	.	.	■	■	(Beyerl, 1978; Brunso-Bechtold et al., 1981; Coleman & Clerici, 1987; Mantyh, 1983)
		M	.	.	.	.	.	
		P	.	.	.	.	.	

Note. ■ *= anatomical division is non-existent at this level; . = negligible projections; + = weak or small projections; ++ = medium projections; +++ = strong or large projections; A = anterior/rostral; M = medial/intermediate; P = posterior/caudal.*

The periaqueductal inputs to the midbrain (Table 2.16), medulla and spinal cord (Table 2.17) arise mostly from the dorsal parts of the PAG, with a few exceptions. This represents a difference from the forebrain, where most periaqueductal axons come from the ventral part.

The regions that receive predominantly ventral PAG inputs are the nucleus incertus (Goto et al., 2001), locus coeruleus (Ennis, Behbehani, Shipley, Van Bockstaele, & Aston-Jones, 1991; Krout, Jansen, & Loewy, 1998.1), substantia nigra (SN) (Gerfen et al., 1982) and

reticulus pontis oralis (Holstege, 1991b; Mantyh, 1983; Shammah-Lagnado, Negrao, Silva, & Ricardo, 1987).

Table 2.16. Projections Targeting the Midbrain, Basal Ganglia and Pons from the PAG/DR at Anterior, Medial and Caudal Levels

		DM	DL	L	VL	DR	References
Magnus Raphe	A	+++	.	+++	■	■	(Abols & Basbaum, 1981; Aghajanian & Wang, 1977; Beitz, Mullett, & Weiner, 1983.56; Holstege, 1991b)
	M	+++	.	+++	+++	.	
	P	+++	.	+++	++	.	
Median Raphe	A	+	++	++			(Behzadi, Kalen, Parvopassu, & Wiklund, 1990.; Mantyh, 1983; Meller & Dennis, 1991.5)
	M	++	++	++	+++		
	P	.	.	+	+++	+++	
Nucleus Incertus	A	.	+	+	■	■	(Goto et al., 2001)
	M	.	+	.	+++	.	
	P	.	.	.	++	+++	
Reticulus Pontis Oralis	A	.	.	++	■	■	(Holstege, 1991b; Mantyh, 1983; Shammah-Lagnado et al., 1987)
	M	.	.	+++	++	+	
	P	.	.	.	++	+	
Cuneiform Nucleus	A				■	■	(Garcia-Rill, Skinner, Gilmore, & Owings, 1983)
	M						
	P	.	.	.	++	+++	
Locus Coeruleus	A	.	.	.	■	■	(Ennis et al., 1991; Krout et al., 1998.1)
	M	.	.	.	.	.	
	P	.	.	.	++	+	
Substantia Nigra	A	.	.	.	■	■	(Gerfen et al., 1982)
	M	.	.	.	++	++	
	P	.	.	.	.	+	
Ventral Tegmental Areal	A	.	.	.	■	■	(Phillipson, 1979)
	M	.	.	.	+	.	
	P	.	.	.	+	.	
Zona Incerta	A	.	.	.	■	■	(Roger & Cadusseau, 1985)
	M	.	.	.	.	.	
	P	.	.	.	.	.	
A5 Noradrenaline Cell Group	A	.	.	.	■	■	(Byrum & Guyenet, 1987.1)
	M	.	.	.	.	.	
	P	.	.	.	.	.	

Note. ■ *= anatomical division is inexistent at this level; . = negligible projections; + = weak or small projections; ++ = medium projections; +++ = strong or large projections; A = anterior/rostral; M = medial/intermediate; P = posterior/caudal.*

The DLPAG displays another singular characteristic, by being the only PAG subdivision that lacks significant output directed at midbrain, medullary or spinal targets. For example, the DMPAG and LPAG have large cell populations targeting the magnus raphe (see Table 2.16) and the ventrolateral medulla (Table 2.17), in stark contrast to the intermediate DLPAG, which shows no efferents (Abols & Basbaum, 1981; Aghajanian & Wang, 1977; Beitz, Mullett, et al., 1983.56; Carrive, 1991; Henderson, Keay, & Bandler, 1998; Holstege, 1991b; Van Bockstaele, Aston-Jones, Pieribone, Ennis, & Shipley, 1991).

A large volume of cells in the PAG, mostly located at the VLPAG division, send both GABAergic and opioid inhibitory projections to the ventrolateral medulla (Bowman, Kumar, Hassan, McMullan, & Goodchild, 2013), and serotonergic projections to the trigeminal nucleus of the spinal cord (Y. Q. Li, Takada, & Mizuno, 1993), indicating that these neurotransmitters are essential for the promotion of ventral PAG-generated analgesia.

Table 2.17. Projections Targeting the Medulla and Spinal Cord from the PAG/DR at Anterior, Medial and Caudal Levels

			DM	DL	L	VL	DR	References
MEDULLA AND SPINAL CORD	Nucleus Tractus Solitarius	A				■	■	(Herbert & Saper, 1992b)
		M				+++		
		P						
	Ventrolateral Medulla	A	+++	.	+++	■	■	(Carrive, 1991; Henderson et al., 1998; Van Bockstaele et al., 1991)
		M	+++	.	+++	++	+	
		P	++	+	++	++	+	
	Spinal Trigeminal Nucleus	A	.	.	.	■	■	(Beitz, Mullett, et al., 1983; Y. Q. Li, Takada, Shinonaga, & Mizuno, 1993)
		M	.	.	.	++	+	
		P	.	.	.	++	+	
	Cervical Spinal Cord	A	.	.	.	■	■	(Holstege, 1991a.; 1991b; Martin, Humbertson Jr., Laxson, Panneton, & Tschismadia, 1979)
		M	.	.	+	.	.	
		P	.	.	.	+	.	
	Lumbar Spinal Cord	A				■	■	
		M						
		P						

Note. ■ *= anatomical division is inexistent at this level; . = negligible projections; + = weak or small projections; ++ = medium projections; +++ = strong or large projections; A = anterior/rostral; M = medial/intermediate; P = posterior/caudal.*

2.2.6. A new parcellation of the PAG: internal and external columns

The DLPAG and LPAG columns are not homogenous within themselves in terms of connections. I therefore propose that there are distinct external and internal parts of these two columns, based on different properties. I label them the dorsolateral PAG, external part (DLPAGe); lateral PAG, external part (LPAGe); dorsolateral PAG, internal part (DLPAGi); and lateral PAG, internal part (LPAGi), and summarize the anatomical findings in Table 2.18.

The projections from the ACC, that exclusively target the DLPAG within the PAG/DR, are more precisely targeted at the external part of the column (DLPAGe) (Beckstead, 1979; Wyss & Sripanidkulchai, 1984). Similarly, the projections from the superior colliculus are concentrated in the DLPAGe, with no terminals in the DLPAGi (Graham, 1977). Medullary projections also terminate selectively in the external parts of the PAG. These include axons from the ventrolateral medulla reaching the LPAGe *and not* the LAPGi (Bjorkeland & Boivie, 1984), and both the cervical and lumbar spinal cord also targeting the DLPAGe and LPAGe exclusively while not projecting to their internal counterparts (Bjorkeland & Boivie, 1984).

As pointed out in Section 2.4.2, projections from the amygdala to the PAG/DR are marked by the paucity of terminals targeting the DLPAG compared to the other columns. When examining the few amygdalar fibers in the DLPAG, it is possible to note that they tend to concentrate on the DLPAGi, closer to the aqueduct (Hopkins & Holstege, 1978; Price & Amaral, 1981; Rizvi et al., 1991). Several hypothalamic areas also tend to prefer the internal parts of the PAG. The medial preoptic area overwhelmingly targets the DLPAGi and LPAGi (Rizvi et al., 1992; Simerly & Swanson, 1988), as do the anterior, lateral, dorsomedial and the caudal ventromedial divisions of the hypothalamus (Conrad & Pfaff, 1976; Saper et al., 1978; Veening et al., 1991).

Table 2.18. Afferents to the internal and external divisions of the DLPAG and LPAG

		DLi	DLe	Li	Le	References
Anterior CG1	A	.	++	no afferents		(Beckstead, 1979; Wyss & Sripanidkulchai, 1984)
	M	.	++			
	P	.	++			
Anterior CG2	A	.	+++	no afferents		(Wyss & Sripanidkulchai, 1984)
	M	.	++			
	P	.	++			
Superior Colliculus	A	.	++			(Graham, 1977)
	M	.	+++			
	P	.				
Ventrolateral Medulla	A	no afferents		.	+++	(Bjorkeland & Boivie, 1984)
	M			.	+++	
	P			.	+++	
Cervical Spinal Cord	A	.	+	.	+++	(Bjorkeland & Boivie, 1984)
	M	.	+	.	+++	
	P	.	.	.	++	
Lumbar Spinal Cord	A	.	+	.	+	(Bjorkeland & Boivie, 1984)
	M	.	++	.	+++	
	P	.	+++	.	++	
Central Nuclei of the Amygdala	A					(Hopkins & Holstege, 1978; Price & Amaral, 1981; Rizvi et al., 1991)
	M	++	.			
	P	++				
Anterior Hypothalamic Area	A	+	.			(Conrad & Pfaff, 1976; Saper et al., 1978)
	M	+	.			
	P	+	.			
Lateral Hypothalamus	A	no afferents		+++	+	(Veening et al., 1991)
	M			+++	.	
	P			+++	.	
Dorsomedial Hypothalamic Nucleus	A	+++	.	++	.	(Veening et al., 1991)
	M	+++	.	++	+	
	P	+++	+	+++	.	
Caudal Ventromedial Hypothalamus	A	+++	+	++	.	(Veening et al., 1991)
	M	+++	+	++	.	
	P	++	+	++	.	

Note for Table 2.18. . = negligible projections; + = weak or small projections; ++ = medium projections; +++ = strong or large projections; A = anterior/rostral; M = medial/intermediate; P = posterior/caudal. DLi:dorsolateral PAG, internal part; DLe: dorsolateral PAG, external part; Li: lateral PAG, internal part; Le: lateral PAG, external part.

2.2.7. Neurochemical profile

Throughout the PAG, cell bodies and axonal processes express a wide range of neurotransmitters and neuropeptides (see Tables 2.19-2.30). Radioimmunoassay, enzymatic isotope assay, and immunohistochemistry have found high concentrations of neurotransmitters such as acetylcholine (Palkovits & Jacobowitz, 1974)**,** histamine (Taylor, Gfeller, & Snyder, 1972), serotonin (Palkovits & Jacobowitz, 1974), GABA (Fahn & Cote, 1968), dopamine (Versteeg, Van Der Gugten, De Jong, & Palkovits, 1976), aspartate (Clements, Madl, Johnson, Larson, & Beitz, 1987) and orexin (Baldo, Daniel, Berridge, & Kelley, 2003), and moderate concentrations of neuropeptides such as encephalin, Substance P, bombesin, angiotensin, and P-lipotropin (Mantyh, 1982b). These are reviewed in more detail in the following subsections.

GABA

The distribution of gamma-aminobutyric acid (GABA) in the PAG/DR is shown in Table 2.19. At both the rostral and intermediate levels, the DL column of the PAG is distinct from the other subdivisions in terms of high numbers of GABA-positive cell bodies. A much smaller number of these cell bodies is present in the lateral and ventral parts, including the DR. This pattern reverses at the more caudal end of the PAG/DR complex, where the ventral and lateral sections show larger numbers of cells expressing GABA compared to the DL region. At all levels, however, the midline sections of the DMPAG and the DR show fewer GABA immunopositive cells than the other regions (Barbaresi, 2005; Belin et al., 1979).

Retrograde labeling has shown that these GABA cells are local interneurons, since they project to the PAG/DR itself, exerting local tonic inhibition on most of the GABA-sensitive cells in the region, with very few efferent projections. This is indicated by lesions of putative external GABAergic sources not significantly reducing the availability of periaqueductal GABA – see Reichling (1991) for review.

As with local cell bodies, GABAergic receptors are more numerous in the DL column of the PAG on all levels of the rostral to caudal axis, for both subtypes A and B; on caudal levels, however, the distribution is more uniform throughout all subdivisions, including the DR (Chu, Albin, Young, & Penney, 1990; Gundlach, 1991).

Table 2.19. Concentrations of GABAergic Cell Bodies, Axonic Processes and Receptors in the PAG/DR Region, at Anterior, Medial and Caudal Levels

		DM	DL	L	VL	DR	References
Cell Bodies	A	.	+++	.			(Barbaresi, 2005; Stamp & Semba, 1995)
	M	.	++	+	++	.	
	P	.	+++	++	+++	.	
Fibers and Terminals	A		++				(Barbaresi, 2005)
	M		++		++		
	P		++		++		
GABA A receptors	A	+	+++	+			(Chu et al., 1990) (Gundlach, 1991)
	M	+	+++	+	+	+	
	P	++	++	++	++	++	
GABA B receptors	A	+	+++	+			(Bowery, Hudson, & Price, 1987; Chu et al., 1990)
	M	+	+++	+	+	+	
	P	+	++	+	+	+	

Note. ■ *= anatomical division is non-existent at this level; . = little detected; + =small amount; ++ = medium amount; +++ = large amount; A = anterior/rostral; M = medial/intermediate; P = posterior/caudal.*

Nitric oxide Table 2.20 describes the distribution of nitric oxide (NO) cell bodies and fibers in the PAG. NADPH-diaphorase labeling is an effective method of locating NO cells in the brain, as NADPH is one of its synthases (Hope, Michael, Knigge, & Vincent, 1991). The PAG region exhibits NADPH-d-positive cells in the DL column and the DR throughout most of its rostro-caudal extent (Barbaresi, Quaranta, Amoroso, Mensa, & Fabri, 2012; Ruiz-Torner, Olucha-Bordonau, Valverde-Navarro, & Martinez-Soriano, 2001). The same pattern is seen with nitric oxide-synthase (Gotti, Sica, Viglietti-Panzica, & Panzica, 2005; Onstott et al., 1993). Interestingly, NO is extremely localized in the DLPAG and the DR with little in the rest of PAG. The volume of local fibers and terminals for NO is concentrated in the DLPAG, VLPAG and the DR, with the DMPAG and LPAG displaying much smaller NO arborization (Carrive & Paxinos, 1994; F. Conti et al., 1988).

NO in the PAG is of interest for the study of emotional and defensive disorders, as the administration of NO donors is known to produce panic-like reactions in rats (Braga, Aguiar, & Guimaraes, 2009), while inhibition of NO synthesis produces anxiety-like behaviors (see

(Guimaraes, Beijamini, Moreira, Aguiar, & de Lucca, 2005; Guimaraes, Deaguiar, Delbel, & Ballejo, 1994) for a review).

Table 2.20.Concentration of Nitric Oxide Cell Bodies and Axonic Processes in the PAG/DR Region, at Anterior, Medial and Caudal Levels

		DM	DL	L	VL	DR	References
Cell Bodies	A	.	+++	.			(Barbaresi et al., 2012; Carrive & Paxinos, 1994; Gonzalez-Hernandez et al., 1992; Onstott et al., 1993; Pilyavskii, Maiskii, Hariri, Peker, & Bulgakova, 1996; Vincent & Kimura, 1992)
	M	.	+++	.	.	++	
	P	.	++	.	.	+++	
Fibers and Terminals	A	+	+++	+			(Carrive & Paxinos, 1994; F. Conti et al., 1988; Ruiz-Torner et al., 2001)
	M	+	+++	+	++	+++	
	P	+	+++	+	+++	+++	

Note. ■ *= anatomical division is non-existent at this level; . = little detected; + =small amount; ++ = medium amount; +++ = large amount; A = anterior/rostral; M = medial/intermediate; P = posterior/caudal.*

Glutamate The pattern of glutamate cell bodies, terminals and receptors in the PAG is presented in Table 2.21. In rodents, glutamatergic cell bodies are present in the DM, L, and VL portions of the PAG, but only in small numbers in the DL and not in any considerable concentration in the DR, with glutaminase being distributed in the same pattern (Clements et al., 1987). However, in at least one report on cats, glutamate cell bodies were shown to be scattered over all identified PAG subdivisions of the feline PAG/DR, showing no recognizable pattern in term of cell bodies or synaptic terminals distribution (Barbaresi, Gazzanelli, & Malatesta, 1997).

Beitz (1990) found that cells in the PAG that project and release glutamate and aspartate to the raphe magnus nucleus do not cluster in specific defined columns, and appear to be spread mostly at the peripheral limits of the PAG.

Various glutamergic receptors are abundant and evenly distributed through the PAG/DR; but with slightly higher binding volume in the dorsal regions, especially for kainate and quisqualate in the DL column (Albin et al., 1990; Azkue, Knopfel, Kuhn, Mateos, & Grandes, 1997; Gundlach, 1991; Tolle, Berthele, Zieglgansberger, Seeburg, & Wisden, 1993).

Table 2.21. Concentrations of Glutamatergic Cell Bodies, Axonic Processes and Receptors in the PAG/DR Region, at Anterior, Medial and Caudal Levels

		DM	DL	L	VL	DR	References
Cell Bodies	A	+++	+	+++			(Barbaresi & Manfrini, 1988; Clements et al., 1987)
	M	+++	+	+++	++	.	
	P	++	+	++	+	.	
Fibers and Terminals	A	++	++	++			(Barbaresi & Manfrini, 1988)
	M	++	++	++	++	+	
	P	++	++	++	++	+	
NMDA receptors	A	++	+	+			(Albin et al., 1990; Tolle et al., 1993)
	M	++	+	+	+	++	
	P	+	+	+	++	++	
Kainate receptors	A	++	+++	++			(Albin et al., 1990) (Gundlach, 1991)
	M	+	+++	+	+	+	
	P	+	+++	+	+	+++	
AMPA (Quisqualate) receptors	A	++	++	+			(Albin et al., 1990; Tolle et al., 1993)
	M	++	++	+	++	++	
	P	+	+	+	++	+	
mGluR receptors	A	+	++	+			(Azkue et al., 1997)
	M	+	++	+	+	+	
	P						

Note. ■ *= anatomical division is inexistent at this level; . = little detected; + =small amount; ++ = medium amount; +++ = large amount; A = anterior/rostral; M = medial/intermediate; P = posterior/caudal.*

In the mammalian nervous system, glutamate is the most abundant excitatory neurotransmitter, serving functions beyond cell signaling and assuming roles in cellular metabolism and intracellular processes. The localization of glutamate as a neurotransmitter is difficult, since all available immunohistochemical methods for detecting glutamate might also detect local glutamate that is simply part of the metabolic pool and may have no cell-signaling role. To appraise localized glutamergic systems with a role in cell signaling, the limitations of the techniques available must be taken into account and compensatory resources must be considered, such as using immunohistochemical and immunocytochemical labeling in conjunction with tracing imaging from putative glutamatergic afferent sites and efferent projections from the PAG.

Acetylcholine Table 2.21 shows concentrations of cholinergic cell bodies, terminals and receptors in the PAG. Cell bodies containing acetylcholine (ACh) are located in the caudal part of the rodent and feline VLPAG, with none of the rest of PAG nor the DR showing any ACh-positive cells (Armstrong, Saper, Levey, Wainer, & Terry, 1983). An investigation of the primate brain indicates the same pattern of scattered VLPAG cholinergic cell bodies (Kimura, McGeer, Peng, & McGeer, 1981). It is important to note that most of these cholinergic cell bodies are located at the border of the VLPAG and the laterodorsal tegmental nucleus (LDTg), which emerges lateral to the DR and ventral to the VLPAG. The LDTg is one of the most densely populated cholinergic centers in the midbrain, and it is conceivable that these detected bodies are actually functionally part of the LDTg, rather than the VLPAG. Despite the DR's closeness to both the VLPAG and LTDg, especially at caudal levels, no significant cholinergic cell bodies are located within its boundaries in rodents or primates.

With the exception of the DMPAG, the PAG subdivisions and the DR display cholinergic processes throughout their extension, with an increase in density towards the caudo-ventral levels (Ruiz-Torner et al., 2001). The terminal fields are limited to the boundaries of the PAG, and no immunoreactivity is seen on the neighboring reticular formation or superior and inferior colliculi (Kimura et al., 1981), demonstrating very specific regional input from cholinergic sources.

While muscarinic receptors are fairly evenly spread throughout the PAG and DR (Gundlach, 1991; Levey, Kitt, Simonds, Price, & Brann, 1991; Wamsley, Lewis, Young, & Kuhar, 1981; Zubieta & Frey, 1993), the nicotinic subtype appears to be more concentrated in the VLPAG and the DR (Skoubis et al., 2006; L. W. Swanson, Simmons, Whiting, & Lindstrom, 1987). In squirrel monkeys, vocalization is mediated by a broad array of neurotransmitters in the PAG, including ACh muscarinic receptors. However, ACh nicotinic receptors have no effect on PAG-elicited vocalizations (C. L. Lu & Jurgens, 1993).

Table 2.22. Concentrations of Cholinergic Cell Bodies, Axonic Processes and Receptors in the PAG/DR Region, at Anterior, Medial and Caudal Levels

		DM	DL	L	VL	DR	References
Cell Bodies	A	.	.	.	■	■	(Armstrong et al., 1983; Kimura et al., 1981)
	M	.	.	.	+	.	
	P	.	.	.	+	.	
Fibers and Terminals	A	.	.	++	■	■	(Ruiz-Torner et al., 2001)
	M	.	+	++	+	+++	
	P	.	++	+	+++	+++	
Nicotinic receptors	A	.	.	.	■	■	(Harfstrand et al., 1988; Quik et al., 2000; Skoubis et al., 2006; L. W. Swanson et al., 1987)
	M	.	.	.			
	P	.	.	.	++	++	
Muscarinic (mostly m2 subtype)	A	.	++	++	■	■	(Gundlach, 1991) (Levey et al., 1991; Wamsley et al., 1981)
	M	.	+++	++	.	.	
	P	++	++	++	++	++	
Muscarinic m3 receptors	A	+	+++	++	■	■	(Zubieta & Frey, 1993)
	M	+	+++	++	+	+	
	P						

Note. ■ *= anatomical division is non-existent at this level; . = little detected; + =small amount; ++ = medium amount; +++ = large amount; A = anterior/rostral; M = medial/intermediate; P = posterior/caudal.*

Catecholamines The catecholamines dopamine, adrenaline and noradrenaline (and their receptors) are more highly concentrated in the PAG/DR region than any other midbrain region (see Table 2.23). While the dorsal portions of the PAG show relatively high concentrations of dopamine and noradrenaline compared to other midbrain regions, these concentrations are much higher in the ventral region and in the DR (Palkovits & Jacobowitz, 1974; Versteeg et al., 1976). Adrenergic and noradrenergic medullary afferents preferentially target the ventral part of the PAG, especially at the rostral level (Herbert & Saper, 1992a; Kwiat & Basbaum, 1990), while dopaminergic cell bodies are found in the ventral region of the PAG (Benarroch et al., 2009; Flores, El Banoua, Galan-Rodriguez, & Fernandez-Espejo, 2004; Flores, Galan-Rodriguez, Ramiro-Fuentes, & Fernandez-Espejo, 2006; J. Lu, Jhou, & Saper, 2006) and the DR (Unguez & Schneider, 1988), but not the dorsal regions.

While dopaminergic D1 and D2 receptors are more common in the telencephalon than in most mesencephalic structures (Camps, Kelly, & Palacios, 1990; Gehlert & Wamsley, 1985), only D2 receptors appear to be functionally present in the dorsolateral PAG, where they mediate defense-like behaviors (G. H. Fletcher & Starr, 1987), while D1 receptors present in the ventral region of the PAG exclusively modulate nociception (Flores et al., 2004; Meyer, Morgan, Kozell, & Ingram, 2009).

A1 and A2 adrenergic receptors are found in the ventral and ventrolateral columns of the PAG and respond in similar ways to adrenergic stimulation (Vaughan, Bandler, & Christie, 1996). These A1 and A2 receptors are also present in the DR, and the ionic mechanism through which noradrenaline excites these cells is similar to the mechanism in the ventrolateral PAG (Pan, Grudt, & Williams, 1994).

Table 2.23. Concentrations of Catecholaminergic Cell Bodies, Axonic Processes and Receptors in the PAG/DR Region, at Anterior, Medial and Caudal Levels

		DM	DL	L	VL	DR	References
Adrenaline/ Noradrenaline Cell Bodies	A	.	.	.	■	■	(Poitras & Parent, 1978; L. W. Swanson & Hartman, 1975)
	M	.	.	.	.	.	
	P	.	.	.	.	.	
Dopamine Cell Bodies	A	.	.	.	■	■	(Meyer et al., 2009; Shimada et al., 1976; L. W. Swanson, 1988)
	M	.	.	.	.	.	
	P	.	.	.	+	.	
Adrenaline/ Noradrenaline Fibers and Terminals	A				■	■	(Herbert & Saper, 1992b; L. W. Swanson & Hartman, 1975; Ungerstedt, 1971)
	M	.	.	.	+++	++	
	P	.	.	+	+++	++	
Dopamine Fibers and Terminals	A	.	.	++	■	■	(Herbert & Saper, 1992b; L. W. Swanson, 1988; Ungerstedt, 1971)
	M	.	.	++	+++	++	
	P	.	.	+	++	++	
Adrenaline alpha 1 receptors	A	.	.	.	■	■	(Day, Campeau, Watson, & Akil, 1997; Pieribone, Nicholas, Dagerlind, & Hokfelt, 1994)
	M	.	.	.	.	++	
	P	.	.	.	.	+++	
Adrenaline alpha 2 receptors	A	.	.	.	■	■	(A. P. Nicholas, V. Pieribone, & T. Hokfelt, 1993a)
	M	.	.	.	.	.	
	P	.	.	+	.	.	
Adrenaline beta 1 receptors	A	.	.	.	■	■	(A. P. Nicholas, V. A. Pieribone, & T. Hokfelt, 1993b; Rainbow, Parsons, & Wolfe, 1984; Wanaka et al., 1989)
	M	.	.	.	.	+	
	P	.	.	.	.	+	
Adrenaline beta 2 receptors	A	.	.	.	■	■	(Nicholas et al., 1993b; Rainbow et al., 1984)
	M	.	.	.	.		
	P	.	.	.	.	+	
Dopamine D1 receptors	A	.	.	.	■	■	(Boyson, McGonigle, & Molinoff, 1986; Weiner et al., 1991)
	M	.	.	.	.	.	
	P	.	.	.	.	.	
Dopamine D2 receptors	A	++	++	++	■	■	(Yokoyama, Okamura, Nakajima, Taguchi, & Ibata, 1994)
	M						
	P	++	++	++	++	+++	

Note. ■ *= anatomical division is non-existent at this level; . = little detected; + =small amount; ++ = medium amount; +++ = large amount; A = anterior/rostral; M = medial/intermediate; P = posterior/caudal.*

Histamine Reports have shown that histamine cells in the midbrain and pons are present during rodent embryonic development, but absent after birth and into maturity (Karlstedt, Nissinen, Michelsen, & Panula, 2001; Nissinen & Panula, 1995). This is true for the PAG, where histaminergic cells do not exist in the mature rodent (Steinbusch, 2009; Watanabe et al., 1984).

The distribution of different subtypes of histaminergic receptors in the PAG is summarized in Table 2.24. The PAG shows a relatively high number of histaminergic receptors, approaching the density of some hypothalamic nuclei (Pollard, Moreau, Arrang, & Schwartz, 1993; Taylor et al., 1972). The role of these receptors in the PAG seem to be centered on vocal control (Jurgens & Lu, 1992; C. L. Lu & Jurgens, 1993), as they do not appear to affect panic-like behaviors (Santos, Huston, & Brandao, 2000) and only have a secondary function in controlling nociception (Thoburn, Hough, Nalwalk, & Mischler, 1994).

Table 2.24. Concentrations of Histaminergic Cell Bodies, Axonic Processes and Receptors in the PAG/DR Region, at Anterior, Medial and Caudal Levels

		DM	DL	L	VL	DR	References
Cell Bodies	A	.	.	.	■	■	(Steinbusch, 2009; Watanabe et al., 1984)
	M	.	.	.	.	.	
	P	.	.	.	.	.	
Fibers and Terminals	A	.	.	++	■	■	(Panula, Pirvola, Auvinen, & Airaksinen, 1989; Watanabe et al., 1984)
	M	++	++	++	++		
	P	.	+	++	++	++	
H1 receptors	A	.	.	.	■	■	(Palacios, Wamsley, & Kuhar, 1981)
	M	.	.	.	.		
	P	.	.	.	.	++	
H2 receptors	A	+	+	+	■	■	(Honrubia, Vilaró, Palacios, & Mengod, 2000; Traiffort et al., 1992; Vizuete et al., 1997)
	M	+	+	+	+	+	
	P	+	+	+	+	++	
H3 receptors	A	+	++	++	■	■	(Pillot et al., 2002; Pollard et al., 1993)
	M	++	++	++	++	+	
	P	++	++	++	++	+	

Note. ■ *= anatomical division is non-existent at this level; . = little detected; + =small amount; ++ = medium amount; +++ = large amount; A = anterior/rostral; M = medial/intermediate; P = posterior/caudal.*

Substance P Substance P is a neurotransmitter present in the brain and spinal cord, where it is known to be involved in pain signaling. In the PAG/DR, substance P is generally uniformly present throughout the rostral-caudal extension, as shown in Table 2.25.

While cell bodies expressing substance P are seen throughout the PAG/DR complex, they appear to be slightly more numerous dorsally at the intermediate level and sparser in the VLPAG and DR. Moving posteriorly, however, substance P-positive cells become more concentrated in the VLPAG and DR (R. P. Liu & Swenberg, 1988; Moss & Basbaum, 1983b).

Although the midbrain region is broadly innervated by substance P fibers and terminals, the PAG/DR can be clearly delineated from its neighboring regions by the pattern of its substance P innervation. In the rostral PAG, substance P processes are more concentrated in the PAG than in the surrounding reticular formation or the deeper layers of the superior colliculus. This pattern persists through the mid and caudal PAG/DR, whereas no significant labeling is seen on surrounding areas like the inferior colliculus (Ljungdahl, Hokfelt, & Nilsson, 1978; Moss & Basbaum, 1983b).

Rostrally, substance P receptors are more densely concentrated in the dorsal portions of the PAG, although, ventrally from the aqueduct, a number of cells within the Edinger-Westphal nucleus also show heavy labeling. More posterior to that, around the midway length of the PAG/DR complex at the level of the middle superior colliculus, concentrations are balanced throughout the radial subdivisions both dorsally and ventrally. Finally, on the caudal extreme, the balanced labelling continues, clearly limited to the PAG/DR only, with neighboring regions like the dorsal tegmental nucleus showing no labeling (Beaujouan, Torrens, Saffroy, & Glowinski, 1986; R. P. Liu & Swenberg, 1988; Mantyh, Hunt, & Maggio, 1984; Rothman, Herkenham, Pert, Liang, & Cascieri, 1984).

Table 2.25. Concentrations of Substance P Cell Bodies, Axonic Processes and Receptors in the PAG/DR Region, at Anterior, Medial and Caudal Levels

		DM	DL	L	VL	DR	References
Cell Bodies	A	++	++	++	■	■	(R. P. Liu & Swenberg, 1988; Moss & Basbaum, 1983b)
	M	++	+++	++	+	+	
	P	++	+	++	++	++	
Fibers and Terminals	A	++	++	++	■	■	(Ljungdahl et al., 1978; Moss & Basbaum, 1983b)
	M	++	++	++	++	++	
	P	++	++	++	++	++	
non-specific receptors	A	+++	+++	++	■	■	(Beaujouan et al., 1986; R. P. Liu & Swenberg, 1988; Mantyh et al., 1984; Rothman et al., 1984)
	M	+++	+++	++	++	++	
	P	++	++	++	+++	++	

Note. ■ *= anatomical division is non-existent at this level; . = little detected; + =small amount; ++ = medium amount; +++ = large amount; A = anterior/rostral; M = medial/intermediate; P = posterior/caudal.*

Serotonin Table 2.26 presents the pattern of serotonergic cell bodies, axonic processes and receptors in the PAG/DR region. The DR is the main site of serotonin, or 5-hydroxytryptamine (5-HT), input to the forebrain and has the largest concentration of serotonergic cell bodies within the PAG/DR complex (Bjorklund, Falck, & Stenevi, 1971). Although many serotonergic cells can also be found in the ventrolateral PAG, especially caudally (Clements, Beitz, Fletcher, & Mullett, 1985; Takeuchi, Kimura, & Sano, 1982), no 5-HT cell bodies are seen in the dorsal divisions of the PAG.

There are serotonergic processes in all the subdivisions of the PAG, but the highest concentrations are in the ventral divisions, with an increase towards the caudal portion of the PAG. This increase in 5-HT concentration towards posterior positions only happens ventrally, with dorsal regions retaining a low level of serotonergic fibers (Clements et al., 1985; Gioia, Tredici, & Bianchi, 1983; Steinbusch, 1981).

The 5-HT_{1A} receptor subtype is present in all divisions of the PAG and DR, although greater numbers are seen in more ventral regions (Pompeiano, Palacios, & Mengod, 1992). A reverse pattern of distribution is observed with the 2A subtype, with the lateral column of the PAG having higher immunoreactivity than the other subdivisions (Appel et al., 1990; Cornea-Hebert,

Riad, Wu, Singh, & Descarries, 1999; Griffiths & Lovick, 2002; Morilak, Garlow, & Ciaranello, 1993; Pazos, Cortes, & Palacios, 1985).

Investigations around dysfunctions related to 5-HT tend to focus on the VLPAG and DR (de Paula Soares & Zangrossi, 2009; Deakin; Graeff, Guimaraes, De Andrade, & Deakin, 1996), as these regions have the largest populations of neurons supplying 5-HT to the forebrain.

Table 2.26. Concentrations of Serotonergic Cell Bodies, Axonic Processes and Receptors in the PAG/DR Region, at Anterior, Medial and Caudal Levels

		DM	DL	L	VL	DR	References
Cell Bodies	A	.	.	.	■	■	(Behzadi et al., 1990; Clements et al., 1985; Di Carlo, Hubbard, & Pate, 1973; Hubbard & Di Carlo, 1974; Leger, Charnay, Dubois, & Jouvet, 1986; Y. Q. Li, Zeng, Dong, Rao, & Shi, 1991; Pin, Jones, & Jouvet, 1969; Poitras & Parent, 1978; Steinbusch, 1981; Takeuchi et al., 1982)
	M	.	.	.	++	+++	
	P	.	.	.	++	+++	
Fibers and Terminals	A	++	++	++	■	■	(Steinbusch, 1981)
	M	++	++	++	+++	+++	
	P	+	+	+	+++	+++	
1A receptors	A				■	■	(Pompeiano et al., 1992)
	M	+	+	++	++	+++	
	P	+	+	++	++	+++	
2A receptors	A	+	+	++	■	■	(Appel et al., 1990; Cornea-Hebert et al., 1999; Griffiths & Lovick, 2002; Morilak et al., 1993; Pazos et al., 1985)
	M	+	+	++	+	+	
	P	+	+	+	+	+	

Note. ■ *= anatomical division is non-existent at this level; . = little detected; + =small amount; ++ = medium amount; +++ = large amount; A = anterior/rostral; M = medial/intermediate; P = posterior/caudal.*

Encephalin, endorphin and opioid receptors

The distribution of endogenous opioid cell bodies, axonic processes and receptors in the PAG is displayed in Table 2.27. No cell bodies express endorphins in the PAG or DR (Bloom, Battenberg, Rossier, Ling, & Guillemin, 1978; Weber & Barchas, 1983; Weber, Roth, & Barchas, 1982), but all subdivisions of the PAG and DR have neurons positive for encephalin.

Rostrally, the proportion of encephalin cells is higher at dorsal levels in the DMPAG and DLPAG; ventrally, this pattern shifts in that cells are more numerous at ventral levels in the VLPAG and DR (Khachaturian, Lewis, & Watson, 1983; Moss, Glazer, & Basbaum, 1983; Murakami, Okamura, Yanaihara, Yanaihara, & Ibata, 1987; Uhl, Goodman, Kuhar, Childers, & Snyder, 1979).

The pattern of innervation of encephalin fibers is less distinct than cell body distribution. Processes are fairly evenly distributed in medium-to-high numbers throughout the PAG and DR (Khachaturian et al., 1983; Moss et al., 1983; Murakami et al., 1987; Sar, Stumpf, Miller, Chang, & Cuatrecasas, 1978; Simantov, Kuhar, Uhl, & Snyder, 1977).

In the brain, delta opioid receptors are concentrated in the forebrain and cortex (Sharif & Hughes, 1989), while other regions, including the PAG and DR, show little-to-no receptor binding or mRNA expression (Allen et al., 1993; Mansour, Khachaturian, Lewis, Akil, & Watson, 1987; Peckys & Landwehrmeyer, 1999; Sharif & Hughes, 1989; Waksman, Hamel, Fournie-Zaluski, & Roques, 1986). Mu opioid receptor mRNA, however, is present in large amounts in all subdivisions of the PAG and DR, although this does not necessarily correspond to sites of receptor binding (Mansour, Fox, Thompson, Akil, & Watson, 1994). One possible explanation for this is that while mu receptor synthesis occurs locally at the level of the soma, the receptor is transported through axons to efferent terminals in distant locations. This hypothesis is supported by the finding that delta opioid receptors in the rat spinal cord are mostly on the presynaptic terminals of cells (Cheng et al., 1995) and that receptor binding is reduced in efferent sites to a lesion (Lamotte, Pert, & Snyder, 1976).

The PAG has a known role in regulating nociception in animals, and is the target of deep brain stimulation treatments for chronic pain in human patients. Higher levels of endorphins can be detected in the ventricular fluid of patients undergoing pain-reducing PAG stimulation, and this reduction in nociception can be counteracted by naloxone administration (Hosobuchi, Rossier, Bloom, & Guillemin, 1979). Even the analgesic effects generated by other structures, like the amygdala, can be hampered by the blockade of PAG opioid receptors (Pavlovic, Cooper, & Bodnar, 1996). This opioid control of pain in the PAG is by the ventral, not dorsal, PAG (Nichols, Thorn, & Berntson, 1989).

The involvement of opioid systems in the PAG goes beyond pain control, however. For instance, the antagonism of mu-receptors in the area can combat the panicolytic effects of fluoxetine (Roncon et al., 2012), and can regulate GABAergic availability and neurotransmission (Vaughan, Ingram, Connor, & Christie, 1997), as well as other emotional

responses mediated by the PAG (De Luca-Vinhas, Macedo, & Brandao, 2006; McNally, Pigg, & Weidemann, 2004; Roncon et al., 2013).

Table 2.27. Concentrations of Endogenous Opioid Cell Bodies, Axonic Processes and Receptors in the PAG/DR Region, at Anterior, Medial and Caudal Levels

		DM	DL	L	VL	DR	References
Endorphins Cell Bodies	A	.	.	.			(Bloom et al., 1978; Weber & Barchas, 1983; Weber et al., 1982)
	M	.	.	.	.	.	
	P	.	.	.	.	.	
Encephalin Cell Bodies	A	+++	+++	.			(Khachaturian et al., 1983; Moss et al., 1983; Murakami et al., 1987; Uhl et al., 1979)
	M	++	+	++	+++	+++	
	P	.	++	++	+++	+++	
Endorphins Fibers and Terminals	A	++	++	++			(Fallon & Leslie, 1986; Weber & Barchas, 1983)
	M	++	++	++	++	++	
	P	++	++	++	++	++	
Encephalin Fibers and Terminals	A	+++	++	.			(Khachaturian et al., 1983; Moss et al., 1983; Murakami et al., 1987; Sar et al., 1978; Simantov et al., 1977)
	M	++	++	+	+++	+++	
	P	+++	+++	++	++	+++	
Mu receptors	A	+	+++	+			(Allen et al., 1993; Gutstein, Mansour, Watson, Akil, & Fields, 1998; Herkenham & Pert, 1982; Mansour et al., 1994; Mansour et al., 1987; Moskowitz & Goodman, 1985; Sharif & Hughes, 1989; Waksman et al., 1986)
	M						
	P	+	++	+	+	+	
Delta receptors	A	.	.	.			(Allen et al., 1993; Mansour et al., 1987; Peckys & Landwehrmeyer, 1999; Sharif & Hughes, 1989; Waksman et al., 1986)
	M	.	.	.	.		
	P	.	.	.	.	.	
Kappa receptors	A	.	+	.			(Gutstein et al., 1998; Mansour et al., 1987; Unterwald, Knapp, & Zukin, 1991)
	M						
	P	+	+	+	++	++	

Note. ■ *= anatomical division is non-existent at this level; . = little detected; + =small amount; ++ = medium amount; +++ = large amount; A = anterior/rostral; M = medial/intermediate; P = posterior/caudal.*

Orexin Orexin is a recently-discovered neuropeptide known to be synthesized by a group of cells in the hypothalamus (hence its alternative name, *hypocretin*). Its pattern of distribution is summarized in Table 2.28. Despite being concentrated in populations of cells limited to the lateral, dorsomedial and a few selected other hypothalamic nuclei, orexin fibers project widely to different parts of the central nervous system, from cortical areas through to the brainstem and medulla, including the PAG/DR (Nambu et al., 1999; Sakurai et al., 1998). Of note, the PAG/DR is very strongly targeted when compared to surrounding structures, such as the superior colliculus and reticular formation, which display much sparser orexin terminals.

Fibers from the hypothalamus terminating in the periaqueductal region demonstrate no special pattern of concentration, with all columns of the PAG and DR showing dense labeling from orexin fibers (Nambu et al., 1999). Exceptions to this localized orexin distribution are the median raphe, located ventrally to the PAG/DR, and the locus coeruleus, located caudally to the PAG/DR. Both regions receive strong orexinergic projections and could be part of a functional system with the PAG/DR.

Table 2.28. Concentrations of Orexin Cell Bodies, Axonic Processes and Receptors in the PAG/DR Region, at Anterior, Medial and Caudal Levels

		DM	DL	L	VL	DR	References
Cell Bodies	A	.	.	.	■	■	(Nambu et al., 1999; Sakurai et al., 1998)
	M	.	.	.	.	.	
	P	.	.	.	.	.	
Fibers and Terminals	A	+++	+++	+++	■	■	(Nambu et al., 1999)
	M	+++	+++	+++	+++	+++	
	P						
OX1 receptors	A	.	.	++	■	■	(Marcus et al., 2001)
	M						
	P	.	.	.	.	++	
OX2 receptors	A	.	.	.	■	■	(Marcus et al., 2001)
	M						
	P	.	.	+	.	+++	

Note. ■ *= anatomical division is non-existent at this level; . = little detected; + =small amount; ++ = medium amount; +++ = large amount; A = anterior/rostral; M = medial/intermediate; P = posterior/caudal.*

Orexin was initially discovered to be involved in hunger and food-seeking behavior, as orexinergic cells are located in regions of the hypothalamus classically associated with food intake. The name thus originates from the Greek word for appetite, *orexis*. While the DR mediates certain aspects of feeding and appetite, and these are modulated by 5-HT (P. J. Fletcher & Coscina, 1993), the PAG could mediate changes in motivational states related to feeding. For instance, the PAG is involved in switching from passive behaviors to active ones, such as hunting and foraging (M. O. Klein et al., 2014; Mota-Ortiz, Sukikara, Felicio, & Canteras, 2009; Sukikara, Mota-Ortiz, Baldo, Felicio, & Canteras, 2006). Further putative roles for orexin that could involve the PAG include arousal, reward seeking and processing (Brisbare-Roch et al., 2007; Harris & Aston-Jones, 2006), and the mediation of sleep/wakefulness (Sakurai, 2005).

Orexin is also able to exert nociceptive control of pain. It dampens the tail flick response in rats when injected in the spinal theca, and has the same efficacy as morphine when injected intravenously (Yamamoto, Nozaki-Taguchi, & Chiba, 2002). This mechanism is independent of the opioid system, as these effects are not antagonized by naloxone (Bingham et al., 2001). While the hypothalamus is capable of generating orexin-mediated nociception, orexin blockade in the PAG neutralizes hypothalamic-generated analgesia (Esmaeili, Reisi, Ezzatpanah, & Haghparast, 2016), indicating that the PAG exerts strong influence over the hypothalamus in this regard.

Cannabinoids

Cannabinoid receptors in the brain are involved in the mediation of the psychotropic effects of Cannabis, mostly through the CB1 receptor. As shown in Table 2.29, the concentration of endocannabinoid receptors in the PAG/DR increases in the caudal aspect (Herkenham, Lynn, de Costa, & Richfield, 1991; Herkenham, Lynn, Johnson, et al., 1991; Matsuda, Bonner, & Lolait, 1993; Tsou, Brown, Sanudo-Pena, Mackie, & Walker, 1998).

Table 2.29. Concentrations of Endocannabinoid Receptors in the PAG/DR Region, at Anterior, Medial and Caudal Levels

		DM	DL	L	VL	DR	References
CB1 receptors	A				■	■	(Moldrich & Wenger, 2000)
	M	++	++	++	+	.	
	P						
CB2 receptors	A	.	.	.	■	■	(Gong et al., 2006)
	M						
	P						
non-specific receptors	A	+	+	+	■	■	(Herkenham, Lynn, de Costa, et al., 1991; Herkenham, Lynn, Johnson, et al., 1991; Matsuda et al., 1993; Tsou et al., 1998)
	M						
	P	+++	+++	++	++	++	

Note. ■ *= anatomical division is non-existent at this level; . = little detected; + =small amount; ++ = medium amount; +++ = large amount; A = anterior/rostral; M = medial/intermediate; P = posterior/caudal.*

Cholecystokinin

Table 2.30 shows the pattern of Cholecystokinin (CCK) cell bodies and axonic processes in the PAG/DR complex. CCK is a hormone originally isolated from the gastrointestinal tract, where it initiates enzymatic secretion in the pancreas and contraction in gall bladder muscles. More recently, CCK has been located in the brain, where its distribution is widespread. Systemic administrations of CCK can promote satiety in rats, while antagonism of CCK receptors in the brain annuls the satiety effect of the hormone (Dourish, Rycroft, & Iversen, 1989).

Synaptic terminals and populations of cell bodies expressing CCK are present in the VLPAG and DR (H. Liu et al., 1994; Loren, Alumets, Hakanson, & Sundler, 1979). CCK molecules can act through GABA and opioid receptors (Wiesenfeld-Hallin, de Arauja Lucas, Alster, Xu, & Hokfelt, 1999) and GABAergic agonists are capable of antagonizing the central effects of CCK (Bradwejn & Demontigny, 1985), indicating a central role for this molecule in regulating panic and anxiety reactions in the PAG (Y. Li & Han, 1989).

Indeed, it appears that CCK facilitates panic-like reactions at the PAG level and also peripherally, with one potentiating the other: intravenous CCK administration can induce panic attacks in both humans (de Montigny, 1989) and animals (Bradwejn, Koszycki, & Shriqui, 1991), and local injections of the peptide in the dorsal PAG in animal models seem to either

facilitate the panicogenic effects of local injections of excitatory amino acids (Mongeau & Marsden, 1997) or have direct panicogenic effects that are blocked by local administration of CCK antagonists (Zanoveli, Netto, Guimaraes, & Zangrossi, 2004).

Table 2.30. Concentrations of CCK Cell Bodies and Axonic Processes in the PAG/DR Region, at Anterior, Medial and Caudal Levels

		DM	DL	L	VL	DR	References
CCK Cell Bodies	A	.	.	+			(Loren et al., 1979)
	M	.	.	.	++	++	
	P	.	.	.	++	++	
CCK Fibers and Terminals	A	+	+++	+			(H. Liu et al., 1994; Loren et al., 1979)
	M	+	+++	+	+	+	
	P	+	+++	+	+	+	

Note. ■ *= anatomical division is non-existent at this level; . = little detected; + =small amount; ++ = medium amount; +++ = large amount; A = anterior/rostral; M = medial/intermediate; P = posterior/caudal.*

Glycine

Glycine is a neurotransmitter with inhibitory properties at the brainstem and spinal cord, and its distribution in the PAG/DR is presented in Table 2.31. Glycine fibers are seen in all columns of the PAG, although they are comparatively underrepresented at the DLPAG (Rampon, Luppi, Fort, Peyron, & Jouvet, 1996). Receptors, however, are absent from most of the PAG at the rostral level, but become more widespread through all columns on the caudal aspect (Zarbin, Wamsley, & Kuhar, 1981).

Glycenergic inputs to the medulla are capable of regulating both vascular (Blessing & Reis, 1983; Guertzenstein & Silver, 1974) and cardiac (Ezure, Tanaka, & Kondo, 2003) changes at local GABA receptors. These effects could be at least partially mediated through glycine cell bodies present at the LPAG and VLPAG (Rampon et al., 1996), given that the LPAG and VLPAG target the ventrolateral medulla (Carrive, 1991; Henderson et al., 1998; Van Bockstaele et al., 1991).

Table 2.31. Concentrations of Glycine Cell Bodies, Axonic Processes and Receptors in the PAG/DR Region, at Anterior, Medial and Caudal Levels

		DM	DL	L	VL	DR	References
Glycine Cell Bodies	A	.	.	++			(Rampon et al., 1996)
	M	.	.	++	++	.	
	P	.	.	+	++	.	
Glycine Fibers and Terminals	A						(Rampon et al., 1996)
	M	++	+	+++	+++	++	
	P						
Glycine receptors	A	.	.	+			(T. Araki et al., 1988)
	M						
	P	++	++	++	++	++	

Note. ■ *= anatomical division is non-existent at this level; . = little detected; + =small amount; ++ = medium amount; +++ = large amount; A = anterior/rostral; M = medial/intermediate; P = posterior/caudal.*

Corticotropin releasing factor

Corticotropin releasing factor (CRF) is a peptide central in the signaling pathways that influence the cascade of stress responses in the body. Cells that release CRF are heavily concentrated in hypothalamic regions, although sizeable populations exist in other sites like the amygdala and the PAG (see Table 2.32).

The ventral PAG contains CRF cells in the lateral column, ventrolateral column and in the dorsal raphe (Merchenthaler, Vigh, Petrusz, & Schally, 1982; Olschowka, O'Donohue, Mueller, & Jacobowitz, 1982). Local axonic processes, though, appear to be segmented more dorsally, mostly at the DLPAG and LPAG, with only a smaller volume at the VLPAG (Olschowka et al., 1982). The CRF fibers at the PAG mostly originate from hypothalamic and amygdalar sites (Gray & Magnuson, 1992).

Table 2.32. Concentrations of Corticotropin Releasing Factor (CRF) Cell Bodies and Axonic Processes in the PAG/DR Region, at Anterior, Medial and Caudal Levels

		DM	DL	L	VL	DR	References
CRF Cell Bodies	A	.	.	+	■	■	(Merchenthaler et al., 1982; Olschowka et al., 1982)
	M	.	.	+	+	.	
	P	.	.	+	+	+	
CRF Fibers and Terminals	A	.	++	++	■	■	(Olschowka et al., 1982)
	M	.	++	++	.	.	
	P	.	++	++	+	.	
Somatostatin Cell Bodies	A	.	.	.	■	■	(Finley, Maderdrut, Roger, & Petrusz, 1981)
	M	.	.	.	++	++	
	P						

Note. ■ *= anatomical division is non-existent at this level; . = little detected; + =small amount; ++ = medium amount; +++ = large amount; A = anterior/rostral; M = medial/intermediate; P = posterior/caudal.*

Neurotensin

The peptide neurotensin, which has a proposed modulatory influence over dopaminergic systems, is present in the human and monkey PAG as one of the most concentrated regions for neurotensin in the midbrain and brain stem (Cooper, Fernstrom, Rorstad, Leeman, & Martin, 1981; Kataoka, Mizuno, & Frohman, 1979). As seen in Table 2.33, neurotensin fibers are evenly distributed over all subdivisions of the mammalian PAG/DR (Jennes, Stumpf, & Kalivas, 1982; Mai, Triepel, & Metz, 1987), while cells are present mostly within the VLPAG and DR, and are known to project to the magnus raphe (Beitz, Shepard, & Wells, 1983).

Centrally administered neurotensin provokes a series of autonomic changes in the rat, including sedation and reduced locomotion. Neurotensin administration in the PAG generates nociception that is dependent on the median raphe but not dependent on opioidergic systems (Al-Rodhan et al., 1991; Behbehani & Pert, 1984). In vitro studies show that neurotensin exerts its effects in the PAG through complex interactions with other receptor systems: while neurotensin release can be induced by opioids (Stiller, Gustafsson, Fried, & Brodin, 1997), its mechanism of action appears to be the inhibition of GABA neurotransmission, which is achieved through the release of glutamate-induced endocannabinoids that bind to the CB1 receptor (Mitchell, Kawahara, & Vaughan, 2009).

Table 2.33. Concentrations of Neurotensin Cell Bodies, Axonic Processes and Receptors in the PAG/DR Region, at Anterior, Medial and Caudal Levels

		DM	DL	L	VL	DR	References
Neurotensin Fibers and Terminals	A	++	+	++	■	■	(Jennes et al., 1982; Mai et al., 1987)
	M	++	++	++	++	++	
	P	++	++	++	++	++	
Neurotensin Cell Bodies	A	.	.	.	■	■	(Beitz, Shepard, et al., 1983; Jennes et al., 1982; Mai et al., 1987)
	M	.	+	.	++	+	
	P	.	.	.	++	++	
Neurotensin receptors (non-specific)	A	+	+++	++	■	■	(Moyse et al., 1987)
	M	+	+++	+	+		
	P	+	+++	+	+	++	

Note. ■ *= anatomical division is non-existent at this level; . = little detected; + =small amount; ++ = medium amount; +++ = large amount; A = anterior/rostral; M = medial/intermediate; P = posterior/caudal.*

Relaxin

Relaxin was first discovered as a peripheral hormone secreted by the reproductive system, capable of inducing changes related to pregnancy and menstrual cycles. Relaxin-3, a variant of the hormone, has since been confirmed to be present in the brain. The locus of synthesis for relaxin in the CNS is the nucleus incertus (NI), a diminutive structure caudal to the PAG/DR, at the floor of the 4th ventricle (Bathgate et al., 2002; Burazin et al., 2002; C. Liu et al., 2003). The NI has widespread efferents, spanning most of the forebrain and midbrain (Goto et al., 2001; Olucha-Bordonau et al., 2003).

Table 2.34 summarizes the distribution of relaxinergic processes and receptors in the PAG/DR. Relaxin fibers originating from the NI are found in high volume across the rostro-caudal extent of all PAG/DR subdivisions (Ma et al., 2007; Ma, Sang, Lanciego, & Gundlach, 2009; Smith et al., 2010). Meanwhile, RXFP-3 relaxin receptors are concentrated in the DLPAG and VLPAG, although they are also found in other PAG/DR subdivisions (Smith et al., 2010).

The relaxin system appears to modulate a wide array of emotional, defensive and cognitive aspects of brain function. In rats, systemic antagonism of the relaxin brain receptor is anxiolytic and antidepressant (Ryan et al., 2013), while agonism induces feeding (Calvez, Lenglos, de Avila, Guevremont, & Timofeeva, 2015). In the amygdala, relaxin impairs emotional conditioning (Ma et al., 2005), and NI lesions impair extinction of fear conditioning (Pereira et

al., 2013). NI neurons induce hippocampal theta when stimulated, and also increase their firing rate when hippocampal theta is evoked by reticular stimulation (Nunez, Cervera-Ferri, Olucha-Bordonau, Ruiz-Torner, & Teruel, 2006). Furthermore, the endogenous release of relaxin at the medial septum enhances spatial learning while at the same time promoting hippocampal theta (Ma, Olucha-Bordonau, et al., 2009), while inhibition of NI neurons blocks spatial learning (Nategh, Nikseresht, Khodagholi, & Motamedi, 2015). The modulatory properties of the relaxin system is long-ranging: NI relaxin cells fire in the presence of CRF (Ma, Blasiak, Olucha-Bordonau, Verberne, & Gundlach, 2013) and in turn are capable of changing firing patterns in the medial PFC (U. Farooq et al., 2013).

Table 2.34. Concentrations of Relaxinergic Axonic Processes and Receptors in the PAG/DR Region, at Anterior, Medial and Caudal Levels

		DM	DL	L	VL	DR	References
Relaxin Fibers and Terminals	A	++	++	++	■	■	(Ma et al., 2007; Ma, Sang, et al., 2009; Smith et al., 2010)
	M	+	+++	+	+++	+	
	P	+++	++	++	+++	+++	
Relaxin Receptors	A	+	+++	+	■	■	(Smith et al., 2010)
	M	+	+++	+	+++	+	
	P	+	+	+	+	++	

Note. ■ *= anatomical division is non-existent at this level; . = little detected; + =small amount; ++ = medium amount; +++ = large amount; A = anterior/rostral; M = medial/intermediate; P = posterior/caudal.*

2.3. Functions within the PAG

The anatomy reviewed so far suggests that there should be considerable functional differentiation of the PAG/DR complex. In this section, I discuss the evidence for functional differentiation not only between the dorsal and ventral parts of the PAG/DR complex, but also along its anterior-posterior axis and between its internal and external portions. The new divisions of the PAG introduced in Section 2.6 account for the distinct functionality of these areas.

Given the PAG's phylogeny and well-conserved state among species, it has long been known as a region that mediates behavioral and autonomic flight-or-fight responses during close-proximity aversive scenarios, and the electrical or chemical stimulation of the PAG is a well-established model for studying panic attacks in animals. Electric stimulation of the PAG in human patients produces an array of symptoms and signs similar to a patient suffering a panic attack; and panic disorder patients show structural and biochemical abnormalities in midbrain structures, including the PAG (see Del-Ben and Graeff (2009) for a review on the subject). Pharmacological interventions known to be effective in treating panic-related symptoms in the clinic, like the administration of 5-HT selective drugs, reduce the responses provoked by PAG electrical or chemical stimulation (Jenck, Moreau, & Martin, 1995). Furthermore, patients diagnosed with panic disorder or with a history of panic attacks are sensitive to panic attacks induced by challenges like the inhalation of carbon dioxide (CO_2) or intravenous infusion of sodium lactate and potassium cyanide, and these challenges also facilitate the production of escape reactions from PAG electrical stimulation in rats (Schimitel et al., 2012).

Prior to the 1980s, the PAG was considered functionally homogenous. However, with the subsequent division of the PAG into columns, each with their own properties, attention shifted to how distinct parts of the PAG are responsible for different *types* of behavioral and autonomic responses – see, for example, S. P. Zhang, Bandler, and Carrive (1990); and reviews by Shipley, Ennis, Rizvi, and Behbehani (1991); Carrive (1993) and Bandler and Shipley (1994).

An early dichotomy in PAG function came from the distinct autonomic responses and defensive scenarios provoked by activation of the dorsal versus ventral extremes of the PAG. Activation of ventral PAG elicits passive behavioral states, including immobility, cataplexy, bradycardia, hypotension and opioid-mediated analgesia. Activation of dorsal PAG, however, elicits active reactions more related to fight/flight, namely vigilance, hyperactivity to stimuli, tachycardia, hypertension and non-opioid analgesia.

To make sense of this dichotomy when discussing the functions of the PAG, defensive distance (R.J. Blanchard, Flannelly, & Blanchard, 1986) must be taken into account. When a threat is imminent and clear (e.g. a rat detecting a cat about to pounce, or a person noticing a snake at close proximity), the PAG will be involved in organizing the defensive response. In contrast, the PAG has no involvement (or only plays a secondary role) in less threatening scenarios where the danger is remote or unclear (e.g. a rat detecting the smell, but not the presence, of a cat, or a person seeing a suspicious figure on the other side of the street).

As discussed in Chapter 1, the elegant evolutionary explanation is that animals resort to active strategies, such as running or fighting, to survive close-proximity threats, while the adaptive response to uncertain or distant threats distant is to freeze, as a reduction in motor activity will decrease the likelihood of detection while the animal can assess the situation further. However, defensive distance alone is insufficient to explain mobility and immobility in laboratory manipulations, and I argue that the animal's assessment of their likelihood of successful escape influences their response to a great extent.

Consider the following two scenarios, and how the escapability of the situation influences the defensive response. In the first scenario, a rat is placed in a small, closed box that has previously been associated with an aversive stimulus. The rat will freeze, even though no actual threat is present, indicating that the animal is reacting to a *potential* (distant) threat. However, when given the opportunity to remove itself from the box by being given access to a separate chamber, it will choose to escape instead, engaging in more active types of defensive and risk assessment behaviors, such as crouch-sniff and stretch postures (Viellard, Baldo, & Canteras, 2016). In contrast, now consider the second scenario in which a rat has been placed in a sealed enclosure with a real predator: an *actual* (proximal) threat. If the rat knows that a way out from danger is possible (say, through a small passage that leads to a hiding burrow), it will remove itself from the area by escaping (or first fighting and then escaping). However, if the rat knows that escape is not possible, then it will resort to an acute state of immobility, called quiescence, to avoid detection. During this state, animals reduce their autonomic responses to such an extent that they become unresponsive to external stimuli. The most extreme case of this passive defensive state is known as tonic immobility or *thanatosis* (Arduino & Gould, 1984), in which animals 'play dead' and stop responding to predator probes and attacks entirely. In some species the behavior includes mimicking death though body posture or the release of putrid scents.

While not always successful, this strategy is adaptive as a last resort, as it may provide the prey with an opportunity to escape. In the same way that animals constantly monitor their environment while freezing due to distant threats, animals engaging in tonic immobility also

monitor their environment and can become mobile when escape is judged possible (Arduino & Gould, 1984). Considering that some predators have no interest in pursuing dead prey and others might shift their attention to other priorities if they perceive their prey to be defeated, an animal using tonic immobility as a defense mechanism at least has a chance of successfully evading their predator.

Thus it is clear that, alongside defensive distance, the *escapability* of the environment is highly influential on the animal's chosen survival strategy. In this section, I thus consider experimental data in light of both of these factors, as they activate distinct circuits within the PAG.

2.4. The dorsal-ventral axis

In broad terms, the dorsal aspects of the PAG are involved in the *production* of different classes of behavior, while the ventral PAG *inhibits* responsiveness to stimuli (see Figure 2.3 and Table 2.35).

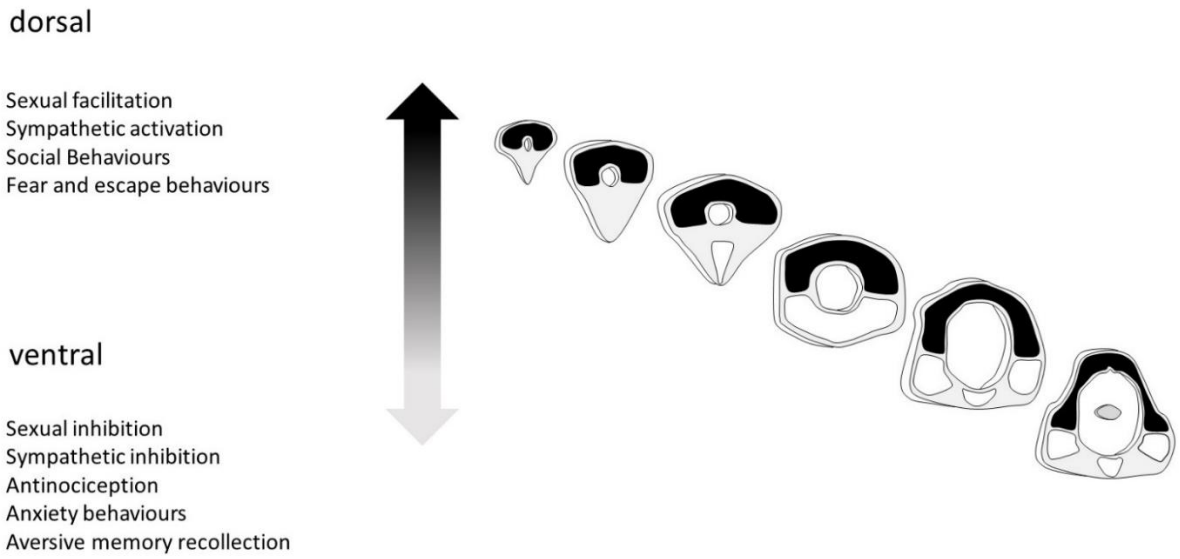

Figure 2.3. The predominant, contrasting functions of the dorsal and ventral PAG.

Lordosis is the curvature of a female rodent's spine, produced in the presence of a desired male. PAG lesions can reduce (or completely abolish) lordosis, particularly when located in the dorsal PAG (Sakuma & Pfaff, 1979b), indicating that this region is crucial in the production of

this behavior. Activation of the ventral PAG, on the other hand, inhibits lordosis (Arendash & Gorski, 1983).

In social encounters, aggression towards a conspecific is more easily elicited from dorsal rather than ventral stimulation (Depaulis, Bandler, & Vergnes, 1989). The flight response seen during encounters with proximal dangers can only be induced from stimulation of the dorsal PAG (Carrive, 1993). Furthermore, escape behavior produced by the elevated T-Maze (ETM, an ethological model of fear), labels more cells in the dorsal PAG in c-Fos experiments (Leite Silveira, Zangrossi Jr, de Barros Viana, Silveira, & Graeff, 2001), as does escape provoked by a blast of ultrasonic sound (Neophytou et al., 2000). Similarly, while hypoxia can cause vigorous escape responses, in vitro studies show that dorsal cells are more responsive to low levels of oxygen than ventral cells (Kramer, Nolan, & Waldrop, 1999).

When faced with an inescapable threat, the best defensive strategy for a rat is quiescence or tonic immobility. It needs to remain still and decrease the probability of being detected: in other words, to reduce its movement, reduce its response to stimuli, and decrease nociception - in anticipation of injury. Excitatory amino acid (EAA) injections in the ventral part of the PAG produce immobility and unresponsiveness (Bandler & Depaulis, 1991), reduce blood pressure (Carrive, 1993) and increase analgesia (Besson, Fardin, & Oliveras, 1991; Fardin, Oliveras, & Besson, 1984). In addition, responses to aversive conditioned memories of an inescapable environment seem to be dependent on the ventral PAG as well, as lesions (Leman, Dielenberg, & Carrive, 2003; Vianna, Graeff, Landeira-Fernandez, & Brandao, 2001) and opioid blockade (Grahn, Maswood, McQueen, Watkins, & Maier, 1999) in the ventral region disrupt conditioned responses, while dorsal interventions do not.

Table 2.35. Functions of the Dorsal and Ventral Extremes of the PAG/DR

Function	Dorsal role	Ventral role	Paradigm	Description	References
Sexual (activation)	Yes	no	Stimulation	Lordosis	(Sakuma & Pfaff, 1979b)
	More	less	Lesion	Lordosis	
Sexual (inhibition)	no	Yes	Stimulation	Lordosis	(Arendash & Gorski, 1983)
Social	More	less	Stimulation	Aggressive behaviour towards conspecific	(Depaulis et al., 1989)
Sympathetic (activation)	Yes	no	EAA	Increase in arterial blood pressure	(Carrive, 1993)
	More	less	Electrophysiology	Neurons responsive to hypoxic states in vitro	(Kramer et al., 1999)
Fear	Yes	no	Stimulation	Flight response	(Carrive, 1993)
	More	less	c-Fos	Encounter with predator	(Canteras & Goto, 1999)
	More	less	c-Fos	Escape behaviour in an ethological model of panic (ETM)	(Leite Silveira et al., 2001)
	More	less	c-Fos	Escape elicited by ultrasonic sound	(Neophytou et al., 2000)
Sympathetic (inhibition)	no	Yes	EAA	Decrease in arterial blood pressure	(Carrive, 1993)
Nociception (inhibition)	no	Yes	Opioid Blockade	Opioid-dependent analgesia	(Nichols et al., 1989)
	no	Yes	Stimulation	Pure analgesia without elicitation of active behaviours	(Besson et al., 1991)
Anxiety	less	More	EAA	Immobility by localized injection	(Bandler & Depaulis, 1991)
Memory Recollection	no	Yes	Lesion	Reduction in conditioned freezing	(Leman et al., 2003)
	no	Yes	Opioid Blockade	reduction in expression of conditioned fear	(Grahn et al., 1999)

2.5. The anterior-posterior axis

The anterior and posterior portions of the PAG show distinct functional properties, including differential control of reproductive traits, maternal behavior and other social and defensive responses (summarized in Figure 2.4 and Table 2.36).

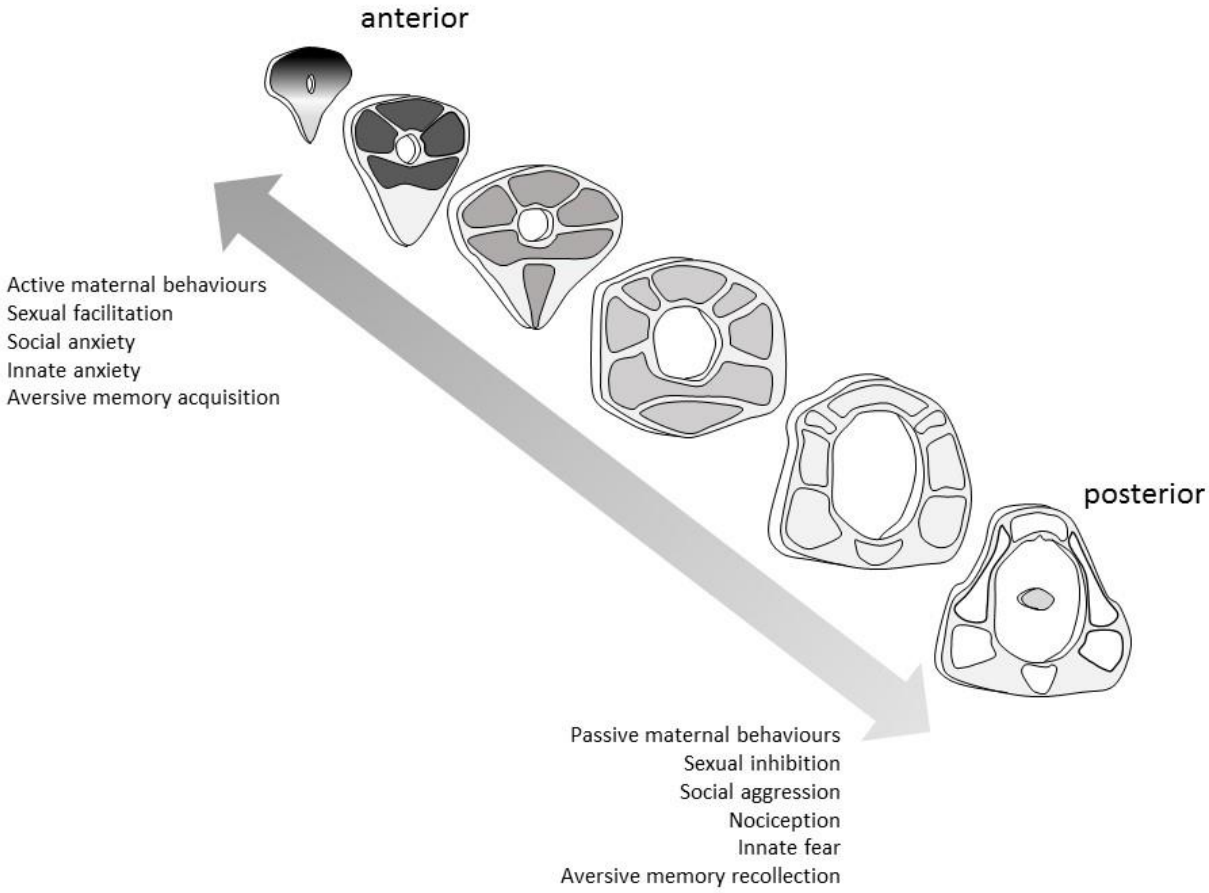

Figure 2.4. The predominant functions of the anterior and posterior PAG.

Lordosis in female rats is more strongly elicited from the anterior parts of the PAG (Sakuma & Pfaff, 1979a), indicating that this portion of the PAG has a role in controlling receptiveness to a partner in copulation. Stimulation of the posterior part, however, inhibits lordosis (Arendash & Gorski, 1983).

Active maternal functions, such as retrieval and licking of pups, are more strongly correlated with the anterior PAG, while passive maternal behaviors like kyphosis (a curvature of the spine presented along with stillness to facilitate nursing) is mediated by the posterior PAG. For example, c-Fos experiments demonstrate stronger labeling in anterior PAG cells after dams actively interact with pups (Lonstein & Stern, 1997a), and lesions of the anterior PAG reduces dam nursing behavior (Sukikara et al., 2006). Meanwhile, the kyphotic posture is

correlated with more c-Fos labeling in the posterior parts of the PAG, and destruction of this region reduces kyphosis more (Lonstein & Stern, 1998).

The role of the PAG in feeding is not well defined. Early studies with animals sustaining midbrain lesions show that destruction of parts of the PAG does not significantly affect feeding (Lyon, Halpern, & Mintz, 1968; Parker & Feldman, 1967). A more recent report, however, showed that muscimol injections in the anterior PAG greatly reduced feeding (Tryon & Mizumori, 2018).

Social behaviors also vary across the anterior-posterior PAG axis. During a social interaction test in which an animal is exposed to a conspecific, kainic acid injections in the anterior PAG lead to the production of strong avoidance behaviors, such as backing away, while injections in the posterior PAG lead to strong escape behaviors, such as running and jumping (Depaulis, Keay, & Bandler, 1992). Furthermore, these behaviors are accompanied by corresponding, specialized vocalizations: anterior stimulation produces vocalizations related to social separation (Kyuhou & Gemba, 1998), while posterior activation evokes vocalizations related to social aggression (Depaulis et al., 1992).

The anterior PAG is associated with freezing, as c-Fos labelling is stronger here when the animal is faced with an inescapable threat, such as a predator (Canteras & Goto, 1999), or a stimulus related to a predator like the scent of a cat (Dielenberg, Hunt, & McGregor, 2001). In contrast, the posterior PAG is more strongly associated with escape behaviors seen during aversive encounters that are more proximal and certain, such as actual attack by a predator. Electrical stimulation of the posterior PAG produces fight or flight (Bandler & Depaulis, 1991), and the inhalation of CO_2 or intravenous injection of potassium cyanide elicit strong escape responses in the rat and concomitantly generate more c-Fos labeling in caudal regions of the PAG (Muller et al., 2017). Similarly, NADP-h activity is stronger in the posterior PAG after a noxious visceral stimulation (Rodella, Rezzani, Agostini, & Bianchi, 1998).

The anterior PAG plays an important role in the acquisition of conditioned fear, while the posterior PAG is involved in its expression. This can be seen through interventions where NMDA blockade in the anterior part of the PAG disrupt the *acquisition* of Pavlovian conditioning to an aversive stimulus, while NMDA blockade in the posterior part disrupts the *expression* of conditioned responses (Souza & Carobrez, 2016). Additional support to this notion comes from c-Fos experiments, which demonstrate that the posterior PAG is more selectively labeled after the expression of conditioned responses (Carrive, Leung, Harris, & Paxinos, 1997).

Table 2.36. Functions of the Anterior and Posterior Extremes of the PAG/DR.

Function	Anterior role	Posterior role	Paradigm	Description	References
Maternal (active)	Strong	weak	c-Fos	Active maternal behaviours (retrieval, licking)	(Lonstein & Stern, 1997a)
	Strong	weak	Lesion	Active maternal behaviours (retrieval, licking)	(Lonstein & Stern, 1998)
Sexual (activation)	Strong	weak	Stimulation	Lordosis facilitation	(Sakuma & Pfaff, 1979a)
Maternal (passive)	weak	Strong	c-Fos	Passive maternal behaviours (kyphosis immobility)	(Lonstein & Stern, 1997b)
	no	Strong	GABAa	Passive maternal behaviours (kyphosis immobility)	(Salzberg, Lonstein, & Stern, 2002)
	no	Strong	Lesion	Passive maternal behaviours (kyphosis immobility)	(Lonstein & Stern, 1998)
Sexual (inhibition)	weak	Strong	Stimulation	Lordosis inhibition	(Arendash & Gorski, 1983)
Social Anxiety	Strong	weak	Stimulation	Social separation vocalizations	(Kyuhou & Gemba, 1998)
	Strong	weak	KA injection	Social avoidance	(Depaulis et al., 1992)
Social Aggression	weak	Strong	KA injection	Social aggression vocalizations	(Depaulis et al., 1992)
	weak	Strong	KA injection	Social escape	(Depaulis et al., 1992)
Anxiety	Strong	no	Stimulation	Freezing	
	Strong	weak	c-Fos	Freezing to predator presence	(Canteras & Goto, 1999)
	Strong	weak	c-Fos	Freezing to exposure to cat odour	(Dielenberg et al., 2001)

Table continued on following page.

(Table 2.36, continued)

Memory Acquisition	Strong	weak	NMDA blockade	Acquisition of aversive classical conditioning	(Souza & Carobrez, 2016)
Nociception	weak	Strong	NADPH-d activity	Noxious visceral stimulation	(Rodella et al., 1998)
Fear	weak	Strong	Stimulation	escape response	(Bandler & Depaulis, 1991)
	no	Strong	c-Fos	Escape to i.v. potassium cyanide or inhaled CO_2	(Muller et al., 2017)
Memory recollection	weak	Strong	c-Fos	Expression of aversive classical conditioning	(Carrive et al., 1997)
	weak	Strong	NMDA blockade	Expression of aversive classical conditioning	(Souza & Carobrez, 2016)

2.6. The interior-exterior axis

The dorsal part of the PAG has traditionally been split into three subdivisions based on function and anatomy: the DMPAG, DLPAG and LPAG (see Table 2.37 for a list of functions). Despite these anatomical separations, a big functional overlap exists across these regions, and many opposing emotional states can be elicited from these areas. While behaviors associated with negative emotions (e.g. fight or flight, social aggression and anxiety) are linked to the dorsal PAG, so too are positively-valenced expressions of sexual receptivity and maternal behavior. In this Chapter, I proposed new internal and external subdivisions for the DLPAG and LPAG. In this functional section, I show experimental evidence that reconciles anatomy with functional specificity. Figure 2.5 summarizes these new divisions, and Tables 2.38 and 2.39 list the functional and anatomical features that distinguish these subdivisions apart.

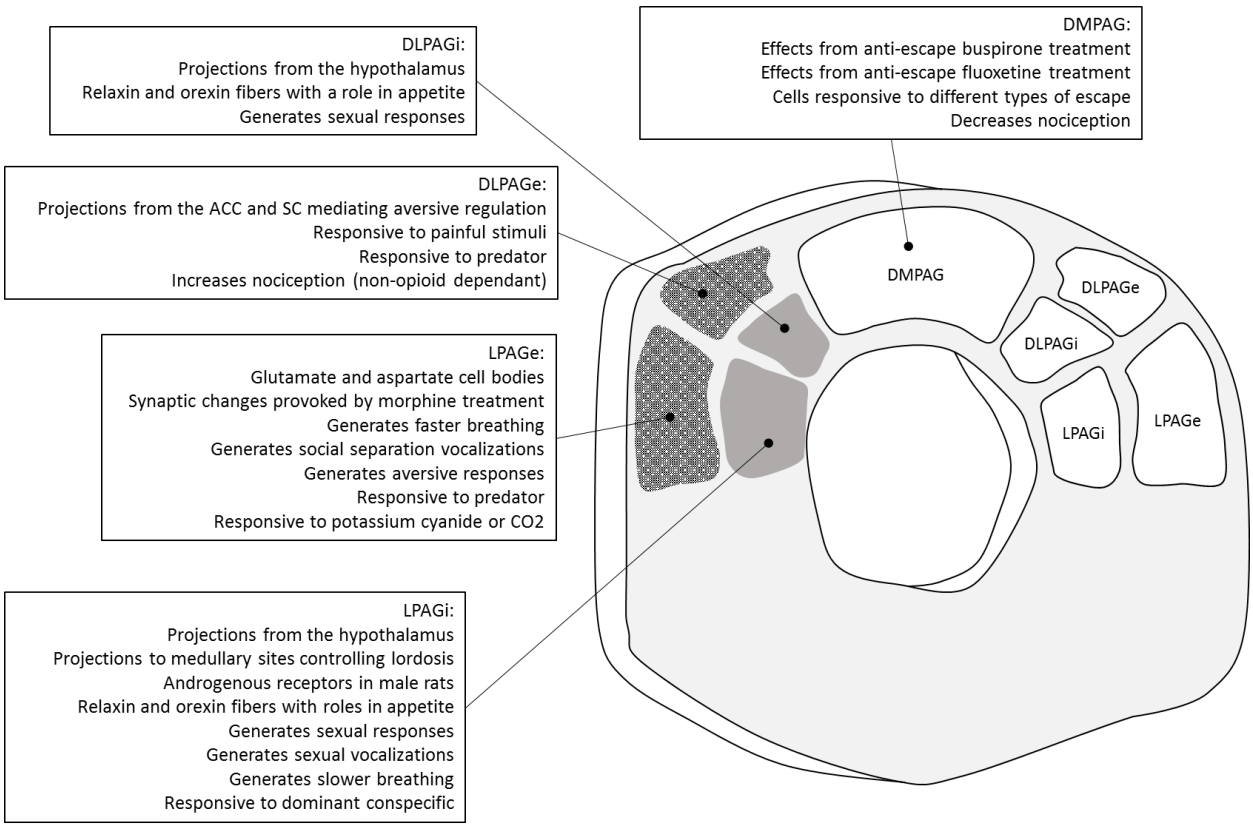

Figure 2.5. The predominant and unique functions and characteristics of the DMPAG and the proposed internal and external subdivisions of the DLPAG and LPAG.

The interior regions of the LPAG and DLPAG are specialized for sexual and social encounters. In male rats, androgen receptors are exclusive to the interior LPAG (Murphy & Hoffman, 2001), and the LPAGi contains cells that project to the nucleus retroambiguus, a region with known involvement in producing lordosis (Vanderhorst, Terasawa, Ralston, & Holstege, 2000). While stimulation of the LPAGi and DLPAGi elicits lordosis in female rats (Ogawa, Kow, McCarthy, Pfaff, & Schwartz-Giblin, 1991), the LPAGi also elicits vocalizations related to sexual courtship (Kyuhou & Gemba, 1998) and slows breathing (Subramanian, Balnave, & Holstege, 2008). In general, the LPAGi seems to be more involved in mediating social interactions than the other regions, as c-Fos labeling in rats is more prominent in this area after social encounters with dominant conspecifics (Motta et al., 2009). In contrast, the external components of the PAG are more strongly correlated with negotiating aversive encounters and pain. Stimulation of the LPAGe generates distress vocalizations (Kyuhou & Gemba, 1998; Subramanian et al., 2008) and faster breathing (Subramanian et al., 2008), and c-Fos labeling is more prominent in the LPAGe after aversive challenges, like forced swimming (Bellchambers, Chieng, Keay, & Christie, 1998), and after flight responses provoked by inhalation of CO_2 or intravenous injection of potassium cyanide (Muller et al., 2017). In

addition, c-Fos labelling is stronger in the DLPAGe of rodents that receive a painful deep muscle stimulus (Keay & Bandler, 1993) or exposure to a cat (Canteras & Goto, 1999), and systemic morphine injections only reduce GABA release in the LPAGe, not the LPAGi (Renno, Mullett, & Beitz, 1992).

Table 2.37. Functions of the Columns of the Dorsal PAG.

Function	Description	DMPAG Role	DLPAG Role	LPAG Role	Paradigm	References
Stress	Forced restraint	Strong	weak	weak	c-Fos	(Lino-de-Oliveira, Sales, Del Bel, Silveira, & Guimaraes, 2001)
Anxiety	Freezing caused by GABAergic blockade in the superior colliculus	Strong	no	no	c-Fos	(Borelli, Ferreira-Netto, & Brandao, 2006)
	Reduction of exploration of open arms in the EPM	Strong	no	no	CRF	(Borelli & Brandao, 2008)
	Defensive behaviours (stretching, flat-back posture)	Strong	no	no	CRF	(Borelli & Brandao, 2008)
Fear	Escape caused by an airjet	Strong	weak	no	c-Fos	(Salchner & Singewald, 2002)
	Escape caused by GABAergic blockade in the superior colliculus	Strong	weak	no	c-Fos	(Borelli et al., 2006)
Fear / 5-HT / 5-HT-1A	Reduction in c-FOS expression after escape caused by an airjet in animals treated w/ fluoxetine	Yes	no	no	c-Fos	(Salchner & Singewald, 2002)
	Acute buspirone	Strong	weak	no	c-Fos	(Lim et al., 2008)
	Chronic buspirone	Yes	no	no	c-Fos	(Lim et al., 2008)
Sympathetic	Renal sympathetic activity	Yes	Yes	Yes	EAA	(Iigaya, Horiuchi, McDowall, & Dampney, 2010)
	Heart rate	weak	Strong	weak	EAA	(Iigaya et al., 2010)
	Arterial blood pressure	weak	Strong	Strong	EAA	(Iigaya et al., 2010)

Table 2.38. Features and Functions of the Internal and External Subdivisions of the DLPAG.

Feature	Description	DLPAGi	DLPAGe	Paradigm	References
Biochemistry	Substance-P synaptic terminals	Yes	no	-	(Moss & Basbaum, 1983b)
	Relaxin-3 synaptic terminals	More	less	-	(Ma et al., 2007)
	Orexin fibers	Yes	no	-	(Baldo et al., 2003)
	NADPH-d positive cell bodies in the juvenile rat	no	Yes	-	(Iwase et al., 1998)
Anatomy	Projections from the amygdala	Yes	no	-	(Hopkins & Holstege, 1978)
	Projections from the hypothalamus	Yes	no	-	(Vertes & Crane, 1996)
	Projections from the superior colliculus	no	Yes	-	(Graham, 1977)
	Projections from the cingulate cortex	no	Yes	-	(Beckstead, 1979)
Sexual	Lordosis	Yes	no	Stimulation	(Ogawa et al., 1991)
Nociception	Deep muscle noxious stimulus	less	More	c-Fos	(Keay & Bandler, 1993)
Fear	Exposure to a cat	less	More	c-Fos	(Canteras & Goto, 1999)

Table 2.39. Features and Functions of the Internal and External Subdivisions of the LPAG

Feature	Description	LPAGi	LPAGe	Paradigm	References
Biochemistry	Encephalin synaptic terminals	Yes	no	-	(Moss et al., 1983)
	Relaxin-3 synaptic terminals	More	less	-	(Ma et al., 2007)
	Substance-P synaptic terminals	Yes	no	-	(Moss & Basbaum, 1983b)
	Androgen receptors in male rats	Yes	no	-	(Murphy & Hoffman, 2001)
	Reduction on the release of GABA after systemic morphine injection	no	Yes	-	(Renno et al., 1992)
	Glutamaergic and aspartate cell bodies	no	Yes	-	(Clements et al., 1987)
Anatomy	Projections from the hypothalamus	Yes	no	-	(Vertes & Crane, 1996)
	Projections to Nucleus Retroambiguus sites controlling lordosis	More	less	-	(Vanderhorst et al., 2000)
Sympathetic	Slower, shallow breathing (apneusis)	Yes	no	Stimulation	(Subramanian et al., 2008)
	Faster, deep breathing (tachypnea)	no	Yes	Stimulation	(Subramanian et al., 2008)

Table 2.39. continued

Feature	Description	LPAGi	LPAGe	Paradigm	References
Sexual	Lordosis reflex	Yes	no	Stimulation	(Ogawa et al., 1991)
	Vocalizations related to sexual courtship	More	less	Stimulation	(Kyuhou & Gemba, 1998)
Social	Exposure to a dominant conspecific	More	less	c-Fos	(Motta et al., 2009)
Vocal	Neurons that fire during vocalizations	no	Yes	Electrophysiology	(Dusterhoft, Hausler, & Jurgens, 2004)
	Vocalizations	less	More	Stimulation	(Subramanian et al., 2008)
Stress	Vocalizations related to social separation	less	More	Stimulation	(Kyuhou & Gemba, 1998)
	Forced swim	less	More	c-Fos	(Bellchambers et al., 1998)
Fear	Aversive responses	no	Yes	Stimulation	(Ogawa et al., 1991)
	Escape provoked by i.v. potassium cyanide or CO_2	no	Yes	c-Fos	(Muller et al., 2017)
	Exposure to a cat	less	More	c-Fos	(Canteras & Goto, 1999)

2.7. Summary

In this Chapter, I reviewed the anatomy and functions of the PAG and attempted to clear some of the confusions about the region. Also, I attempted to highlight potential functions and roles in which the PAG appears to be significantly involved, although rarely acknowledged in the literature.

The PAG has been traditionally associated with two main phenomena (and both of them quite unpleasant in nature): pain and panic attacks. Although the role of the PAG on these two negative aspects of the mind are undeniable, and investigations on how the PAG manages them yielded strong advancements in our understanding and treatment of these states, this is hardly the whole picture for this region of the brain.

I proposed here that the PAG also has a strong role in regulating appetitive functions, mainly sexual responses, although recent evidence points out to the possibility of its involvement in feeding as well. Based on function, anatomy and biochemistry, I propose here that the dorsolateral and lateral columns of the PAG need to be further subdivided. I propose the existence of internal (i.e. closer to the aqueduct) subdivisions that are functionally and anatomically distinct from the parts that are in the periphery of the PAG.

Clearly, all the hypotheses generated here in this Chapter cannot be tested by a single person, in the short course of his doctoral studies. Many of the appetitive roles of the PAG, its involvement in the pathogenesis of depression, and direct functional proof of the newly suggested subdivisions of the PAG would require more time, expertise and collaborations with different groups than a single PhD project allows to.

In the next Chapters I will try to address at least one of my claims here: that different portions of the PAG in anterior-posterior axis are involved in distinct roles in the motivational spectrum, specially anxiety and panic. At the end of this thesis (Chapter 6) I will return to the ideas presented here in this review, along with the findings from the experimental Chapters, in an attempt to show how these findings impact our understanding of the PAG, the nature of motivational states, and the theories that we build in order to comprehend them. For the moment, however, let us move to the experiments that will tackle a few of the hypothesis and ideas presented in this Chapter.

Chapter 3. General methods

This Chapter summarizes the common methods used to acquire all the experimental data reported in this thesis. Animal housing, handling, surgery, acquisition setup, histological procedures, and data processing were all common across the different experiments. Details regarding the behavioral procedures, electrical stimulation, drug administration and statistical analysis that are unique to each experiment are given separately in each experimental Chapter.

I used two batches of rats in this thesis. The first batch (from now on called Multipolar Batch) was implanted with multi-polar, high-density arrays (28 channels total) and were used to validate the procedures, and to gather baseline LFP data during PAG and RPO stimulation. The second batch of rats (from now on, Bipolar Batch) was implanted with bipolar and tripolar electrodes (8 channels total), and were used to gather PAG and RPO stimulation data and test the intracranial effects of drugs. The bipolar batch matched the multipolar batch in having activity recorded from the left prelimbic cortex (PrL) and the left and right hippocampus (HPC). Also, all animals had bipolar stimulating electrodes implanted in the right reticulus pontis oralis (RPO) and left periaqueductal grey (PAG) and a guide cannula for intracerebral drug injections aimed at the midline nucleus incertus (NI). Drug injections were not carried out through the cannula in the multipolar batch because of the age of the animals after extensive electrical testing.

Animal welfare standards were in accordance with the University of Otago Animal Welfare guidelines; and all the surgical and experimental manipulations were approved by the University of Otago Animal Ethics Committee (protocol numbers AEC 29/12, and AEC 10/16).

3.1. Animal housing, handling

A total of thirty-nine male Sprague-Dawley rats were used in this project (n=29 for multipolar batch, and n=10 for bipolar batch). They weighed between 150-200 gm on arrival. All animals were sourced from the Hercus-Taieri breeding colony of the University of Otago. Upon arriving at the psychology department housing space, rats were paired in cages in order to avoid stress from social isolation, and given ad-libitum access to food and water. Cages were located in a temperature (20-22º C) controlled room, on a 12h light-dark cycle with lights on at 6am. All experimental data were collected during the light period of the cycle.

Before any experimental manipulation, rats were given 10 days to acclimatize to the laboratory, and were handled daily. Weight progression was assessed daily, and after the initial

10 days the animals were scheduled for surgery if body weight had reached a minimum of 300 grams.

3.2. Electrodes

3.2.1. Multipolar arrays

Animals in this batch were implanted in the recording areas described in more detail below (bilateral HPC and left PrL), but with a set of custom-built multipolar arrays. These electrodes were manufactured from insulated nichrome wires (0.001" diameter, California Fine Wire Company, USA). These wires could be arranged in any spacing configuration using our laboratory's novel method for array building. First, a section of 15cm of nichrome wire had its insulation at one of the ends removed by exposing it to a heat gun at 400° C for 30 seconds. This uninsulated part of the wire (around 1.5cm) was then wrapped around a 1cm piece of silver wire. By attaching a heated needle to a stereotaxic arm, small sheets of plastic could be punctured at close spacing (between 200 and 500 µm in this project; see Figure 3.1). The individual nichrome wires were then threaded through the holes. As each wire was threaded, the other end of it that was wrapped around the piece of silver wire was then soldered to a pin in a mini array socket with 32 pins (Ironwood, USA).

After each nichrome wire was threaded through the plastic, the wires were twisted together (Figure 3.2, panel A). A small amount of cyanoacrylate-based adhesive (Loctite 401, UK) was applied to the top side of the plastic sheet where the wires were inserted, and a fine tungsten rod (0.009" gauge) was added in parallel for structural rigidity. After 24 hours to allow curing of the adhesive, the wires on the other side of the plastic sheet were cut with a surgical scalpel and the finished array was unglued from the plastic sheet (Figure 3.2, panel B).

For HPC arrays, eight recording tips were spaced 200 µm apart, in order to cover the dorsal hippocampus in the dorso-ventral axis. For the prefrontal cortex, eleven tips were spaced 500 µm apart in order to cover most of the medial wall of the prefrontal cortex.

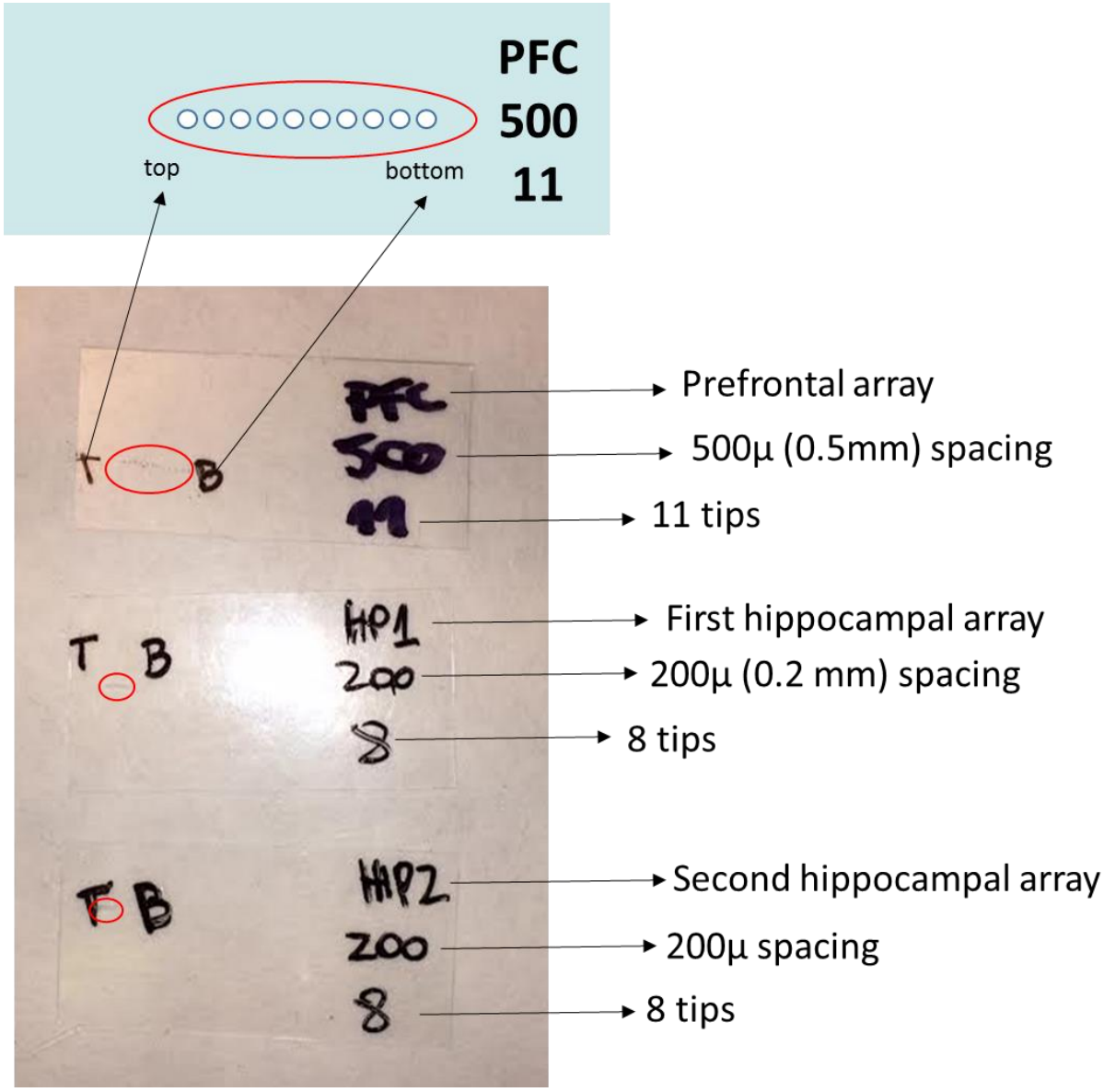

Figure 3.1. Sheets of plastic punctured at different distances for array building. Punctures were made at either 500µ or 200µ distances for prefrontal and hippocampal arrays, respectively. The two hippocampal sheets were the same as each other.

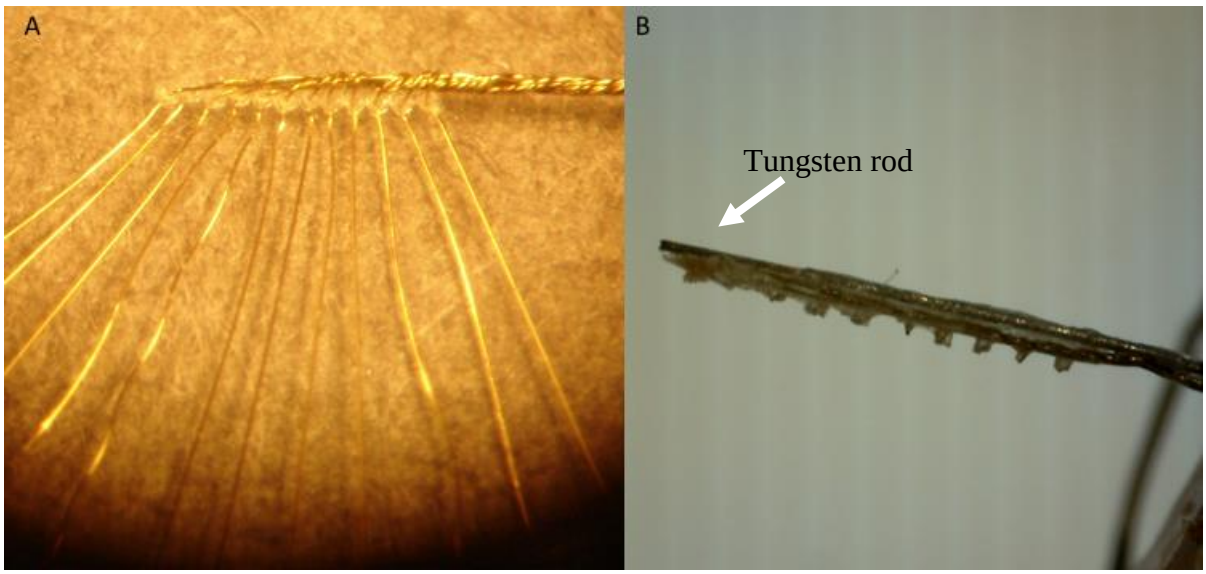

Figure 3.2. A: Nichrome wires threaded through the punctured plastic sheet, and then twisted. B: Finalized PrL array including tungsten rod used to maintain rigidity during implantation.

3.2.2. Bipolar recording

All the recording electrodes for this batch of animals were built from twisted, PFA-insulated stainless steel wires with a 0.005” thickness (AM-Systems, USA). Each of these wires had their ends bared and soldered to male gold pins using phosphoric acid flux. During implantation surgery, these pins were inserted into a McIntyre connector (Molino & McIntyre, 1972).

Recording electrodes for PrL were composed of three stainless steel wires twisted together. Tip separation for this tripolar setup was 1mm, so the three tips would span the whole dorso-ventral height of the PrL and minimize stereotaxic imprecision. Out of the three tips, two of them were selected later in post processing as the bipolar pair for analysis.

Electrodes for the left and right HPC were composed of two twisted wires each, with a tip separation of 0.6mm with one tip aimed at the hippocampal fissure and the other at stratum oriens of CA1.

3.2.3. Ground, reference and stimulating electrodes

For both the multipolar and bipolar batches, signals in the recorded regions were acquired by referencing against a common, distant electrode in the animal's skull. During post-processing, further subtractions between two local signals from each region resulted in a more localized "bipolar” signal, which was used for analysis.

For this common reference, a section of PFA-insulated stainless steel wire had the insulation stripped from each end and one end was then soldered to the head of a jeweler's screw using phosphoric acid flux. During surgery, this screw was fixed to the skull area just behind lambda. The ground wire was a length of bare silver wire (0.005" diameter, AM Systems, USA), and was wrapped around the outside of the implant prior to suturing. Both RPO and PAG stimulating electrodes were composed of the type of insulated bipolar twisted wires described above. Tip separation for both pairs was 0.5mm.

3.3. Surgical methods

All instruments, swabs, towels, etc. were sterilized via autoclave before use and were placed on a sterile field during surgery. Stainless steel screws and electrodes were placed in 70% alcohol for at least 5 hours. All animals received a prophylactic dose of antibiotic treatment (Amphoprim, 30mg/kg), 30 minutes prior to the beginning of surgery.

The multipolar batch of rats in this project was anesthetized for surgery using an injectable solution. Halfway through this project our laboratory surgical suite was updated with a new inhalant anesthetic system, which was used for the animals in the bipolar batch.

The rats operated with injectable anesthesia were given ketamine and medetomidine (75mg/kg and 0.5mg/kg, s.c.) and given additional injections of ketamine if necessary, as determined by toe pinch reflex. As soon as voluntary movement ceased, atropine (0.05mg/kg, s.c.) was administered to reduce the secretion of fluids in the respiratory tract and aid breathing.

For inhalation anesthesia, an isoflurane evaporator (E-Z Anesthesia, USA) was used. Animals were first placed in an induction chamber connected to the machine, until lightly anesthetized for ease of handling, and then removed from the chamber, and administered buprenorphine (0.1mg/kg, s.c.) for additional pain control. While still under anesthesia, the animal's scalp was shaved, rubbed with 70% alcohol and then infiltrated with Marcaine (0.4 ml/kg) and Lidocaine (0.2 ml/kg) subcutaneously. The animal was then moved to the stereotaxic frame; and a breathing cone installed over the nose bar of the stereotaxic frame delivered oxygen mixed with isoflurane at a rate of 1.5 liter/minute. The percentage of oxygen/isoflurane mix was regulated between 2% and 3% depending on the animal's toe-pinch reflex and breathing responses. Then, Tricin (Jurox, Australia) was applied to the animals eyes, which were also covered with a wet cotton pad for protection. The animal's head was then secured to the stereotaxic frame using non-traumatic ear bars, and the tongue was gently pulled out from the mouth to aid breathing.

The animal's scalp was then swabbed with Betadine, and the head and body were covered with a plastic sheet that had been soaked in 70% alcohol for at least 15 minutes and acted as a sterile surgical field. During surgery, all animals rested on a heated pad in order to maintain body temperature.

A single midline incision was made on the scalp through the sterile field. Superficial muscles were pushed to either side with a sterile swab and the surface of the skull scraped clean until the cranial fissures were made visible. The edges of the incision were kept open with skin retractors.

A sterile needle was mounted to the stereotaxic arm, and the dorsal-ventral height of lambda was taken. The needle was then moved forward along the anterior-posterior axis, and placed over bregma. The nose bar height was then adjusted so bregma would be placed on the same level as lambda, achieving the flat-skull position.

After proper placement of the rat in the frame, a dental drill was mounted to the stereotaxic arm, and holes for the electrodes were drilled in the skull. The coordinates for implantation are shown in Table 3.1. For the left dorsal PAG, the stereotaxic arm was placed at a 16 degree angle and, for the nucleus incertus, the stereotaxic arm was positioned at a 10 degree angle and the nose bar was dropped to -12.5mm from horizontal zero, both in order to avoid damage to the blood vessel plexus beneath lambda. The dorsal-ventral coordinates used for implanting the guide cannula (Plastic One, USA) were calculated so the tip would rest 1mm above the NI. A scheme of the implantation is presented in Figure 3.3.

Table 3.1. Coordinates for stereotaxic implantations.

	A-P (reference)		M-L	D-V (skull)	Angle	Nose Bar
Left PrL	+2.76mm	(Bregma)	+0.60mm	-4.50mm	0°	flat skull
Left HPC	-3.8mm	(Bregma)	+2.50mm	-2.90mm	0°	flat skull
Right HPC	-3.8mm	(Bregma)	-2.50mm	-2.90mm	0°	flat skull
Right RPO	-7mm	(Bregma)	-1.60mm	-6.50mm	0°	flat skull
Left dPAG	+1.32mm	(Lambda)	+2.30mm	-4.50mm	16°	flat skull
NI	-2.8mm	(Lambda)	+0.62mm	-5.16mm	10°	-12.5mm

Note: A-P: anterior-posterio; M-L: medial-lateral; D-V: dorsal-ventral; PrL: prelimbic cortex; HPC: hippocampus; RPO: reticular pontis oralis; dPAG: dorsal periaqueductal gray.

After the placement of the holes for the electrodes and the guide cannula, holes for the stainless steel jeweler's screws were drilled. Seven screws were fixed to the edges of the incision in order to secure the electrodes and cannula to the skull. The reference electrode supplied an eighth screw and was fixed posterior and lateral to lambda.

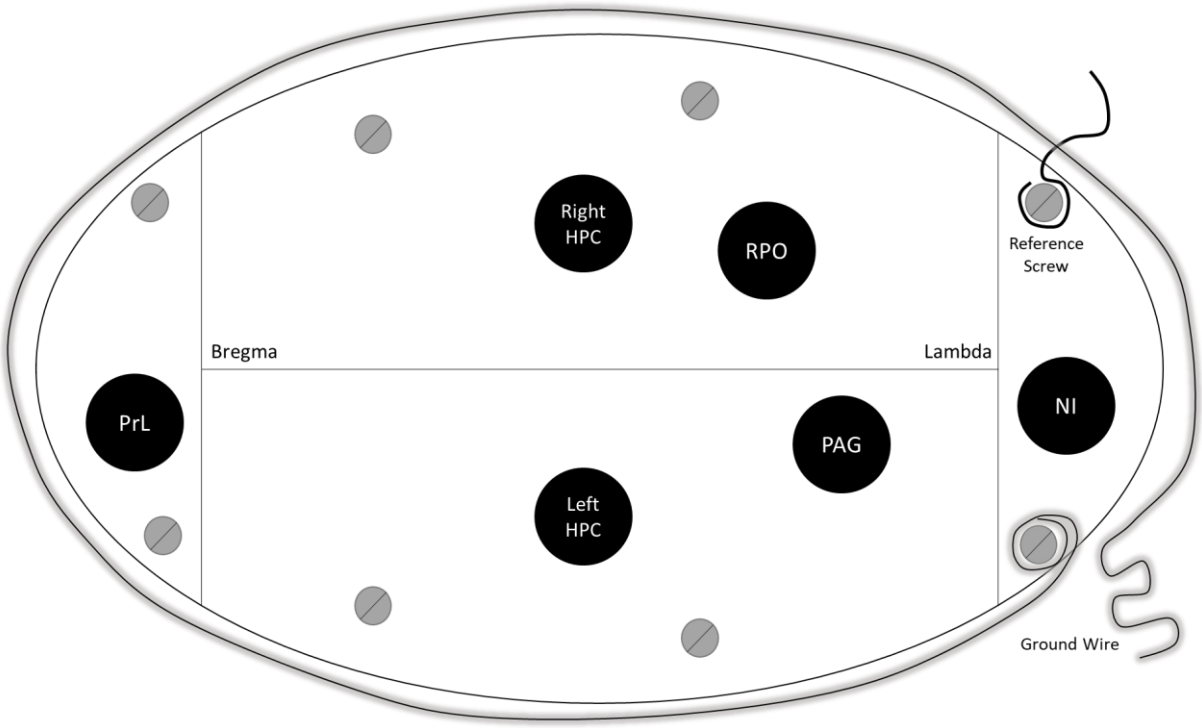

Figure 3.3. Schematic top view of rat's skull during implantation surgery. Placement of structural and reference screws (grey) are displayed, along with craniotomy holes (black) for electrode and cannula implantation. The posterior-most right side screw served as a reference electrode, and the posterior-most right side screw was used to secure the uninsulated silver ground wire.

The electrodes and the cannula were placed over their respective craniotomy sites one at a time, and slowly lowered into the brain. After the electrode or cannula was inserted, dental cement was applied to the site and the electrode was secured to the nearest screw. This process was repeated for each electrode until all of them were in position.

The posterior left screw was left exposed, and the end of a bare silver wire was wrapped to it. Then, the wire was tightly wrapped around the circumference of the incision on the outside of the screws and underneath the skin. Finally, dental cement was applied to the top of the implant to cover all the wires (with the exception of the silver bare wire) and hold the connector on an appropriate position.

For animals that received injectable anesthesia, antisedan (atipamezole, 2.5mg/kg s.c.) was administered at the end to reverse the effects of the medetomidine and speed recovery. For animals that received gas anesthesia, the oxygen/isoflurane was dropped to 0% and animals received pure oxygen for 10 minutes. In both cases, carprofen (5mg/kg, s.c.) was given to relieve post-operative pain. During surgery, 10ml of 0.9% physiological saline was administered s.c. in doses of 2ml in order to maintain hydration.

The animals were then individually housed in a clean cage with free access to food and water. The animal's well-being and recovery were monitored for seven days according to the University of Otago Animal Welfare guidelines using a standard monitoring sheet. After full recovery, rats were grouped back into their original pairs.

3.4. Behavioral apparatus

All animals were tested in a modified operant chamber (width: 24.5cm, height: 18.5cm, depth: 30cm), with its levers, lights and feeding mechanisms removed. All walls were made out of transparent acrylic, except for the back one which was made out of aluminium. This operant box was placed inside a second chamber, which apart from a small hole on the ceiling through which the recording cable ran, was fully sealed from external light and noise. Illumination inside the chamber was provided by a non-aversive red light, and a fan provided air recirculation and background noise. A small video camera inside the larger chamber provided a live video feed for experimenter observation.

Prior to any data collection, for 5 consecutive days, the rats were individually placed inside the observation box and allowed to explore for fifty minutes. Before each exposure, the walls and floor of the observation box were cleaned with a 10% ethanol solution and allowed to dry.

3.5. Electrical stimulation response thresholds

Stimulating currents for the PAG and RPO electrodes were delivered by a custom built, constant current isolated stimulator controlled by custom software programmed in Visual Basic 6. Stimulation was set at 100 Hz with monophasic pulses with a width of 0.1 ms. Trains for the RPO stimulation were set to 1 second duration, and PAG trains were set to 8 seconds maximum duration.

In order to determine the ideal currents necessary to drive the desired responses from the PAG and RPO, rats were tested daily before data acquisition. They were individually placed in the observation chamber, the recording cable attached to their head stage and given 30 minutes to habituate before testing.

First, the current for appropriate RPO responses was established. When animals voluntarily ceased moving, an initial current of 10µA was delivered in a 1-second train. High intensity currents can provoke undesired motor reactions in free moving animals, so during the delivery of the current the animal's behavior and real time LFPs were observed. We defined the ideal response based on repeated stimulation that provoked clear, elicited hippocampal theta from the stimulation train with no evoked motor reactions. If no induced theta or motor reactions were noticed, the stimulating current was increased in 5µA steps until the highest current that caused no motor responses was reached.

Following determination of RPO-stimulation values, the animals were tested for PAG-evoked responses. The goal for the PAG stimulation was to establish the minimum current intensity necessary to induce the emotional response of freezing. Stimulation trains were 8 second long, and the first current was set at 10uA, with increases in 5µA steps until the desired freezing behavior was evoked.

After repeated PAG stimulations at the freezing threshold, RPO stimulations were conducted in order to verify that the desired hippocampal responses were still being elicited. In all cases, the currents established for the RPO-stimulation before PAG activations were still effective in inducing hippocampal theta rhythmicity.

3.6. Data acquisition and processing

Local field potentials were acquired by a Micro1401 (CED, UK) at a sampling rate of 512 Hz. The signal was passed through Grass Model 15 amplifiers, and hardware gain was set at x5,000 for all acquired data. The signals acquired from the recording electrodes were referenced to a recording screw positioned at the posterior part of the rat's skull behind lambda in a zone that is thought to be electrically silent. For data processing, the files were down-sampled to 256 Hz using the in-built cubic spline interpolation in Spike2 (CED, UK), band passed at 2-30 Hz and exported to Matlab (Mathworks, USA).

Referencing from a common, distant electrode has been shown to bias the interpretation of signals and to cause spurious correlations (Lalla, Rueda Orozco, Jurado-Parras, Brovelli, & Robbe, 2017; Shirhatti, Borthakur, & Ray, 2016). In order to minimize this, subtractions of the signal in the PrL and HPC were performed between local pairs of electrodes. Based on the histological reconstruction, the electrodes centered in our regions of interested (left HPC, right HPC and PrL) were re-referenced to their closest neighbor. All data analysis was then performed on the three resulting localized signals from the left HPC, right HPC and PrL.

As described in the acknowledgements section of this thesis, MatLab routines were designed and adapted by Dr Calvin Young. He also advised, supervised and provided training on how to conduct the analysis through a Spike2-MatLab-SPSS workflow. The acquisition, handling and processing of the datasets were done by me under his supervision and guidance.

3.6.1. Spectral analysis

The time-frequency analyses reported here were done with 1-second windows with 50% overlap between them. All spectral analyses were carried out using the multi-taper method, with three tapers and a numerical bandwidth product of 5 using the Chronux package (http://chronux.org/, (Bokil, Andrews, Kulkarni, Mehta, & Mitra, 2010; Mitra, 2007) and with a cut-off frequency set to 30 Hz. For this project, theta was defined as 5 to 10 Hz and z-scored power spectral density for this band was calculated relative to the rest of the frequency spectrum.

3.6.2. Pairwise phase consistency analysis

Supplementary to coherence analysis, pairwise phase consistency analysis (PPC) was also employed in this study. PPC calculates the distribution of the relative angular distances between two Hilbert-transformed signals, and estimates the phase coupling from the two based on the outcome. PPC, similar to coherence and phase-lock value, indicates how much two separate signals are "synchronized" based on the phase of their oscillations. These measures are generally taken to represent an estimation of the degree of relationship between two brain regions. However, unlike spectral coherence or phase-lock value estimates, PPC has been demonstrated to be free of the biases that come from a small number of observations in a sample (Vinck, van Wingerden, Womelsdorf, Fries, & Pennartz, 2010). With this in mind, this thesis uses the more traditional measure of coherence, alongside the PPC measure, to infer the relationship between the neural oscillations of different regions.

3.6.3. Partial directed coherence analysis

To assess the direction of theta modulation between HPC and PrL, we employed the Partial Directed Coherence (PDC) method developed by Baccala and Sameshima (2001) – also see Young and Eggermont (2009) for discussion and used before in our laboratory (Ruan, Young, & McNaughton, 2017; Young, Ruan, & McNaughton, 2017).

3.7. Statistical analysis

For all experiments in this thesis, each measure of interest had their variance distribution analyzed for normality. The r-squareds between the means and the variances of the samples

were calculated, and the data were power transformed when necessary before repeated measures ANOVAs were performed. For the ANOVAs, orthogonal polynomial contrasts were extracted for dimensional factors using SPSS (IBM, USA). The interactions between these contrasts were assessed, and the linear and quadratic components derived, where the significant interactions between the different levels of treatments can be captured by significant polynomial trends. The use of these methods allow for 1 degree-of-freedom contrasts, which prevent the effects of sphericity; 1 degree-of-freedom contrasts are also statistical measures that are recommended in the *Publication Manual of the American Psychological Association* (Kirk, 2013).

For experiments in Chapter 4, the data were arranged to test the hypothesis that our two electric stimulation treatments (PAG and RPO) produce different states from their respective unstimulated periods (sham) and between themselves. Also, we anticipated that measurements in the two hippocampi would be different from the ones in the PrL. Therefore, the contrasts assessed were *PAG/RPO x Stim x Region*, where "PAG/RPO" represents either stimulation of the PAG or stimulation of the RPO, "Stim" represents either real electrical stimulation or sham stimulation, and "region" represent LFP measurements in the two hippocampi and the prelimbic cortex. This model anticipates a significant difference between the states produced by PAG and RPO stimulation, and this would be seen in the form of a linear trend between the two. Likewise, it is expected that the two hippocampi would behave similarly, and the PrL would show different activity from the other two. In this case, a significant quadratic trend between left HPC vs PrL vs right HPC (treated as levels of a dimensional factor) would capture this.

For experiments in Chapter 5, the same general organization of stimulation and LFP regions was followed for hypothesis testing but including also factors related to drug treatments. We tested 4 compounds: CDP, Buspirone, RXFP3-A2, and R3B(1-22)R. We first tested CDP, buspirone and saline. Then, in a separate test, we analyzed RXFP3-A2, R3B(1-22)R and saline. In these statistical tests, the highest level of interaction assessed was *Stim x Drug x Region x Time x Injection*, where "Stim" represents either PAG stimulation, RPO stimulation or Sham stimulation, "Drug" represents saline and two of our experimental compounds, "Region" represents our LFP measurements in the two hippocampi and the prelimbic cortex, "Time" represents one block of time before the injection of drugs and two blocks after, and "Injection" represents animals that received drug injections in two different brain regions. Similar to the arrangement in Chapter 4, a difference between PAG and RPO states would be expected in the form of a linear trend, and hippocampi x PrL differences would be seen in the form of a quadratic trend. For CDP and Buspirone, our hypothesis was arranged to test a quadratic effect

from saline, indicating that both drugs produce the same effects, and the effects are different from saline. If the two compounds have different effects, this would be captured by a linear trend between the two. For RXFP3-A2 and R3B(1-22)R, a linear trend is expected – indicating that the two peptides produce opposing effects. This expectation arises from the two drugs being an agonist and antagonist of the RFXP3 receptor, respectively.

The data and results presented in Chapter 4 come from raw, untransformed values. This was decided once the transformed numbers yielded p-values in the ANOVA that *were not* radically different from the p-values from those for the raw numbers. Therefore, in order to keep interpretation of the numbers easy, the untransformed numbers and their statistical test results are reported there.

For data in the experiments of Chapter 5, we used unchanged raw values following the same logic described above, with the exception of the measures of coherence and PPC. These two variables presented skewed variances, and transformations were used to correct this. For the CDP/Buspirone and relaxin Agonist/Antagonist experiments, coherence was arcsine transformed, and PPC was transformed to the power of 0.12 (1/8 power transform), respectively.

3.8. Histological methods

After all testing was concluded, animals were euthanized with pentobarbitone sodium (100mg/kg, i.p.). A transcardial perfusion was performed with 60ml of 0.9% saline solution, followed by 60ml of a 10% paraformaldehyde solution, followed by 30ml of a 30% sucrose-10% formaldehyde solution for cryoprotection.

Afterwards, the brains were removed and placed in a vial containing 200ml of 10% paraformaldehyde solution, and stored in a cool environment for 24 hours. After this, the liquid was drained and replaced with a 30% sucrose-10% formaldehyde solution for cryoprotection, and left to saturate for five days minimum.

The brains were then blocked and placed on a microtome (Leica 1320, Germany), covered with a cryoprotecting gel (VWR Chemicals, Germany) and frozen with carbon dioxide. The tissue was sectioned at 90µm thickness, and wet mounted on gelatin-coated glass slides. The slides were then left to dry for at least 12 hours before proceeding to staining.

The sections were stained in 1.3% thionin protocol (following an adapted protocol from L.W. Swanson (1992) coverslipped with a mounting medium (DPX, Merck, Germany), and at least 24 hours allowed for drying. The sectioned and mounted slices were then digitized using

a digital macro camera and the photo files were used to reconstruct electrode and cannula placements according to the atlas of Paxinos and Watson (2007).

Chapter 4. Cortico-hippocampal oscillations and interactions during PAG-generated freezing

4.1. Introduction

The PAG is a central locus for the control of aversive and defensive responses (Chapter 2). Stepwise increases in electrical or chemical stimulation of the dorsal PAG evoke a hierarchy of behavioral and autonomic responses like those of animals exposed to predatory threats. At lower levels of stimulation, animals display strong freezing behavior; at higher levels, animals eventually perform an escape response that consists of running and/or jumping, similarly to the response seen in animals that are in close contact with predators (Sudre, de Barros, Sudre, & Schenberg, 1993).

Dorsal PAG *escape* behavior has been extensively studied at the pharmacological level, and it is taken as a reliable proxy for fear responses and panic attacks in animals (Jenck et al., 1995). Dorsal PAG-induced *freezing*, however, has not been much studied. In experiments with rodents, freezing is generally induced by placing animals inside an operant box and delivering small electric foot shocks. After previously experiencing the painful stimulus and not being able to remove themselves from the environment, rats engage in freezing behavior. This freezing (either innate or conditioned) response is generally seen as a measure of anxiety, as it is responsive to anxiolytic drugs (L. H. Conti, Maciver, Ferkany, & Abreu, 1990).

The PAG appears to be part of the networks mediating freezing responses and anxiety. Lesion studies indicate more precisely that destruction of the ventral, but not the dorsal PAG, disrupts conditioned freezing responses (Grahn et al., 1999; Leman et al., 2003). Also, several experiments indicate ventral PAG activation during conditioned freezing responses. Interestingly, however, while destruction of the ventral PAG disrupts conditioned freezing, it does not inhibit freezing elicited by stimulation of the dorsal PAG (Vianna et al., 2001). These indicate that while at the phenomenological level both ventral and dorsal PAG freezing behaviors look similar, their etiology are distinct.

If the ventral, rather than the dorsal PAG, is necessary for conditioned freezing responses, how can dorsal PAG-generated freezing be explained? In one study (Canteras & Goto, 1999), c-Fos labeling indicated strong dorsal PAG activity in rats exposed to a cat. According to the authors “during the 10 min of the predatory encounter, all five animals exposed to the cat expressed a robust freezing response (…) and several episodes of vigorous running and jumping escape behaviours (…)”. Considering that both freezing and escape behaviors happened

concomitantly, it becomes hard to interpret which behavior primarily drove dorsal PAG labelling. Another c-Fos study suffers from the same limitation, in which animals were exposed to cat odor and given the opportunity to escape from the environment of exposure into an enclosed box: animals exposed to the experimental condition escaped more frequently into the hiding place and had more strongly expressed c-Fos in the dorsal PAG (Canteras & Goto, 1999; Dielenberg et al., 2001).

Chapter 2 provides some answers about the nature of dorsal PAG responses. There, I proposed that the anterior PAG is involved in anxiety-like behaviors, related to distal or ambiguous threats, and the posterior PAG is involved in panic-like behaviors, related to immediate and certain threats. Those propositions, while based on reports in the literature, have not been put to direct experimental test.

In animal research, the defining behavioral expression of anxiety is taken to be freezing (immobility). Panic/fear reactions, are taken to be represented by vigorous running and escaping. Whenever an animal is immobile, the dominating circuits producing immobility must also be inhibiting movement; and the same can be said about the circuits producing escape from a threat and at the same time inhibiting immobility systems. As a demonstration of this, experiments shows that conditioned anxiety responses (immobility) inhibit panic-like responses (running) induced by electrical stimulation of the PAG (Magierek, Ramos, da Silveira-Filho, Nogueira, & Landeira-Fernandez, 2003). Also, in humans that suffer from panic disorder, states of relaxation or clinical techniques that cause reductions of anxiety can produce panic attacks (Cohen, Barlow, & Blanchard, 1985; D. F. Klein, 1993; Mellman & Uhde, 1989). Furthermore, in both animals and humans, anxiety enhances pain sensitivity while fear reduces it (Rhudy & Meagher, 2000). These appear to show that anxiety and fear compete and balance each other in order to produce behavior inhibition and activation through different sensory, motivational and cognitive systems in the brain.

In mammals, the occurrence of movement seems to overlap with the occurrence of electrical field oscillations at the theta band in the hippocampus. Early evidence showed that the faster animals move, the faster the frequency and stronger the amplitude of hippocampal theta is (McFarland, Teitelbaum, & Hedges, 1975). The co-occurrence of movement and theta is so ubiquitous that one of the first conceptualizations of hippocampal theta was as a signal of locomotor action and motor planning (see Buzsaki, 2002 for an overview). It was later demonstrated, however, that hippocampal theta can sometimes be absent when animals are engaged in motor activity. As an example, theta does not occur during repetitive, stereotyped behaviors (Kemp & Kaada, 1975). Also, hippocampal theta can occur when animals are

immobile, leading some to the separate theta into two types: type I theta, that appears during movement and is not abolished after administration of atropine; and type II theta, that appears during immobility and in animals under surgical anesthesia, and can be abolished by atropine (Kramis, 1975).

Artificially elicited theta through reticular stimulation does not provoke movement at the appropriate intensity, and is reduced by anxiolytic-only drugs (McNaughton, Kocsis, & Hajós, 2007). This led to the notion that hippocampal theta might also be a neural mechanism subserving anxiety processes (J. A. Gray & N. McNaughton, 2000; McNaughton & Gray, 2000). But theta seems to be related not only to anxiety, but perhaps more generally to the importance (either positive or negative) of relevant stimuli and actions. As demonstrations of this, hunger and food availability (Ford, Bremner, & Richie, 1970; Munn, Tyree, McNaughton, & Bilkey, 2015; Routtenberg, 1968), predator presence (Sainsbury, Heynen, & Montoya, 1987), operant learning (Feder & Ranck, 1973; Lopes da Silva & Kamp, 1969), and novel stimuli (Kemp & Kaada, 1975) generate hippocampal theta. On the other hand, irrelevant stimuli or stimuli that the organism was habituated to (Kemp & Kaada, 1975; Sainsbury, Harris, & Rowland, 1987), already learned and automatic behaviors (Feder & Ranck, 1973) and consummatory acts (Routtenberg, 1968) do not generate theta.

If the circuits commanding panic-like responses, as witnessed at the behavioral level, are in a state of competition with anxiety-like circuits, then the neural signals associated with these states should also show opposing trends. As indicated above, previous research points to increased hippocampal theta rhythm as a potential anxiety signal in the brain. So, stimulation of PAG regions with known involvement in anxiety (namely the anterior portion) should evoke increases and decreases in hippocampal theta. Conversely, stimulation of the regions involved in panic (i.e., more posterior portions) should reduce hippocampal theta.

Both panic- and anxiety-like processes are, however, also orchestrated by cortical regions. Structures in the medial wall of the prefrontal cortex have been implicated in the modulation of basic defensive functions. For instance, the anterior cingulate cortex (ACC) is a node in the pain processing network of the brain, and it has been suggested more specifically as a center responsible for the affective component of painful events (Fuchs, Peng, Boyette-Davis, & Uhelski, 2014; Hsu et al., 2013).

Sitting ventrally to the ACC is the prelimbic cortex (PrL). This cortical division sends strong projections to the PAG and, in return, receives projections from the ventral PAG as well (Chapter 2). The PrL has strong modulatory influence over defensive circuits in the brain,

including influence over the dorsal raphe (DR) which is capable of influencing PAG activity. Disinhibition of the PrL can promote elevations in extracellular 5-HT in the DR, and in turn cause escape responses in the rat (Yamashita, Spiacci, Hassel, Lowry, & Zangrossi, 2017). The PrL is also implicated in the control of conditioned responses. Electrical stimulation of this region increases conditioned responses and prevents animals from extinguishing the acquired association (Vidal-Gonzalez, Vidal-Gonzalez, Rauch, & Quirk, 2006). It has also been proposed that the PrL can modulate short term affective memories and feed this information to the striatum and limbic circuits, greatly modulating emotional processes (Vertes, 2006).

Understanding how different brain structures react dynamically and interact during these states can be important to elucidate the nature of PAG-induced freezing. If the states induced by activation of the PAG are reflective of panic and/or anxiety disorders, then understanding how large assembles of neurons behave during these states should illuminate and broaden our understanding of fear- and panic-generating systems in the brain.

So, it is proposed here that hippocampal theta activity serves as an underlying neural mechanism that allows for the emergence of behaviors, functions and emotional states that require the coordination of large assembles of cell populations in different brain locations. Considering that the PAG-induced freezing state could be an anxiety-like state of conflict, it would be expected that the emergence of this behavior would correlate with enhanced theta oscillations in the hippocampus. But structures like the PrL, on the other hand, can influence subcortical structures like the PAG via the DR, and induce panic responses (i.e. avoidance responses *away* from danger) which are ethologically opposite to conflict-, and anxiety-like freezing.

In this Chapter, I investigate changes in HPC and PrL field potentials during behavioral states induced by PAG stimulation. If hippocampal theta reflects an underlying neural mechanism necessary for the generation of anxiety states, we would expect that increases and decreases in theta activity should reflect increases and decreases in anxiety. In this section, responses to the RPO electrical stimulation method will be used as a comparing tool against the responses produced by electrical stimulation of the PAG.

In this Chapter we will also evaluate if the anterior PAG is capable of generating distinct cortico-hippocampal responses than more caudal portions of the PAG, as predicted by the findings in Chapter 2. Although stimulation of both the anterior and middle PAG is capable of evoking immobility and freezing in the rat, Chapter 2 of this thesis presented anatomical, biochemical and functional evidence that indicates that these two PAG regions are not similar.

Could the freezing behavior elicited by stimulation of different levels of the PAG in the anterior-posterior axis be electrophysiologically different while behaviorally similar?

With these in mind, we anticipate that: 1) middle PAG stimulations, at the freezing threshold, will *reduce* hippocampal and PrL theta power and/or frequency; 2) anterior PAG stimulations, at the freezing threshold, will *increase* hippocampal and PrL theta power and/or frequency and 3) anterior and posterior PAG stimulations will differently affect cortico-hippocampal coherence.

4.2. Methods

For this experiment, ten Sprague-Dawley rats were initially used. Two animals had to be removed from the study due to health complications, and a third one had stimulating electrodes located outside of the regions of interest, making the final number of animals used seven. The housing, surgical, and recording procedures are described in the general methods section in Chapter 3.

4.2.1. Behavioral apparatus

All animals were tested in a modified operant chamber (width: 24.5cm, height: 18.5cm, depth: 30cm), with its levers, lights and feeding mechanisms removed. All walls were made out of transparent acrylic, except for the back one which was made out of aluminium. It was placed inside a second chamber, which apart from a small hole on the ceiling through which the recording cable ran, was fully sealed from external light and noise. Illumination inside the chamber was provided by a non-aversive red light, and a fan provided air recirculation and background noise. A small video camera inside the larger chamber provided a live video feed for experimenter observation.

Prior to any data collection, for 5 consecutive days, the rats were individually placed inside the observation box and allowed to explore for fifty minutes. Before each exposure, the walls and floor of the observation box were cleaned with a 10% ethanol solution and allowed to dry.

4.2.2. Electrical stimulation response thresholds

In order to determine the ideal currents necessary to drive the desired responses from the PAG and RPO, rats were tested daily before data acquisition. They were individually placed in the observation chamber, the recording cable attached to their head stage and given 30 minutes to habituate before testing.

First, the current for appropriate RPO responses was established. When animals voluntarily ceased moving, an initial current of 10μA was delivered in a 1-second train (the parameters for

the stimulation are detailed in the methods section of Chapter 3). High intensity currents can provoke undesired motor reactions in free moving animals, so during the delivery of the current the animal's behavior and real time LFPs were observed. We defined the ideal response based on repeated stimulation that provoked clear, elicited hippocampal theta from the stimulation train with no evoked motor reactions. If no induced theta or motor reactions were noticed, the stimulating current was increased in 5μA steps until the highest current that caused no motor responses was reached.

Following determination of RPO-stimulation values, the animals were tested for PAG-evoked responses. The goal for the PAG stimulation was to establish the minimum current intensity necessary to induce the emotional response of freezing. Stimulation trains were 8 second long, and the first current was set at 10uA, with increases in 5μA steps until the desired freezing behavior was evoked.

After repeated PAG stimulations at the freezing threshold, RPO stimulations were conducted in order to verify that the desired hippocampal responses were still being elicited. In all cases, the currents established for the RPO-stimulation before PAG activations were still effective in inducing hippocampal theta rhythmicity.

4.2.3. Recording sessions

For the data presented in this section, rats were tested in 10-minute sessions on each of five days. LFP activity from the bilateral HPC and left PrL were recorded according to the detailed methods in Chapter 3. For each session, rats were consecutively stimulated at the RPO and PAG-freezing thresholds established before. The first 1-second RPO train was delivered, followed 30 seconds later by an 8-second PAG train, and by the end of each session the rat had received 10 stimulations of each type. At the end of the session, the stimulating current for PAG was increased in steps of 5μA until an escape response was induced, and the session was finished. The experimental timeline is illustrated in Figure 4.1.

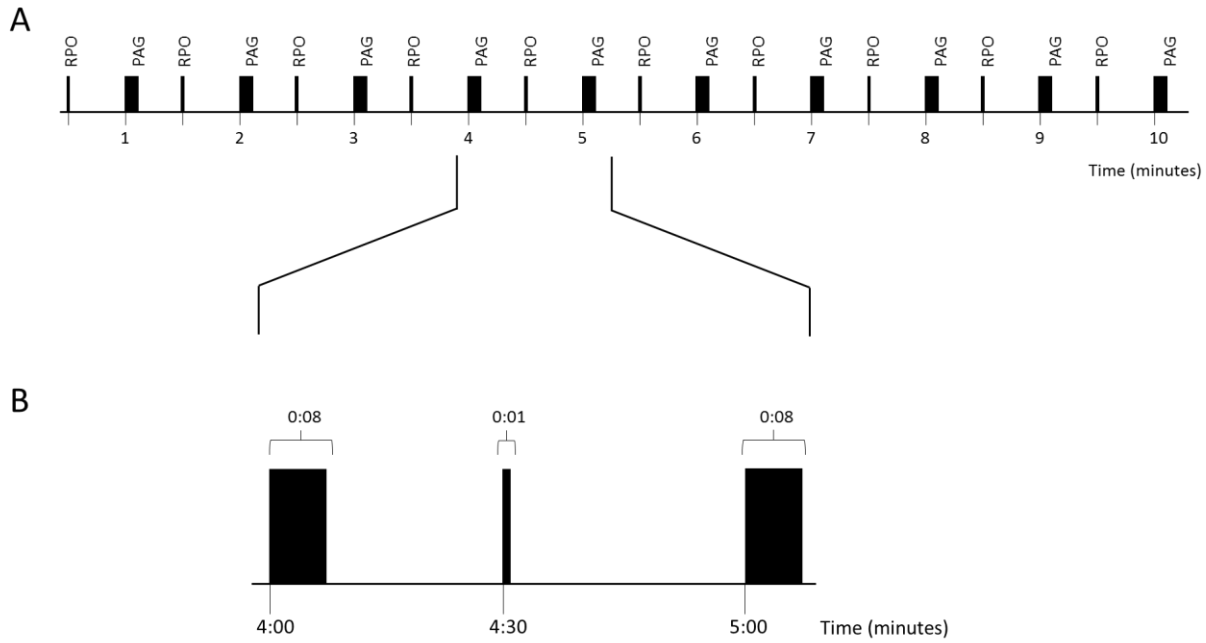

Figure 4.1. Timeline of experiment. A: time interval between stimulations. RPO and PAG stimulation trains are presented each 30 seconds, alternating between the two. B: view of a single minute of the experimental session. PAG trains last 8 seconds, and RPO ones 1 second.

4.2.4. Data processing

Given that PAG stimulation periods are 8 times longer than RPO ones, 1-second segments of EEG were extracted from each stimulation event in order to adequately compare the effects of the two stimulation types. 1-second periods of data before the onset of each event were extracted from each epoch, and treated as control "sham" stimulations, and 1-second periods after the onset were used for assessing stimulation effects (see Figure 4.2).

After segmentation of the data, each epoch was individually computed for power, instant frequency, coherence, PPC and PDC as described in the methods section on Chapter 3. All 10 trials of each type within the session were then averaged for each measure within the theta range (5 to 10 Hz).

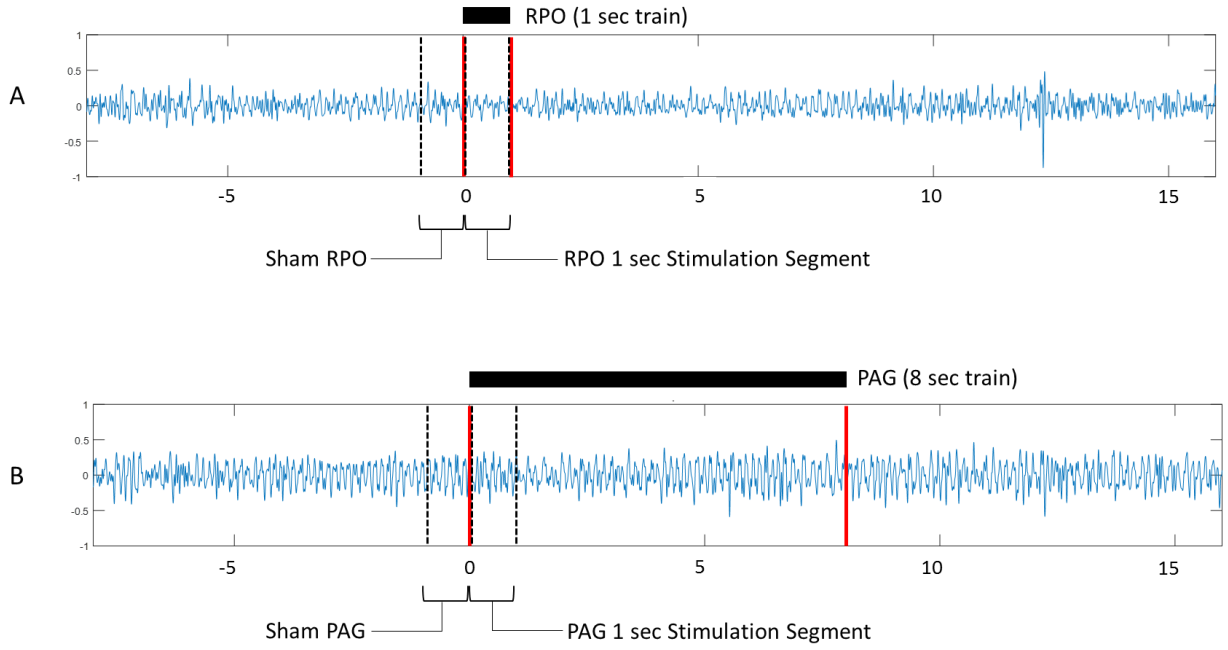

Figure 4.2. EEG segmentation from original RPO (A) and PAG (B) stimulation periods, demarcated by vertical red lines. Two 1-second segments of data before and after the onset of stimulation (0 second on X-axis) were used as "sham stimulation" and "real stimulation" epochs for analysis, respectively.

4.3. PAG-induced responses vs. RPO-induced responses

4.3.1. Histology

After data acquisition, electrode placements were verified histologically. All subjects included in this experiment had recording electrodes located in the left PrL, as shown in Figure 4.3, and HPC as shown in Figure 4.4. Stimulating electrodes located in the PAG and RPO are shown in Figures 4.5 and 4.6 respectively.

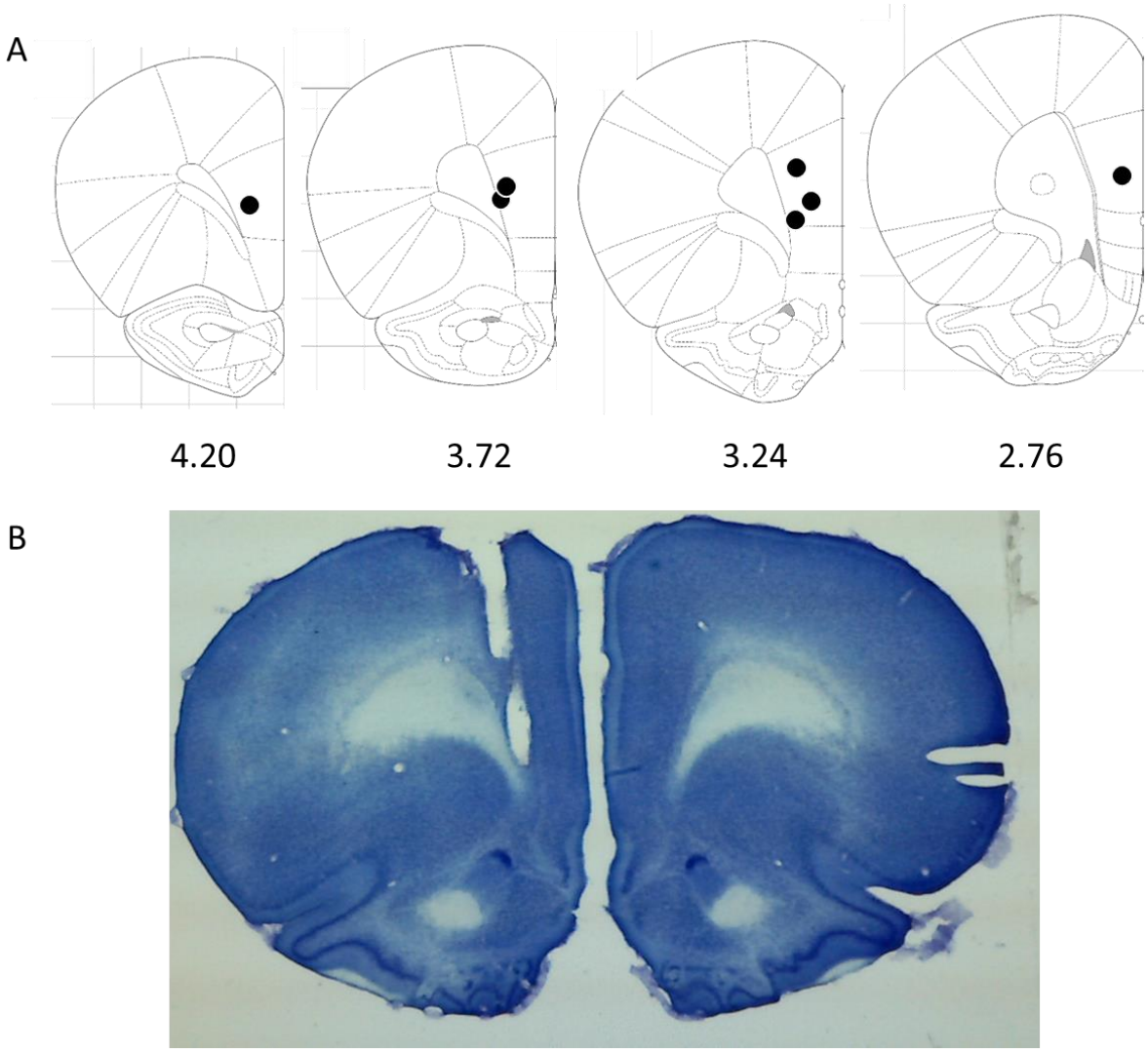

Figure 4.3. Histological placements of recording electrodes for the left PrL. Black dots in panel A show the centerpoint between the two pairs of electrodes in each rat that were used for analysis. A-P coordinates from bregma are indicated. Panel B is a representative photomicrograph showing the electrode trace through the medial wall of the prefrontal cortex.

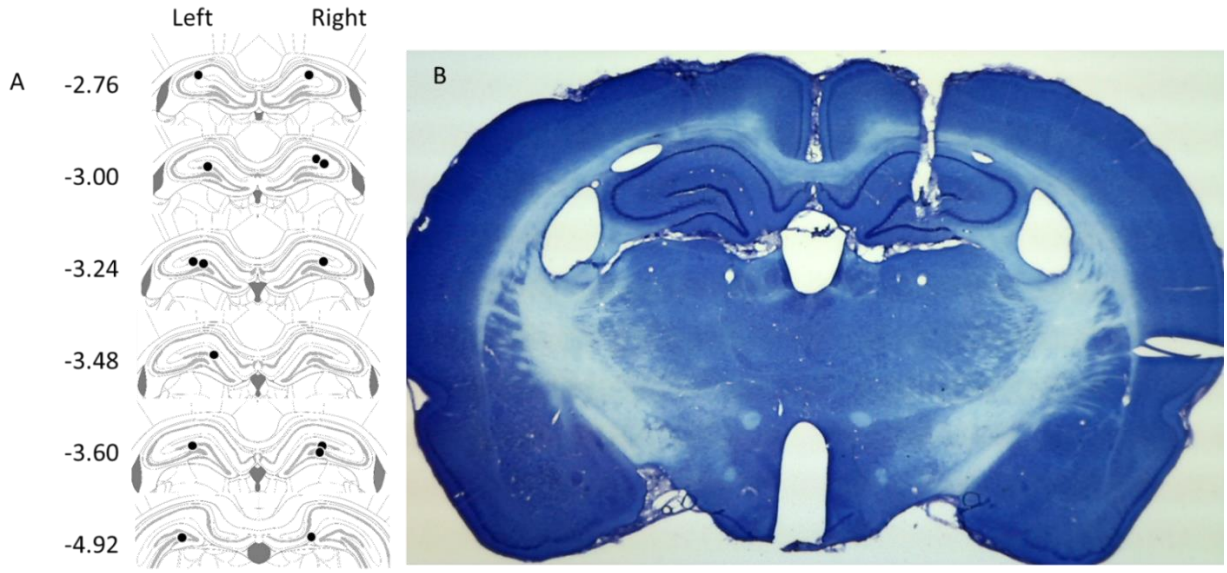

Figure 4.4. Histological placements of recording electrodes for the left and right HPC. Black dots in panel A show the centerpoint between the two pairs of electrodes in each rat that were used for analysis. A-P coordinates from bregma are indicated. Panel B is a representative photomicrograph showing the electrode trace through the right hippocampus.

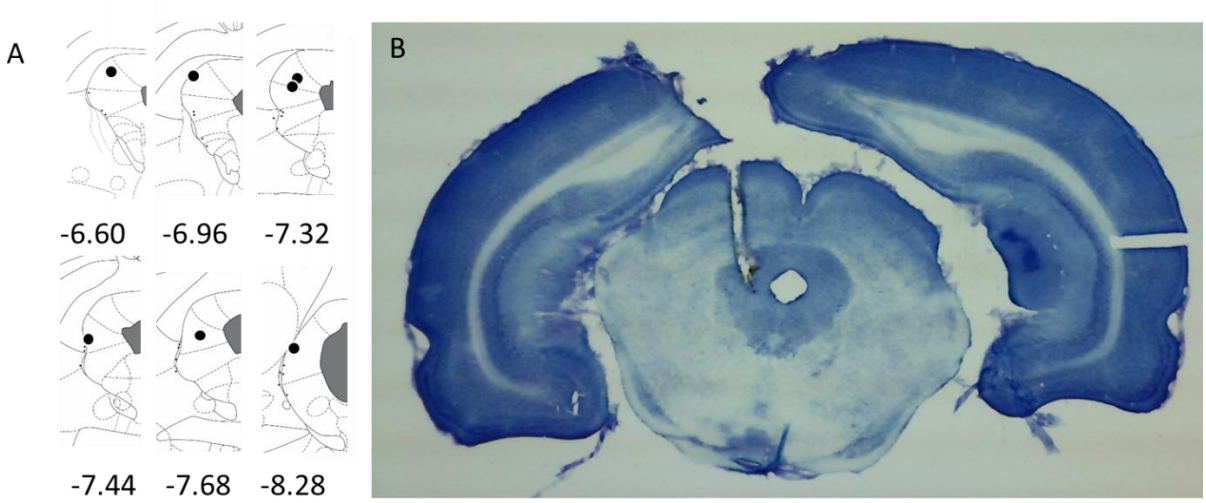

Figure 4.5. Histological placements of stimulating electrodes for the PAG. . Black dots in panel A indicate location of the anode of the two stimulating tips in each rat. A-P coordinates from bregma are indicated. Panel B is a representative photomicrograph showing the electrode trace through the left PAG.

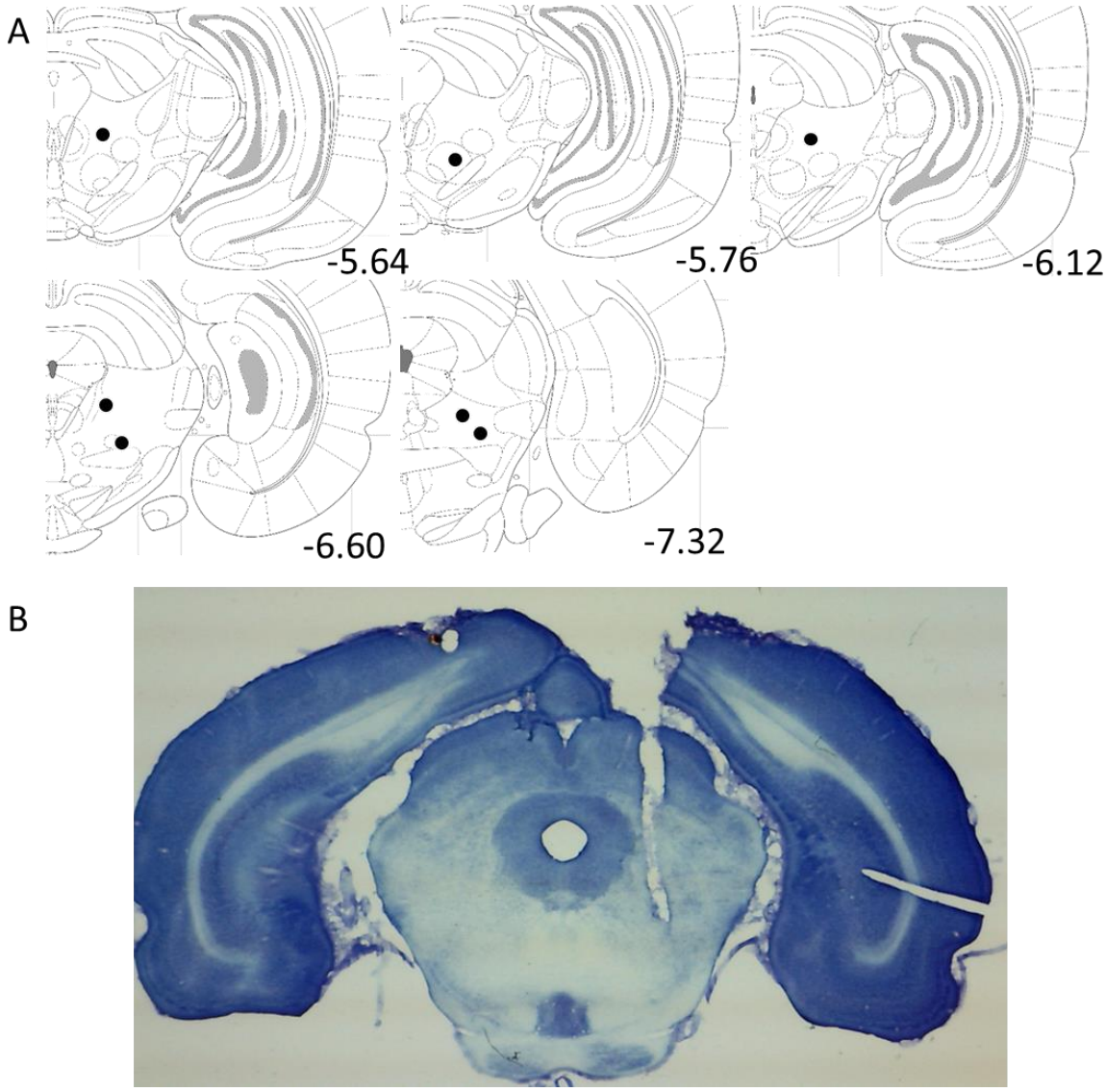

Figure 4.6. Histological placements of stimulating electrodes for the RPO. Black dots in panel A indicate location of the anode of the two stimulating tips in each rat. A-P coordinates from bregma are indicated. Panel B is a representative photomicrograph showing the electrode trace through the right hemisphere.

4.3.2. Results

Behavioral and neural effects of stimulation. For RPO stimulation, an average of 57µA was found to be the maximum intensity that evoked theta rhythmicity with no motor manifestations, with ±4µA (S.E.M.) variations from one day to the next.

For PAG stimulation, an average of 68µA was established as the minimum current that caused clear, repeatable, evoked freezing, with a variation of ±6.5µA (S.E.M) across different days. These effective PAG currents caused evident freezing in animals, characterized by the arrest of ongoing motor activity, with the animal resting all four pawns on the ground.

Occasionally, these changes in posture would be accompanied by visible changes in breathing and/or cardiac patterns, noticeable by faster breathing movements in the thoraxic region. Other occasional occurrences included micturition and defecation, and sometimes head scanning. A few seconds after the stimulation train finished, rats stopped freezing and returned to normal behavior.

Power spectral density during PAG stimulation. Before conducting comparisons between the effects of PAG and RPO stimulations with segmented 1-second periods, spectral analysis was performed on 24-second epochs of PAG stimulation, which included the 8-second periods before and after the delivery of the stimulus train as well as the 8 s period of stimulation.

As shown in Figure 4.7, PAG stimulations provoke marked changes in HPC and left PrL field potentials that are bound to the stimulation period. As seen in panel A, LFP amplitude is greatly diminished, especially at the hippocampus during the stimulation period. Spectrograms in panel B show that in both left and right HPC, before stimulation, the dominating power band is 5Hz (this is consistent with the rat being restricted in an operant chamber, in which the animal is confined to slower and smaller movements, which produce lower frequency theta). During stimulation this band still is the dominating one, but power is greatly reduced. Once stimulation is turned off, activity in this band returns, with a rebound effect of showing stronger power than during pre-stimulation. For the left PrL, the pre-stimulation period shows dominating bands bellow 5Hz – although some relative activity is also present at higher frequencies, unlike the HPC. During stimulation, as seen with the HPC, power in the dominating bands is greatly diminished. Immediately after stimulation is turned off, a small rebound in power happens, but in the following seconds power is generally reduced to a level below the pre-stimulation period.

Theta power. Results for LFP power in the theta band are presented in Figure 4.8. For PAG stimulation, the overall pattern is that stimulation of this area causes a large decrease in LFP power. As seen in in panel A, power is decreased by approximately a third during stimulation (stimulation [linear], $F(1,6) = 52.61$, $p < 0.001$). In the same panel, we can see that RPO stimulation appeared to cause a slight increase in mean power, but this was not significant (stimulation [linear], $F(1,6) = 0.98$, $p = 0.36$). Panel B shows the LFP power value for L-HPC during sham and RPO stimulation. Most of the increase in power during stimulation, seen in panel A, came from this region. The increase, however, was not significant (stimulation [linear], $F(1,6) = 1.61$, $p = 0.25$).

Panel C presents the detailed view of LFP power by region and stimulation type, and the quadratic components for each state. No statistically significant changes were seen for specific

regions; the reduction in power seen during PAG stimulation affected all three regions similarly. For RPO, there appears to be a slight positive curve during sham, that is reversed and becomes negative during stimulation; this, however, was not a significant change (Stimulation [linear] x Region [quadratic], $F(1,6) = 1.78$, $p = 0.230$).

Frequency. The effect of stimulation on HPC and left PrL frequency is presented in Figure 4.9. Panels A and B show that both PAG and RPO stimulation significantly reduced frequencies across the regions (PAG stimulation [linear], $F(1,6) = 11.93$, $p = 0.014$; RPO stimulation [linear], $F(1,6) = 50.40$, $p < 0.001$).

Panel C shows the changes promoted by the stimulation in the relationship between the recorded areas. The reductions in frequency coming from PAG stimulation originate almost entirely from a reduction in left PrL frequency, with HPC frequency remaining largely unchanged (PAG stimulation [linear] x Region [quadratic], $F(1,6) = 298.60$, $p < 0.001$).

Theta coherence and PPC. No significant effects of either stimulation were seen between the stimulation states for PPC and coherence measures (Figure 4.10). Panel A shows the PPC numbers by pairs, averaged across both sham and stimulation states of PAG and RPO. In general, the left and right HPC are 3 times more coherent among themselves than they are with the PrL. This is captured by the significant trend that shows the left and right HPC having higher PPC scores (Region [quadratic], $F(1,6) = 7.61$, $p = 0.02$). No differences were seen between PPC levels of the hippocampi against the PrL, meaning that the left HPC has the same levels of synchronicity with the PrL as the right HPC (Region [linear], $F(1,6) = 0.02$, $p = 0.87$). Panel B shows the PPC levels for each state of stimulation. No significant differences were seen between the sham and stimulated periods of both PAG and RPO. Panel C shows the coherence measures for PAG and RPO stimulations; again, no significant changes were seen in coherence between sham and stimulation of both PAG and RPO.

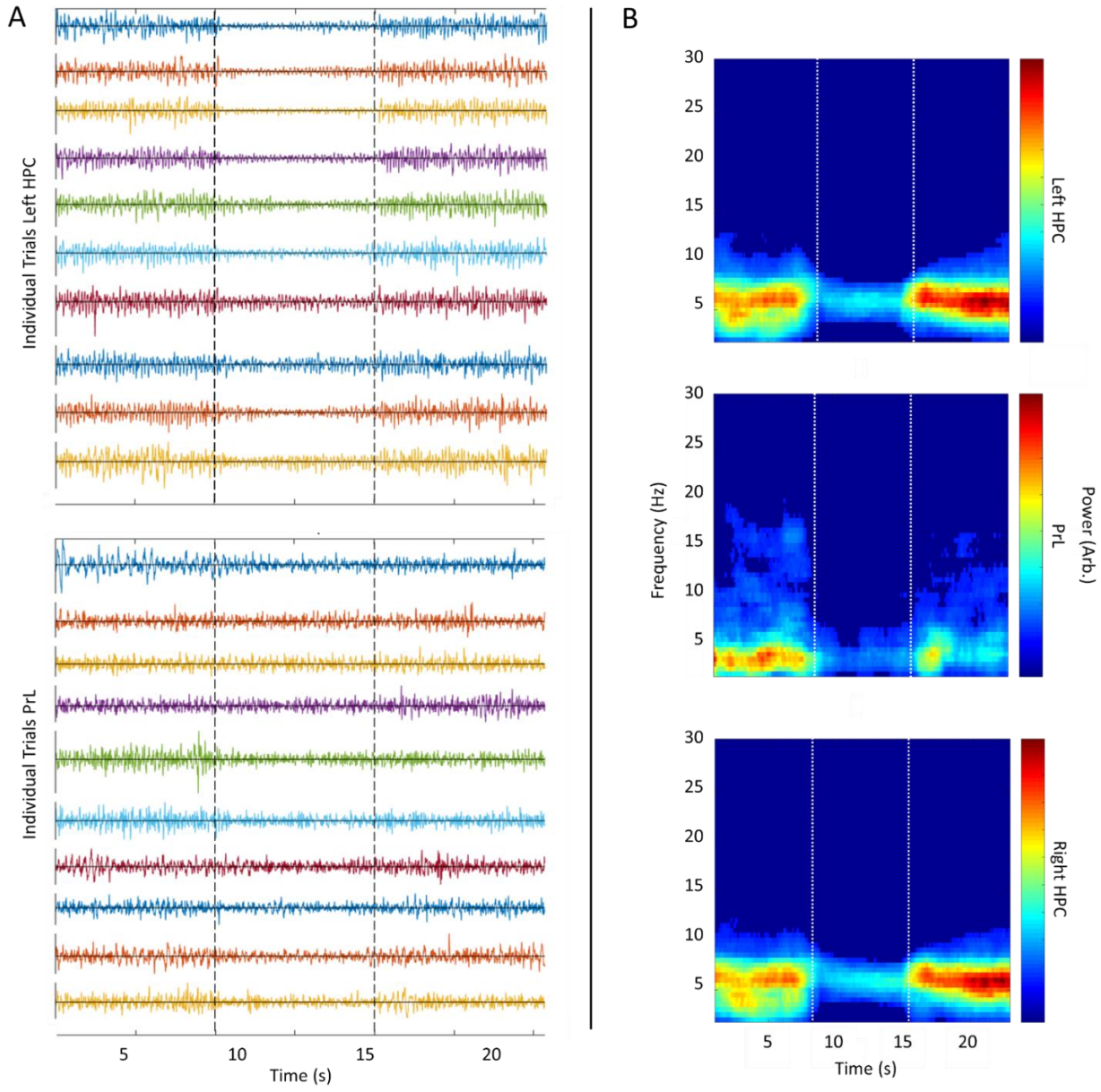

Figure 4.7. LFP activity under PAG stimulation for a representative rat. Event epochs are comprised of a total of 24 seconds including 8 second periods before, during and after stimulation. A: Each panel presents raw LFP of ten individual trials of PAG stimulation, with stimulation periods indicated by black dashed lines at the center. Top: Left HPC; bottom: left PrL. Panel B shows spectrograms for relative power (averaged trials). From top to bottom: Left HPC, left PrL and right HPC spectrograms, with PAG-stimulation periods delimited by white dashed lines at the center.

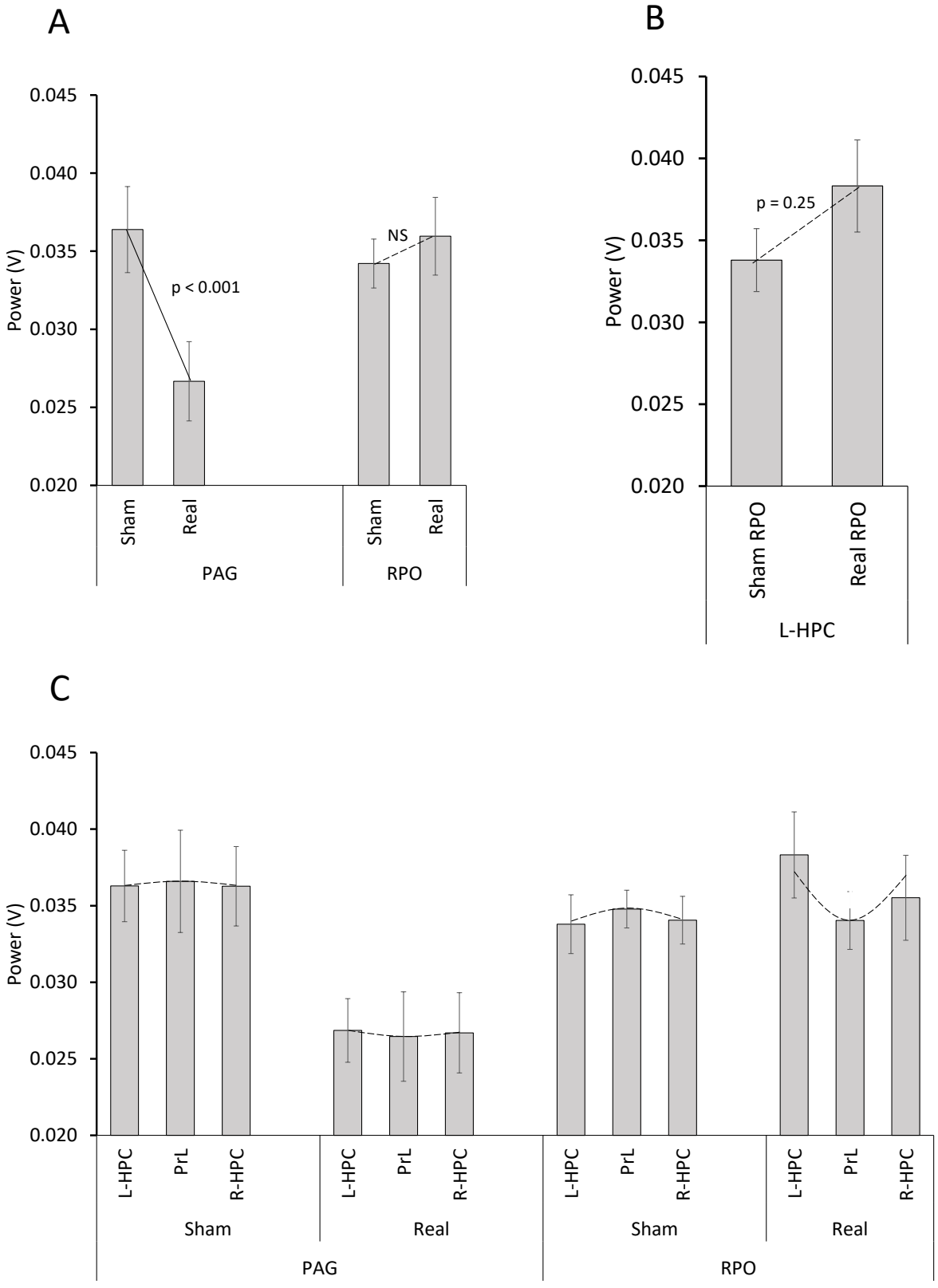

Figure 4.8. Theta power during real and sham stimulations of PAG and RPO (n=7). Panel A shows the overall effects of stimulation, with the activity of the regions averaged. PAG stimulation promotes a significant decrease in LFP power, and RPO promotes a non-significant increase in LFP power. Panel B shows a non-significant increase in hippocampal power during RPO stimulation. Panel C shows a detailed view of LFP power in all regions, with their quadratic curves fitted. Power was significantly decreased during PAG stimulation

at both the hippocampal sites and the left PrL. RPO stimulation promotes a non-significant change in the quadratic relationship between left PrL and the HPC sites. Solid lines indicate statistically significant differences, and dashed lines indicate non-significant differences.

PDC. In order to tell if the changes seen during stimulation are being led by specific regions, Partial Directed Coherence analysis was conducted. Figure 4.11 illustrates PDC measures during sham and real stimulations. During PAG stimulation (panel A), information flowing from the left HPC to the right HPC and to the left PrL is reduced. Meanwhile, the flow from the left PrL to the left HPC is increased. Panel B in the same picture shows that RPO stimulation mostly keeps the dynamics between the regions unaltered, with the exception of an increase in flow from the left HPC to the left PrL.

Figure 4.12 presents the results from the PDC analysis in more detail. Panels A and B present PDC measures averaged across real and sham stimulations of both types. In general terms, panel A shows that the flow of information from the two HPC sites to the left PrL is larger than the bilateral flow between the two hippocampi. Statistically, this is demonstrated by a significant difference between the flow of information in the two HPC → left PrL direction compared to L-HPC → R-HPC (Region [quadratic], $F(1,6) = 11.20$, $p = 0.02$). The right HPC tends to more strongly influence left PrL than the left HPC, although the differences are not significant (Region [linear], $F(1,6) = 6.48$, $p = 0.051$).

Panel B displays the flow of information from left PrL to both right and left HPC, and compares it to how the left and right HPC talk between themselves. In general, it cannot be said that PrL influences either HPC anymore than the two HPC influence each other (Region [quadratic], ($F(1,6) = 1.56$, $p = 0.266$). Although the power of PrL to modulate activity in the HPC is not any larger than the influence that left and right HPC have on each other, the image also show that PrL influences the left HPC more than it influences the right HPC (Region [linear], $F(1,6) = 23.69$, $p = 0.005$).

Panels C and D show PDC measures during stimulation. In general, stimulations of both PAG and RPO did not produce large changes. First, PAG stimulation did not cause any significant changes in the flow of information between the areas studied (PAG Stimulation [linear], $F(1,6) = 3.28$, $p = 0.130$). RPO stimulation, however, caused changes albeit small ones. During sham, we see a significant linear difference between L-HPC → left PrL and R-HPC → left PrL, and no quadratic difference between the flow of the two HPC to left PrL against HPC → HPC. These indicate that during non-stimulated periods the right HPC is sending more information to the left PrL than the left HPC, and left to right HPC communication is not

significantly different than the averaged flow of information from both HPC to the left PrL. However, during stimulation, L-HPC → PrL increases, making it now significantly higher than HPC → HPC communication, and as high as R-HPC → left PrL (RPO stimulation [linear], $F(1,6) = 7.74$, $p = 0.039$; RPO stimulation [quadratic], $F(1,6) = 15.52$, $p = 0.011$).

Panel D shows that the flow of information from left PrL to both HPC and from right HPC to left HPC are generally unaffected by both PAG and RPO stimulation compared to sham (Stimulation [linear] x real/sham [linear] x region [linear], $F(1,6) = 1.22$, $p = 0.319$; Stimulation [linear] x real/sham [linear] x region [quadratic], $F(1,6) = 0.079$, $p = 0.079$).

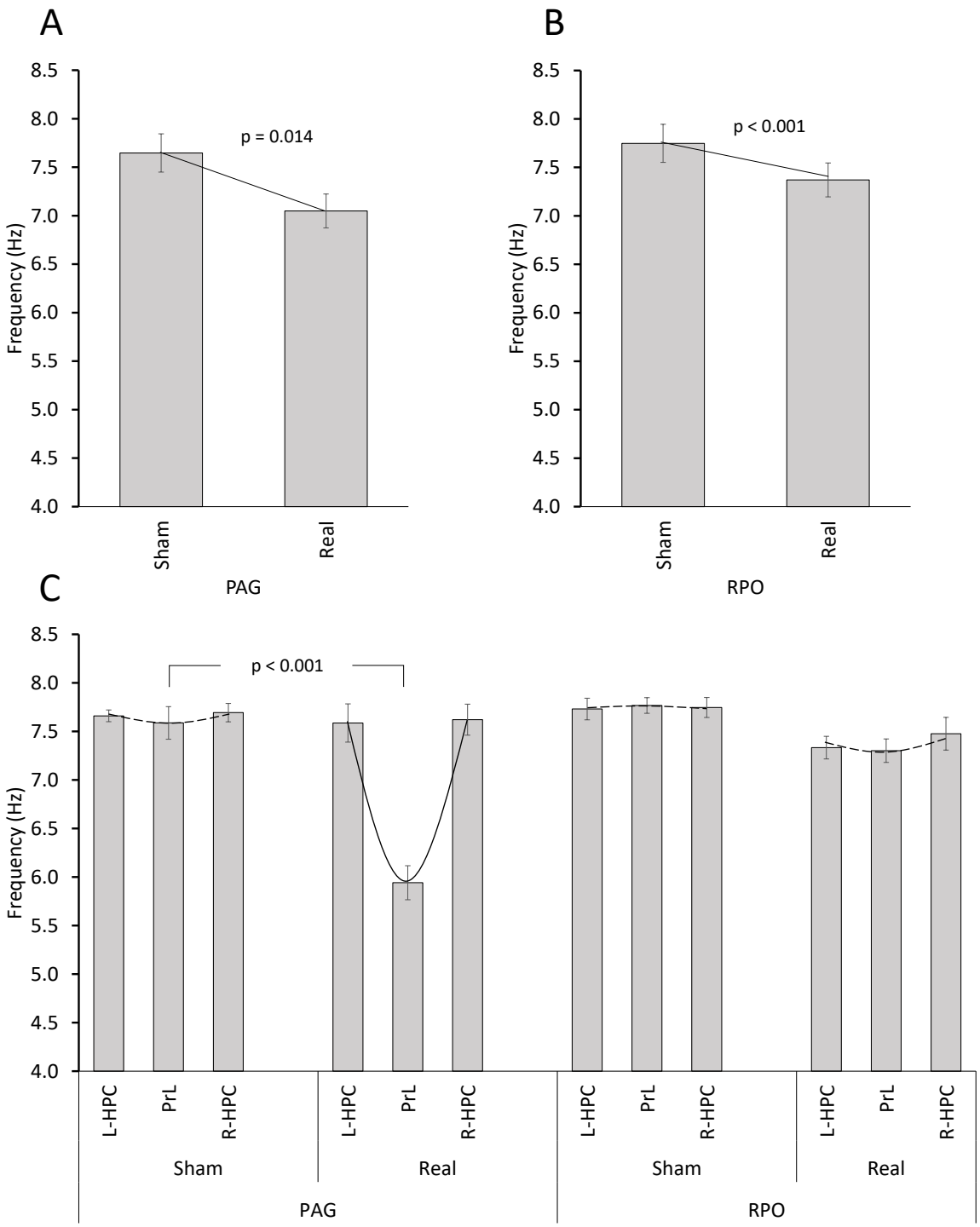

Figure 4.9. Frequency changes during sham and real stimulations of the PAG and RPO (n=7). Both PAG (panel A) and RPO (panel B) stimulations promote a general decrease in frequency from baseline across regions. Panel C shows the effects of stimulation in each region separately. The reductions in frequency coming from PAG stimulation are mostly due to decreases in left PrL, with hippocampal sites remaining mostly unchanged. The image shows the quadratic curve and the changes promoted by stimulation. Solid lines indicate statistically significant differences, and dashed lines indicate non-significant differences.

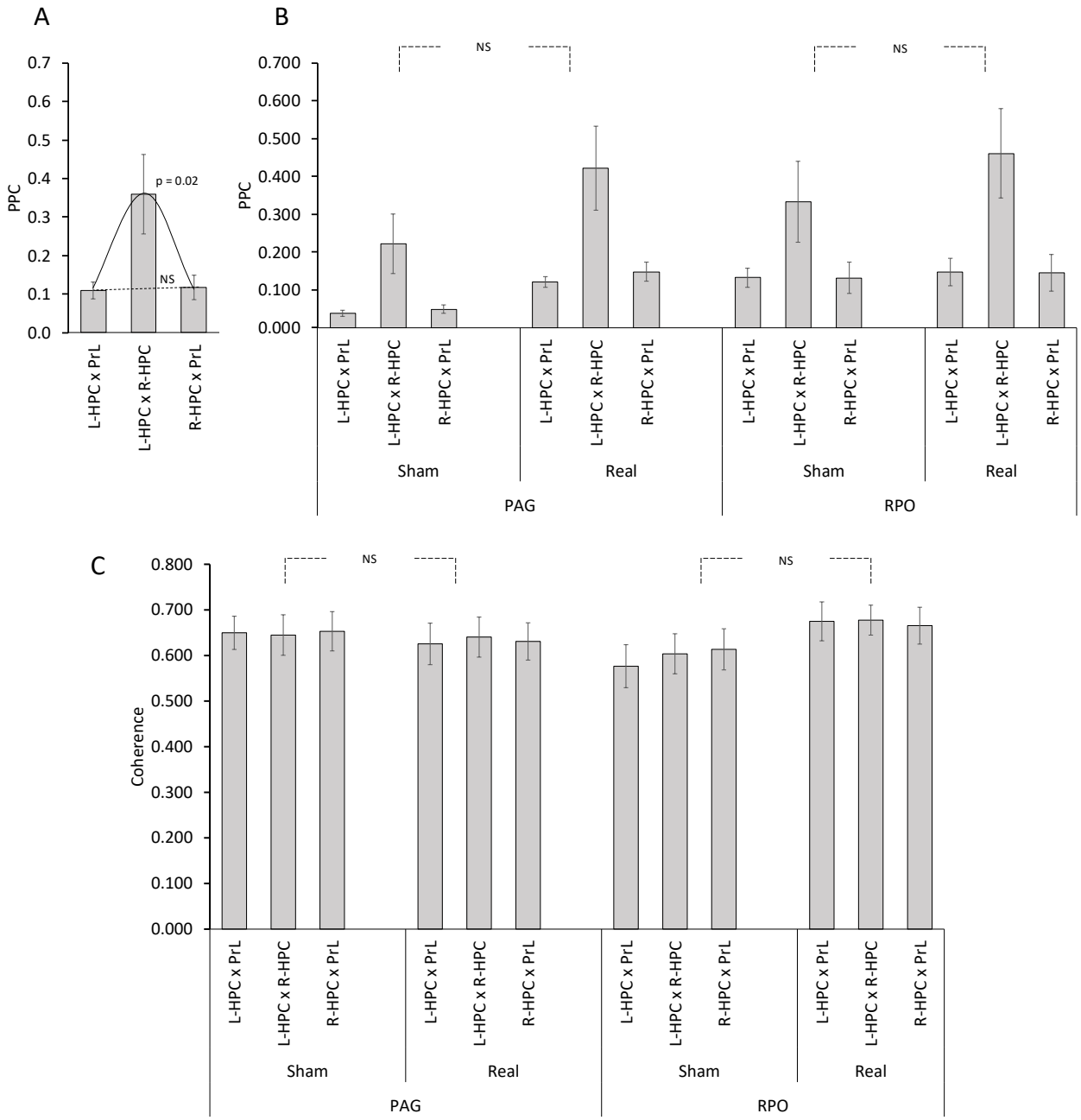

Figure 4.10. Pairwise Phase Consistency (PPC) and coherence for PAG and RPO stimulation (n=7). Panel A shows the average PPC between regions, averaged across sham and real types of both stimulation. Panel B and C show the detailed view for each state, respectively for PPC and coherence. Solid lines indicate statistically significant differences, and dashed lines indicate non-significant differences.

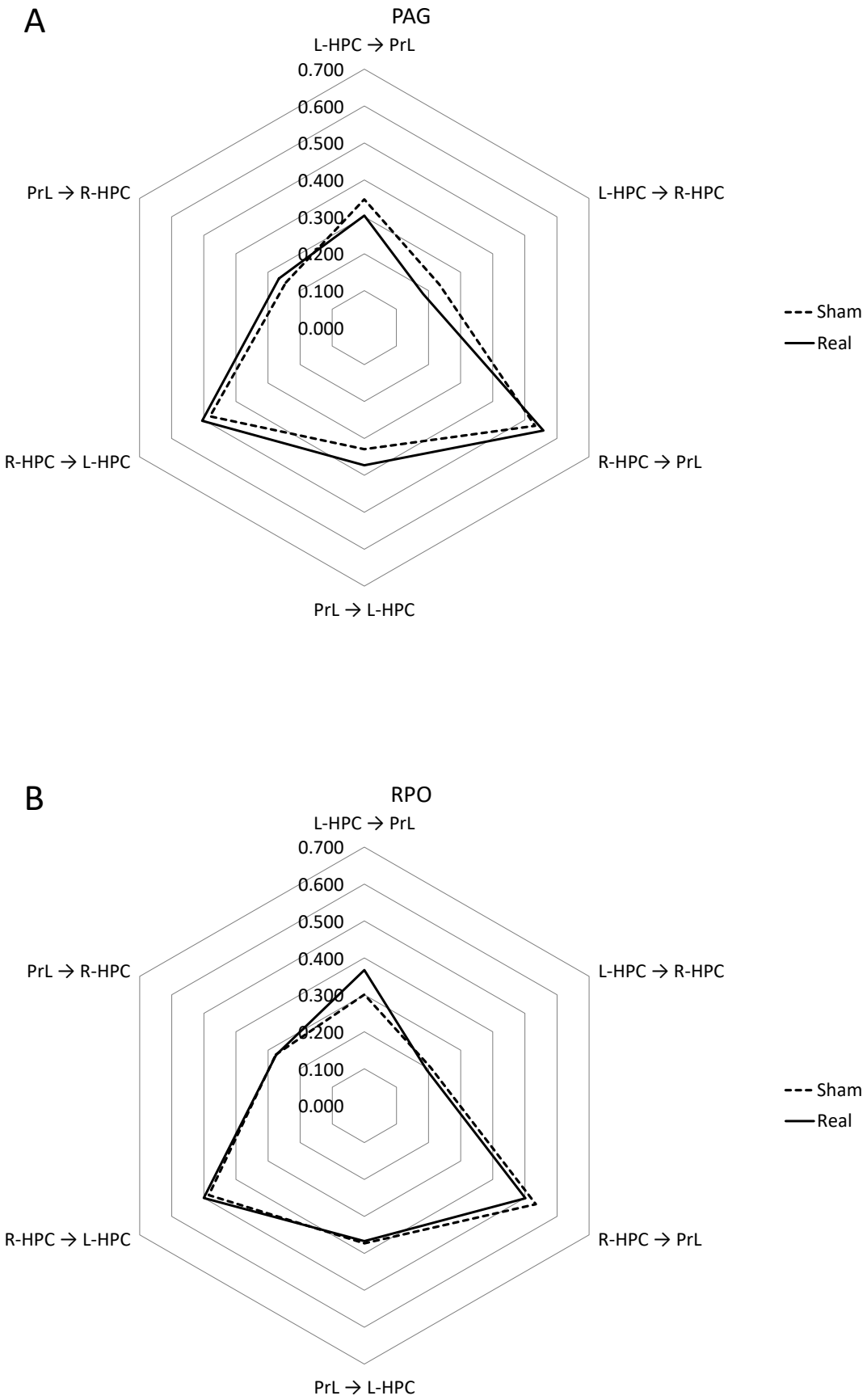

Figure 4.11. PDC during PAG stimulation (A) and RPO stimulation (B). The same results are also shown in bar graph form, and with more detailed explanation, in Figure 4.12.

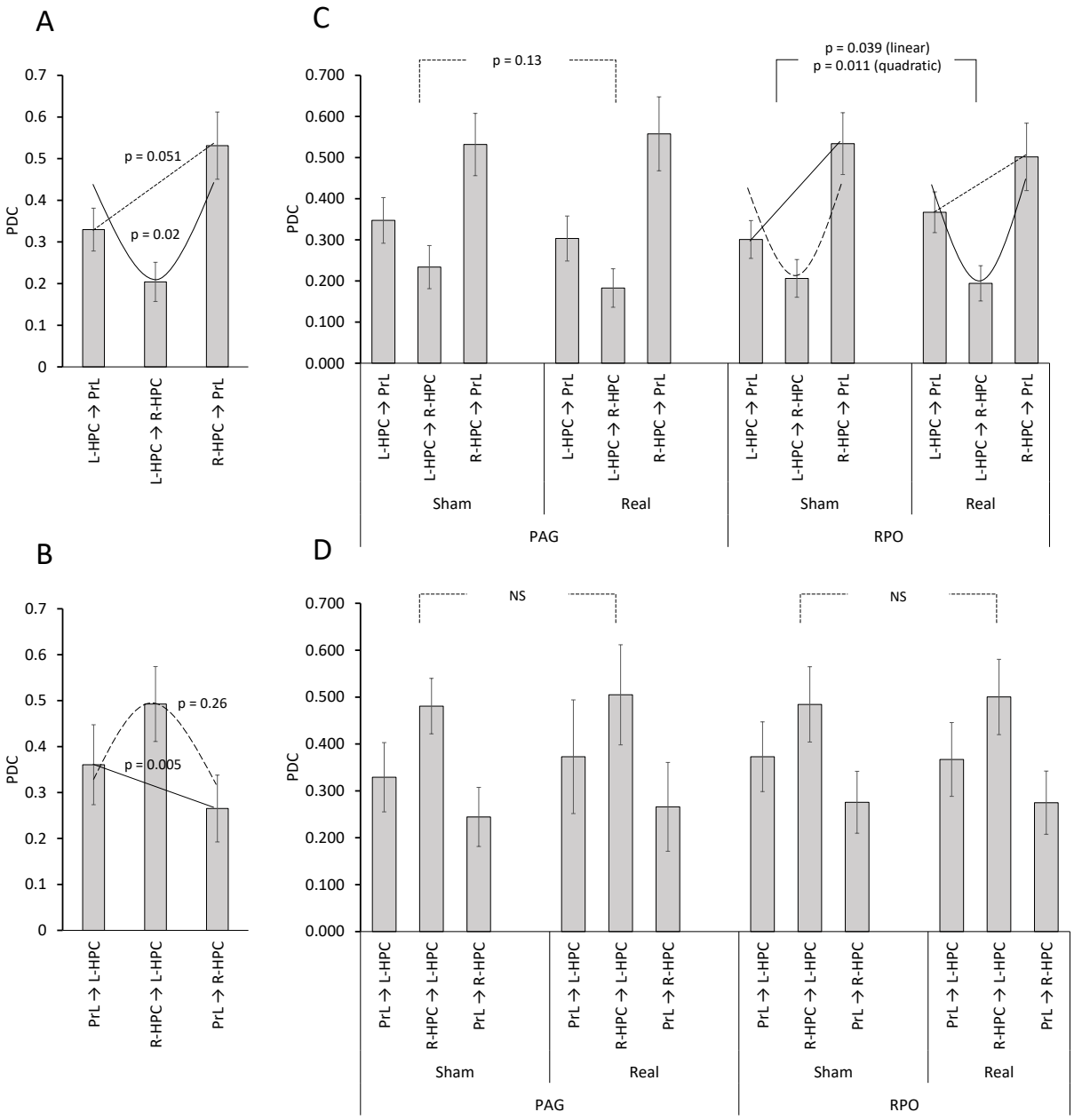

Figure 4.12. Statistical results for PDC. Panel A shows PDC activity averaged across PAG, RPO, Sham and Real states for L-HPC → left PrL, L-HPC → R-HPC and R-HPC → left PrL, along with linear and quadratic relationships. Panel B shows PDC activity averaged across PAG, RPO, Sham and Real states for left PrL → L-HPC, R-HPC → L-HPC and left PrL → R-HPC along with linear and quadratic relationships. Panels C and D show detailed effects of stimulation on the same pairs in A and B, respectively. Solid lines indicate statically significant differences, and dashed lines indicate non-significant differences (NS = non-significant).

4.4. Anterior PAG vs. Mid PAG

In the first part of this Chapter, the general effects of PAG stimulation that also generated freezing were investigated on a series of LFP measures. Subjects in that experiment, however, had stimulating electrodes placed mostly in the medial portion of the PAG. In order to assess whether the more anterior PAG produces similar effects, five rats with PAG stimulating electrodes placed in the anterior PAG (aPAG) were tested and analyzed in the same way, and compared with the same medial PAG (mPAG) animals.

As described in the first part of this Chapter, daily pre-test sessions were conducted in order to define the minimum PAG stimulation threshold capable of producing behavioral responses. The methodology for the second group of rats was the same as for the previous group.

4.4.1. Histology

The location of the recording electrodes for the left PrL and HPC, and stimulating electrodes for the PAG are shown in Figures 4.13, 4.14 and 4.15, respectively.

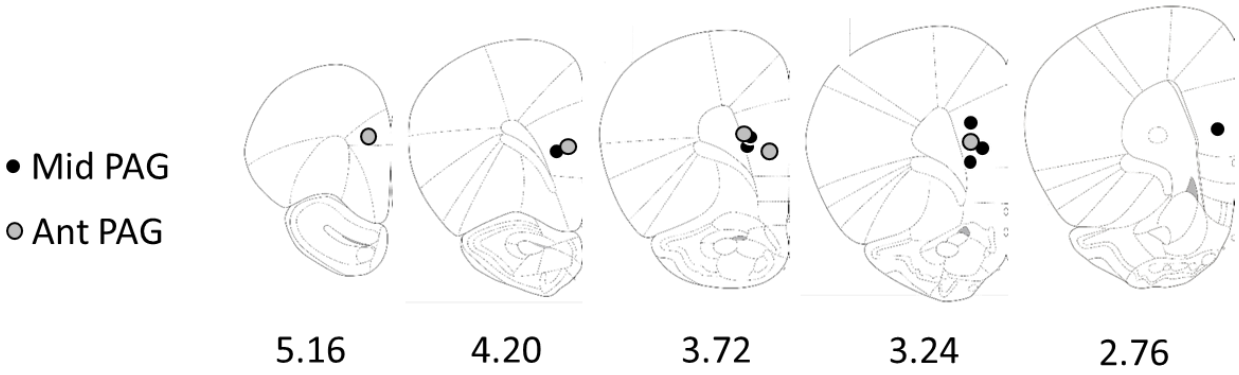

Figure 4.13. Histological placements of recording electrodes for the left PrL. Black dots show the centerpoint between the two pairs of electrodes in each rat in the mPAG group. Grey dots show the centerpoint between the two pairs of electrodes in each rat in the aPAG group. A-P coordinates from bregma are indicated.

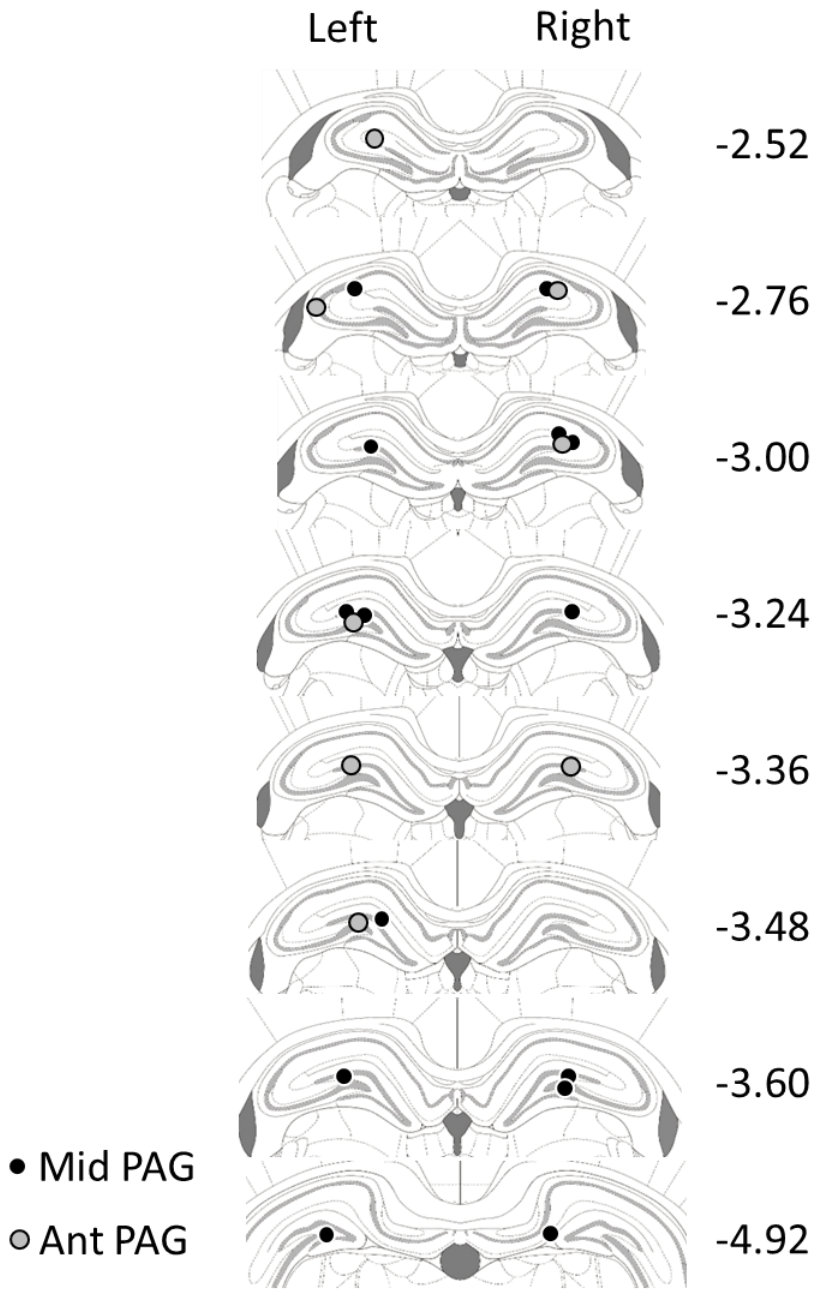

Figure 4.14. Histological placements of recording electrodes for the left and right HPC. Black dots show the centerpoint between the two pairs of electrodes in each rat for the mPAG group. Grey dots show the centerpoint between the two pairs of electrodes in each rat for the aPAG group. A-P coordinates from bregma are indicated.

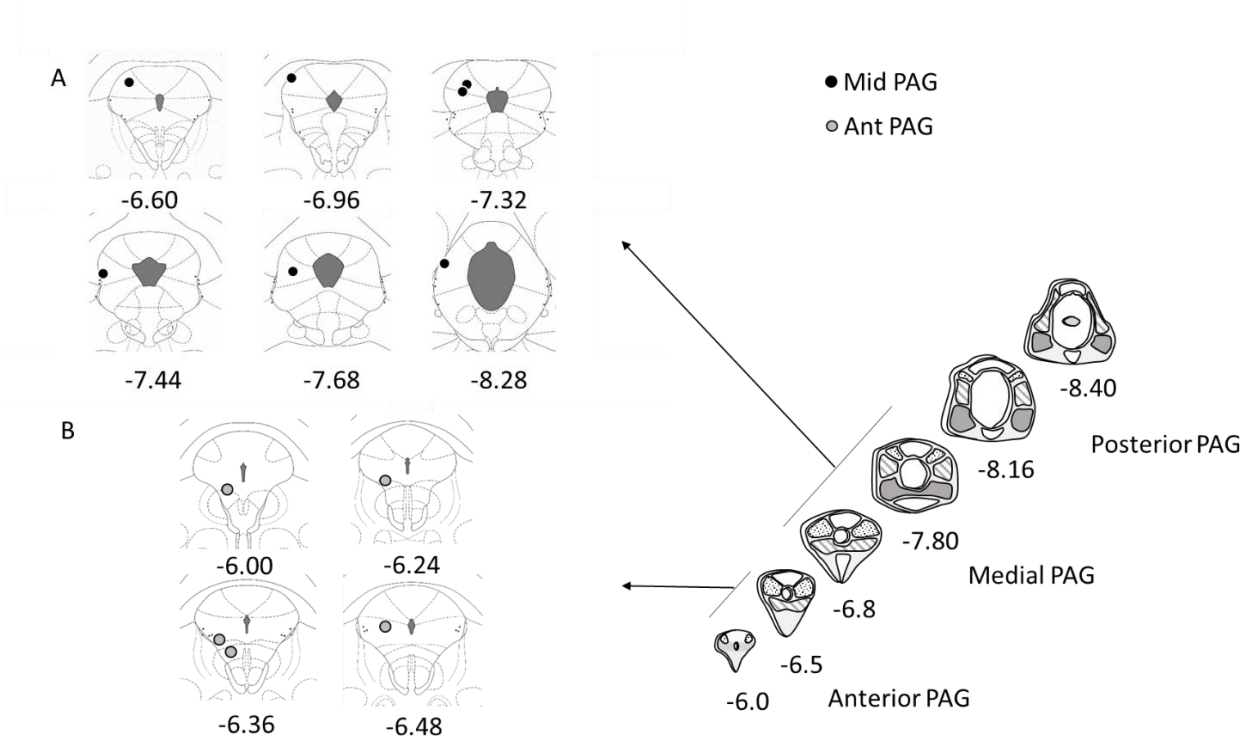

Figure 4.15. Histological reconstruction of PAG stimulating electrode placements. Black dots in panel A indicate location of the anode of the two stimulating tips in the animals in the mPAG group. Panel B shows the location of the anode of the two stimulating tips in animals in the aPAG. On the right, the concentration of the stimulating regions for each group is indicated in the anterior-posterior axis of the PAG.

4.4.2. Results

Effects of electrical stimulation. The behaviors elicited by stimulation in the two groups were distinct. As described before, mPAG animals would freeze during stimulation, and occasionally head scanning and faster breathing patterns would occur in some animals. Rats in the aPAG group presented this freezing behavior as well, but the occurrence of higher rates of breathing was more consistent and intense than the other group. The aPAG animals also displayed strong sniffing and occasional facial contractions during stimulation, which were completely absent in the mPAG rats.

For rats with aPAG electrode placements, the average minimum electric current that caused freezing was 428µA, with a variation of ±6.9µA (S.E.M) in different days of testing. This minimum threshold for freezing is considerably higher than the one for animals stimulated in the mPAG (68µA, ±6.5µA), and an independent sample, two tailed t-test showed these differences were reliable ($t(10) = -3.88$, $p = 0.003$).

Upon increase of the stimulation current (96uA, ±9.6μA as a group average), animals in the mPAG group would consistently present escape behaviors, characterized by forward running in circles while the stimulation train was on. Subjects in the aPAG group, however, were more resistant to change of behaviors with higher currents. Most animals in this group failed to consistently show escape behaviors with stronger stimulations and would usually remain in the freezing state. Occasionally, higher currents in the aPAG group would cause backing reactions. This motor reaction was characterized by backwards locomotion, with a strong arched back and lowered head. In some other animals, higher currents provoked strong, contralateral head turning. These two behaviors are unique to aPAG animals, as no animals in the mPAG group displayed backing or head turning during stimulation.

Power spectral density during PAG stimulation. Figure 4.16 presents spectrograms for activity in the HPC and left PrL for an animal under mPAG stimulation (left column; same images presented in Figure 4.2) and an animal under aPAG stimulation. As demonstrated before, mPAG stimulation reduces theta power on all three channels of interest. aPAG stimulation, on the other hand, increases hippocampal theta power on the ~15Hz band. One thing to note is that pre-stimulation epochs are different between the animals from different groups. For instance, the representative aPAG animal in image 4.2 show a much wider band of strong HPC activity between 5 and 15 Hz than the mPAG animal.

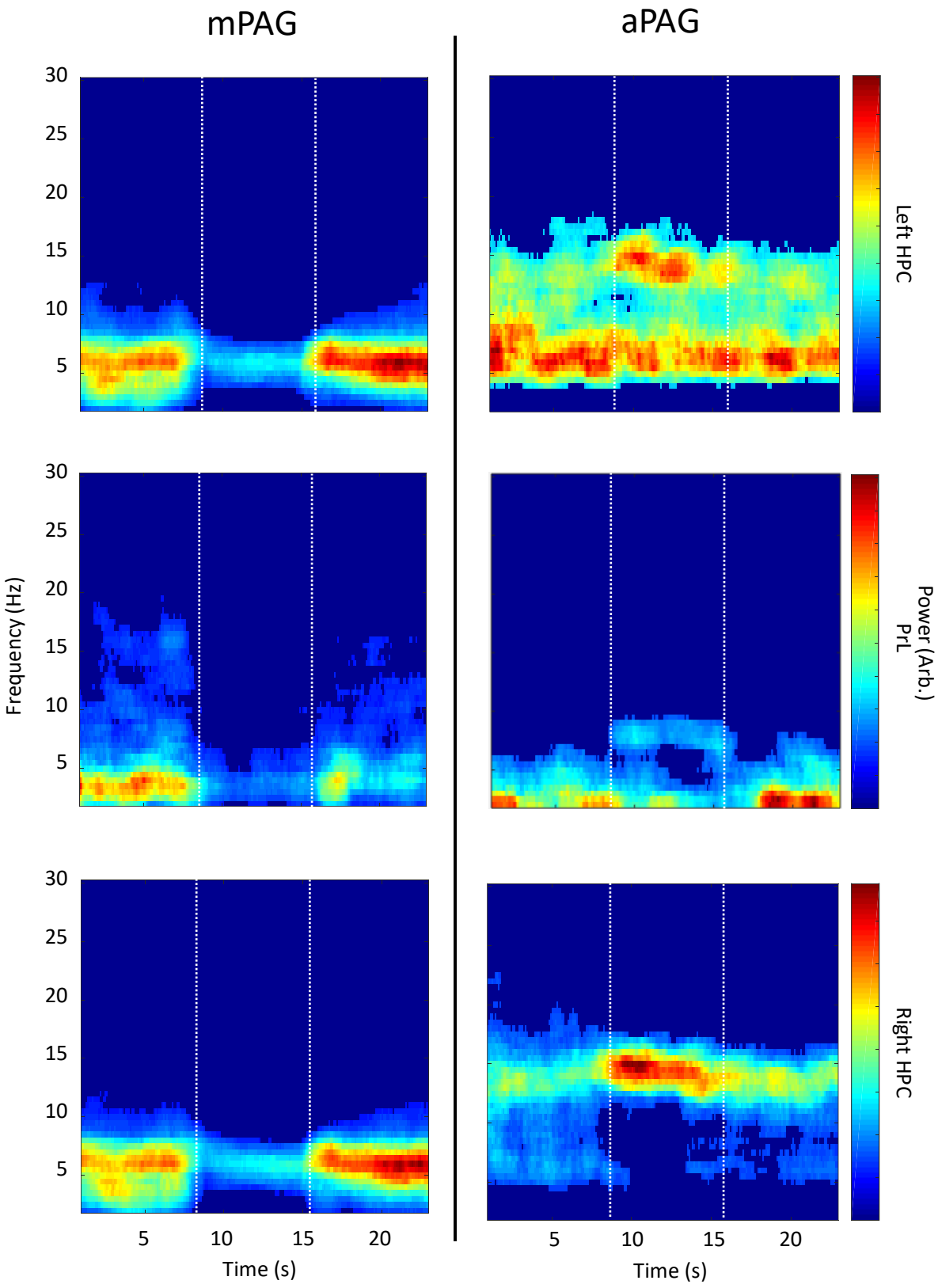

Figure 4.16. LFP activity under stimulation of the medial PAG (left column) and anterior PAG (right column) of one representative rat in each group (10 individual trials averaged). Event epochs are comprised of a total of 24 seconds including 8 second periods before, during and after stimulation.

Theta power. The effects of stimulation of the mPAG and aPAG are shown in Figure 4.17. In panel A, we can see how mPAG and aPAG differently affect theta power on all averaged regions. As established in the previous section in this Chapter, mPAG stimulation significantly reduces power over the average of all regions. aPAG stimulation, on the other hand, may show a marginal effect in increasing theta power (Stimulation [linear], $F(1,4) = 2.86$, $p = 0.166$). Panel B shows a detailed view, per recorded region, of the effects of mPAG and aPAG stimulations. It is possible to see that mPAG stimulation equally reduces power on both HPC and the left PrL. aPAG stimulation, however, increases power on all regions, and most noticeably in left PrL. On the sham scenario, left PrL LFP power is significantly smaller than the average of the two HPC (Region [quadratic], $F(1,4) = 22.78$, $p = 0.009$). During stimulation, however, left PrL power increases and becomes indistinguishable from HPC (Region [quadratic], $F(1,4) = 0.31$, $p = 0.608$). In order to evaluate if the increases in left PrL and right HPC power seen on panel B are statistically significant between sham and stimulation states, post-hoc analysis were conducted on these channels separately and are presented in panel C. Increases in left PrL power are only marginally significant (Stimulation [linear], $F(1,4) = 2.46$, $p = 0.192$). The increase in right HPC power, however, was shown to be significant (Stimulation [linear], $F(1,4) = 13.71$, $p = 0.021$). As seen with the power spectral density heat maps, a difference exists in the pre-stimulation periods (sham stimulation) of the two groups of animals. For instance, the LFP power of the three regions is not different in the pre-stimulation period of animals in the mPAG group; on the other hand, power for the PrL is much smaller than the power for the hippocampal regions in the aPAG animals.

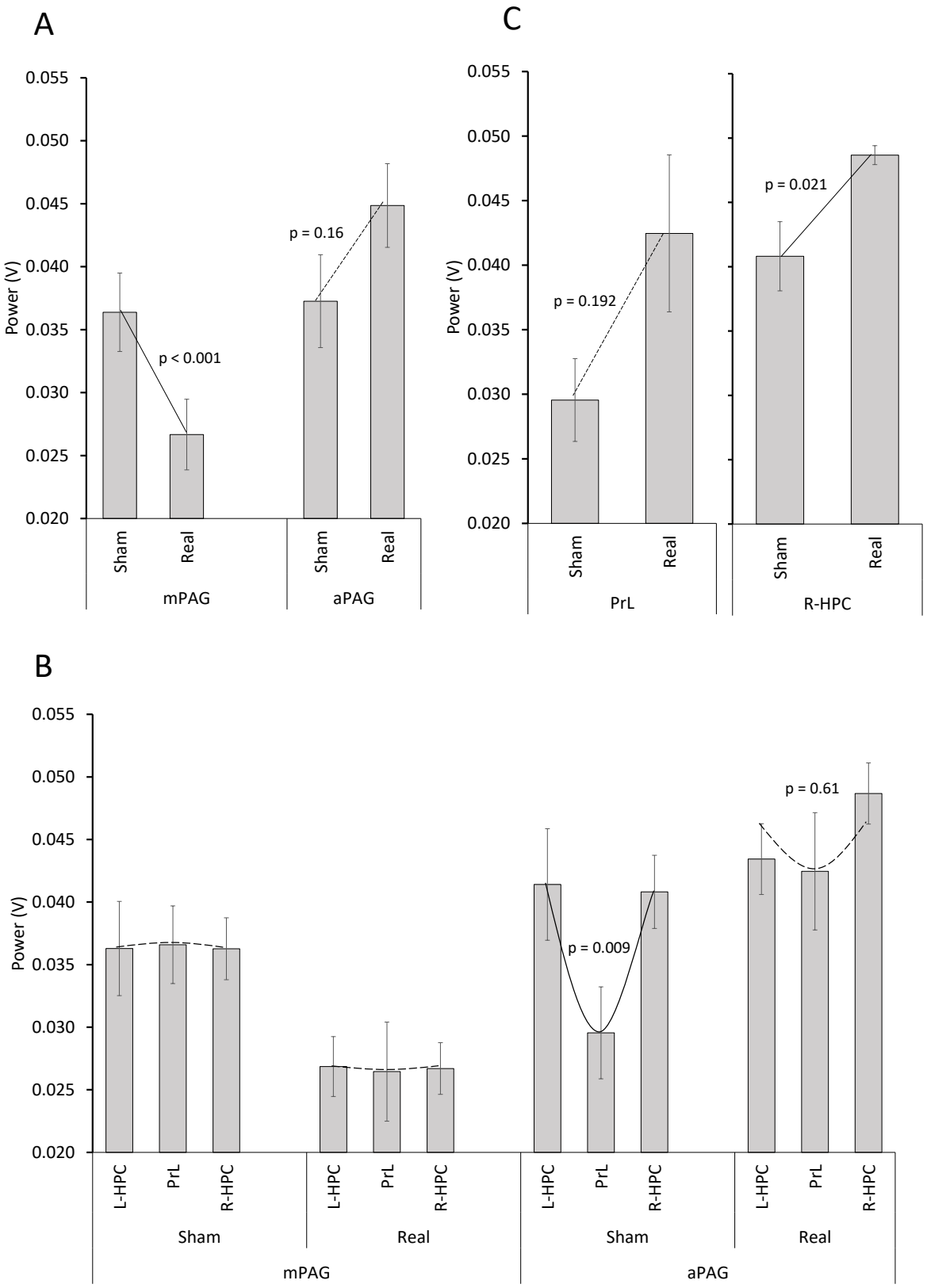

Figure 4.17. Theta power during real and sham stimulations of medial PAG (n=7) and anterior PAG (n=5). Panel A presents the changes promoted by mPAG and aPAG stimulations on the general activity of the regions, averaged. mPAG stimulation promotes a significant decrease in power, while aPAG promotes a marginally non-significant global increase. Panel B shows results per individual channels. mPAG promotes equal decreases in HPC and left PrL power. aPAG stimulation produces an increase in left PrL and right HPC

power, which is significantly reflected on their quadratic curves. Panel C shows post-hoc tests comparing sham and stimulation effects on left PrL and right HPC. Solid lines indicate statically significant differences, and dashed lines indicate non-significant differences.

Frequency. Figure 4.18 summarizes the effects of stimulation on frequency. While mPAG activation greatly reduces left PrL frequency, aPAG stimulation does not promote the same strong frequency changes (Stimulation [linear] x region [linear], $F(1,4) = 0.049$, $p = 0.83$; Stimulation [linear] x region [quadratic], $F(1,4) = 5.71$, $p = 0.075$).

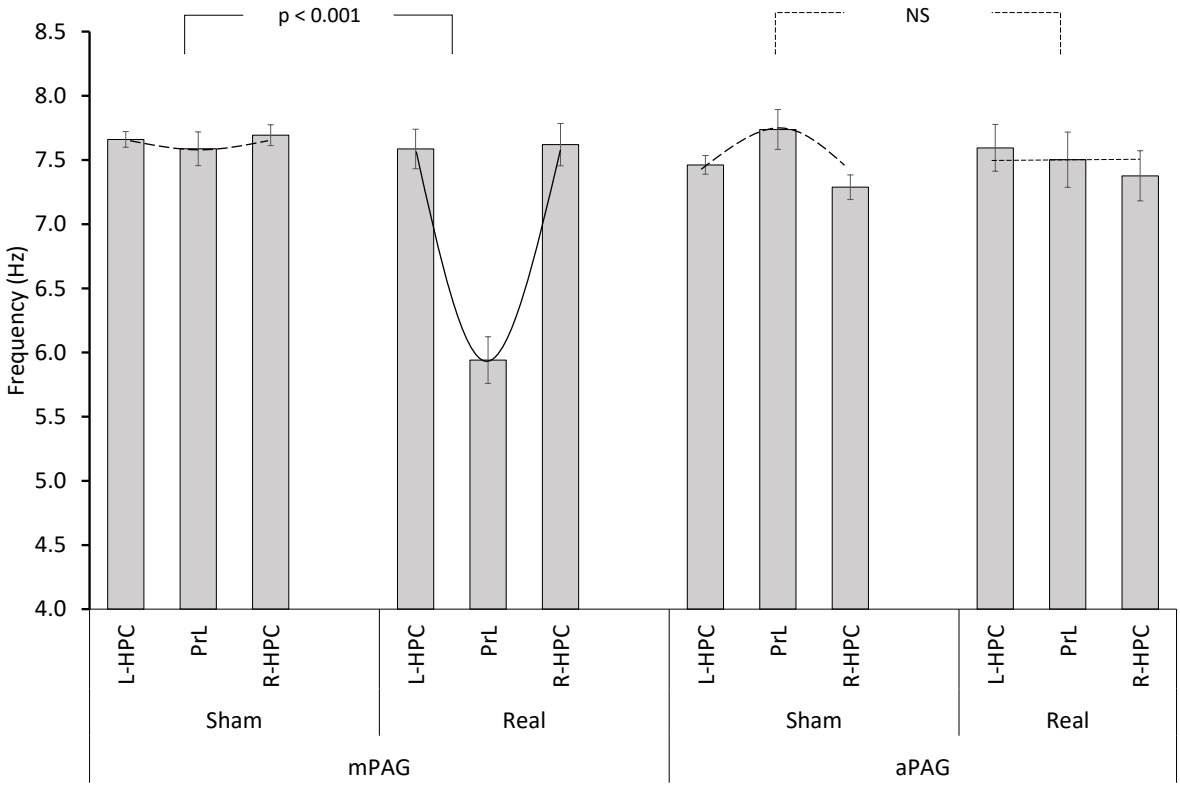

Figure 4.18. Frequency changes during real and sham stimulations of the mPAG (n=7) and aPAG (n=5). mPAG induces significant decreases in left PrL frequency, but aPAG effects are non-significant. Solid lines indicate statically significant differences, and dashed lines indicate non-significant differences (NS = non-significant).

Theta PPC and coherence. Figure 4.19 shows the results of stimulation on PPC and coherence. For PPC, no significant effects of stimulation were seen between groups for the two HPC against PrL (Stimulation [linear] x Region [quadratic] x PAG group, $F(1,10) = 0.02$, $p = 0.87$) or between the two HPC (Stimulation [linear] x Region [linear] x PAG group, $F(1,10) = 0.96$, $p = 0.35$).

In the same way, no changes were seen in coherence measures (Stimulation [linear] x region [quadratic] x PAG group, $F(1,10) = 3.80$, $p = 0.08$; Stimulation [linear] x region [linear] x PAG

group, $F(1,10) = 0.70$, $p = 0.42$). As seen with other measures, it is important to note that coherence between the two groups of rats is different in the pre-stimulation period. A comparison of the sham periods between the two groups reveals that they are different (Region [quadratic] x PAG group, $F(1,10) = 11.91$, $p = 0.006$), indicating that in the mPAG group the activity of the PrL is more similar to the two HPC than it is in the aPAG group.

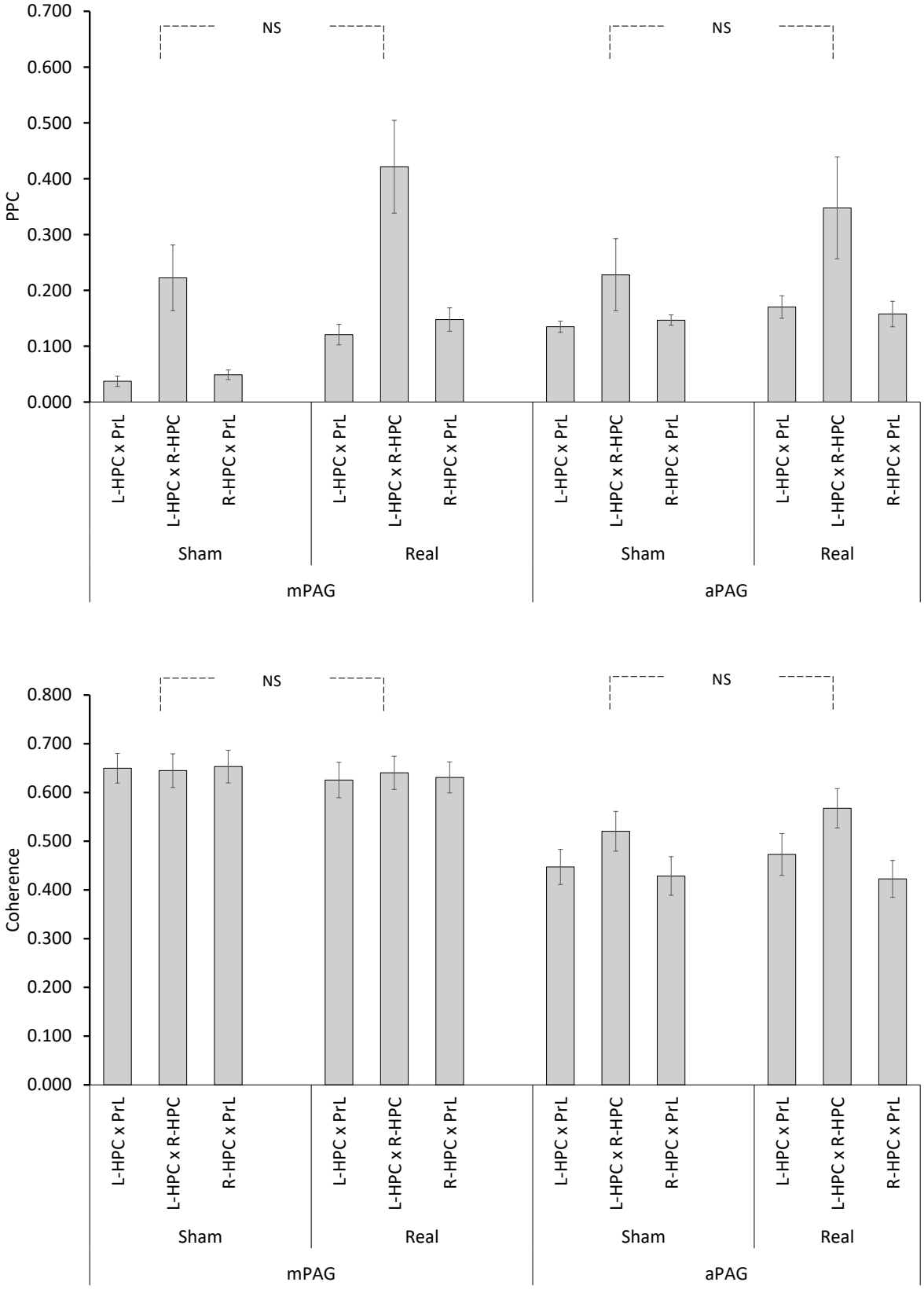

Figure 4.19. Pairwise Phase Consistency (panel A) and coherence (panel B) for mPAG (n=7) and aPAG (n=5).

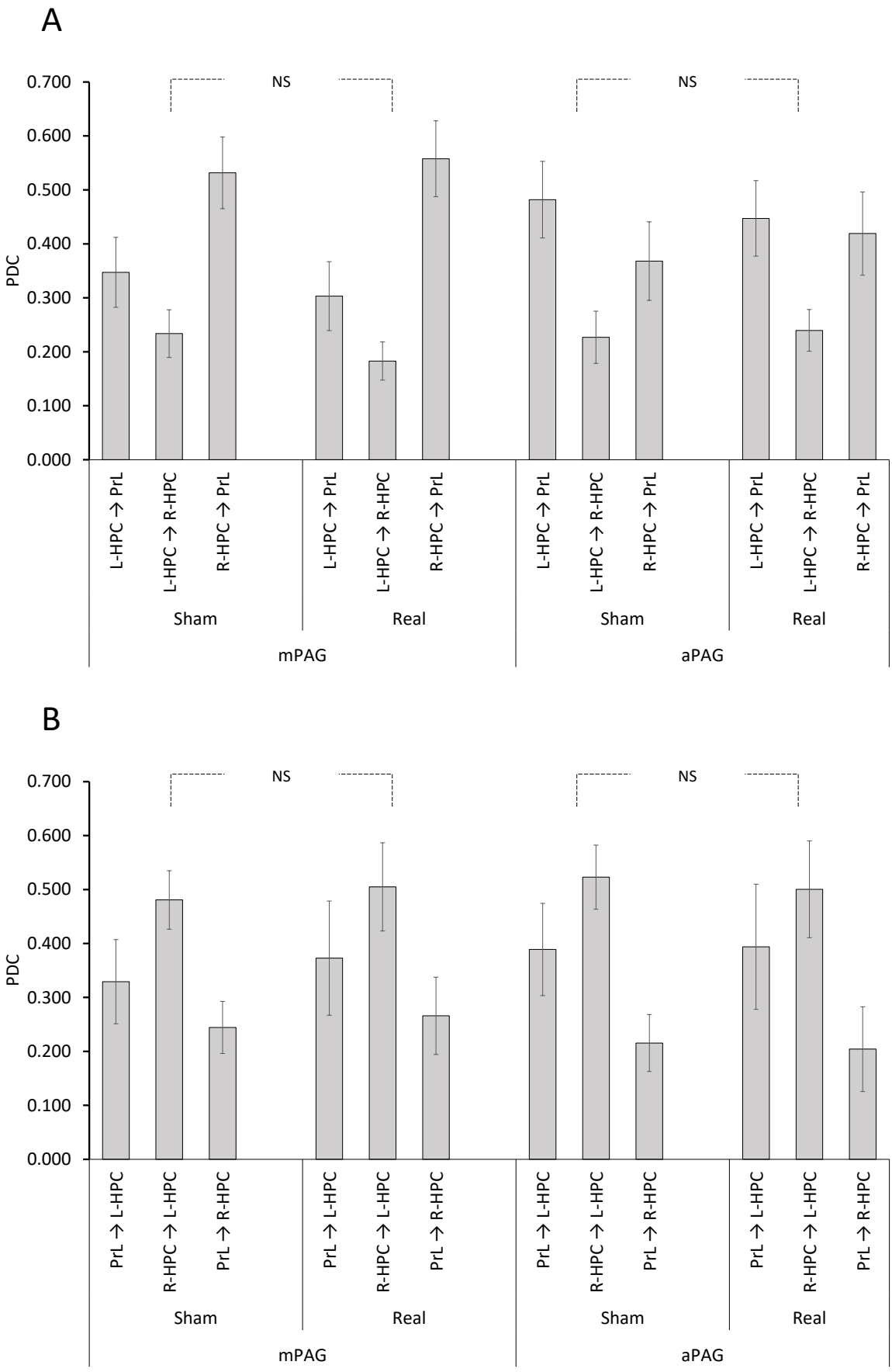

Figure 4.20. PDC activity during sham and stimulation states of mPAG and aPAG. Panel A shows L-HPC → left PrL, L-HPC → R-HPC and R-HPC → left PrL, and panel B shows left

PrL → L-HPC, R-HPC → L-HPC and left PrL → R-HPC. Dashed lines indicate statically non-significant differences (NS = non-significant).

PDC. Results for PDC are shown in Figure 4.20. Panel A shows PDC scores for the flow of information going from the HPC to left PrL, and from left HPC to right HPC. Although the baseline sham of the two groups of rats is slightly different (the dominance of the right HPC over left PrL, seen in the mPAG group, is reversed in the aPAG group), no actual effect of stimulation was present (Stimulation [linear] x region [linear] x PAG group, $F(1,9) = 0.047$, $p = 0.83$; Stimulation [linear] x region [quadratic] x PAG group, $F(1,9) = 0.703$, $p = 0.42$).

Panel B shows PDC for left PrL influence over HPC, compared against the right HPC influence over left HPC. Again, no significant differences were found between sham and stimulation states for both groups (Stimulation [linear] x region [linear] x PAG group, $F(1,9) = 0.029$, $p = 0.87$; Stimulation [linear] x region [quadratic] x PAG group, $F(1,9) = 0.008$, $p = 0.93$).

4.5. Summary and data discussion

In this Chapter, an electrophysiological investigation of the properties of freezing generated by PAG stimulation was conducted. Free-moving animals had their local field potential activity recorded from the prelimbic cortex and both sides of the hippocampus. Measures of theta power, frequency, coherence and causation between areas were assessed during electrical stimulation of the PAG that provoked freezing responses.

The first finding was that stimulations of the mPAG that also induced freezing caused marked and significant reductions in the amplitude of hippocampal and prefrontal theta. These reductions were bound to the stimulation period, and ceased as soon as stimulation was terminated. After electrical stimulation was ceased, spectrograms showed a rebound effect of theta power in the hippocampus, with stronger activity than what was seen in the pre-stimulation period.

In general, both hippocampal and prefrontal LFP power were reduced by approximately 1/3 during mPAG stimulation, and this reduction was statistically robust ($p<0.001$). In contrast, while mPAG generated a *reduction* of power in all areas, RPO stimulation produced an *increase* of power in the left hippocampus – although this RPO-increase was not statically significant.

Another strong change seen during mPAG stimulation was a large reduction in frequency, but selectively at the prefrontal cortex – no changes in frequency happened at either of the

hippocampi. On average, mPAG stimulation caused a drop of 1.5Hz in the dominant frequencies present in the prefrontal cortex that was strongly significant ($p < 0.001$). RPO stimulation also caused a significant reduction in frequency in both hippocampi and the prefrontal cortex ($p < 0.001$). Compared to the mPAG, however, this drop was relatively small at around 0.5 Hz ($F = 50.40$).

This drop in frequency during RPO stimulation, despite being very small when compared to the equivalent PAG effect, is unexpected. Usually, hippocampal frequency is increased during reticular stimulation (Green & Arduini, 1954; McNaughton & Sedgwick, 1978; Vertes, 1981). Previous studies in the free moving rat have shown that reticular stimulation using the same parameters and type of electrodes as the current one, have evoked hippocampal theta at the range of 7-8Hz using 50μA of current amplitude (McNaughton & Sedgwick, 1978; Figure 1). The investigation presented here also used stimulation currents averaging 50uA, and also produced hippocampal theta around the range of 7-8Hz; the crucial difference is that in the results presented here, hippocampal frequency was already at 7.5Hz before the onset of stimulation. One possibility for this is that repeated, concurrent activation of the PAG at the threshold of freezing could have changed basal activity in the hippocampus. It is very likely that during the inter-stimulation periods, when no manipulations are made and the animal is behaving freely, spontaneous activity in the hippocampus was stronger than usual. This would be due to activation of the PAG producing emotional states that lasted beyond the stimulation period. Crucially, this explanation would imply that RPO stimulation can override input from PAG or related areas in generating theta frequency. This would be possible if the PAG effect was mediated by RPO, with the 100Hz RPO stimulation antidromically activating the PAG input pathway to block incoming input.

Coherence measures indicate that, either before or during stimulations, all the regions recorded from were similarly synchronized to each other. This, however, was different with PPC. PPC indicated that activity in the two hippocampi was more similar between themselves than the activity between the hippocampi and the prefrontal cortex. Stimulations of the mPAG and RPO, however, did not change these patterns of synchronization. Measures of pairwise phase consistency, used to infer if changes seen in one signal might be caused by another, remained largely unmodified during electrical activations.

Since mPAG stimulation caused marked changes in power and frequency, we employed partial directed coherence measures to infer if these changes could be being led by any of the regions recorded in this study. At their resting state, before any stimulation of any kind was delivered, it was seen that the right hippocampus “leads” activity seen in the prefrontal cortex

and left hippocampus – more precisely however, the only statistically significant inference here was that the right HPC leads the PrL more than the left HPC does, and this was a marginal significance at best ($p = 0.039$). The only stimulation effect that was seen was during RPO activation, when the influence of the left hippocampus over the prefrontal cortex was elevated enough for it not to be statistically any different from the influence that the right hippocampus commands; putting in another words, at the resting state the right HPC influences activity in the PrL more than the left HPC, but during RPO stimulation both hippocampi equally influence activity seen in the PrL. No changes were seen during mPAG stimulation.

After establishing what changes were seen during the freezing response produced by mPAG stimulation, we assessed the effects of aPAG-induced freezing in a different group of animals. The first difference seen was that aPAG activation caused *increases* in power while mPAG caused decreases. However, the spectrograms comparing the two groups shows that the pre-stimulation activity between the two groups of animals was different. Stronger activity at higher frequencies was seen during these baseline epochs of aPAG animals compared to the mPAG group.

The increases in power promoted by aPAG stimulation were greater at the prefrontal cortex and the right hippocampus. The quadratic effect seen between the prefrontal cortex and the two hippocampi seen at pre-stimulation ($p = 0.009$) became statically insignificant during stimulation ($p = 0.61$); in other words, during pre-stimulation prefrontal power was smaller than hippocampal power, but during stimulation power in this region increased to levels that made it similar to the hippocampus.

Another difference between the two groups was seen in frequency. aPAG activation *did not* produce the same reduction in prefrontal frequency as the one seen with mPAG. Although stimulation of the aPAG did not cause any significant changes in the frequency of either of the hippocampi or the prefrontal cortex, it is important to point out that a trend is present (quadratic between sham and real stimulation, $F = 5.71$, $p = 0.075$). Although not significant, it is possible to see in Figure 4.16 that the quadratic trend of sham is eliminated during aPAG stimulation, indicated by the increase in hippocampal frequency.

For measures of synchronicity or causality, no differences caused by stimulation were seen in either group. Stimulations of the aPAG and mPAG did not produce changes in coherence, pairwise phase consistency and phase-directed coherence.

Essentially, there are two strong and significant results from these experiments:

1) mPAG provokes strong *reductions* in theta amplitude in the prelimbic cortex and hippocampus, while aPAG provokes *increases* in theta amplitude, especially in the prelimbic cortex;
2) mPAG provokes strong *reductions* in the dominant frequency in the prelimbic cortex, while aPAG provokes *no changes* in the dominant frequency in the prelimbic cortex.

Although the evoked changes in hippocampal activity suggest a role of PAG regions and hippocampal theta in anxiety and panic, there are some important caveats and unanswered questions. Firstly, other frequency bands of LFP activity were not examined in this study. It is uncertain if, for example, lower or higher frequency bands are also changed in the same way as theta during the manipulations done in the current experiments. If changes to theta are also accompanied by changes in other bands, then the specificity of the proposed PAG-induced signal would be diminished, and instead more general increases and decreases of hippocampal activity are more akin to PAG induced states rather than a single frequency band. Secondly, drastically opposed hippocampal theta effects were obtained while the same behavior (immobility) was evoked. While defensive immobility and increased hippocampal theta are generally seen as proxies of anxiety/conflict and therefore their co-occurrence is expected, it becomes harder to see how the same behavior of immobility (anxiety) would also happen concomitantly with the opposing state of lower hippocampal theta. One possibility is that, although both look extremely similar, immobility evoked by the aPAG and mPAG represent different classes of emotional responses. Perhaps aPAG immobility represents conflict/anxiety, while mPAG immobility represents anticipatory fear and a preparatory, pre-motor state prior to escape. While the phenomenon of PAG-induced escape reaction is well studied and is taken to be a model for panic attacks, the phenomenon of PAG-induced immobility is not well understood or well explained at all, leaving it open for interpretations.

But before we can further discuss the meaning of these results for the way we understand the PAG, defensive systems, fear and anxiety, we will first take a look at another experiment, reported in in the next Chapter that may help us more with these questions.

Chapter 5. Pharmacological manipulation of a region in the theta-generating system: how anxiolytic drugs in the nucleus incertus affect PAG-evoked responses

5.1. Introduction

The nucleus incertus (NI) is a small pontine nucleus, sitting on the floor of the 4th ventricle. Despite its small dimensions, the cells in the NI project widely to diverse regions in the brain, including strong projections to the PAG and dorsal raphe (Chapter 3), septum and parahippocampal cortices (Goto et al., 2001; Olucha-Bordonau et al., 2003).

The main neurotransmitter system in the NI is relaxin-3. Relaxin-3 is a highly conserved neuropeptide, being present in insects (Nassel & Vanden Broeck, 2016), fish (Donizetti et al., 2008), rodents (Ma et al., 2007), primates (Ma, Sang, et al., 2009) and humans (C. Liu et al., 2003). In the brain, the presence of cells expressing relaxin-3 is highest in the NI, where it is co-expressed by cells alongside GABA (Ma et al., 2007). Cells expressing relaxin-3 are also abundant in the PAG and DR, making these two of the regions with the largest concentrations of cell bodies expressing the neuropeptide in the brain after the NI (Smith, Ryan, Hosken, Ma, & Gundlach, 2011). Of the four relaxin receptors identified, RXFP-3 is the one for which distribution in the brain is more stably conserved across rodents and primates (Gundlach et al., 2009). Besides high concentrations in the NI, the RXFP-3 receptor and/or its mRNA is also strongly expressed in the amygdaloid complex, septum, hippocampal formation, PAG and DR, and several pontine structures surrounding the NI (Smith et al., 2010).

Given the widespread connections of the NI and relaxin-3 presence in critical brain regions known to control arousal, anxiety and learning, interest in the involvement of NI peaked in recent years. In initial experiments, electrical stimulation of the NI in anesthetized rats evoked theta rhythmicity in the hippocampus (Nunez et al., 2006). In the same report, electrolytic lesions and $GABA_A$ agonism via muscimol of the NI were both sufficient to abolish theta oscillations evoked by RPO stimulation. Later reports confirmed that NI cells respond during RPO-induced hippocampal theta, and demonstrated that NI field potentials are phase-locked with the hippocampus in the theta band (Cervera-Ferri et al., 2011; Martinez-Bellver et al., 2015). These reports indicate that the NI is an important node in the ascending arousal system, probably acting as a relay station between the reticular formation and the hippocampus/septum, and that it modulates hippocampal theta.

The NI has been shown to be involved in stress responses, and to be active during stressful events. The NI is rich in CRF1 receptors (corticotropin release factor), most of which are present in cells that also express relaxin-3, and that respond to systemic injections of CRF (Tanaka et al., 2005). Infusion of CRF into the NI also reduces neuronal firing of cells in the prelimbic cortex (Usman Farooq et al., 2013). Exposure to the elevated plus maze in rats cause c-Fos labeling in the NI, as do the administration of an anxiogenic inverse agonist of the $GABA_A$ benzodiazepine receptor (Lawther et al., 2015).

Systemic injections of an agonist of the RXFP-3 receptor indicate some anxiolytic effects. Animals that received central injections of the agonist displayed decrease anxiety-like behaviors in the light-dark box task and the elevated plus maze (Ryan et al., 2013). In this same report, injections of RXFP-3 agonist also reduced depression-like behaviors in the forced swim test, but only in animals that have been previously exposed to test, indicating some anti-stress functions of the receptor system. In a RXFP-3 knockout mouse model, however, animals were shown to be hypoactive and to locomote less than control animals (Hosken, Sutton, Smith, & Gundlach, 2015), probably indicating that any antidepressive or anti-stress effects of activating the RXFP-3 receptor in the forced swim test could be cofounds from enhanced motor activity. Two other reports on RXFP-3 gene knockout mice confirmed that animals with the gene deletion are more hyporeactive, and also failed to show any behavioral changes in anxiolytic tests such as the open field test, elevated-plus maze test, light-dark box test and novel object exploration test (Smith, Hosken, Sutton, Lawrence, & Gundlach, 2012; Smith, Lawrence, Sutton, & Gundlach, 2009). This lack of change in the gene deleted animals could be explained by a later investigation showing that central administration of relaxin-3 agonist did not change behaviors in anxiety tests, but did counteract some of the anxiogenic effects of an inverse agonist of the $GABA_A$ benzodiazepine receptor (C. Zhang et al., 2015).

Although evidence of involvement of both the NI and RXFP-3 systems in the control of hippocampal theta rhythm is plentiful, its exact role in controlling anxiety-like behaviors is unclear. Equally, while anatomical and immunohistochemical evidence supports the notion that the NI has some form of influence over the PAG, no direct experimental evidence of NI modulation over PAG and its behaviors is available.

In Chapter 4, I demonstrated how mPAG stimulation provokes a reduction in hippocampal and prefrontal theta power, along with reductions in prefrontal frequency as well. In this Chapter, I aim to investigate how manipulations of the serotonergic, benzodiazepinergic, and both the agonism and antagonism of RXFP-3 in the NI and surrounding areas affect the activity evoked by PAG and RPO stimulation.

If RPO activation is indicative of anxiety, and PAG activation indicative of fear/panic, I expect that changes in one system will not happen in the other, or that the changes will occur in opposing directions; that is, if the anxiolytic drugs in the NI reduce RPO-induced hippocampal power, I expect these drugs to have no effect on PAG-induced hippocampal power – or to cause changes in a different direction, by increasing power.

Therefore, the experiments in this Chapter have two objectives:

1) To understand if pharmacological manipulation of NI receptor systems change PAG-induced states in the hippocampus and prefrontal cortex, and;
2) To test the hypothesis that mPAG-induced states are different from RPO-induced states, supporting the view that the cortico and hippocampal changes observed during mPAG stimulation on Chapter 5 are not anxiety-related but more likely fear-related.

5.2. Methods

For this experiment, a subgroup of 6 Sprague-Dawley rats from the cohort used in the first experiment in Chapter 4 were used. These animals had bipolar stimulating electrodes implanted in the mPAG and RPO, LFP recording electrodes placed bilaterally in the hippocampus, and a guide cannula implanted at the NI. The housing, surgical, recording, behavioral procedures, apparatus and data processing are described in the general methods section in Chapter 4.

5.2.1. Intracerebral microinjections

The drugs used in this investigation were: Chlordiazepoxide (CDP), a benzodiazepine anxiolytic; Buspirone, a 5-HT_{1A} receptor agonist anxiolytic; RXFP3-A2, a RXFP-3 receptor selective agonist (Shabanpoor et al., 2012); R3B(1-22)R, a RXFP-3 receptor antagonist (Haugaard-Kedstrom et al., 2011). CDP and Buspirone were purchased from Sigma (USA) and the two relaxin peptides were synthesized and supplied by Professor Andrew Gundlach of the Florey Institute and the University of Melbourne (Victoria, Australia). All compounds were dissolved in physiological saline (0.9% NaCl; 2mg/ml) and the volume injected was 0.5µL based on previous studies (Ma et al., 2017; Nategh et al., 2015) and preliminary data from our laboratory. Physiological saline was used as control. 24 hours were allowed between each drug administration, and a counterbalanced design was used in this experiment, with animals receiving all drugs in different orders.

5.2.2. Experimental session and design

After the animal was placed inside of the experimental chamber and the recording cable was connected to its head implant, an injecting cannula was inserted into the guide cannula cemented to the rat's head implant. The tip of this injecting cannula was set to protrude 1mm beyond the tip of the guide cannula, and to reach the NI. A polyethylene tube was attached to the injecting cannula, and connected to a 1µL glass syringe (Hamilton, USA). All drugs were injected at a rate of 0.25uL/min by an automatic syringe pump (Razel Scientific, USA). Once the drug trial session began, the animals were not disturbed by experimenter intrusion.

The doors for the observation box and acoustic chamber were closed, and the animals were allowed a 2 minute period for acclimatization. After this, the experimental session proper was initiated. Each session lasted around 20 minutes, and involved sequential RPO and PAG electrical stimulation trains as described in Chapter 4, and also illustrated here in Figure 5.1: a 1-second RPO train, followed 30 seconds later by an 8-second PAG train, for the duration of the session. After an initial baseline period of 5 minutes, the injection pump was turned on and infusion of the experimental solution begun. The progress of the injection was monitored by the movement of a small air bubble inside of the polyethylene tube. The injection time for 0.5µL was on average 2:00 minutes, after which the pump was turned off and the animal remained inside the chamber for 10 more minutes.

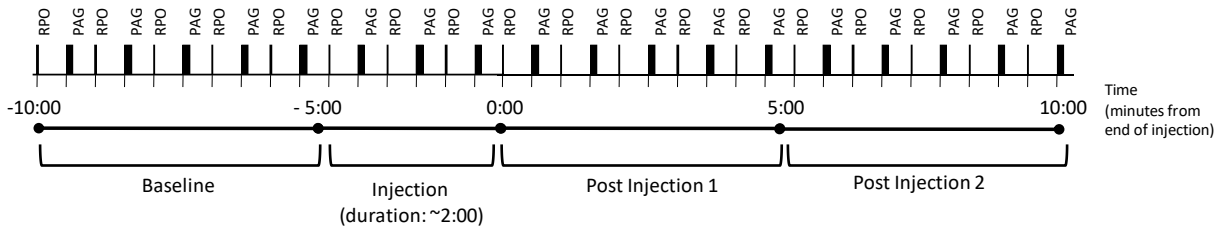

Figure 5.1. Components of the experimental session. Each session lasted approximately 20 minutes. Data from the baseline period (a block of 5 minutes previous to the start of drug injection), from post injection 1 (a block of 5 minutes immediately following end of injection) and post injection 2 (a blocks of 5 minutes following post injection 1) were used for analysis in this experiment. Each 5 minute block contains 5 samples of the three types of stimulation (PAG, RPO and Sham).

5.2.3. Data processing

Similar to what was described in Chapter 4, LFP data segments based on the onset of stimulation trains were extracted for analysis. For this Chapter, three segments were produced:

a “sham” condition, corresponding to a 1-second unstimulated period before the onset of PAG stimulation; a PAG condition, corresponding to the initial 1-second period of the PAG; and a RPO condition, corresponding to the whole 1-second RPO train. Since no general differences were seen between “sham PAG” and “sham RPO” in Chapter 4, in this experiment a single “sham” period was used for simplicity, also allowing the extraction of stimulation effects as a quadratic component and differences between PAG and RPO as a linear component.

For statistical analysis, these stimulation periods were then averaged across three time blocks as seen in Figure 5.1.: a pre-injection control block (baseline); an immediate post-injection block (post injection 1) and a later post-injection block (post injection 2). Each block contains 5 averaged stimulation periods for each stimulation type (PAG, RPO and sham). The effects of the drugs were extracted as the quadratic component of time (i.e. the difference between post injection 1 and the average of the periods before and after it). Similarly, for analysis, the drug conditions were ordered as CDP, saline, Buspirone so that general anxiolytic action could be assessed as a quadratic component; and agonist, saline, antagonist so that the RXFP-3 effect overall could be assessed as a linear component.

5.2.4. Histology

The localization of the recording and stimulating electrodes are shown in in Figures 4.3 to 4.6 in Chapter 4. The localization of the cannula tips and estimated spread of the injected fluids are shown here in Figure 5.2.

The diffusion of fluids from the centerpoint of injection sites in brain tissue is estimated to be around 1mm for a 0.5µL volume (Myers, 1966). Based on this, the histological reconstructions show that of the animals included in this study, three had injection tips that fell within a 1mm radius of the right NI. Three other rats in which the dispersion of the drugs was estimated to have not reached the NI were used as control animals (outside of NI, *OS*). Of these three rats in the OS group, two had injections in the right locus coeruleus and surrounding structures, such as the dorsal part of the subcoeruleus nucleus, the central grey of the pons and several small trigeminal nuclei, and the last one had injections limited to a small portion of the pontine reticular nucleus. No lesions or necrosis at the injection site were observed in any of the animals tested.

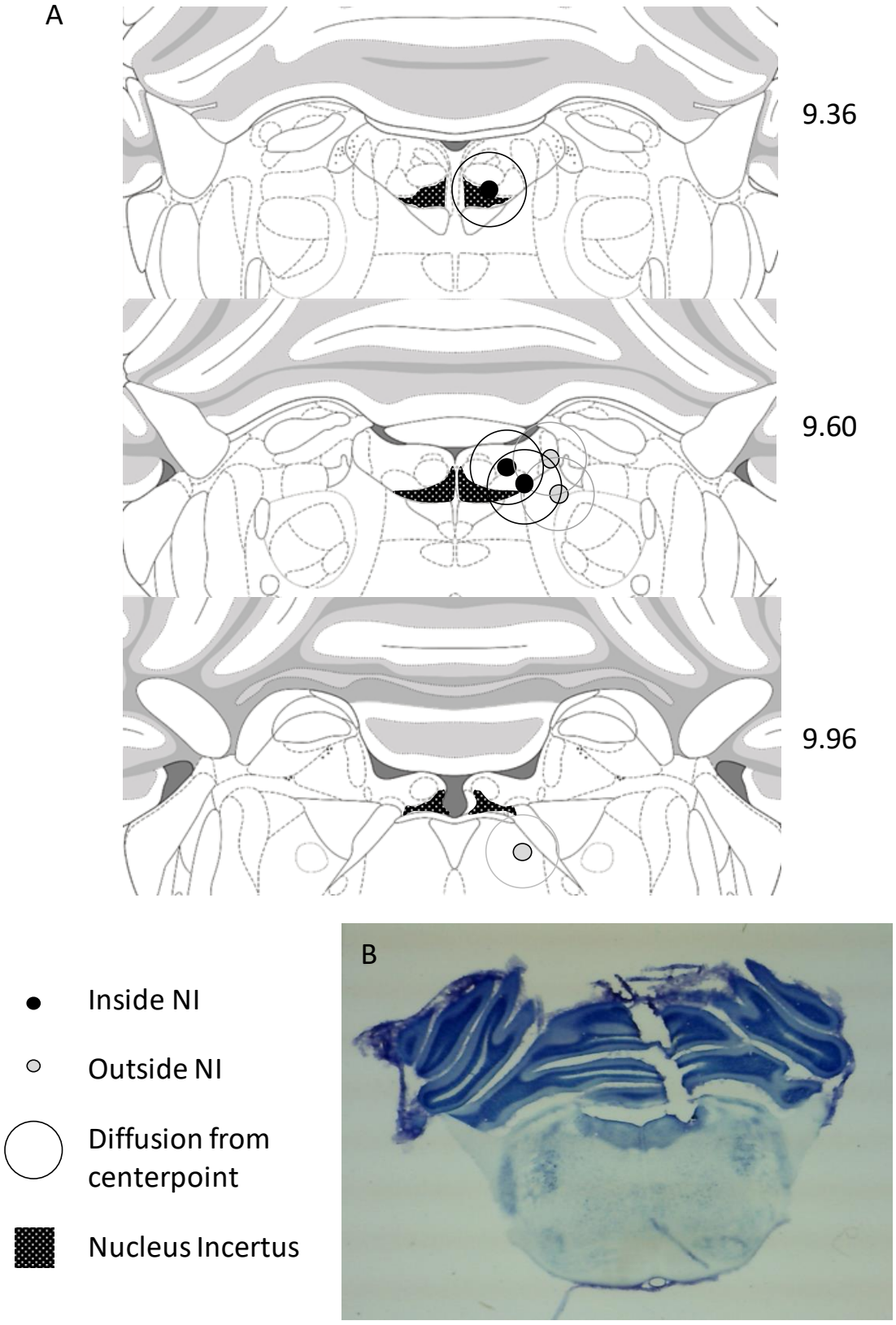

Figure 5.2. Histological reconstruction of sites of injection. Panel A shows the location of the tips of the injector cannula, along with the estimated diffusion of the compounds. Panel B shows the cannula tract in the brain of a representative rat.

5.3. Results

Note: some result figures mentioned in the text are located at the postscript section at the end of the thesis. These figures are identified by the letter P before their numbering, which is sequential with the figures included in this chapter.

5.3.1. CDP and buspirone

Theta power. The overall means summarizing theta power findings under CDP, saline and Buspirone is shown in Figure P5.3 (Postscript). An initial statistical analysis revealed significant interactions that were group dependent (Stim [linear] x Drug [linear] x Region [linear] x Time [quadratic], $F(1,4) = 31.6$, $p = 0.005$). Post hoc tests were conducted with the two groups separately in order to detect which one was the source of the detected effect. These effects were revealed to be significant in the animals that received drug injections in the NI (Stim [linear] x Drug [linear] x Region [linear] x Time [quadratic], $F(1,2) = 65.62$, $p = 0.015$), but not the ones with injection outside of the NI (Stim [linear] x Drug [linear] x Region [linear] x Time [quadratic], $F(1,2) = 3.43$, $p = 0.205$).

The significant contrasts are summarized in Figure 5.4. Let us focus in panel A of Figure 5.4 which details the effects of drugs during PAG stimulation. The left portion of the image shows LFP power levels for the two hippocampi sites under the CDP condition. No significant changes between the time points are seen, either in the form of a linear or quadratic trend. Moving to the right side of the image, we see the same brain regions under the Buspirone treatment. In here, it is possible to see that the L-HPC shows a significant quadratic trend of time, with increased LFP power being registered in the post injection 1 time point; this trend is not seen in the R-HPC or in any of the regions under CDP. Down below, in panel B, we see the effects of the two drugs during RPO stimulation. This panel shows that neither CDP nor Buspirone display a quadratic trend of time.

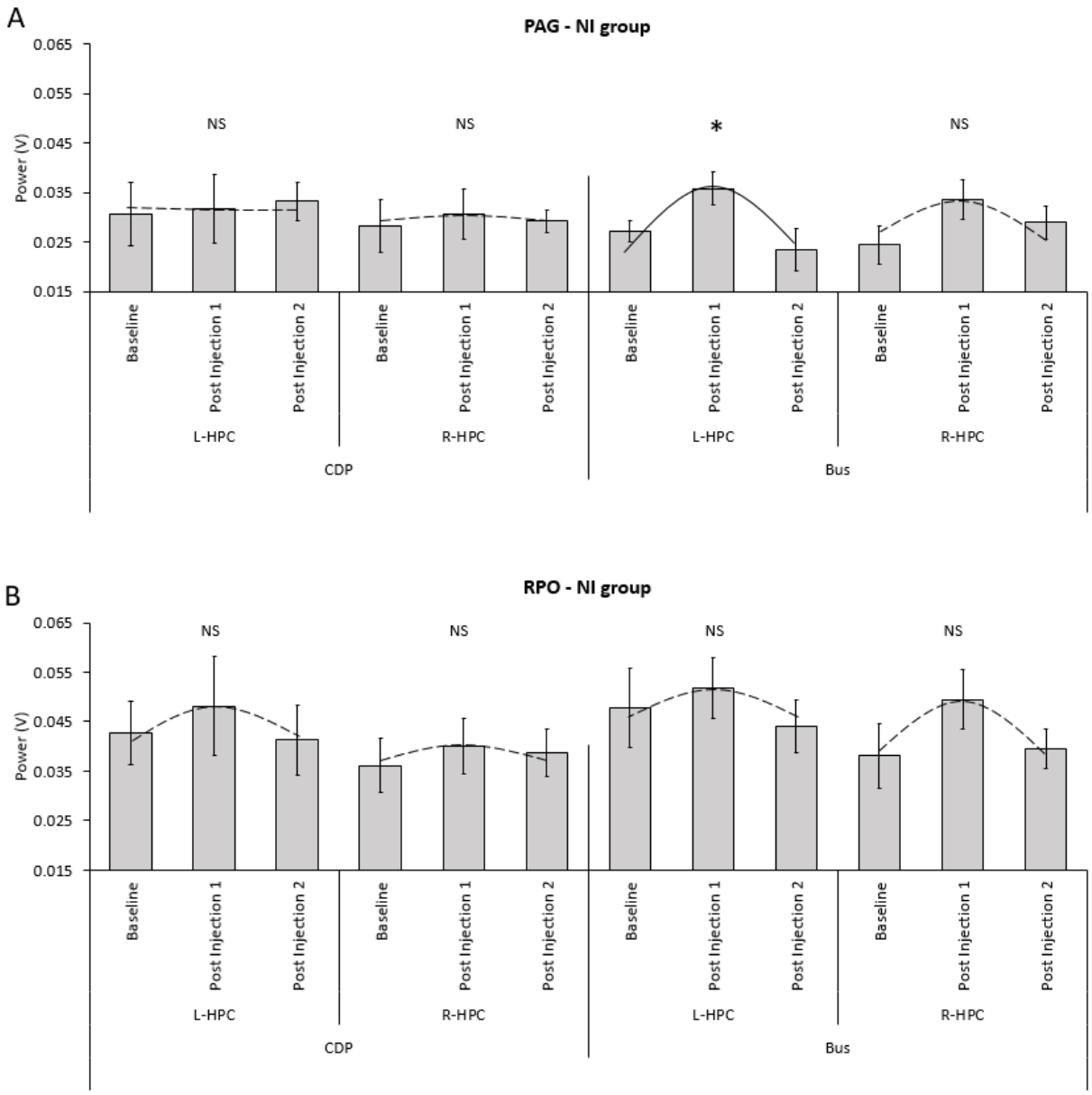

*Figure 5.3. Summary of LFP power data in the significant contrast of Stim x Drug x Region x Time (linear, linear, linear, quadratic) in the NI injection group. Panel A: PAG stimulation. Panel B: RPO group. NS = non-significant; * = significant.*

Frequency. The overall means summarizing frequency findings under CDP, saline and Buspirone are shown in Figure P5.5 (Postscript), and a significant group effect was observed (Stim [linear] x Drug [quadratic] x Region [quadratic] x Time [linear], $F(1,4) = 12.40$, $p = 0.024$). A post hoc of the NI group did not show significance in this contrast (Stim [linear] x Drug [quadratic] x Region [quadratic] x Time [linear], $F(1,2) = 2.97$, $p = 0.227$), and the effect was revealed to come from the OS animals (Stim [linear] x Drug [quadratic] x Region [quadratic] x Time [linear], $F(1,2) = 20.55$, $p = 0.045$).

These results indicate that in the OS group, but not NI, both CDP and Buspirone promote reductions in hippocampal frequency in relation to PrL frequency, during only one type of stimulation. Figure 5.6 summarizes the significant contrasts in the OS group. In panel A, we can see the magnitude of the quadratic effect over time; that is, the difference in the quadratic trend of stimulation and drug from baseline to post injection 2. In it, we can see that the largest decrease in frequency comes from the drug treatment during RPO stimulation. Panels B and C show frequency patterns during PAG and RPO stimulation, respectively. At the right side of the image, we can see that the quadratic effect of drug comes mostly from Buspirone during RPO, but not PAG stimulation.

Theta coherence and PPC. No group dependent effects were seen in coherence. By pooling the groups together (Figure P5.7, Postscript), a significant interaction was found (Stim [linear] x Drug [quadratic] x Region [linear] x Time [quadratic], $F(1,4) = 16.81$, $p = 0.015$). Figure 5.8 compares the effects of drugs over PAG and RPO stimulation. Panel A shows the quadratic effect of time, indicating that the experimental drugs increased coherence between the R-HPC and PrL during RPO stimulation only. This drug effect on RPO only was confirmed by a post hoc tests of each stimulation group separately (Sham stim: drug [quadratic] x region [linear] x time [quadratic], $F(1,5) = 0.13$, $p = 0.72$; PAG stim: drug [quadratic] x region [linear] x time [quadratic], $F(1,5) = 0.20$, $p = 0.66$; RPO stim: drug [quadratic] x region [linear] x time [quadratic], $F(1,5) = 24.97$, $p = 0.004$). Panels B and C show PAG and RPO stimulation results, respectively. In panel C, R-HPC x PrL coherence under CDP and Buspirone increase at post injection 1; however, the baseline levels of these drugs is also lower than the others.

Another apparent effect seems to be one of time. Figure 5.7 shows that in almost all stim x drug cases, coherence tends to decrease in post injection periods compared to baseline. It is unlikely that this is a pure drug effect, as the reduction also happens during saline treatment x stimulation. The exception to this trend is the combination of saline x sham stimulation, where no reductions in coherence are seen. Therefore, it appears that the reductions in coherence over time are a mix of the after effects of the stimulations and drugs, as during the combination of sham stim and saline no changes in coherence occur over time.

For PPC, analysis revealed a group effect, albeit marginally significant (Stim [linear] x Drug [linear] x Region [linear] x Time [linear] x Injection group, $F(1,4) = 7.80$, $p = 0.049$). The group means are shown in Figure P5.9 (Postscript). A comparison of the two groups on the significant contrast interactions is shown in Figure 5.10. No group trend appears significant, and post hoc analysis did not show any significant effects by group (NI: Stim [linear] x Drug [linear] x

Region [linear] x Time [linear], $F(1,2) = 5.20$, $p = 0.150$; OS: Stim [linear] x Drug [linear] x Region [linear] x Time [linear], $F(1,2) = 3.77$, $p = 0.192$).

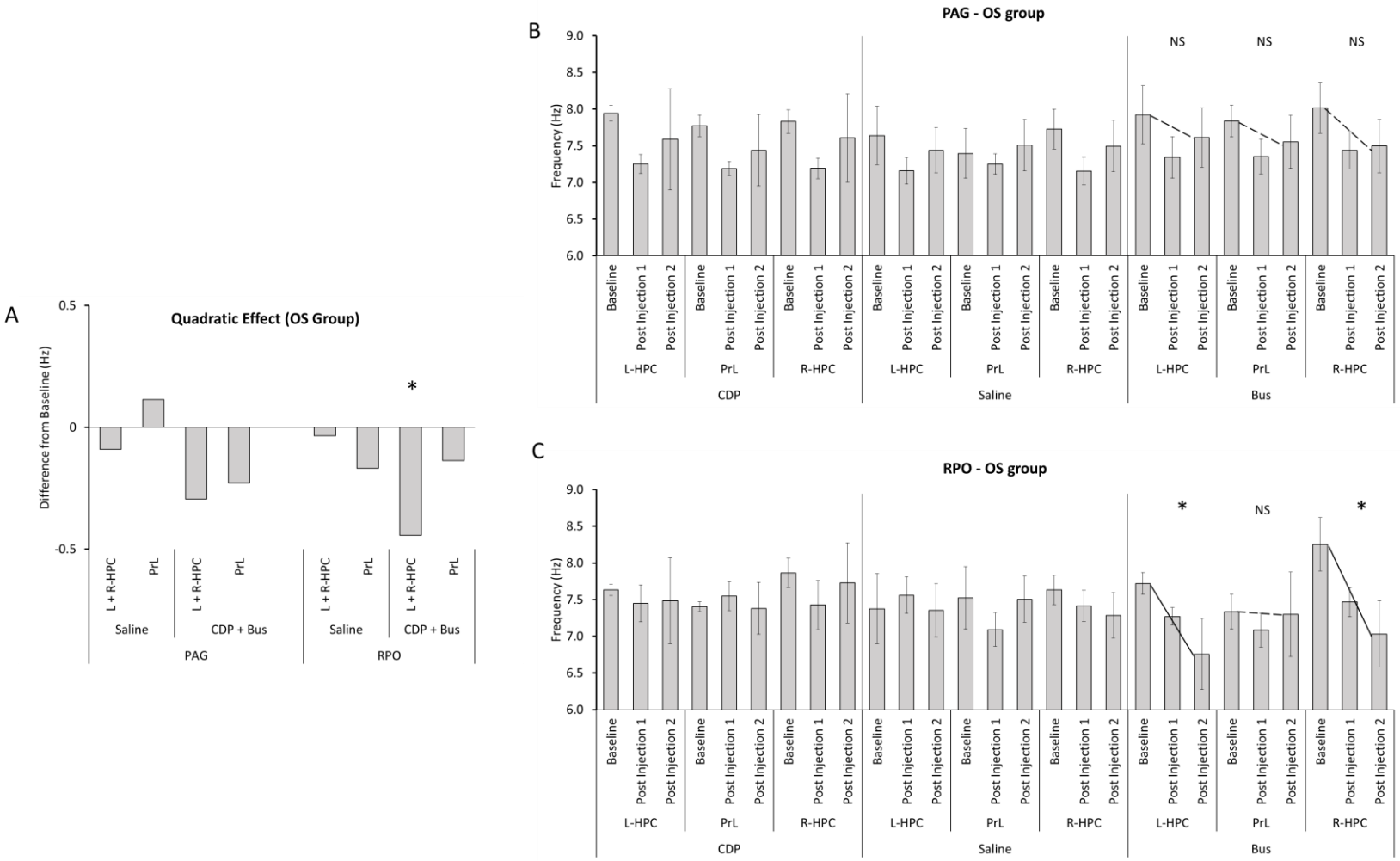

*Figure 5.4. Summary of LFP frequency data in the significant contrast of Stim x Drug x Region x Time x Injection (linear, quadratic, quadratic, linear) in the OS injection group (N=2). Panel A: The quadratic effect a factor of time under both PAG and RPO stimulations. Panel B: Effect of drugs over time during PAG stimulation. Panel C: Effect of drugs over time during RPO stimulation. NS = non-significant; * = significant.*

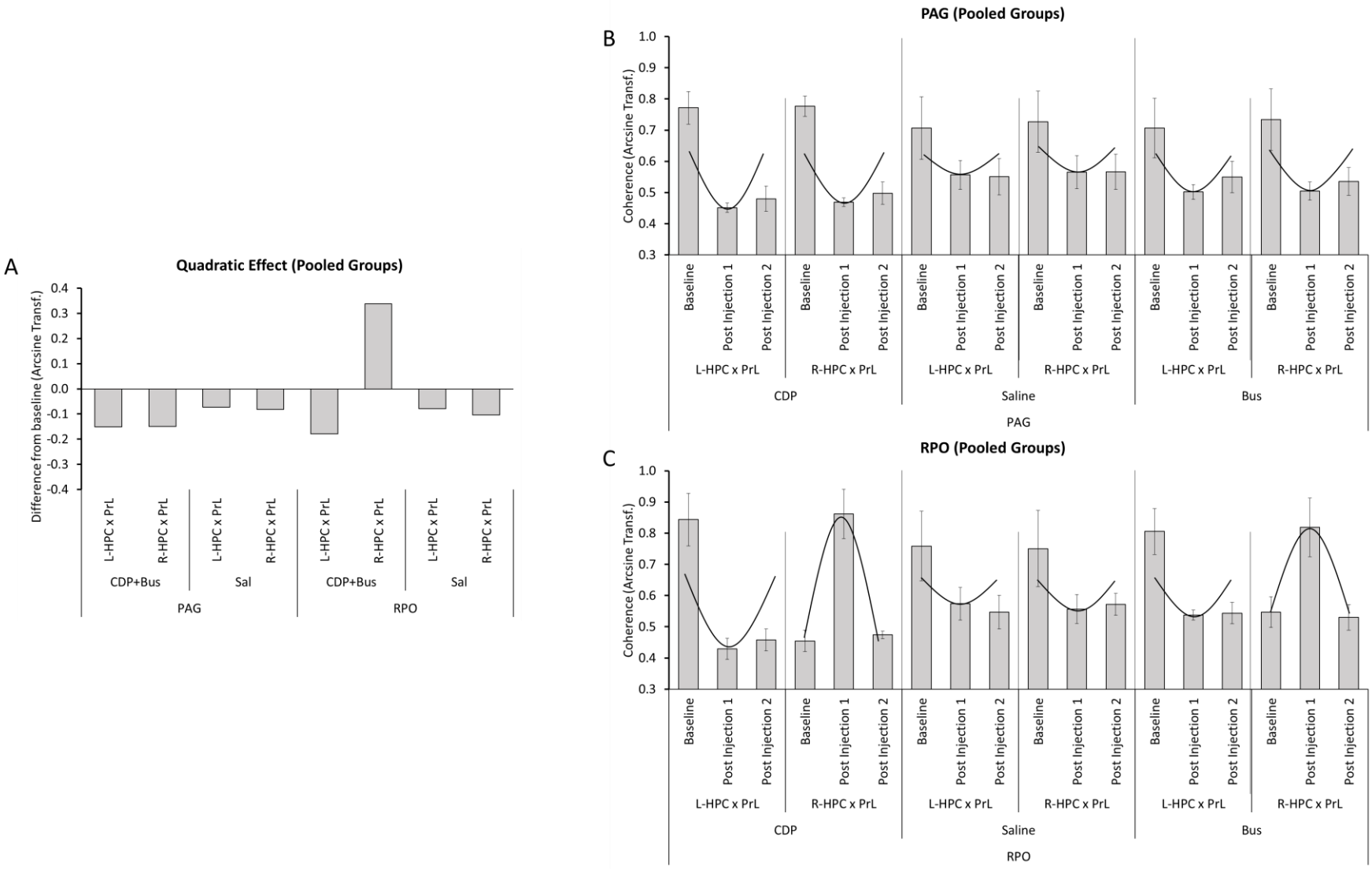

*Figure 5.5. Summary of coherence data in the significant contrast of Stim x Drug x Region x Time (linear, quadratic, linear quadratic) with injection groups pooled (N=6). Panel A: The quadratic effect as a factor of time under both PAG and RPO stimulations. Panel A: Effect of drugs over time during PAG stimulation. Panel B: Effect of drugs over time during RPO stimulation. NS = non-significant; * = significant.*

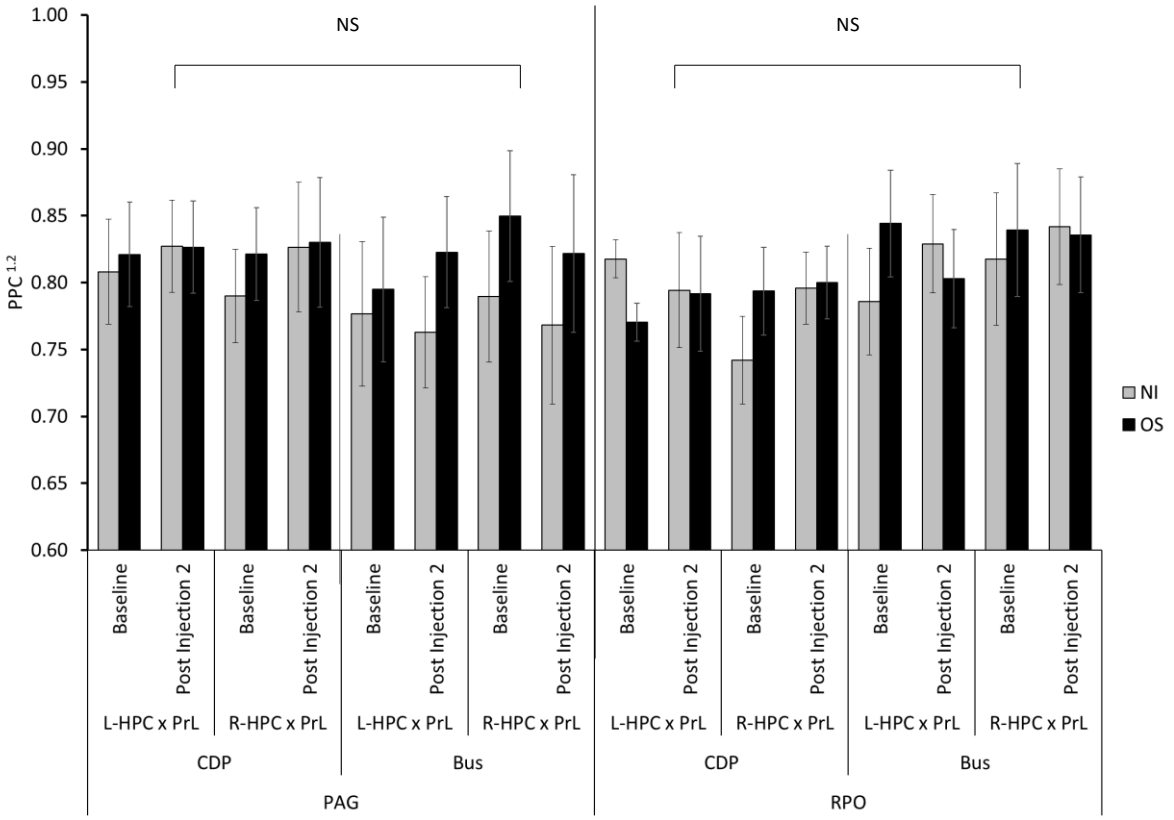

Figure 5.6. Summary of PPC data in the contrast of Stim x Drug x Region x Time (linear, linear, linear, linear), with both groups shown (NI, N=3; OS N=3). NS = non-significant.

5.3.2. RXFP3-A2 and R2B(1-22)R

Theta power. A difference between groups was seen in the highest level of interactions (Stim [linear] x Drug [quadratic] x Region [linear] x Time [quadratic] x Injection group, $F(1,4) = 20.05$, $p = 0.011$). The overall trends for both groups are shown in Figure P5.11 (Postscript). Post hoc tests of groups revealed the effect to be present in the NI group (Stim [linear] x Drug [quadratic] x Region [linear] x Time [quadratic], $F(1,2) = 4049.98$, $p < 0.000$), but not in the OS group (Stim [linear] x Drug [quadratic] x Region [linear] x Time [quadratic], $F(1,2) = 1.57$, $p = 0.337$).

Figure 5.12 shows the significant contrasts in this analysis. Panel A shows the quadratic difference between post injection 1 and the average of baseline and post injection 2. The largest change between the drug treatments and saline is seen on the left hippocampus during PAG stimulation; under saline treatment, L-HPC power drops in post injection period 1, and this is counteracted by the drug treatments which increase power in the same region. Although a somewhat similar trend is seen with the R-HPC during RPO stimulation, this effect was not

proved to be significant. Panel B shows the overall trends and quadratic lines fitted to the graphs. It is possible to see that L-HPC under PAG stimulation is the only region that went from a negative quadratic shape in saline to a positive one under drug treatments, while all combinations of stimulation, region and drugs showed only positive quadratic trends.

Frequency. Figure P5.13 (Postscript) shows the overall pattern of drugs effects under PAG and RPO stimulation. Statistical test showed that there was a group dependent effect with two significant complex interaction at the highest level (Stim [linear] x Drug [linear] x Region [linear] x Time [quadratic] x Injection group, $F(1,4) = 39.40$, $p = 0.003$; and Stim [linear] x Drug [quadratic] x Region [quadratic] x Time [linear] x Injection group, $F(1,4) = 26.56$, $p = 0.007$). Post hoc analysis showed that the effect was coming from the OS group (Stim [linear] x Drug [linear] x Region [linear] x Time [quadratic], $F(1,2) = 170.11$, $p = 0.006$ and Stim [linear] x Drug [quadratic] x Region [quadratic] x Time [linear], $F(1,2) = 181.41$, $p = 0.005$) and not from the NI group (Stim [linear] x Drug [linear] x Region [linear] x Time [quadratic], $F(1,2) = 6.69$, $p = 0.123$ and Stim [linear] x Drug [quadratic] x Region [quadratic] x Time [linear], $F(1,2) = 6.60$, $p = 0.129$, respectively).

This initial result points to PAG stimulation being different from RPO stimulation (linear component of stim) with all other factors showing both significant linear and quadratic elements. Within the OS group, post hocs of PAG and Sham stimulation do not hold significance in the contrasts (PAG: Drug [linear] x Region [linear] x Time [quadratic], $F(1,2) = 2.38$, $p = 0.263$ and Drug [quadratic] x Region [quadratic] x Time [linear], $F(1,2) = 0.16$, $p = 0.725$; Sham: Drug [linear] x Region [linear] x Time [quadratic], $F(1,2) = 2.57$, $p = 0.250$ and Drug [quadratic] x Region [quadratic] x Time [linear], $F(1,2) = 0.72$, $p = 0.485$). Testing of the RPO stimulation, however, showed that one of the contrasts was significant (Drug [linear] x Region [linear] x Time [quadratic], ($F(1,2) = 19.48$, $p = 0.048$), but not the other (Drug [quadratic] x Region [quadratic] x Time [linear] ($F(1,2) = 3.11$, $p = 0.220$).

These results indicate that RXFP3-A2, but not R3B(1-22)R, reduce R-HPC frequency during RPO stimulation, but not during PAG, in animals in the OS group, but not the ones in the NI group. This is summarized in Figure 5.14.

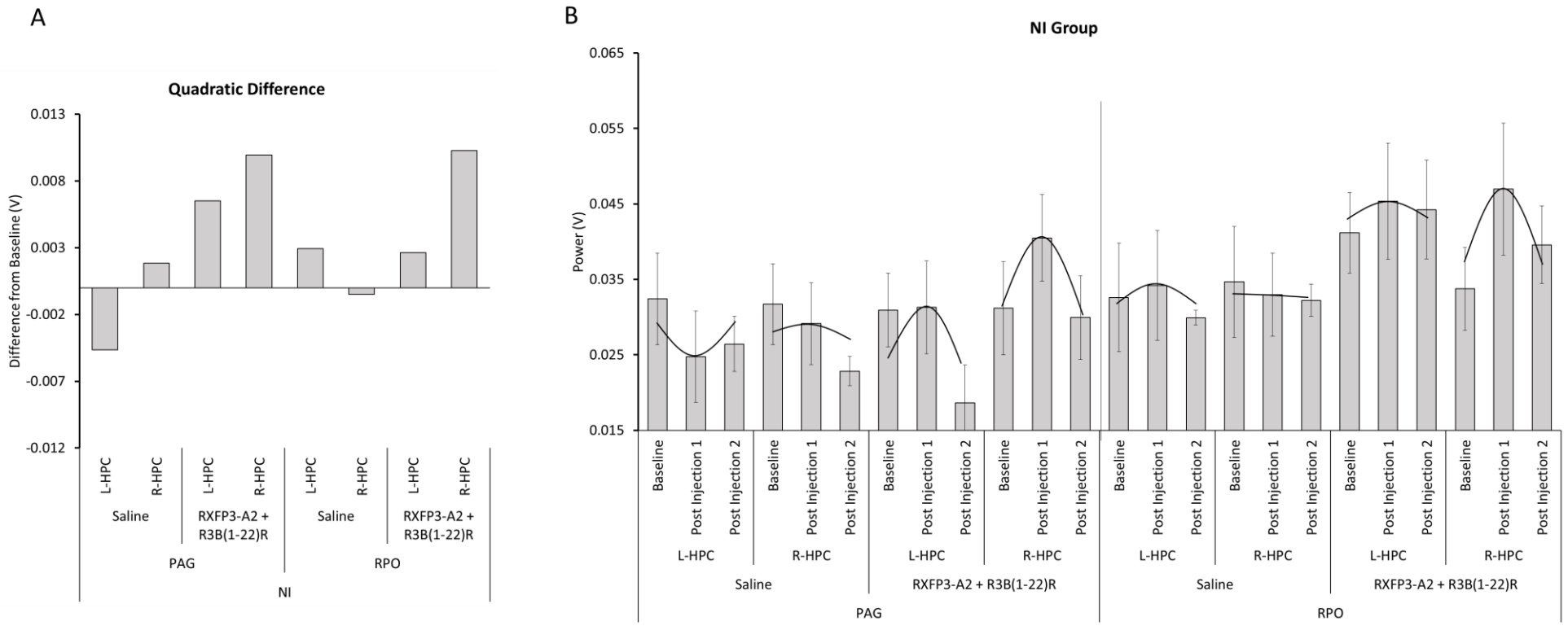

Figure 5.7. Summary of LFP power data in the significant contrast of Stim x Drug x Region x Time (linear, quadratic, linear, quadratic) in the NI injection group (N=3). Panel A: The quadratic effect as a factor of time under both PAG and RPO stimulations. Panel B: Effect of drugs over time during PAG and RPO stimulation.

Theta coherence and PPC. Trends for coherence under stimulation and drug treatments, for both groups, are shown in Figure P5.15 (Postscript). There were no significant interactions of the highest level between groups (Stim [linear] x Drug [linear] x Region [quadratic] x Time [linear], $F(1,4) = 6.28$, $p = 0.066$; Stim [quadratic] x Drug [linear] x Region [quadratic] x Time [linear], $F(1,4) = 4.20$, $p = 0.110$). With the groups pooled together, no significant interactions were found either (Stim [linear] x Drug [linear] x Region [quadratic] x Time [linear], $F(1,4) = 0.97$, $p = 0.380$; Stim [quadratic] x Drug [linear] x Region [quadratic] x Time [linear], $F(1,4) = 5.84$, $p = 0.073$).

Trends for PPC are shown in Figure P5.16 (Postscript). Analysis revealed two group-dependent trends at the highest level of interactions (Stim [linear] x Drug [linear] x Region [linear] x Time [quadratic], $F(1,4) = 8.74$, $p = 0.042$; and Stim [quadratic] x Drug [linear] x Region [linear] x Time [quadratic], $F(1,4) = 8.53$, $p = 0.043$). Post hoc tests of groups did not show any significant interactions for the contrasts of interest (NI group: Stim [linear] x Drug [linear] x Region [linear] x Time [quadratic], $F(1,2) = 0.79$, $p = 0.467$ and Stim [quadratic] x Drug [linear] x Region [linear] x Time [quadratic], $F(1,2) = 10.11$, $p = 0.086$; OS group: Stim [linear] x Drug [linear] x Region [linear] x Time [quadratic], $F(1,2) = 10.89$, $p = 0.081$ and Stim [quadratic] x Drug [linear] x Region [linear] x Time [quadratic], $F(1,2) < 0.000$, $p = 0.98$). The data from the two groups are compared in Figure P5.17 (Postscript).

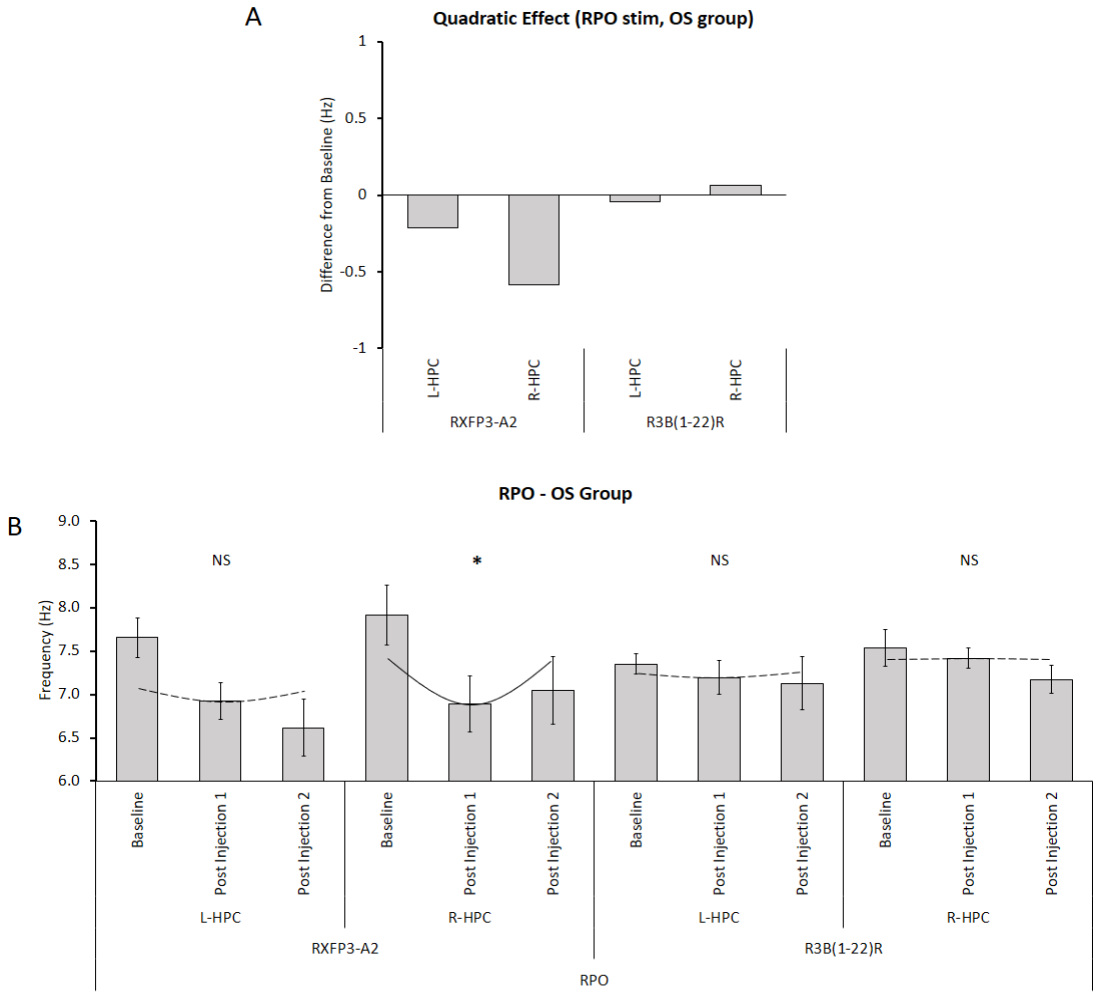

*Figure 5.8. Summary of LFP frequency data in the significant contrast of Drug x Region x Time (linear, linear, quadratic) in the OS injection group during RPO stimulation (N=3). Panel A: The quadratic effect as a factor of time under RPO stimulation. Panel B: Effect of drugs over time during RPO stimulation. NS = non-significant. * = significant.*

5.4. Summary and data discussion

In this Chapter, the effect of two anxiolytic drugs (CDP and Buspirone) and an agonist and an antagonist of the RFXP3 receptor (RXFP3-A2 and R3B(1-22)R – referred to from now on as agonist and antagonist for clarity) were assessed on PAG- and RPO-elicited LFP oscillations. CDP and buspirone were selected for their shared anxiolytic effects, despite different pharmacodynamics: CDP acts on the benzodiazepine receptor, enhancing $GABA_A$ receptor activity, and buspirone acts as an agonist of the $5\text{-}HT_{1A}$ receptor. The interest in the RFXP3 peptides stems from the tentative involvement of the RFPX3 receptor in the regulation of motivational and emotional states in the brain. The drugs were administered intracerebrally in the Nucleus Incertus, as this region has strong projections to the PAG, and is known to modulate

hippocampal theta. A second group of animals, with injections to structures surrounding the NI, were also used in this experiment. The expectation in this experiment is that NI has a dual purpose of regulating fear (by influencing PAG) and anxiety (by influencing reticular-induced hippocampal theta).

In Chapter 5, I demonstrated how activation of the mPAG at the freezing threshold caused marked reductions in hippocampal and prelimbic LFP power, and also reductions in prelimbic frequency. RPO stimulation, on the other hand, is known to provoke increases in hippocampal power and frequency. This RPO-elicited hippocampal activity is a reliable method of testing the efficacy of anxiolytic drugs. The nature of this PAG-induced signal in hippocampal and cortical oscillations, on the other hand, is unknown.

The experiments in the current Chapter had several purposes. First, there are two pharmacological questions that need to be answered: 1) do benzodiaze receptor and 5-HT_{1A} receptor manipulations in the NI change RPO-elicited hippocampal responses; and 2) do relaxin-3 agonism and antagonism also change RPO-elicited hippocampal responses? If the answer to these questions is Yes, and these drugs are shown to cause changes, then another question of interest is: 3) are these drugs causing similar or different changes to PAG- and RPO-induced states? This last question is of particular interest in order to elucidate the nature and meaning of the PAG-induced changes demonstrated in Chapter 5.

Table 5.1. Summary of results from CDP and Buspirone analysis in this Chapter.

		PAG	Sham	RPO
CDP / BUS	Power	Between Group F = 31.6 NI Group F = 65.62 OS Group F = 3.43 Buspirone @ NI ↑ hippocampal power	no detected effect	no detected effect
	Frequency	no detected effect	no detected effect	Between Group F = 12.40 NI Group F = 2.97 OS Group F = 20.55 CDP+Bus @ OS ↓ hippocampal frequency
	Coherence	no detected effect	no detected effect	No Group Effect, Pooled F = 16.81 PAG F = 0.20; Sham F = 0.13 RPO F = 24.97 Time effects / baseline shift
	PPC	no detected effect	no detected effect	Between Group F = 7.80 NI Group F = 5.20 OS Group F = 3.77 no detected effect

p-value: < 0.04 | from 0.04 to 0.1 | > 0.1 Effects from: Nucleus Incertus | Outside Areas

Table 5.2. Summary of results from RXFP3-A2 (ago) and R3B(1-22)R (ant) analysis in this Chapter.

		PAG	Sham	RPO
AGO / ANT	Power	Between Group F = 20.05 NI Group F = 4049.98 OS Group = 1.57 Ant+Ago @ NI ↑ hippocampal power	no detected effect	no detected effect
	Frequency	no detected effect	no detected effect	Between Group F = 39.40 NI Group F = 6.69 OS Group = 170.11 Ago @ OS ↓ hippocampal frequency
	Coherence	no detected effect	no detected effect	Between Groups F = 6.28; 4.20 Pooled Groups F = 0.97; 5.84 no detected effect
	PPC	no detected effect	no detected effect	Between Group F = 8.74; 8.53 NI Group F = 0.79, 10.11 OS Group F = 10.89; 0.00 no detected effect

p-value: < 0.04 | from 0.04 to 0.1 | > 0.1 Effects from: Nucleus Incertus | Outside Areas

Tables 5.1 and 5.2 summarize the findings of this Chapter. As demonstrated in the previous Chapter, PAG stimulation *reduces* hippocampal power dramatically; in this Chapter, buspirone was shown to *increase* hippocampal power, partially counteracting the effects of PAG stimulation. This effect was strongly connected to manipulations of the NI but not the OS group ($F = 65.62$ vs. $F = 3.43$). Also, this change was only seen during PAG stimulation, and not during sham or RPO stimulation, indicating a pathway-specific drug effect. Similarly, the same results were found with relaxin agonist and antagonist manipulations, where both compounds *increased* hippocampal power during PAG stimulation only.

Analysis of frequency also showed consistent, stimulation-depend effects of drugs: CDP and buspirone both *reduced* hippocampal frequency during RPO stimulation only, but not during PAG stimulation. With the relaxin peptides, the RFXP3 agonist also reduced hippocampal frequency during RPO stimulation only. Unlike the power results, however, these effects of the drugs were observed in animals that received injections *outside* of the NI but not inside.

With the two measures of neural synchronicity used here (coherence and PPC), results are less clear. In the CDP/Bus analysis, no group effect was detected with coherence; that is, if the injection of drugs provoked changes, these changes are independent of *where* the injections were performed. In the image summarizing the overall effects of drugs over coherence (Figure 5.7) it is possible to see a striking effect of time; that is, even during saline injection, coherence between the regions tend to *decrease* over time. While in a sense this is a blow to any experimental inference (that is, the interpretability of the effect of drugs), a peculiar pattern is evident: coherence tends to remain stable over time during saline injections under sham stimulation only. This points to the possibility that the reductions in coherence observed here are probably a compound effect of repeated stimulations *and* the effect of drugs.

By conducting statistical analysis on coherence measures with the two injection groups pooled together, a strong effect was observed in the RPO group but not in the PAG or Sham groups ($F = 24.97$, $F = 0.20$, $F = 0.13$, respectively). In here, we see a second unexpected, albeit consistent, result (showed also in Figure 5.8): in the CDP and buspirone sessions, compared to saline, coherence was greatly increased after injection of the drugs, even if a possible common effect of time affected both the drug and saline groups. However, this change only occurs because coherence during the baseline period (the blocks of time *before* any drug was infused) was much lower than what was seen in saline sessions. While this could be seen as an experimental fluke, this shift was only seen in R-HPC x L-PrL coherence, and not in the coherence among other regions. As a reminder, the animals in this project had electrodes

implanted in the right hemisphere for reticular stimulation, and in the left hemisphere for PAG stimulation. It would be possible that the changed right hippocampus/left PrL coherence seen here could also be a partial effect of lateralization of stimulation.

More crucially, no unusual baseline shifts were seen in the same animals when these were tested with the relaxin compounds (Figure 5.15). For the relaxin peptides, no significant between group effects were observed. A failure to detect any significant effects remained after pooling the two groups together.

For PPC, both with CDP x Buspirone and Agonist x Antagonist, initial group effects were detected. In both cases, these were modest in terms of significance and effect sizes (between F= 7.80 and 8.74). CDP x Buspirone, post hocs did not show any strong effects or significance; for agonist x antagonist, although no statically significance was observed, the separation of the two groups yielded an increase of the observed F-ratio. Each group showed strong effects in different contrasts (F = 10.11 for NI; F = 10.89 for OS), indicating some unique interactions in each group. This result indicates that, unlike CDP and buspirone, the relaxin compounds appear to cause real changes in coherence; however, in order to reach higher levels of significance and precision, a study with a larger sample size is required here.

Perhaps the first pattern to emerge with these results is that changes caused by drugs were stimulation-dependent. That is, no changes in power, frequency or neural synchronicity were seen during the basal states of sham stimulation. If the PAG- and RPO-induced neural signals are to be interpreted as being proxies of fear and anxiety, these results indicate that drug manipulations in the NI and outside areas do not affect the baseline functioning of the recorded cortico-hippocampal circuits, and only modify neural patterns during fear and anxiety states.

The second pattern seen in these results is that the drug effects were selective to either PAG or RPO, but not common to both. For example, 5-HT_{1A} and RXFP-3 manipulations in the NI increased hippocampal power during PAG, but not during RPO stimulation; similarly, infusion of drugs outside of the NI reduced hippocampal power during RPO, but not PAG stimulation.

Changes to RPO-induced activity. In previous experiments with urethane-anesthetized animals, muscimol injections in the NI reduced the field potential power of RPO-evoked hippocampal theta (Nunez et al., 2006). The current experiments conducted in this project, with free moving animals, were unable to replicate these findings. This discrepancy in findings could be explained by the different reasons. Firstly, although both CDP and muscimol act on the GABAergic receptor system, the mechanism of action of the two drugs are distinct. CDP binds to the benzodiazepine receptor, enhancing $GABA_A$ receptor activity (i.e. amplifying the effects

of GABA when that is released), while muscimol, binds directly to the $GABA_A$ receptor (acting like release of GABA). Different results from CDP and muscimol experiments could be expected if the GABAergic receptor population in the NI is underrepresented for the benzodiazepine receptor. Another possibility is the fact that the effects of CDP rely on the endogenous GABA present in the region, while muscimol does not, therefore making it possible that CDP effects on the $GABA_A$ receptor are not potent enough to induce changes in hippocampal theta. Failure to replicate findings from muscimol experiments using CDP have been reported before (Dudchenko & Sarter, 1992). Finally, another factor is that previous experiments used urethane-anesthetized animals. Under the effects of urethane, it is possible that other nodes in the theta-generating system were inactive, giving the NI a more prominent role than what it would otherwise have in free moving animals.

The results of the current experiment, however, showed reliable effects on the reduction of hippocampal frequency. Once again surprisingly (but in line with the above findings with power measures), injections outside the NI were the most effective in reducing theta frequency. As anticipated by other authors (McNaughton, Kocsis, & Hajos, 2007), CDP and buspirone, two drugs that have the same anxiolytic clinical effects despite their different pharmacology, were efficient in reducing hippocampal theta. A third drug, the relaxin-3 receptor agonist RXFP3-A2, was also effective in reducing hippocampal theta. In the group in which theta frequency reductions were significant, the injections were centered in the locus coeruleus and other small nuclei in the pontine tegmentum. Cholinergic activation of the locus coeruleus produces hippocampal theta in halothane-anesthetized animals (Berridge & Foote, 1991), a find supported by evidence that in free moving animals, optogenetic activation of locus coeruleus neurons produces cortical theta (Carter et al., 2010). The results from this Chapter are in concurrence with these findings, and add new possibilities to the involvement of benzodiazepinergic, serotonergic and relaxinergic receptor systems in the locus coeruleus controlling theta rhythmicity in the hippocampus.

Changes to PAG-induced activity. The nucleus incertus had more influence on hippocampal states provoked by PAG- than RPO-stimulation. Administration of buspirone, but not CDP, in the NI was effective in increasing hippocampal theta power during PAG stimulation. $5\text{-}HT_{1A}$, the receptor to which buspirone has the highest binding affinity, is present in the cells of the NI that also express relaxin-3 (Miyamoto, Watanabe, & Tanaka, 2008). In this same publication, central 5-HT depletion by administration of *p*-chlorophenylalanine caused a marked increase in the expression of relaxin-3 gene expression in the NI. Although the precise mechanisms throughout which serotonin regulates relaxin-3 in the NI is unclear, the

results presented in this Chapter and these previous findings suggest that they could happen through 5-HT_{1A} receptors.

Perhaps the most consequential finding in the current experiments is that buspirone/5-HT_{1A} *and not* CDP/$GABA_A$ caused changes in PAG- *but no*t RPO-stimulation states. 5-HT_{1A} receptor binding is reduced in patients with a diagnosis of panic disorder (Nash et al., 2008). In rats, activating the 5-HT_{1A} receptor in the dorsomedial hypothalamus inhibits panic-like reactions from the electrical stimulation of the same region (de Bortoli, Yamashita, & Zangrossi, 2013). Fluoxetine, a drug with known anti-panic effects, enhances 5-HT_{1A} receptor activity in the PAG (Zanoveli, Nogueira, & Zangrossi, 2007), and blocking the same receptor in the dorsal PAG also blocks the anti-panic effects of the drug (Zanoveli et al., 2010). Given our knowledge of the PAG and 5-HT_{1A} receptors involvement in panic, and of how the NI has strong projections to the PAG, the results of the buspirone experiment in this Chapter reinforce the 5-HT_{1A} involvement in panic and indicate that the NI could also be a strong regulatory node in the panic/fear system. Also, one of the hypotheses proposed in this thesis is that the reductions in hippocampal theta produced by PAG stimulation (Chapter 4) could be a proxy for a fear/panic signal. The results from buspirone testing in this Chapter are supporting evidence for this notion.

The experiments in this Chapter had two objectives. The first one was a "smaller scale" goal; it was an attempt to demonstrate that the nucleus incertus, a region with known regulatory roles in anxiety and in hippocampal theta, was also capable of modulating the effects of PAG stimulation demonstrated in Chapter 4. Indeed, the results presented here support this hypothesis, with the NI reducing the effects provoked by PAG stimulation, although findings from the NI influencing RPO-stimulation hippocampal theta in anesthetized animals could not be replicated in free-moving rats. The second, "larger scale" goal in this Chapter was an investigation aimed at better characterizing the nature of the PAG-induced states in Chapter 4. The hypothesis going into the current experiments was that these PAG-induced states were more akin to a neural substrate of panic rather than one of anxiety. The results here appear to confirm this suggestion. In the next Chapter I attempt to unify all of the findings from the Chapters 3, 4 and 5 into a cohesive view of the PAG and some of its functions.

Chapter 6. Discussion

In the previous Chapters of this thesis I presented a literature review and experimental data addressing the nature and functions of the PAG/DR complex. Discussion of the detailed implications was provided in the relevant Chapters. Below I start with a summary of the conclusions of those detailed discussions. All the data presented so far indicate that the PAG is endowed with both anxiety/conflict and withdrawal/fear components as well as appetitive ones. In this conclusion Chapter, I will present a unified view of the PAG based on the evidence of the previous Chapters, and propose a new model of how the PAG controls the systems that help solve the problems of approach, withdrawal and conflict. Also, I will propose that the PAG/DR is responsible for reducing general activity when the organism is presented with scenarios that are not resolvable.

In the first Chapter of this thesis, I described how the need to move appropriately to external cues is the most fundamental force driving the development and evolution of nervous systems. The first rudimentary nerve cells and systems emerged to guide the organism towards appetitive and safe stimuli, and away from aversive and dangerous ones. My argument was that as evolution built more complex, centralized, nervous systems capable of more elaborated, abstract thinking and planning, the demands that created these systems remained the same as before: the need to move according to environmental pressures. Features of the human mind that *seem* unique within the animal kingdom, such as planning for the future, anticipating outcomes, creative thinking, communication and cooperation with others, are all side-effects of pressure for better adaptation that maximizes positive and avoids negative outcomes. Although the human mind can appear different to the rest of the animal kingdom, its features are only more complex variations of the same simplistic behaviors approach and withdrawal of the early jellyfish. Movement is, in the end, the fundamental requirement that shaped all animals.

In Chapters 1 and 2 I talked about anxiety (conceptualized as conflict) and fear (conceptualized as withdrawal/moving away) as two elements that guide motivation and movement in animals. Anxiety and fear appear to be opposing mental phenomena, where one is capable of inhibiting the other. The most evident aspect of this competition between the two is how their corresponding animal behaviors are completely different by nature: in most cases, anxiety/conflict requires stopping all movement, whereas fear/withdrawal requires active movement. Whenever an animal is immobile, the dominating circuits producing immobility must also be inhibiting movement; and the same can be said about the circuits producing escape

from a threat and at the same time inhibiting immobility systems. These led to the pursuit of whether or not the PAG can produce signals that correspond to anxiety and fear.

In Chapter 4, I talk about hippocampal theta and how it can be a strong signal of arousal and emotion in the brain. In the same Chapter, I presented experimental evidence that the freezing provoked by aPAG stimulation generates high amplitude, high frequency hippocampal theta, while mPAG-generated freezing induces low amplitude, low frequency hippocampal theta. The rationale that guided these experiments, presented in Chapter 2, was that the aPAG is more involved in anxiety-like processes, and the mPAG is more involved in fear/panic-processes, and the results from the experiments seem to confirm this notion. Also, follow-up experiments in Chapter 5 confirmed that manipulations of the 5-HT system (similar to the ones that can reduce panic-like behaviors in the rat), but not manipulations of the GABAergic system (more related to anxiety and the mechanism through which most anxiety drugs act on) changed the hippocampal states induced by mPAG stimulation. This, again, was another strong evidence supporting the possibilities that were raised in Chapter 2.

In the summary sections of each of the experimental Chapters I presented detailed arguments and explanations to support why I believe that PAG has anxiety and panic components. With these theoretical and empirical evidence from the review and experimental Chapters in mind, now I would like to present a unified view of the PAG/DR and its roles.

6.1. Reconceptualizing the PAG/DR complex

Classically, the main body of research regarding the PAG has focused on its aversive properties. However, other studies have branched out to show that not only does the PAG also contribute towards appetitive motivational states and behaviors – such as social interactions, pro-sexual behaviors and vocalizations, food and water intake (Parker & Feldman, 1967), and even speech control in humans (Holstege & Subramanian, 2016) – it may in fact be essential to their operation.

For instance, the PAG was initially considered of secondary importance for sexual behaviors, playing a modulatory role, either facilitating or inhibiting the sexual behaviors generated by hypothalamic sites like the preoptic area and the ventral hypothalamus (Arendash & Gorski, 1983; McCarthy, Pfaff, & Schwartz-Giblin, 1991; Sirinathsinghji, 1985). However, although direct electrical stimulation of either the preoptic area or the PAG in male rats leads to sexual behaviors, lesion studies have shown that destruction of the PAG completely abolishes these sexual reactions while destruction of the preoptic area alone does not (Marson, 2004). Similarly, although stimulating either the dorsal PAG or the hypothalamus of a female rat will

lead to lordosis, lesioning the dorsal PAG completely abolishes the behavior while hypothalamic lesions do not (Sakuma & Pfaff, 1979b). These findings indicate that the PAG's role in controlling appetitive functions is as fundamental as its role in generating aversive states. This conceptualization of the role of PAG sees it as a set of key nodes in the survival circuits proposed by LeDoux (2012) and, essentially, a complete conserved remnant of the most primitive integrated control of motivated behavior.

Given the established dual role of the PAG in generating appetitive as well as aggressive-defensive states, Chapter 2 proposed a new subdivision for the dorsal parts of the PAG that are concerned with mediating appetitive behavior. In addition, I also proposed that conflict between appetitive-driving regions and aversive-driving regions could be at least partially mediated by the DLPAG, with its unique set of connections and chemical properties. Furthermore, I hypothesized that conflicts of this nature elicit activation of the VLPAG in order to shut down overt behaviors until the neural conflict is resolved, and propose that chronic exposure to unresolved scenarios would result in long-term changes to the DR neurons that feed serotonin to the PAG and forebrain, causing long-lasting changes in motivational states, such as learned helplessness (discussed in Chapter 2).

It is important to highlight that the PAG is concerned with *close-proximity* goals (as discussed in Chapters 1 and 2). Although the PAG drives behavior towards appetitive stimuli and away from aversive ones, these positive and negative stimuli need to be unambiguous and close in both space and time for primary control to be by the PAG; distant and future projections of a potential cost or benefit will not strongly engage the PAG. The PAG thus plays a fundamental role in driving actions that help attain close appetitive goals, such as consummating copulation with a partner, but there is no evidence nor any expectation that the region would have a central role in driving behavior toward distant goals, such as sustaining long-term activity that will only bear fruit in the future. However, while the PAG is not a motivational driver for distant goals, it certainly is a potential disruptor of them. For instance, in a natural setting, if an animal is engaged in an ongoing task and then detects the presence of a close-proximity threat, activation of the PAG would inhibit all the circuits involved in the performance of that task, and produce the appropriate defensive behavior: fight, flight or immobility, depending on environmental cues.

The concept of the PAG as a purely aversive region must be amended to include its functions in driving behavior towards appetitive goals. Based on data from Chapter 2, I propose here a more precise definition of the dorsal PAG as a region driving close-range motivational states, which may be either aversive (the DMPAG) or appetitive (the LPAGi). I also

conceptualize the role of the ventral parts of the PAG (VLPAG and DR) as *stopping action* in scenarios where aversive and appetitive stimuli are concurrently present. Immediate stopping in a conflict scenario is mostly conducted by the VLPAG, probably through inputs from the DLPAG and DR. The DLPAG acts as a hub that receives input from relevant cortical and subcortical regions that aid in resolving these motivational conflicts. I propose that the effects of repeated conflicts generate a more systemic reduction in motivational drive, which is mediated by the DR sending inhibitory inputs to the motivational regions of the PAG and the forebrain. These ideas would not only reinforce the involvement of the PAG in appetitive functions, but it would also be – to the best of my knowledge – the first formal suggestions that the PAG/DR is strongly involved with the pathogenesis of depression.

6.2. Approach, avoidance and conflict: a new perspective of the PAG

The necessity to approach positive stimuli and to move away from negative ones has been a central feature of psychological and biological theory (Corr, 2013). Simple organisms are endowed with rudimentary tools that conduct movement towards appetitive cues and away from aversive ones. In the more complex mammalian brain, it is recognized that circuitry evolved to deal with approaching and avoiding internal representations of goals, rather than simple environmental cues (Cloninger & Gilligan, 1987). The fundamental conceptual shift in assuming the existence of internal goal representations is that now organisms can develop the ability to compare these two opposing goal representations, and decide on the optimal strategy for action. Frequently, situations can be ambiguous in that neither moving towards nor away from the goal seem ideal. In this scenario, a third system in the brain, parallel to the approach and avoidance ones, emerges to deal with conflict between these positive and negative representations. The organism can halt locomotion, and engage in further analysis based on other external and internal indicators.

As outlined by McNaughton et al. (2016), the PAG is theorized to be part of the approach-avoidance-conflict system at its lowest level of defensive and appetitive distance. In Chapter 1, I presented a schematic image from McNaughton, DeYoung, and Corr in which the PAG was assigned a role only in the avoidance and conflict systems. That image was one of the drivers of the main missions of this thesis: to properly incorporate the PAG into a cohesive, unified theoretical view of motivational systems in the brain. In Figure 6.1, I present an updated version of that scheme, modified here with data from Chapter 2. On this view, since it is a phylogenetically old and well-conserved structure, the PAG deals with direct and unambiguous scenarios of all types present at close range. Anatomical and functional evidence summarized

in Chapter 2 points to the PAG as a locus for dealing with actual (or object-specific) stimuli, such as physical contact with a predator or a mate. Meanwhile structures located hierarchically above it deal with potential (or object-general) stimuli that might be located further away in spatial distance and/or time.

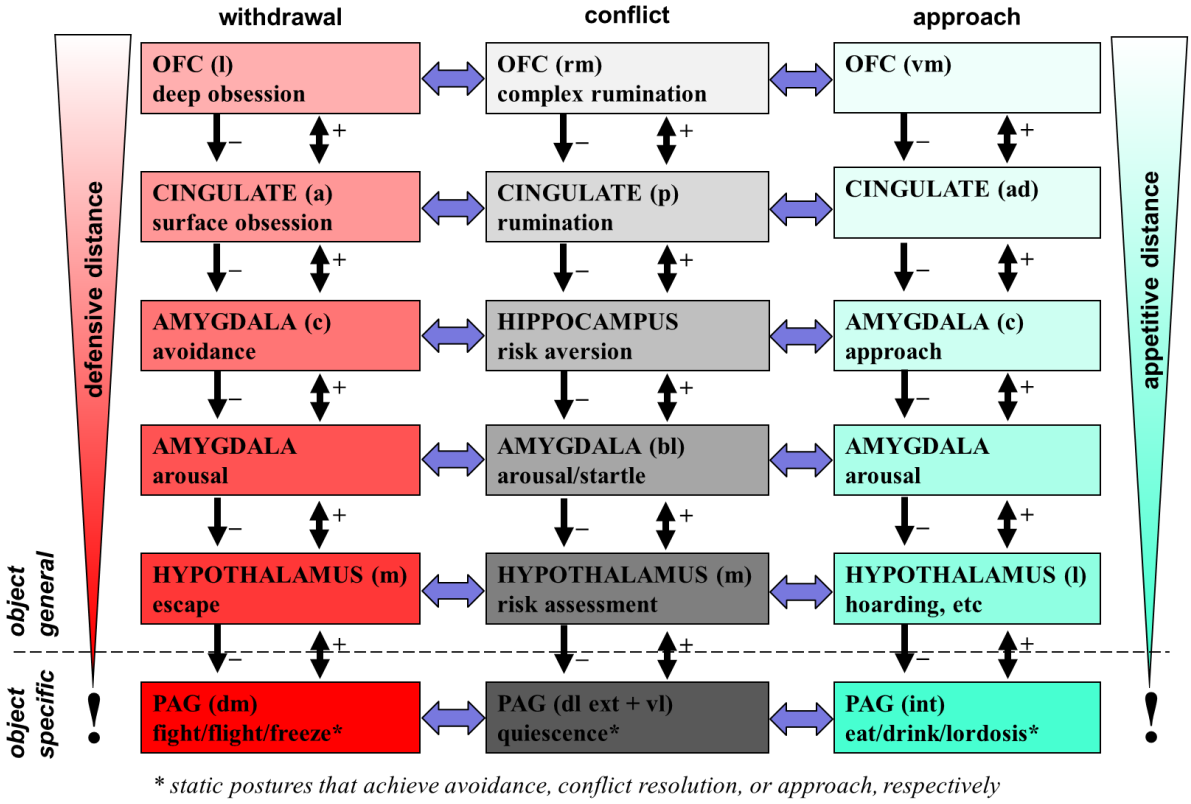

Figure 6.1. Approach, withdrawal and conflict systems in the brain. Adapted and updated from Figure 7 in McNaughton et al. (2016)

6.3. Negative and positive goals: the dorsal PAG as a motivational driver

Experimental evidence shows that of all dorsal subdivisions of the PAG, the DMPAG is the one most involved in mediating reactions to proximal, aversive stimuli (Figure 6.2). For instance, rats exposed to a strong jet of air produce vigorous motor activities, such as flight and running reactions. This paradigm is thought to be a model for studying panic in animals, as the reactions to the air jet are reduced by treatment with known panicolytic drugs (Salchner & Singewald, 2002). In c-Fos experiments, rats subjected to the air jet test show stronger labeling in the DMPAG compared to the other PAG divisions, and treatment with fluoxetine, a drug with known panic-reducing properties, is more efficient in reducing c-Fos labeling in the DMPAG (Salchner & Singewald, 2002). After GABAergic blockade in the superior colliculus,

which is known to cause panic-like reactions, c-Fos labeling becomes markedly stronger in the DMPAG than in neighboring regions for rats that present with running and jumping (Borelli et al., 2006).

In a mouse line selectively bred for aggressive behaviors, c-Fos labeling is not significantly different in the PAG columns of animals exposed to sensory cues of another animal, such as sight or odor. However, labelling of the DMPAG is stronger when mice have *direct* physical contact with another animal (Haller, Toth, Halasz, & De Boer, 2006). Further support for the DMPAG as a center for dealing with direct and immediate aversive situations, is that c-Fos labelling is also stronger in this region for animals that have been physically, forcibly restrained (Lino-de-Oliveira et al., 2001).

Appetitive reactions appear to be dependent on the two identified internal parts of the PAG: the DLPAGi and LPAGi (Chapter 2). The lordosis reflex, for instance, is more easily elicited from the internal parts of the PAG using localized electrical stimulation (Ogawa et al., 1991). Similarly, in guinea pigs, vocalizations related to sexual courtship are also produced more efficiently by stimulating the DLPAGi and LPAGi (Kyuhou & Gemba, 1998). Even autonomic responses are different in the interior parts of the PAG: electrical stimulation of the LPAGi provokes slow, shallow breathing (apneusis) while the LPAGe produces much faster and deeper tachypnea, as in aversive reactions (Subramanian et al., 2008). Recently, single unit recording investigations in the PAG of free moving animals showed that a larger proportion of cells in the LPAG fire than cells in the DLPAG when the animals receive food rewards (Tryon & Mizumori, 2018).

Several areas of the hypothalamus that have a known involvement in sexual behavior and regulating feeding project to the internal parts of the PAG and not the external ones. The medial preoptic area targets the DLPAi and LPAGi only (Rizvi et al., 1992; Simerly & Swanson, 1988), and so do the lateral, dorsomedial and ventromedial hypothalamic areas (Veening et al., 1991). Also unique to the interior divisions of the PAG is the presence of synaptic terminals releasing relaxin (Ma et al., 2007), a peptide with modulatory effects on feeding (Smith et al., 2011).

What potential functional differences, if any, exist between the DLPAGi and LPAGi remain unresolved, however. It could be that the LPAGi is more concerned with generating sexual behaviors than the DLPAGi, as androgen receptors are present to a much smaller degree in the dorsolateral column compared to the lateral (Murphy & Hoffman, 2001). Also, projections from the medial preoptic area, a region known to promote sexual behaviors, are more abundant in the LPAG (Rizvi et al., 1992), and the nucleus retroambiguus, a medullary region that generates

lordosis, is targeted by LPAG neurons but not DLPAG ones (Vanderhorst et al., 2000). The DLPAGi could either be dealing with other classes of appetitive goals, such as feeding, or it could be responsible for a different aspect of appetitive processing altogether.

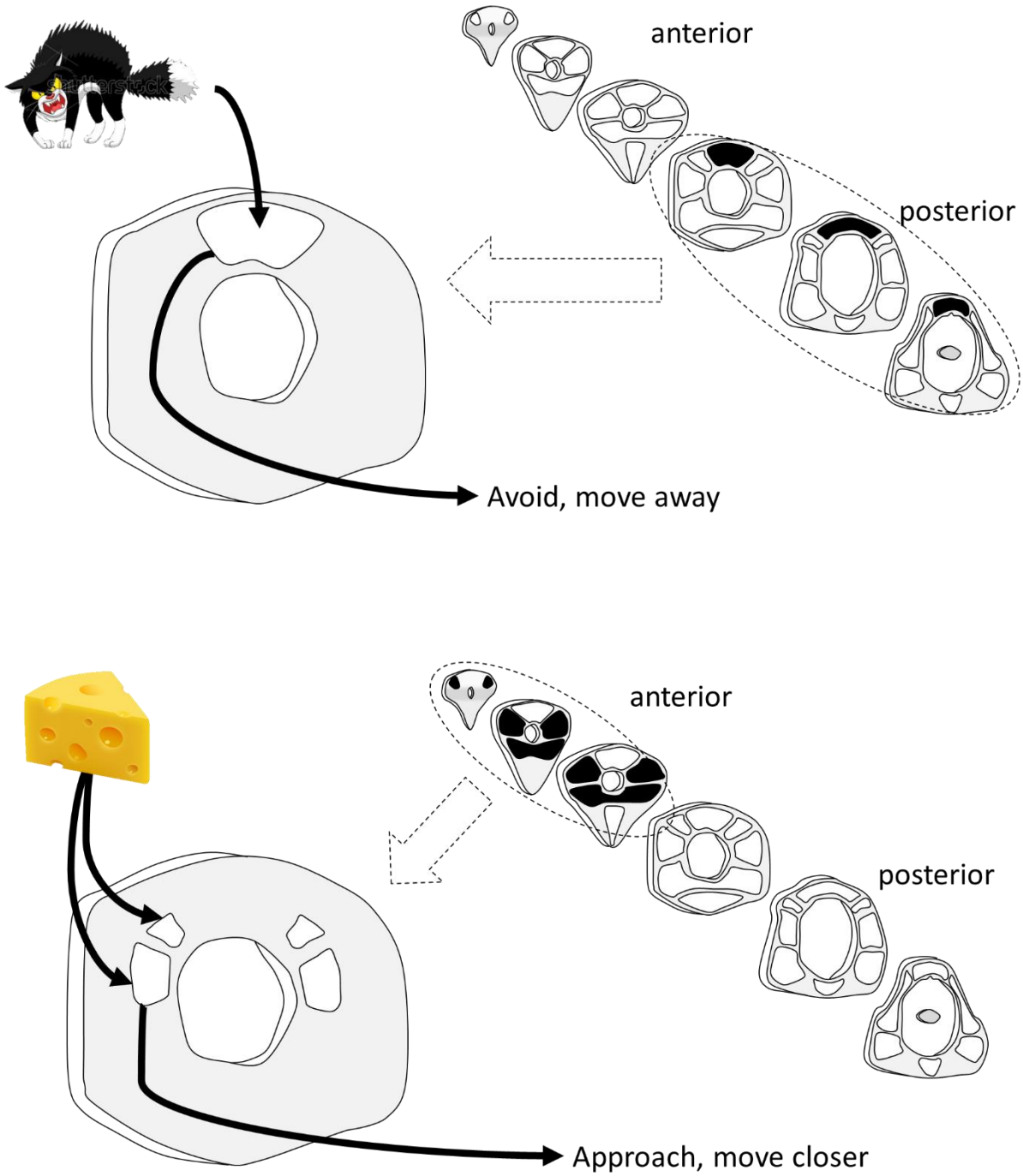

Figure 6.2. Above: DMPAG neurons at intermediate and posterior sites of the PAG initiate behaviors to deal with an aversive stimulus. Below: internal PAG neurons at more anterior sites initiate behaviors to deal with an appetitive stimulus.

6.4. Motivational conflicts: the DLPAG and VLPAG

Upon analysis of its chemical and anatomical properties, the DLPAG shows itself to be a distinct component of the periaqueductal grey (Chapter 2). In terms of internal connections with the other subdivisions of the PAG/DR, the DLPAG is the only region that does not receive projections from the ventrally located columns and DR (Jansen, Farkas, Mac Sams, & Loewy, 1998; Vertes, 1991), but does receive axons from the DMPAG. Therefore, the activities in which the LPAG and VLPAG are more engaged, such as cardiovascular control and production of immobility, are not relayed back to the DLPAG. It could be, however, that the responses generated by the DMPAG concerning escape from a threat are channeled to the DLPAG. While only receiving limited PAG input, the DLPAG sends outputs to all other PAG divisions, indicating that while its inputs of signals are narrowly located, its outputs are much broader.

Also unique to the DLPAG are the concentrated projections that it receives from dorsal pre-mammillary (PMd) neurons compared to other columns (Canteras & Swanson, 1992). The PMd is a region that seems to selectively respond to some modalities of threat. In rats exposed to a predator or predator's odor at the end of a runway, lesions of the PMd greatly reduce defensive freezing and increase the number of approaches toward the threatening stimuli (Markham, Blanchard, Canteras, Cuyno, & Blanchard, 2004). Interestingly, however, lesions of this area do not affect freezing induced by the very direct and unambiguous negative effects of a painful electric shock (Markham et al., 2004). The PMd seems to modulate responses to uncertain risk, such as proximal predator cures, rather than direct and certain threats, like the painful experience of an electric shock.

The exterior portion of the column, the DLPAGe, is the only region in the whole PAG/DR complex that receives projections from the anterior cingulate cortex (ACC; Figure 6.3; also (Beckstead, 1979; Floyd et al., 2000; Meller & Dennis, 1986; Wyss & Sripanidkulchai, 1984). In humans, the ACC responds to different *perceptions* of the unpleasantness of a painful stimulus, rather than the stimulus itself (Rainville, Duncan, Price, Carrier, & Bushnell, 1997). As reviewed by Fuchs et al. (2014), the ACC in animals serve the same function of processing the affective component of pain, while keeping nociception intact. Experiments with lesions of the ACC did not reduce sensory pain processing, and lesioned animals effectively withdraw from painfully stimuli, indicating that nociceptive processing is intact in the absence of the ACC. However, emotional elements associated with the painful stimulus, such as avoidance of a place where pain was previously experienced, are abolished. Further corroborating this, higher c-Fos labelling in the ACC was registered for animals that spent time in a place *associated* with a painful stimulus, but no difference in ACC activity was found for actual painful stimulation.

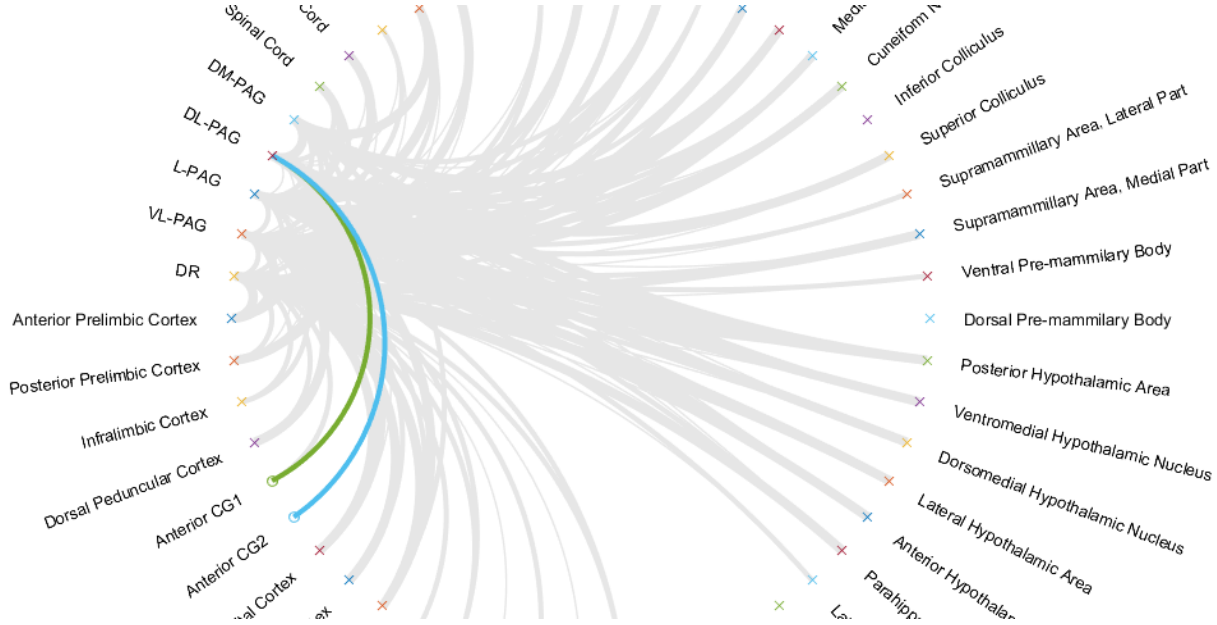

Figure 6.3. Projections from the anterior cingulate cortex to the PAG/DR. Cingulate projections target the DL column exclusively, not projecting to any of the other subdivisions in significant volumes. Line thickness indicates volume of terminals sent to the area.

At the same time, the DLPAG receives fewer projections from the amygdala than other PAG regions, as illustrated in Figure 6.4 (Hopkins & Holstege, 1978; Price & Amaral, 1981; Rizvi et al., 1991), and those present are found in the DLPAGi, but not the DLPAGe (Hopkins & Holstege, 1978; Price & Amaral, 1981; Rizvi et al., 1991). While the amygdala is known to play a prominent role in emotional processing, its precise function remains unresolved. A theory proposed by J. A. Gray and N. McNaughton (2000) posits that the amygdala is a region tasked with increasing or decreasing arousal, and this in turn can positively or negatively modulate emotional responses. Therefore it is possible that outputs from the amygdala are not fundamental for the systems involved in conflict solving. The amygdala would be *potentiating* an organism to approach or avoid behaviors, but would not play a role in solving conflicts between the two.

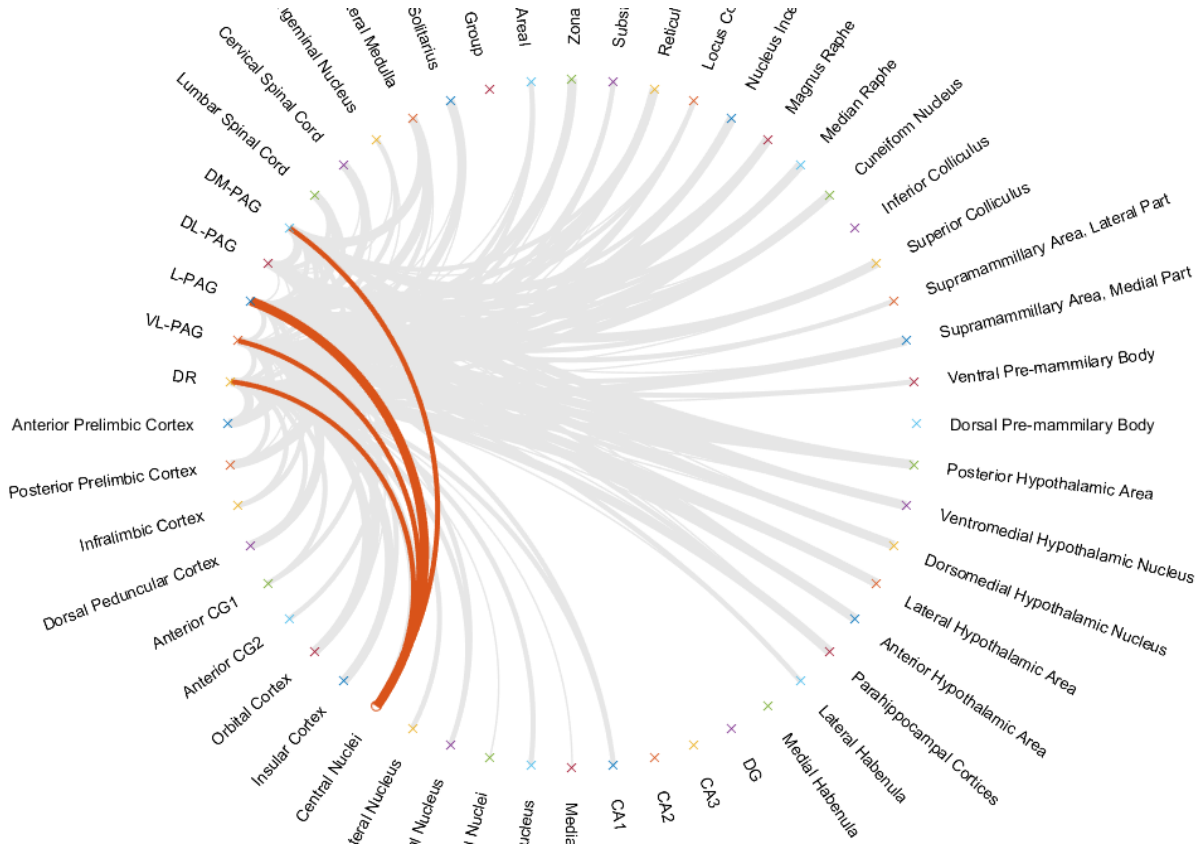

Figure 6.4. Projections from the Central Nuclei of the amygdala to the PAG/DR. Amygdalar projections intensely target all PAG/DR subdivisions, with the exception of the DL column to which it has fewer terminals. Line thickness indicates volume of terminals sent to the area.

The DLPAGe appears to be a local conflict resolution area in the PAG, where immediate appetitive input from external and local sources, and immediate aversive input from the DMPAG, converge. If we conceptualize the conflict between opposing motivational forces as the core of anxiety, then the DLPAGe emerges as the root of close-proximity anxiety phenomena (see Figure 6.5).

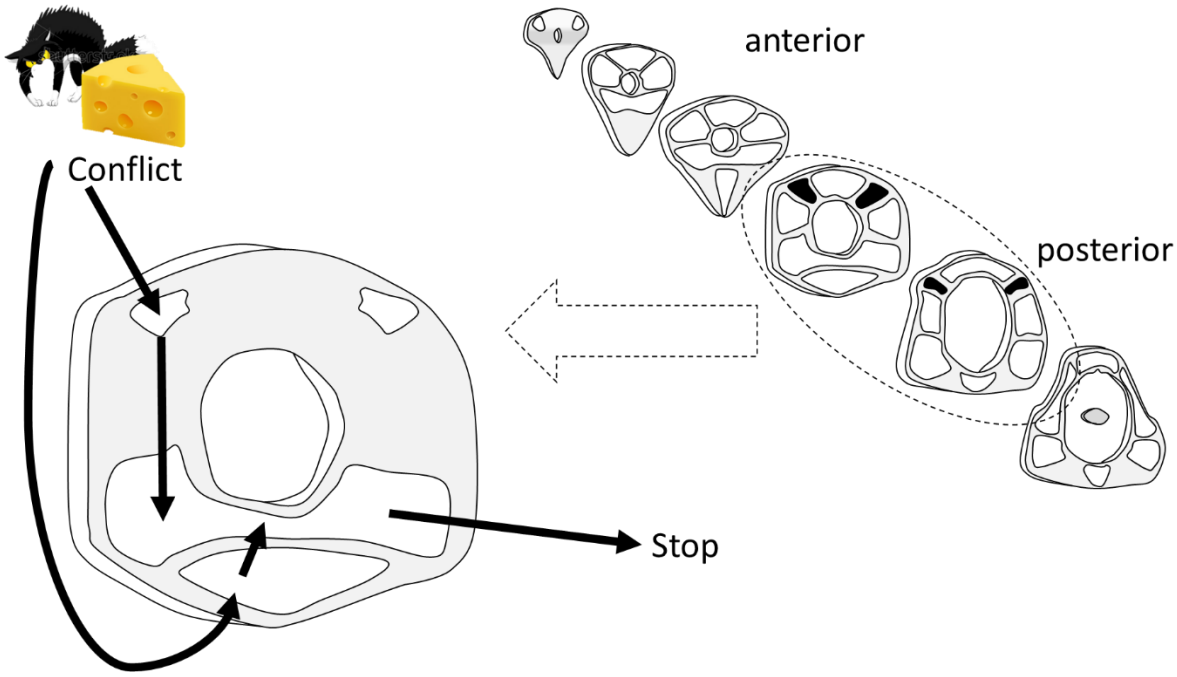

Figure 6.5. Unique inputs from sensory and cortical areas reaching the DLPAGe might help detect and solve conflicts. Upon detection of a conflict, DLPAGe neurons at intermediate and posterior sites of the PAG signal VLPAG and DR neurons to stop motor action until the conflict is resolved.

The magnus raphe and the ventrolateral medulla are two of the main sites of descending efferent outputs of the PAG. And yet, the DLPAG sends no projections to these two areas when compared to the other divisions (Abols & Basbaum, 1981; Aghajanian & Wang, 1977; Beitz, Mullett, et al., 1983; Bjorkeland & Boivie, 1984; Carrive, 1991; Henderson et al., 1998; Herbert & Saper, 1992b; Holstege, 1991b; Van Bockstaele et al., 1991). In fact, the only real significant outputs of the DLPAG column is to itself and the other PAG divisions (Jansen et al., 1998); also Figure 6.6). If the DLPAG's role is indeed in mediating and resolving conflicts locally, it would not need to send descending information in order to generate motor output: upon activation, the DLPAGe would signal the VLPAG to halt motor activity until the conflict between approaching and withdrawing from the stimulus is resolved. Indeed, freezing caused by activation of the DLPAG induces c-Fos labeling only in a small set of regions, one of which is the VLPAG (Borelli, Ferreira-Netto, Coimbra, & Brandao, 2005). Meanwhile, information from ascending areas like the ACC and PMd could help the DLPAG resolve the conflict, by integrating the respective affective and contextual cues originating from these areas.

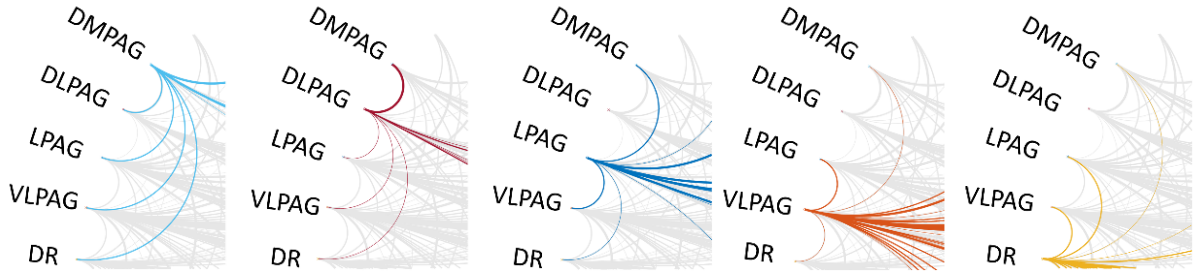

Figure 6.6. Intra-PAG/DR connections. From left to right: projections from the DMPAG, DLPAG, LPAG, VLPAG and DR to other subdivisions. The DLPAG is the only subdivision that does not receive projections from its ventral counterparts. Line thickness indicates volume of terminals sent to the area.

Another feature that bolsters the idea of the DLPAG as an anxiety/conflict area is the higher concentration of GABAergic receptors within the dorsolateral borders (Bowery et al., 1987; Chu et al., 1990; Gundlach, 1991). All classic anxiolytics rely on GABAergic receptors in order to produce their effect, and injections of the benzodiazepine receptor agonist midazolam into the dorsal PAG reduces anxiety-related behaviors in rats (Russo, Guimaraes, De Aguiar, & Graeff, 1993).

Unlike fear, which produces reductions in nociception, anxiety-like reactions cause an enhancement of pain perception in both human and animals (Rhudy & Meagher, 2000). CCK fibers, which are involved in increasing nociception, are present in overwhelmingly larger volumes in the DLPAG (H. Liu et al., 1994; Loren et al., 1979) and, not coincidentally, injections of CCK in the DLPAG produce hyperalgesia (Lovick, 2008). In contrast, the fear-inducing DMPAG produces reductions in nociception (de Freitas et al., 2014; de Freitas, Medeiros, Khan, & Coimbra, 2016).

Direct experimental evidence for the DLPAG as an anxiety region comes from pharmacological investigations using the elevated plus maze (EPM) (Bertoglio, Anzini, Lino-de-Oliveira, & Carobrez, 2005). Novel and open environments are known to be anxiogenic for rats, as they involve uncertainty and exposure to potential threats. Rats who have been treated with anxiolytic drugs like benzodiazepines will show decreased anxiety defined by spending more time exploring the open arms of the EPM, but only upon their first encounter with the maze. If they have prior experience with the EPM, systemic benzodiazepine administration no longer has this effect, a phenomenon called ‘one-trial tolerance’. In order to address whether or not the DLPAG might be involved this benzodiazepine-resistant anxiogenic state, Bertoglio et al. (2005) administered intra-DLPAG injections of lidocaine into rats submitted to the test. Lidocaine acts by blocking sodium channels, silencing regional cell activity. After blocking

DLPAG activity, the anxiolytic effects of systemic benzodiazepine injections returned on trial 2 of the EPM, indicating that this region is indeed involved in the anxiety-like effects of the one-trial tolerance phenomenon.

Table 6.1. Internal Representations of Acute and Resolvable and Unresolvable Goals in the Rat's PAG, the Actions Produced by the Structures Involved, and Analogous Human Pathological Manifestations

	ACUTE SCENARIO			
	RESOLVABLE		UNRESOVABLE	SPECIFICITY
STIMULUS	CHEESE	CAT	CHEESE + CAT	
INTERNAL VALUE	good	bad	ambiguous	different internal values
EMPLOYED STRATEGY	to approach	to avoid	conflict	different goal representations
PAG NEURAL DYNAMICS	inhibits avoidance systems and/or activates approach systems	activates avoidance systems and/or inhibits approach systems	inhibits both approach and avoidance, receives ascending input to help resolve conflict	different neural dynamics
RAT BEHAVIOUR IN RELATION TO GOAL	active towards	active away	neither towards nor away; engages in risk analysis	different behaviours
OUTCOME	successful approach	successful avoidance	dependent on the conflict resolution	different outcomes
HUMAN PATHOLOGICAL EQUIVALENT	mania-related disorders	phobia-related disorders	anxiety-related disorders	different pathologies
PAG CIRCUITRY MOST HEAVLY INVOLVED	anterior LPAGi (behav state) + LPAGe (autonomic)	posterior DMPAG (behav state) + LPAGe (autonomic)	DLPAGe (conflict resolution) + VLPAG (behavioural suppression until resolution)	different PAG regions

6.5. Acute and chronic unresolvable goals and conflicts: the VLPAG and DR as general inhibitors of behavior and neuronal activity

The two preceding sections considered the ways in which the PAG/DR complex deals with *acute* appetitive, aversive and conflict scenarios. As summarized in Table 6.1, acute scenarios that are easily acted upon (moving towards cheese or away from a cat) are resolved quickly, while a slight delay is introduced if both desirable and undesirable options are presented

simultaneously, while the PAG engages behaviors to access the situation and receives further information from supporting regions of the nervous system. Despite this slight delay, the acute nature of the scenario assumes that its unresolvability is only temporary, and a conclusion is eventually reached.

In both human and animal contexts, however, organisms can be chronically subjected to situations where either approaching, avoiding or trying to resolve conflicts are chronically impossible goals to be achieved. Perhaps one of the earliest conceptualizations of the effects of chronic unresolvability was postulated by Martin Seligman as the theory of learned helplessness (Abramson, Seligman, & Teasdale, 1978). In Seligman's initial learned helplessness studies, dogs with no prior experience of electric shock would quickly learn how to avoid it by jumping over a barrier, while those who were first exposed to a series of inescapable shocks would not take the opportunity to escape when it was finally presented. Later investigations found the same results in cats, rats, fish and humans. In rodents, for example, the presentation of a repeated, inescapable and aversive stimulus causes long-term reductions in general responsiveness: reducing social interaction (Short & Maier, 1993) and sexual performance (Holmer, Rodman, Helmreich, & Parfitt, 2003), reducing food intake (Dess, Minor, & Brewer, 1989); and causing weight loss even when control and shocked rats consume the same number of calories, indicating changes in metabolic rate (Dess, Raizer, Chapman, & Garcia, 1988).

The phenomenology of learned helplessness in animals resembles the symptomology of depression in humans: a general reduction of pleasure or interest in activities, change in appetite, diminished sexual libido (Mathew & Weinman, 1982) and social interaction (Hirschfeld et al., 2000). Drugs that are known to have effective antidepressant effects in humans are also efficient in reducing the deleterious effects of inescapable aversive stimuli in animals, indicating this to be a possible analogue to depression in experimental animals (Willner, 1984).

The most accepted hypothesis for the molecular basis of depression postulates that monoaminergic systems in the brain, in particular 5-HT, are disrupted in depression (Delgado, 2000; Hirschfeld, 2000). This hypothesis resonates with the fact that the vast majority of validated antidepressants available today are tapping mechanisms in monoaminergic neurotransmission.

The DR is one of the main serotonergic centers in the brain, and its main function appears to be the release of 5-HT in the forebrain, although it also sends descending projections. Changes in neurotransmitter expression within the DR have been reported in depressed patients (Bach-Mizrachi et al., 2008) as well as reductions in tissue volume of this region (Lee et al.,

2011). In animal studies, the majority of antidepressant drugs alter firing rates of DR cells (Scuvée-Moreau & Dresse, 1979).

Antidepressant drugs are also capable of ameliorating symptoms of panic in humans (Lydiard & Ballenger, 1987; Wilkinson, Balestrieri, Ruggeri, & Bellantuono, 2009). Animal studies have shown that systemic and localized administration of antidepressants reduces panic-like responses in ethological models of panic (Zangrossi & Graeff, 2014), and antidepressant treatment increases the electric current threshold necessary to provoke escape reactions triggered by the dorsal PAG stimulations (Schenberg, Capucho, Vatanabe, & Vargas, 2002). The elicitation of panic-like reactions through electrical stimulation of the dPAG is also inhibited in animals that have been chronically exposed to inescapable aversive stimuli (Quintino-dos-Santos et al., 2014). It is believed that this inhibition of dPAG cells is due to projections from the DR, since changing volumes of extracellular 5-HT in the DR reduce the panic responses evoked by dPAG stimulation (Yamashita et al., 2017). These results indicates that the DR keeps the dPAG under inhibition in acute, short term scenarios (during risk assessment, for example) or chronic, long-term ones (during depression). This dynamic is summarized in Figure 6.7.

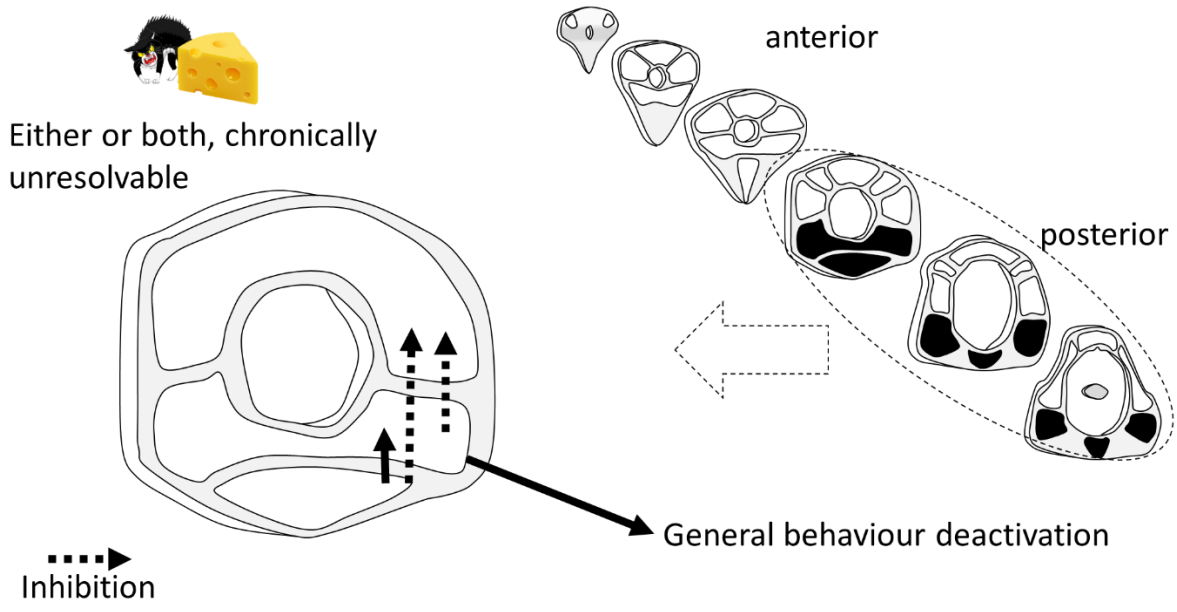

Figure 6.7. Repeated unresolvable scenarios cause long-term changes in serotonergic patterns in the DR, which in turn promote general inhibition in the dorsal PAG and its roles in aversive and appetitive motivation. Concurrently, descending signals from the VLPAG promote general inhibitions in motor, nociceptive and sympathetic activity.

If the DMPAG is concerned with governing motivational states to move away from aversive stimuli, and the LPAGi to move towards appetitive ones, we would expect changes in these regions in depressive states. While we lack direct experimental evidence for this, indirect evidence points to this possibility. The lordosis reflex, which is strongly dependent on the LPAGi, is reduced after pharmacological (Uphouse, Caldarola-Pastuszka, & Droge, 1992) and electrical (Arendash & Gorski, 1983) stimulations of the DR, while lesions of the DR greatly increase spontaneous lordosis (Kakeyama & Yamanouchi, 1993). The DR also reduces other appetitive behaviors related to the internal parts of the dorsal PAG: inhibition of 5-HT cells in the DR increases appetite in satiated rats (P. J. Fletcher & Coscina, 1993), and antagonism of CRF (which reduces the 5-HT neurotransmission) increases social interaction in rats (Lukkes, Vuong, Scholl, Oliver, & Forster, 2009). In humans, major depressive disorder is quite often accompanied by decreases in appetite, sexual libido and social interactions (Hirschfeld et al., 2000; Mathew & Weinman, 1982; Paykel, 1977).

Rats electrically stimulated in the ventral PAG assume a relaxed body position, with no muscle tone, decreased cardiovascular activation, and a lack of reaction to disturbances caused by the experimenter or the presence of another rat in the experimental chamber (Depaulis, Keay, & Bandler, 1994). This behavioral pattern is similar to when rats suffer social defeat and display a hyporeactive state after losing a confrontation. Corroborating the role of the ventral PAG in social defeat, socially defeated animals display preferential activation of ventral PAG cells (Kroes, Burgdorf, Otto, Panksepp, & Moskal, 2007). This trend of ventral PAG activation in socially defeated animals is also seen in a range of other markers, such as overexpression of catecholamine receptors, growth factors and preferential c-Fos expression (Vasconcelos, Stein, & de Almeida, 2015). Furthermore, rats that have been repeatedly exposed to an inescapable negative stimulus in learned helplessness studies display both the hyporeactive behavioral pattern and ventral PAG changes seen in social defeat.

It is possible that the motor and autonomic functions that are reduced in depressive states are being mediated by the VLPAG, given its properties as a general inhibitor of nociception, motor activity, and cardiovascular responses. Investigations of DeltaFosB expression support the view of the VLPAG role in the symptomology of depression. Transcription factors like DeltaFosB are proteins capable of altering how mRNA encodes certain sections of the genetic code. It is believed that DeltaFosB accumulation in certain brain areas is capable of producing stable, long-term changes in the pattern of activity of cells – a mechanism that explains long-term changes in behavior caused by environmental effects (McClung & Nestler, 2003; Nestler, Barrot, & Self, 2001). It has been shown, for example, that frequent drug intake changes

DeltaFosB levels in discreet brain areas, which could contribute to the behavioral, motivational and cognitive changes seen in drug addiction (Nestler et al., 2001). In terms of depression, mice displaying depression-like symptoms after exposure to inescapable shocks also show elevated expression of DeltaFosB in the VLPAG, indicating that the VLPAG is involved in the stable, chronic changes seen in depressive states (Berton et al., 2007). Although pain perception in depression is controversial, more than one study has shown that depressed patients do indeed display reduced nociception. In one particular experimental design, researchers reduced the fear and anticipatory anxiety associated with the delivery of a painful stimulus by giving participants control over the intensity and timing of shocks (Adler & Gattaz, 1993). This methodology revealed that depressed patients have a higher pain tolerance, and that lower thresholds for pain perception are correlated with anxiety rather than depression (Silvestrini, 1989; Ward et al., 1982). Given the prevalent comorbidity between depression and anxiety in humans (Hirschfeld, 2001), many autonomic findings from studies of depressed patients are probably confounds from anxiety.

Table 6.2. Internal Representations of Chronic, Unresolvable Goals in the Rat's PAG, the Actions Produced by the Structures Involved, and Analogous Human Pathological Manifestations

	CHRONIC SCENARIO			
	UNRESOLVABLE			SPECIFICITY
STIMULUS	CHEESE	CAT	CHEESE + CAT	
INTERNAL VALUE	formerly good, now failure	formerly bad, now failure	formerly ambiguous, now failure	all same internal values
EMPLOYED STRATEGY	repeated failure (to approach)	repeated failure (to avoid)	repeated failure (to resolve)	all same employed strategies
PAG NEURAL DYNAMICS	inhibits approach and avoidance systems **(?)**	inhibits approach and avoidance systems	inhibits approach and avoidance systems **(?)**	all same neural dynamics **(?)**
RAT BEHAVIOUR IN RELATION TO GOAL	passivity, hyporeactivity, unresponsiveness **(?)**	passivity, hyporeactivity, unresponsiveness	passivity, hyporeactivity, unresponsiveness **(?)**	all same behaviours **(?)**
OUTCOME	repeatedly unresolved	repeatedly unresolved	repeatedly unresolved	all same outcomes
HUMAN PATHOLOGICAL EQUIVALENT	frustration, stress, depression **(?)**	frustration, stress depression	frustration, stress, depression	all same pathologies **(?)**
PAG CIRCUITRY MOSTLY INVOLVED	posterior VLPAG + DR + dysregulated modulatory inputs **(?)**	posterior VLPAG + DR + dysregulated modulatory inputs	posterior VLPAG + DR + dysregulated modulatory inputs **(?)**	all same PAG regions **(?)**

Note. Question marks (?) indicate predictions from this model that have not yet been experimentally demonstrated.

As presented in Table 6.2, I propose that modulatory inputs that have been dysregulated by inescapable and unresolvable events reach the DR, altering its baseline activity. In turn, the DR promotes tonic inhibition of the dorsal parts of the PAG, which accounts for the reduced approach and avoidance responses to some scenarios in animals and humans displaying depression-like symptoms. At the same time, the VLPAG inhibits motor, sympathetic and nociceptive functions.

However, since there are no direct projections from either the DR or the VLPAG to the DLPAG (recall Figure 6.6), this model predicts that the DLPAG would be spared from the

inhibition produced by depression. If the DLPAG controls anxiety as I propose, then the anxiety symptoms of animals with depression symptoms should remain unaffected. Indeed, inescapably shocked rats do not reduce their exploration of novel and open environments (Short & Maier, 1993) or the open arms on the EPM (Grahn, Kalman, Brennan, Watkins, & Maier, 1995; Quintino-dos-Santos et al., 2014), even though their social interactions (Short & Maier, 1993) and DPAG-driven escape responses (Quintino-dos-Santos et al., 2014) are reduced.

6.6. Final remarks

In this thesis, I presented a detailed anatomical and functional picture of the periaqueductal grey. This anatomical and functional data provided evidence for new subdivisions within the PAG and argued that DR should be included as a functional part of the coherent complex that surrounds the aqueduct. This additional complexity is consistent with the demonstration that, along with its classical role in panic, the PAG plays a role in appetitive states, anxiety and depression. Indeed, this thesis provided experimental evidence indicating that the anxiety propositions seems to be true.

My aim was to present a new, more complete, theoretical picture of how the different parts of the PAG contribute to the distinct functions attributed to the region. I showed that the DMPAG, especially at more caudal levels, is responsible for driving the organism away from threats. On the other hand, at more rostral levels the proposed new subdivisions of the PAG, the DLPAGi and LPAGi, drive the organism towards appetitive stimuli, especially reproductive ones. In situations of motivational conflicts, a local circuit including the DLPAGe, VLPAG and DR halts overt simple motivated behavior, while the organism gathers sensory and cognitive information in order to solve the conflict. I demonstrated how that afferents unique to the DLPAGe can be responsible for decision making during conflicts. When conflict becomes chronic and approach/avoidance problems insoluble, I presented a model that explains how the VLPAG and DR are responsible for long term reductions in general motor and autonomic activity. This is done by inhibition of ascending and descending sites, and also local inhibition of the dorsal PAG. Overall, then, a case is made for the PAG representing the bottom, highly conserved, level of the hierarchically organized systems controlling integrated motivated behavior.

Many novel ideas have been proposed (and backed by voluminous amounts of data) in this thesis. Since testing all of them would be simply impossible for this project, I focused in the proposition that the PAG can increase hippocampal theta (anxiety) and also decrease it (fear).

In Chapters 4 and 5 I provided empirical demonstrations of how this hypothesis presented here can be confirmed.

Conceptually, these findings should be a guide for future research and treatment of anxiety, panic and depression. The PAG, conventionally seen as a center for panic only, is also an important locus in the circuits mediating other motivated behavior and so important for other psychiatric disorders.

References

Abols, I. A., & Basbaum, A. I. (1981). Afferent connections of the rostral medulla of the cat: a neural substrate for midbrain-medullary interactions in the modulation of pain. *The Journal of comparative neurology, 201*(2), 285-297. doi:10.1002/cne.902010211

Abrahamson, E. E., & Moore, R. Y. (2001). The posterior hypothalamic area: chemoarchitecture and afferent connections. *Brain research, 889*(1-2), 1-22.

Abramson, L. Y., Seligman, M. E., & Teasdale, J. D. (1978). Learned helplessness in humans: critique and reformulation. *J Abnorm Psychol, 87*(1), 49-74.

Adler, G., & Gattaz, W. F. (1993). Pain perception threshold in major depression. *Biological psychiatry, 34*(10), 687-689.

Adolphs, R., Tranel, D., Damasio, H., & Damasio, A. (1994). Impaired recognition of emotion in facial expressions following bilateral damage to the human amygdala. *Nature, 372*(6507), 669-672. doi:10.1038/372669a0

Aghajanian, G. K., & Wang, R. Y. (1977). Habenular and other midbrain raphe afferents demonstrated by a modified retrograde tracing technique. *Brain research, 122*(2), 229-242.

Al-Rodhan, N. R. F., Richelson, E., Gilbert, J. A., McCormick, D. J., Kanba, K. S., Pfenning, M. A., . . . Yaksh, T. L. (1991). Structure-antinociceptive activity of neurotensin and some novel analogues in the periaqueductal gray region of the brainstem. *Brain research, 557*(1-2), 227-235. doi:10.1016/0006-8993(91)90139-m

Albin, R. L., Makowiec, R. L., Hollingsworth, Z., Dure, L. S. t., Penney, J. B., & Young, A. B. (1990). Excitatory amino acid binding sites in the periaqueductal gray of the rat. *Neurosci Lett, 118*(1), 112-115.

Allen, D. L., Johnson, A. E., Tempel, A., Zukin, R. S., Luine, V. N., & McEwen, B. S. (1993). Serotonergic lesions decrease mu- and delta-opiate receptor binding in discrete areas of the hypothalamus and in the midbrain central gray. *Brain research, 625*, 269-275.

Amaral, D. G., & Cowan, W. M. (1980). Subcortical afferents to the hippocampal formation in the monkey. *The Journal of comparative neurology, 189*(4), 573-591. doi:10.1002/cne.901890402

An, X., Bandler, R., Ongur, D., & Price, J. L. (1998). Prefrontal cortical projections to longitudinal columns in the midbrain periaqueductal gray in macaque monkeys. *The Journal of comparative neurology, 401*(4), 455-479.

Appel, N. M., Mitchell, W. M., Garlick, R. K., Glennon, R. A., Teitler, M., & Desouza, E. B. (1990). Autoradiographic Characterization of (+-)-1-(2,5-Dimethoxy-4-[I-125]Iodophenyl)-2-Aminopropane ([I-125]Doi) Binding to 5-Ht2 and 5-Ht1c Receptors in Rat-Brain. *Journal of Pharmacology and Experimental Therapeutics, 255*(2), 843-857.

Appell, P. P., & Behan, M. (1990). Sources of Subcortical Gabaergic Projections to the Superior Colliculus in the Cat. *Journal of Comparative Neurology, 302*(1), 143-158. doi:DOI 10.1002/cne.903020111

Araki, M., McGeer, P. L., & Kimura, H. (1988). The efferent projections of the rat lateral habenular nucleus revealed by the PHA-L anterograde tracing method. *Brain research, 441*(1-2), 319-330.

Araki, T., Yamano, M., Murakami, T., Wanaka, A., Betz, H., & Tohyama, M. (1988). Localization of Glycine Receptors in the Rat Central Nervous-System - an Immunocytochemical Analysis Using Monoclonal-Antibody. *Neuroscience, 25*(2), 613-624. doi:Doi 10.1016/0306-4522(88)90263-1

Arduino, P. J., & Gould, J. L. (1984). Is tonic immobility adaptive? *Animal Behaviour, 32*(3), 921-923.

Arendash, G. W., & Gorski, R. A. (1983). Suppression of lordotic responsiveness in the female rat during mesencephalic electrical stimulation. *Pharmacol Biochem Behav, 19*(2), 351-357.

Armstrong, D. M., Saper, C. B., Levey, A. I., Wainer, B. H., & Terry, R. D. (1983). Distribution of cholinergic neurons in rat brain: demonstrated by the immunocytochemical localization of choline acetyltransferase. *The Journal of comparative neurology, 216*(1), 53-68. doi:10.1002/cne.902160106

Azkue, J. J., Knopfel, T., Kuhn, R., Mateos, J. M., & Grandes, P. (1997). Distribution of the metabotropic glutamate receptor subtype mGluR5 in rat midbrain periaqueductal grey and relationship with ascending spinofugal afferents. *Neurosci Lett, 228*(1), 1-4.

Azmitia, E. C., & Segal, M. (1978a). An autoradiographic analysis of the differential ascending projections of the dorsal and median raphe nuclei in the rat. *The Journal of comparative neurology, 179*(3), 641-667.

Azmitia, E. C., & Segal, M. (1978b). An autoradiographic analysis of the differential ascending projections of the dorsal and median raphe nuclei in the rat. *The Journal of comparative neurology, 179*(3), 641-667. doi:10.1002/cne.901790311

Baccala, L. A., & Sameshima, K. (2001). Partial directed coherence: a new concept in neural structure determination. *Biol Cybern, 84*(6), 463-474. doi:10.1007/PL00007990

Bach-Mizrachi, H., Underwood, M. D., Tin, A., Ellis, S. P., Mann, J. J., & Arango, V. (2008). Elevated expression of tryptophan hydroxylase-2 mRNA at the neuronal level in the dorsal and median raphe nuclei of depressed suicides. *Molecular psychiatry, 13*(5), 507-513, 465. doi:10.1038/sj.mp.4002143

Bach, D. R., Hurlemann, R., & Dolan, R. J. (2013). Unimpaired discrimination of fearful prosody after amygdala lesion. *Neuropsychologia, 51*(11), 2070-2074. doi:10.1016/j.neuropsychologia.2013.07.005

Baldo, B. A., Daniel, R. A., Berridge, C. W., & Kelley, A. E. (2003). Overlapping distributions of orexin/hypocretin- and dopamine-beta-hydroxylase immunoreactive fibers in rat brain regions mediating arousal, motivation, and stress. *The Journal of comparative neurology, 464*(2), 220-237. doi:10.1002/cne.10783

Baldwin, D. (1998). Depression and panic: Comorbidity. *Eur Psychiatry, 13 Suppl 2*, 65s-70s. doi:10.1016/S0924-9338(98)80016-3

Bandler, R., Carrive, P., & Depaulis, A. (1991). Emerging Principles of Organization of the Midbrain Periaqueductal Gray-Matter - Introduction. *Midbrain Periaqueductal Gray Matter, 213*, 1-8.

Bandler, R., & Depaulis, A. (1991). Midbrain Periaqueductal Gray Control of Defensive Behavior in the Cat and the Rat. *Midbrain Periaqueductal Gray Matter, 213*, 175-198.

Bandler, R., & Shipley, M. T. (1994). Columnar organization in the midbrain periaqueductal gray: Modules for emotional expression? *Trends in Neuroscience, 17*, 379-389.

Barbaresi, P. (1998). Immunocytochemical localization of substance P receptor in rat periaqueductal gray matter: a light and electron microscopic study. *The Journal of comparative neurology, 398*(4), 473-490.

Barbaresi, P. (2005). GABA-immunoreactive neurons and terminals in the cat periaqueductal gray matter: a light and electron microscopic study. *J Neurocytol, 34*(6), 471-487. doi:10.1007/s11068-006-9440-7

Barbaresi, P., Gazzanelli, G., & Malatesta, M. (1997). Glutamate-positive neurons and terminals in the cat periaqueductal gray matter (PAG): a light and electron microscopic immunocytochemical study. *The Journal of comparative neurology, 383*(3), 381-396.

Barbaresi, P., & Manfrini, E. (1988). Glutamate decarboxylase-immunoreactive neurons and terminals in the periaqueductal gray of the rat. *Neuroscience, 27*(1), 183-191.

Barbaresi, P., Quaranta, A., Amoroso, S., Mensa, E., & Fabri, M. (2012). Immunocytochemical localization of calretinin-containing neurons in the rat periaqueductal gray and

colocalization with enzymes producing nitric oxide: a double, double-labeling study. *Synapse, 66*(4), 291-307. doi:10.1002/syn.21509

Bass, A. H. (2008). Steroid-dependent plasticity of vocal motor systems: novel insights from teleost fish. *Brain Res Rev, 57*(2), 299-308. doi:10.1016/j.brainresrev.2007.04.006

Bass, A. H., & McKibben, J. R. (2003). Neural mechanisms and behaviors for acoustic communication in teleost fish. *Prog Neurobiol, 69*(1), 1-26. doi:10.1016/s0301-0082(03)00004-2

Bass, A. H., Rose, G. J., & Pritz, M. B. (2005). Auditory Midbrain of Fish, Amphibians, and Reptiles: Model Systems for Understanding Auditory Function.

Batelaan, N., Smit, F., de Graaf, R., van Balkom, A., Vollebergh, W., & Beekman, A. (2007). Economic costs of full-blown and subthreshold panic disorder. *J Affect Disord, 104*(1-3), 127-136. doi:10.1016/j.jad.2007.03.013

Bathgate, R. A., Samuel, C. S., Burazin, T. C., Layfield, S., Claasz, A. A., Reytomas, I. G., . . . Tregear, G. W. (2002). Human relaxin gene 3 (H3) and the equivalent mouse relaxin (M3) gene. Novel members of the relaxin peptide family. *The Journal of biological chemistry, 277*(2), 1148-1157. doi:10.1074/jbc.M107882200

Beart, P. M., Summers, R. J., Stephenson, J. A., Cook, C. J., & Christie, M. J. (1990). Excitatory amino acid projections to the periaqueductal gray in the rat: a retrograde transport study utilizing D[3H]aspartate and [3H]GABA. *Neuroscience, 34*(1), 163-176.

Beaujouan, J. C., Torrens, Y., Saffroy, M., & Glowinski, J. (1986). Quantitative autoradiographic analysis of the distribution of binding sites for [125I]Bolton Hunter derivatives of eledoisin and substance P in the rat brain. *Neuroscience, 18*(4), 857-875.

Becker, B., Mihov, Y., Scheele, D., Kendrick, K. M., Feinstein, J. S., Matusch, A., . . . Hurlemann, R. (2012). Fear processing and social networking in the absence of a functional amygdala. *Biological psychiatry, 72*(1), 70-77. doi:10.1016/j.biopsych.2011.11.024

Beckstead, R. M. (1979). Autoradiographic Examination of Cortico-Cortical and Sub-Cortical Projections of the Mediodorsal-Projection (Prefrontal) Cortex in the Rat. *Journal of Comparative Neurology, 184*(1), 43-62. doi:DOI 10.1002/cne.901840104

Beckstead, R. M., Domesick, V. B., & Nauta, W. J. (1979). Efferent connections of the substantia nigra and ventral tegmental area in the rat. *Brain research, 175*(2), 191-217.

Behbehani, M. M. (1995). Functional characteristics of the midbrain periaqueductal gray. *Progress in Neurobiology, 46*, 575-605.

Behbehani, M. M., & Pert, A. (1984). A Mechanism for the Analgesic Effect of Neurotensin as Revealed by Behavioral and Electrophysiological Techniques. *Brain research, 324*(1), 35-42. doi:Doi 10.1016/0006-8993(84)90619-X

Behzadi, G., Kalen, P., Parvopassu, F., & Wiklund, L. (1990). Afferents to the median raphe nucleus of the rat: retrograde cholera toxin and wheat germ conjugated horseradish peroxidase tracing, and selective D-[3H]aspartate labelling of possible excitatory amino acid inputs. *Neuroscience, 37*(1), 77-100.

Beitz, A. J. (1985). The midbrain periaqueductal gray in the rat. I. Nuclear volume, cell number, density, orientation, and regional subdivisions. *The Journal of comparative neurology, 237*(4), 445-459. doi:10.1002/cne.902370403

Beitz, A. J. (1989). Possible origin of glutamatergic projections to the midbrain periaqueductal gray and deep layer of the superior colliculus of the rat. *Brain Res Bull, 23*(1-2), 25-35.

Beitz, A. J. (1990). Relationship of Glutamate and Aspartate to the Periaqueductal Gray-Raphe Magnus Projection - Analysis Using Immunocytochemistry and Microdialysis. *Journal of Histochemistry & Cytochemistry, 38*(12), 1755-1765.

Beitz, A. J., Mullett, M. A., & Weiner, L. L. (1983). The periaqueductal gray projections to the rat spinal trigeminal, raphe magnus, gigantocellular pars alpha and paragigantocellular nuclei arise from separate neurons. *Brain research, 288*(1-2), 307-314.

Beitz, A. J., & Shepard, R. D. (1985). The midbrain periaqueductal gray in the rat. II. A Golgi analysis. *The Journal of comparative neurology, 237*(4), 460-475. doi:10.1002/cne.902370404

Beitz, A. J., Shepard, R. D., & Wells, W. E. (1983). The periaqueductal gray-raphe magnus projection contains somatostatin, neurotensin and serotonin but not cholecystokinin.

Belin, M. F., Aguera, M., Tappaz, M., McRae-Deguerce, A., Bobillier, P., & Pujol, J. F. (1979). GABA-accumulating neurons in the nucleus raphe dorsalis and periaqueductal gray in the rat: a biochemical and autoradiographic study. *Brain research, 170*, 279-297.

Bellchambers, C. E., Chieng, B., Keay, K. A., & Christie, M. J. (1998). Swim-stress but not opioid withdrawal increases expression of c-Fos immunoreactivity in rat periaqueductal gray neurons which project to the rostral ventromedial medulla.

Benarroch, E. E., Schmeichel, A. M., Dugger, B. N., Sandroni, P., Parisi, J. E., & Low, P. A. (2009). Dopamine cell loss in the periaqueductal gray in multiple system atrophy and Lewy body dementia. *Neurology, 73*(2), 106-112. doi:10.1212/WNL.0b013e3181ad53e7

Berridge, C. W., & Foote, S. L. (1991). Effects of locus coeruleus activation on electroencephalographic activity in neocortex and hippocampus. *The Journal of neuroscience, 11*(10), 3135-3145.

Bertoglio, L. J., Anzini, C., Lino-de-Oliveira, C., & Carobrez, A. P. (2005). Enhanced dorsolateral periaqueductal gray activity counteracts the anxiolytic response to midazolam on the elevated plus-maze Trial 2 in rats. *Behavioural brain research, 162*(1), 99-107. doi:10.1016/j.bbr.2005.03.010

Berton, O., Covington, H. E., 3rd, Ebner, K., Tsankova, N. M., Carle, T. L., Ulery, P., . . . Nestler, E. J. (2007). Induction of deltaFosB in the periaqueductal gray by stress promotes active coping responses. *Neuron, 55*(2), 289-300. doi:10.1016/j.neuron.2007.06.033

Besson, J. M., Fardin, V., & Oliveras, J. L. (1991). Analgesia Produced by Stimulation of the Periaqueductal Gray-Matter - True Antinoceptive Effects Versus Stress Effects. *Midbrain Periaqueductal Gray Matter, 213*, 121-138.

Beyerl, B. D. (1978). Afferent projections to the central nucleus of the inferior colliculus in the rat. *Brain research, 145*(2), 209-223.

Bingham, S., Davey, P. T., Babbs, A. J., Irving, E. A., Sammons, M. J., Wyles, M., . . . Parsons, A. A. (2001). Orexin-A, an hypothalamic peptide with analgesic properties. *Pain, 92*(1-2), 81-90.

Bjorkeland, M., & Boivie, J. (1984). The termination of spinomesencephalic fibers in cat. An experimental anatomical study. *Anat Embryol (Berl), 170*(3), 265-277.

Bjorklund, A., Falck, B., & Stenevi, U. (1971). Classification of monoamine neurones in the rat mesencephalon: distribution of a new monoamine neurone system. *Brain research, 32*(2), 269-285.

Blanchard, D. C., & Blanchard, R. J. (1988). Ethoexperimental approaches to the biology of emotion. *Annual Review of Psychology, 39*, 43-68. doi:10.1146/annurev.psych.39.1.43

Blanchard, D. C., Griebel, G., & Blanchard, R. J. (2003). The Mouse Defense Test Battery: pharmacological and behavioral assays for anxiety and panic. *Eur J Pharmacol, 463*(1-3), 97-116. doi:10.1016/s0014-2999(03)01276-7

Blanchard, R. J., & Blanchard, D. C. (1989). Antipredator defensive behaviors in a visible burrow system. *J Comp Psychol, 103*(1), 70-82.

Blanchard, R. J., Flannelly, K. J., & Blanchard, D. C. (1986). Defensive Behaviour of Laboratory and Wild Rattus novergicus. *Journal of Comparative Psychology*.

Blessing, W. W., & Reis, D. J. (1983). Evidence That Gaba and Glycine-Like Inputs Inhibit Vasodepressor Neurons in the Caudal Ventrolateral Medulla of the Rabbit. *Neuroscience Letters, 37*(1), 57-62. doi:Doi 10.1016/0304-3940(83)90504-9

Blomqvist, A., & Craig, A. D. (1991). Organization of Spinal and Trigeminal Input to the Pag. *Midbrain Periaqueductal Gray Matter, 213*, 345-363.

Bloom, F., Battenberg, E., Rossier, J., Ling, N., & Guillemin, R. (1978). Neurons Containing Beta-Endorphin in Rat-Brain Exist Separately from Those Containing Enkephalin - Immunocytochemical Studies. *Proceedings of the National Academy of Sciences of the United States of America, 75*(3), 1591-1595. doi:DOI 10.1073/pnas.75.3.1591

Bobillier, P., Petitjean, F., Salvert, D., Ligier, M., & Seguin, S. (1975). Differential projections of the nucleus raphe dorsalis and nucleus raphe centralis as revealed by autoradiography.

Bobillier, P., Seguin, S., Petitjean, F., Salvert, D., Touret, M., & Jouvet, M. (1976). The raphe nuclei of the cat brainstem: a topographical atlas of their efferent projections as revealed by autoradiography. *Brain research, 113*, 449-486.

Bokil, H., Andrews, P., Kulkarni, J. E., Mehta, S., & Mitra, P. P. (2010). Chronux: a platform for analyzing neural signals. *J Neurosci Methods, 192*(1), 146-151. doi:10.1016/j.jneumeth.2010.06.020

Borelli, K. G., & Brandao, M. L. (2008). Effects of ovine CRF injections into the dorsomedial, dorsolateral and lateral columns of the periaqueductal gray: a functional role for the dorsomedial column. *Hormones and behavior, 53*(1), 40-50. doi:10.1016/j.yhbeh.2007.08.013

Borelli, K. G., Ferreira-Netto, C., & Brandao, M. L. (2006). Distribution of Fos immunoreactivity in the rat brain after freezing or escape elicited by inhibition of glutamic acid decarboxylase or antagonism of GABA-A receptors in the inferior colliculus. *Behavioural brain research, 170*(1), 84-93. doi:10.1016/j.bbr.2006.02.015

Borelli, K. G., Ferreira-Netto, C., Coimbra, N. C., & Brandao, M. L. (2005). Fos-like immunoreactivity in the brain associated with freezing or escape induced by inhibition of either glutamic acid decarboxylase or GABAA receptors in the dorsal periaqueductal gray. *Brain research, 1051*(1-2), 100-111. doi:10.1016/j.brainres.2005.05.068

Bowery, N. G., Hudson, A. L., & Price, G. W. (1987). Gaba-a and Gaba-B Receptor-Site Distribution in the Rat Central-Nervous-System. *Neuroscience, 20*(2), 365-383. doi:Doi 10.1016/0306-4522(87)90098-4

Bowman, B. R., Kumar, N. N., Hassan, S. F., McMullan, S., & Goodchild, A. K. (2013). Brain sources of inhibitory input to the rat rostral ventrolateral medulla. *The Journal of comparative neurology, 521*(1), 213-232. doi:10.1002/cne.23175

Boyson, S. J., McGonigle, P., & Molinoff, P. B. (1986). Quantitative autoradiographic localization of the D1 and D2 subtypes of dopamine receptors in rat brain. *The Journal of neuroscience, 6*(11), 3177-3188.

Bradwejn, J., & Demontigny, C. (1985). Antagonism of Cholecystokinin-Induced Activation by Benzodiazepine Receptor Agonists - Microiontophoretic Studies in the Rat Hippocampus. *Annals of the New York Academy of Sciences, 448*(Jul), 575-580. doi:DOI 10.1111/j.1749-6632.1985.tb29954.x

Bradwejn, J., Koszycki, D., & Shriqui, C. (1991). Enhanced sensitivity to cholecystokinin tetrapeptide in panic disorder. Clinical and behavioral findings. *Arch Gen Psychiatry, 48*(7), 603-610.

Braga, A. A., Aguiar, D. C., & Guimaraes, F. S. (2009). NOC-9, a selective nitric oxide donor, induces flight reactions in the dorsolateral periaqueductal gray of rats by activating soluble guanylate cyclase. *Neurosci Lett, 459*(2), 79-83. doi:10.1016/j.neulet.2009.05.009

Brandao, M. L., Anseloni, V. Z., Pandossio, J. E., De Araujo, J. E., & Castilho, V. M. (1999). Neurochemical mechanisms of the defensive behavior in the dorsal midbrain. *Neuroscience and biobehavioral reviews, 23*(6), 863-875.

Brandao, M. L., Cardoso, S. H., Melo, L. L., Motta, V., & Coimbra, N. C. (1994). Neural substrate of defensive behavior in the midbrain tectum. *Neuroscience and biobehavioral reviews, 18*(3), 339-346.

Brisbare-Roch, C., Dingemanse, J., Koberstein, R., Hoever, P., Aissaoui, H., Flores, S., . . . Jenck, F. (2007). Promotion of sleep by targeting the orexin system in rats, dogs and humans. *Nat Med, 13*(2), 150-155. doi:10.1038/nm1544

Brunso-Bechtold, J. K., Thompson, G. C., & Masterton, R. B. (1981). HRP study of the organization of auditory afferents ascending to central nucleus of inferior colliculus in cat. *The Journal of comparative neurology, 197*(4), 705-722. doi:10.1002/cne.901970410

Bucher, D., & Anderson, P. A. V. (2015). Evolution of the first nervous systems - what can we surmise? *Journal of Experimental Biology, 218*(4), 501-503. doi:10.1242/jeb.111799

Burazin, T. C., Bathgate, R. A., Macris, M., Layfield, S., Gundlach, A. L., & Tregear, G. W. (2002). Restricted, but abundant, expression of the novel rat gene-3 (R3) relaxin in the dorsal tegmental region of brain. *J Neurochem, 82*(6), 1553-1557.

Buzsaki, G. (2002). Theta oscillations in the hippocampus. *Neuron, 33*(3), 325-340.

Byrum, C. E., & Guyenet, P. G. (1987). Afferent and efferent connections of the A5 noradrenergic cell group in the rat. *The Journal of comparative neurology, 261*(4), 529-542. doi:10.1002/cne.902610406

Calvez, J., Lenglos, C., de Avila, C., Guevremont, G., & Timofeeva, E. (2015). Differential effects of central administration of relaxin-3 on food intake and hypothalamic neuropeptides in male and female rats. *Genes, brain, and behavior, 14*(7), 550-563. doi:10.1111/gbb.12236

Camps, M., Kelly, P. H., & Palacios, J. M. (1990). Autoradiographic Localization of Dopamine D1 and D2 Receptors in the Brain of Several Mammalian-Species. *Journal of Neural Transmission-General Section, 80*(2), 105-127. doi:Doi 10.1007/Bf01257077

Canteras, N. S., & Goto, M. (1999). Fos-like immunoreactivity in the periaqueductal gray of rats exposed to a natural predator. *Neuroreport, 10*(2), 413-418. doi:Doi 10.1097/00001756-199902050-00037

Canteras, N. S., Simerly, R. B., & Swanson, L. W. (1992). Projections of the ventral premammillary nucleus. *The Journal of comparative neurology, 324*(2), 195-212. doi:10.1002/cne.903240205

Canteras, N. S., & Swanson, L. W. (1992). The dorsal premammilary nucleus: An unusual component of the mammilary body.

Carrive, P. (1991). Functional-Organization of Pag Neurons Controlling Regional Vascular Beds. *Midbrain Periaqueductal Gray Matter, 213*, 67-&.

Carrive, P. (1993). The periaqueductal gray and defensive behavior: functional representation and neuronal organization. *Behavioural brain research, 58*(1-2), 27-47.

Carrive, P., Leung, P., Harris, J., & Paxinos, G. (1997). Conditioned fear to context is associated with increased fos expression in the caudal ventrolateral region of the midbrain periaqueductal gray. *Neuroscience, 78*(1), 165-177. doi:Doi 10.1016/S0306-4522(97)83047-3

Carrive, P., & Paxinos, G. (1994). The supraoculomotor cap: a region revealed by NADPH diaphorase histochemistry. *Neuroreport, 5*(17), 2257-2260.

Carter, M. E., Yizhar, O., Chikahisa, S., Nguyen, H., Adamantidis, A., Nishino, S., . . . de Lecea, L. (2010). Tuning arousal with optogenetic modulation of locus coeruleus neurons. *Nature neuroscience, 13*(12), 1526-1533. doi:10.1038/nn.2682

Cervera-Ferri, A., Guerrero-Martinez, J., Bataller-Mompean, M., Taberner-Cortes, A., Martinez-Ricos, J., Ruiz-Torner, A., & Teruel-Marti, V. (2011). Theta synchronization between the hippocampus and the nucleus incertus in urethane-anesthetized rats. *Experimental brain research, 211*(2), 177-192. doi:10.1007/s00221-011-2666-3

Cheng, P. Y., Svingos, A. L., Wang, H., Clarke, C. L., Jenab, S., Beczkowska, I. W., . . . Pickel, V. M. (1995). Ultrastructural Immunolabeling Shows Prominent Presynaptic Vesicular Localization of Delta-Opioid Receptor within Both Enkephalin-Containing and Nonenkephalin-Containing Axon Terminals in the Superficial Layers of the Rat Cervical Spinal-Cord. *Journal of Neuroscience, 15*(9), 5976-5988.

Chu, D. C. M., Albin, R. L., Young, A. B., & Penney, J. B. (1990). Distribution and Kinetics of Gaba-B Binding-Sites in Rat Central-Nervous-System - a Quantitative Autoradiographic Study. *Neuroscience, 34*(2), 341-357. doi:Doi 10.1016/0306-4522(90)90144-S

Churchland, P. S. (1986). *Neurophilosophy: toward a unified science of the mind-brain*: MIT Press.

Clements, J. R., Beitz, A. J., Fletcher, T. F., & Mullett, M. A. (1985). Immunocytochemical localization of serotonin in the rat periaqueductal gray: a quantitative light and electron microscopic study. *The Journal of comparative neurology, 236*(1), 60-70. doi:10.1002/cne.902360106

Clements, J. R., Madl, J. E., Johnson, R. L., Larson, A. A., & Beitz, A. J. (1987). Localization of glutamate, glutaminase, aspartate and aspartate aminotransferase in the rat midbrain periaqueductal gray. *Experimental brain research, 67*(3), 594-602.

Cloninger, C. R., & Gilligan, S. B. (1987). Neurogenetic mechanisms of learning: a phylogenetic perspective. *J Psychiatr Res, 21*(4), 457-472.

Coffield, J. A., Bowen, K. K., & Miletic, V. (1992). Retrograde Tracing of Projections between the Nucleus Submedius, the Ventrolateral Orbital Cortex, and the Midbrain in the Rat. *Journal of Comparative Neurology, 321*(3), 488-499. doi:DOI 10.1002/cne.903210314

Cohen, A. S., Barlow, D. H., & Blanchard, E. B. (1985). Psychophysiology of relaxation-associated panic attacks. *J Abnorm Psychol, 94*(1), 96-101.

Coleman, J. R., & Clerici, W. J. (1987). Sources of projections to subdivisions of the inferior colliculus in the rat. *The Journal of comparative neurology, 262*(2), 215-226. doi:10.1002/cne.902620204

Comoli, E., Ribeiro-Barbosa, E. R., & Canteras, N. S. (2000). Afferent connections of the dorsal premammillary nucleus. *The Journal of comparative neurology, 423*(1), 83-98.

Conaco, C., Bassett, D. S., Zhou, H., Arcila, M. L., Degnan, S. M., Degnan, B. M., & Kosik, K. S. (2012). Functionalization of a protosynaptic gene expression network. *Proc Natl Acad Sci U S A, 109 Suppl 1*, 10612-10618. doi:10.1073/pnas.1201890109

Conde, F., Maire-Lepoivre, E., Audinat, E., & Crepel, F. (1995). Afferent connections of the medial frontal cortex of the rat. II. Cortical and subcortical afferents. *The Journal of comparative neurology, 352*(4), 567-593. doi:10.1002/cne.903520407

Conrad, L. C., & Pfaff, D. W. (1976). Efferents from medial basal forebrain and hypothalamus in the rat. II. An autoradiographic study of the anterior hypothalamus. *The Journal of comparative neurology, 169*(2), 221-261. doi:10.1002/cne.901690206

Conti, F., Barbaresi, P., & Fabri, M. (1988). Cytochrome oxidase histochemistry reveals regional subdivisions in the rat periaqueductal gray matter. *Neuroscience, 24*(2), 629-633.

Conti, L. H., Maciver, C. R., Ferkany, J. W., & Abreu, M. E. (1990). Footshock-Induced Freezing Behavior in Rats as a Model for Assessing Anxiolytics. *Psychopharmacology (Berl), 102*(4), 492-497. doi:Doi 10.1007/Bf02247130

Cooper, P. E., Fernstrom, M. H., Rorstad, O. P., Leeman, S. E., & Martin, J. B. (1981). The regional distribution of somatostatin, substance P and neurotensin in human brain. *Brain research, 218*(1-2), 219-232.

Cornea-Hebert, V., Riad, M., Wu, C., Singh, S. K., & Descarries, L. (1999). Cellular and subcellular distribution of the serotonin 5-HT2A receptor in the central nervous system of adult rat. *The Journal of comparative neurology, 409*(2), 187-209.

Corr, P. J. (2013). Approach and Avoidance Behaviour: Multiple Systems and their Interactions. *Emotion Review, 5*(3), 285-290. doi:10.1177/1754073913477507

Craig, A. D., Jr., Wiegand, S. J., & Price, J. L. (1982). The thalamo-cortical projection of the nucleus submedius in the cat. *The Journal of comparative neurology, 206*(1), 28-48. doi:10.1002/cne.902060105

Day, H. E., Campeau, S., Watson, S. J., Jr., & Akil, H. (1997). Distribution of alpha 1a-, alpha 1b- and alpha 1d-adrenergic receptor mRNA in the rat brain and spinal cord. *Journal of chemical neuroanatomy, 13*(2), 115-139.

de Bortoli, V. C., Yamashita, P. S., & Zangrossi, H., Jr. (2013). 5-HT1A and 5-HT2A receptor control of a panic-like defensive response in the rat dorsomedial hypothalamic nucleus. *J Psychopharmacol, 27*(12), 1116-1123. doi:10.1177/0269881113492900

de Freitas, R. L., de Oliveira, R. C., de Oliveira, R., Paschoalin-Maurin, T., de Aguiar Correa, F. M., & Coimbra, N. C. (2014). The role of dorsomedial and ventrolateral columns of the periaqueductal gray matter and in situ 5-HT(2)A and 5-HT(2)C serotonergic receptors in post-ictal antinociception. *Synapse, 68*(1), 16-30. doi:10.1002/syn.21697

de Freitas, R. L., Medeiros, P., Khan, A. U., & Coimbra, N. C. (2016). micro1 -Opioid receptors in the dorsomedial and ventrolateral columns of the periaqueductal grey matter are critical for the enhancement of post-ictal antinociception. *Synapse, 70*(12), 519-530. doi:10.1002/syn.21926

De Luca-Vinhas, M. C., Macedo, C. E., & Brandao, M. L. (2006). Pharmacological assessment of the freezing, antinociception, and exploratory behavior organized in the ventrolateral periaqueductal gray. *Pain, 121*(1-2), 94-104. doi:10.1016/j.pain.2005.12.008

de Montigny, C. (1989). Cholecystokinin tetrapeptide induces panic-like attacks in healthy volunteers. Preliminary findings. *Arch Gen Psychiatry, 46*(6), 511-517.

de Paula Soares, V., & Zangrossi, H., Jr. (2009). Stimulation of 5-HT1A or 5-HT2A receptors in the ventrolateral periaqueductal gray causes anxiolytic-, but not panicolytic-like effect in rats. *Behavioural brain research, 197*(1), 178-185. doi:10.1016/j.bbr.2008.08.027

Deakin, J. The role of serotonin in depression and anxiety.

Del-Ben, C. M., & Graeff, F. G. (2009). Panic Disorder: Is the PAG Involved? *Neural Plasticity*. doi:10.1155/2009/108135

Delatour, B., & Witter, M. P. (2002). Projections from the parahippocampal region to the prefrontal cortex in the rat: evidence of multiple pathways. *The European journal of neuroscience, 15*(8), 1400-1407.

Delgado, P. L. (2000). Depression: the case for a monoamine deficiency. *J Clin Psychiatry, 61 Suppl 6*, 7-11.

Depaulis, A., Bandler, R., & Vergnes, M. (1989). Characterization of pretentorial periaqueductal gray matter neurons mediating intraspecific defensive behaviors in the rat by microinjections of kainic acid. *Brain research, 486*(1), 121-132.

Depaulis, A., Keay, K. A., & Bandler, R. (1992). Longitudinal neuronal organization of defensive reactions in the midbrain periaqueductal gray region of the rat. *Experimental brain research, 90*(2), 307-318.

Depaulis, A., Keay, K. A., & Bandler, R. (1994). Quiescence and hyporeactivity evoked by activation of cell bodies in the ventrolateral midbrain periaqueductal gray of the rat. *Experimental brain research*.

Descarries, L., Watkins, K. C., Garcia, S., & Beaudet, A. (1982). The serotonin neurons in nucleus raphe dorsalis of adult rat: a light and electron microscope radioautographic study. *The Journal of comparative neurology, 207*(3), 239-254. doi:10.1002/cne.902070305

Dess, N. K., Minor, T. R., & Brewer, J. (1989). Suppression of feeding and body weight by inescapable shock: modulation by quinine adulteration, stress reinstatement, and controllability. *Physiol Behav, 45*(5), 975-983.

Dess, N. K., Raizer, J., Chapman, C. D., & Garcia, J. (1988). Stressors in the learned helplessness paradigm: effects on body weight and conditioned taste aversion in rats. *Physiol Behav, 44*(4-5), 483-490.

Di Carlo, V., Hubbard, J. E., & Pate, P. (1973). Fluorescence histochemistry of monoamine-containing cell bodies in the brain stem of the squirrel monkey (Saimiri sciureus). IV. An atlas. *The Journal of comparative neurology, 152*(4), 347-372. doi:10.1002/cne.901520404

Dielenberg, R. A., Hunt, G. E., & McGregor, I. S. (2001). 'When a rat smells a cat': The distribution of Fos immunoreactivity in rat brain following exposure to a predatory odor. *Neuroscience, 104*(4), 1085-1097. doi:Doi 10.1016/S0306-4522(01)00150-6

Donizetti, A., Grossi, M., Pariante, P., D'Aniello, E., Izzo, G., Minucci, S., & Aniello, F. (2008). Two neuron clusters in the stem of postembryonic zebrafish brain specifically express relaxin-3 gene: first evidence of nucleus incertus in fish. *Dev Dyn, 237*(12), 3864-3869. doi:10.1002/dvdy.21786

Dourish, C. T., Rycroft, W., & Iversen, S. D. (1989). Postponement of satiety by blockade of brain cholecystokinin (CCK-B) receptors. *Science, 245*(4925), 1509-1511.

Dubbeldam, J. L., & den Boer-Visser, A. M. (2002). The central mesencephalic grey in birds: nucleus intercollicularis and substantia grisea centralis. *Brain Res Bull, 57*(3-4), 349-352.

Dudchenko, P., & Sarter, M. (1992). Failure of a Chlordiazepoxide to Reproduce the Behavioral-Effects of Muscimol Administered into the Basal Forebrain. *Behavioural brain research, 47*(2), 202-205. doi:Doi 10.1016/S0166-4328(05)80127-5

Dusterhoft, F., Hausler, U., & Jurgens, U. (2004). Neuronal activity in the periaqueductal gray and bordering structures during vocal communication in the squirrel monkey. *Neuroscience, 123*(1), 53-60. doi:10.1016/S0306-4522(03)00612-2

Edwards, S. B., & de Olmos, J. S. (1976). Autoradiographic studies of the projections of the midbrain reticular formation: ascending projections of nucleus cuneiformis. *The Journal of comparative neurology, 165*(4), 417-431. doi:10.1002/cne.901650403

Ennis, M., Behbehani, M., Shipley, M. T., Van Bockstaele, E. J., & Aston-Jones, G. (1991). Projections from the periaqueductal gray to the rostromedial pericoerulear region and nucleus locus coeruleus: anatomic and physiologic studies. *The Journal of comparative neurology, 306*(3), 480-494. doi:10.1002/cne.903060311

Esmaeili, M. H., Reisi, Z., Ezzatpanah, S., & Haghparast, A. (2016). Functional interaction between orexin-1 and CB1 receptors in the periaqueductal gray matter during antinociception induced by chemical stimulation of the lateral hypothalamus in rats. *European journal of pain, 20*(10), 1753-1762. doi:10.1002/ejp.899

Esposito, A., Demeurisse, G., Alberti, B., & Fabbro, F. (1999). Complete mutism after midbrain periaqueductal gray lesion. *Neuroreport, 10*(4), 681-685.

Ezure, K., Tanaka, I., & Kondo, M. (2003). Glycine is used as a transmitter by decrementing expiratory neurons of the ventrolateral medulla in the rat. *Journal of Neuroscience, 23*(26), 8941-8948.

Fahn, S., & Cote, L. J. (1968). Regional distribution of gamma-aminobutyric acid (GABA) in brain of the rhesus monkey. *J Neurochem, 15*(3), 209-213.

Fallon, J. H., & Leslie, F. M. (1986). Distribution of dynorphin and enkephalin peptides in the rat brain. *The Journal of comparative neurology, 249*(3), 293-336. doi:10.1002/cne.902490302

Fanselow, M. S., & Lester, L. S. (1988). A functional behavioristic approach to aversively motivated behavior: Predatory imminence as a determinant of the topography of defensive behavior.

Fardin, V., Oliveras, J. L., & Besson, J. M. (1984). A reinvestigation of the analgesic effects induced by stimulation of the periaqueductal gray matter in the rat. I. The production of behavioral side effects together with analgesia. *Brain research, 306*(1-2), 105-123.

Farooq, U., Rajkumar, R., Sukumaran, S., Wu, Y., Tan, W. H., & Dawe, G. S. (2013). Corticotropin-releasing factor infusion into nucleus incertus suppresses medial prefrontal cortical activity and hippocampo-medial prefrontal cortical long-term potentiation. *The European journal of neuroscience, 38*(4), 2516-2525. doi:10.1111/ejn.12242

Farooq, U., Rajkumar, R., Sukumaran, S., Wu, Y., Tan, W. H., & Dawe, G. S. (2013). Corticotropin-releasing factor infusion into nucleus incertus suppresses medial prefrontal cortical activity and hippocampo-medial prefrontal cortical long-term potentiation. *European Journal of Neuroscience, 38*(4), 2516-2525.

Feder, R., & Ranck, J. B., Jr. (1973). Studies on single neurons in dorsal hippocampal formation and septum in unrestrained rats. II. Hippocampal slow waves and theta cell firing during bar pressing and other behaviors. *Exp Neurol, 41*(2), 532-555. doi:10.1016/0014-4886(73)90291-4

Fernandez De Molina, A., & Hunsperger, R. W. (1962). Organization of the subcortical system governing defence and flight reactions in the cat. *The Journal of physiology, 160*, 200-213.

Finley, J. C., Maderdrut, J. L., Roger, L. J., & Petrusz, P. (1981). The immunocytochemical localization of somatostatin-containing neurons in the rat central nervous system. *Neuroscience, 6*(11), 2173-2192.

Fletcher, G. H., & Starr, M. S. (1987). Behavioural evidence for the functionality of D-2 but not D-1 dopamine receptors at multiple brain sites in the 6-hydroxydopamine-lesioned rat.

Fletcher, P. J., & Coscina, D. V. (1993). Injecting 5-HT into the PVN does not prevent feeding induced by injecting 8-OH-DPAT into the raphe. *Pharmacology Biochemistry and Behavior, 46*(2), 487-491. doi:10.1016/0091-3057(93)90385-7

Flores, J. A., El Banoua, F., Galan-Rodriguez, B., & Fernandez-Espejo, E. (2004). Opiate anti-nociception is attenuated following lesion of large dopamine neurons of the periaqueductal grey: critical role for D1 (not D2) dopamine receptors. *Pain, 110*(1-2), 205-214. doi:10.1016/j.pain.2004.03.036

Flores, J. A., Galan-Rodriguez, B., Ramiro-Fuentes, S., & Fernandez-Espejo, E. (2006). Role for dopamine neurons of the rostral linear nucleus and periaqueductal gray in the rewarding and sensitizing properties of heroin. *Neuropsychopharmacology, 31*(7), 1475-1488. doi:10.1038/sj.npp.1300946

Floyd, N. S., Price, J. L., Ferry, A. T., Keay, K. A., & Bandler, R. (2000). Orbitomedial prefrontal cortical projections to distinct longitudinal columns of the periaqueductal gray in the rat. *The Journal of comparative neurology, 422*(4), 556-578.

Floyd, N. S., Price, J. L., Ferry, A. T., Keay, K. A., & Bandler, R. (2001). Orbitomedial prefrontal cortical projections to hypothalamus in the rat. *Journal of Comparative Neurology, 432*(3), 307-328.

Ford, J. G., Bremner, F. J., & Richie, W. R. (1970). The effect of hours of food deprivation on hippocampal theta rhythm. *Neuropsychologia, 8*(1), 65-73.

Franklin, T. B., Silva, B. A., Perova, Z., Marrone, L., Masferrer, M. E., Zhan, Y., . . . Gross, C. T. (2017). Prefrontal cortical control of a brainstem social behavior circuit. *Nature neuroscience*. doi:10.1038/nn.4470

Fuchs, P. N., Peng, Y. B., Boyette-Davis, J. A., & Uhelski, M. L. (2014). The anterior cingulate cortex and pain processing. *Front Integr Neurosci, 8*, 35. doi:10.3389/fnint.2014.00035

Garcia-Rill, E., Skinner, R. D., Gilmore, S. A., & Owings, R. (1983). Connections of the mesencephalic locomotor region (MLR) II. Afferents and efferents. *Brain Res Bull, 10*(1), 63-71.

Gehlert, D. R., & Wamsley, J. K. (1985). Dopamine receptors in the rat brain: quantitative autoradiographic localization using [3H]sulpiride. *Neurochemistry International, 7*(4), 717-723. doi:http://dx.doi.org/10.1016/0197-0186(85)90070-1

Gerfen, C. R., Staines, W. A., Arbuthnott, G. W., & Fibiger, H. C. (1982). Crossed connections of the substantia nigra in the rat. *The Journal of comparative neurology, 207*(3), 283-303. doi:10.1002/cne.902070308

Gioia, M., Bianchi, R., & Tredici, G. (1984). Cytoarchitecture of the periaqueductal gray matter in the cat: a quantitative Nissl study. *Acta Anat (Basel), 119*(2), 113-117.

Gioia, M., Tredici, G., & Bianchi, R. (1983). The ultrastructure of the periaqueductal gray matter of the cat. *J Submicrosc Cytol, 15*(4), 1013-1026.

Gong, J. P., Onaivi, E. S., Ishiguro, H., Liu, Q. R., Tagliaferro, P. A., Brusco, A., & Uhl, G. R. (2006). Cannabinoid CB2 receptors: immunohistochemical localization in rat brain. *Brain research, 1071*(1), 10-23. doi:10.1016/j.brainres.2005.11.035

Gonzalez-Hernandez, T., Conde-Sendin, M., & Meyer, G. (1992). Laminar distribution and morphology of NADPH-diaphorase containing neurons in the superior colliculus and underlying periaqueductal gray of the rat. *Anat Embryol (Berl), 186*(3), 245-250.

Gonzaloruiz, A., Alonso, A., Sanz, J. M., & Llinas, R. R. (1992). Afferent-Projections to the Mammillary Complex of the Rat, with Special Reference to Those from Surrounding Hypothalamic Regions. *Journal of Comparative Neurology, 321*(2), 277-299. doi:DOI 10.1002/cne.903210208

Goto, M., Swanson, L. W., & Canteras, N. S. (2001). Connections of the nucleus incertus. *The Journal of comparative neurology, 438*(1), 86-122.

Gotti, S., Sica, M., Viglietti-Panzica, C., & Panzica, G. (2005). Distribution of nitric oxide synthase immunoreactivity in the mouse brain. *Microsc Res Tech, 68*(1), 13-35. doi:10.1002/jemt.20219

Graeff, F. G., Guimaraes, F. S., De Andrade, T. G., & Deakin, J. F. (1996). Role of 5-HT in stress, anxiety, and depression. *Pharmacol Biochem Behav, 54*(1), 129-141.

Graham, J. (1977). An autoradiographic study of the efferent connections of the superior colliculus in the cat. *The Journal of comparative neurology, 173*(4), 629-654. doi:10.1002/cne.901730403

Grahn, R. E., Kalman, B. A., Brennan, F. X., Watkins, L. R., & Maier, S. F. (1995). The elevated plus-maze is not sensitive to the effect of stressor controllability in rats.

Grahn, R. E., Maswood, S., McQueen, M. B., Watkins, L. R., & Maier, S. F. (1999). Opioid-dependent effects of inescapable shock on escape behavior and conditioned fear responding are mediated by the dorsal raphe nucleus. *Behavioural brain research, 99*(2), 153-167.

Gray, J. A., & McNaughton, N. (2000). *The Neuropsychology of Anxiety: An enquiry into the functions of the septo-hippocampal system* (2nd ed.). Oxford: Oxford University Press.

Gray, J. A., & McNaughton, N. (2000). *The Neuropsychology of Anxiety: An Enquiry into the Functions of the Septo-Hippocampal System (2 ed.)*. Oxford: Oxford University Press.

Gray, T. S., & Magnuson, D. J. (1992). Peptide immunoreactive neurons in the amygdala and the bed nucleus of the stria terminalis project to the midbrain central gray in the rat. *Peptides, 13*(3), 451-460.

Green, J. D., & Arduini, A. A. (1954). Hippocampal electrical activity in arousal. *Journal of neurophysiology, 17*(6), 533-557. doi:10.1152/jn.1954.17.6.533

Griffiths, J. L., & Lovick, T. A. (2002). Co-localization of 5-HT2A-receptor- and GABA-immunoreactivity in neurones in the periaqueductal grey matter of the rat. *Neuroscience Letters, 326*(3), 151-154. doi:Pii S0304-3940(02)00182-9

Doi 10.1016/S0304-3940(02)00182-9

Gross, C. T., & Canteras, N. S. (2012). The many paths to fear. *Nature reviews Neuroscience, 13*(9), 651-658. doi:10.1038/nrn3301

Guertzenstein, P. G., & Silver, A. (1974). Fall in blood pressure produced from discrete regions of the ventral surface of the medulla by glycine and lesions. *The Journal of physiology, 242*(2), 489-503.

Guimaraes, F. S., Beijamini, V., Moreira, F. A., Aguiar, D. C., & de Lucca, A. C. (2005). Role of nitric oxide in brain regions related to defensive reactions. *Neuroscience and biobehavioral reviews, 29*(8), 1313-1322. doi:10.1016/j.neubiorev.2005.03.026

Guimaraes, F. S., Deaguiar, J. C., Delbel, E. A., & Ballejo, G. (1994). Anxiolytic Effect of Nitric-Oxide Synthase Inhibitors Microinjected into the Dorsal Central Grey. *Neuroreport, 5*(15), 1929-1932. doi:Doi 10.1097/00001756-199410000-00022

Gundlach, A. L. (1991). Regional subdivisions in the midbrain periaqueductal gray of the cat revealed by in vitro receptor autoradiography. *Midbrain Periaqueductal Gray Matter*.

Gundlach, A. L., Ma, S., Sang, Q., Shen, P. J., Piccenna, L., Sedaghat, K., . . . Sutton, S. W. (2009). Relaxin family peptides and receptors in mammalian brain. *Annals of the New York Academy of Sciences, 1160*, 226-235. doi:10.1111/j.1749-6632.2009.03956.x

Gutstein, H. B., Mansour, A., Watson, S. J., Akil, H., & Fields, H. L. (1998). Mu and kappa opioid receptors in periaqueductal gray and rostral ventromedial medulla. *Neuroreport, 9*(8), 1777-1781.

Haller, J., Toth, M., Halasz, J., & De Boer, S. F. (2006). Patterns of violent aggression-induced brain c-fos expression in male mice selected for aggressiveness. *Physiol Behav, 88*(1-2), 173-182. doi:10.1016/j.physbeh.2006.03.030

Hamilton, B. L. (1973a). Cytoarchitectural subdivisions of the periaqueductal gray matter in the cat. *The Journal of comparative neurology, 149*(1), 1-27. doi:10.1002/cne.901490102

Hamilton, B. L. (1973b). Projections of the nuclei of the periaqueductal gray matter in the cat. *The Journal of comparative neurology, 152*(1), 45-58. doi:10.1002/cne.901520104

Harfstrand, A., Adem, A., Fuxe, K., Agnati, L., Andersson, K., & Nordberg, A. (1988). Distribution of nicotinic cholinergic receptors in the rat tel- and diencephalon: a quantitative receptor autoradiographical study using [3H]-acetylcholine, [alpha-125I]bungarotoxin and [3H]nicotine. *Acta Physiol Scand, 132*(1), 1-14. doi:10.1111/j.1748-1716.1988.tb08291.x

Harris, G. C., & Aston-Jones, G. (2006). Arousal and reward: a dichotomy in orexin function. *Trends Neurosci, 29*(10), 571-577. doi:10.1016/j.tins.2006.08.002

Hasue, R. H., & Shammah-Lagnado, S. J. (2002). Origin of the dopaminergic innervation of the central extended amygdala and accumbens shell: a combined retrograde tracing and immunohistochemical study in the rat. *The Journal of comparative neurology, 454*(1), 15-33. doi:10.1002/cne.10420

Haugaard-Kedstrom, L. M., Shabanpoor, F., Hossain, M. A., Clark, R. J., Ryan, P. J., Craik, D. J., . . . Rosengren, K. J. (2011). Design, synthesis, and characterization of a single-chain peptide antagonist for the relaxin-3 receptor RXFP3. *J Am Chem Soc, 133*(13), 4965-4974. doi:10.1021/ja110567j

Hayakawa, T., Ito, H., & Zyo, K. (1993). Neuroanatomical study of afferent projections to the supramammillary nucleus of the rat. *Anat Embryol (Berl), 188*(2), 139-148.

Henderson, L. A., Keay, K. A., & Bandler, R. (1998). The ventrolateral periaqueductal gray projects to caudal brainstem depressor regions: a functional-anatomical and physiological study. *Neuroscience, 82*(1), 201-221.

Herbert, H., & Saper, C. B. (1992a). Organization of medullary adrenergic and noradrenergic projections to the periaqueductal gray matter in the rat. *The Journal of comparative neurology, 315*, 34-52.

Herbert, H., & Saper, C. B. (1992b). Organization of medullary adrenergic and noradrenergic projections to the periaqueductal gray matter in the rat. *The Journal of comparative neurology, 315*(1), 34-52. doi:10.1002/cne.903150104

Herkenham, M., Lynn, A. B., de Costa, B. R., & Richfield, E. K. (1991). Neuronal localization of cannabinoid receptors in the basal ganglia of the rat. *Brain research, 547*(2), 267-274.

Herkenham, M., Lynn, A. B., Johnson, M. R., Melvin, L. S., de Costa, B. R., & Rice, K. C. (1991). Characterization and localization of cannabinoid receptors in rat brain: a quantitative in vitro autoradiographic study. *The Journal of neuroscience, 11*(2), 563-583.

Herkenham, M., & Nauta, W. J. (1977). Afferent connections of the habenular nuclei in the rat. A horseradish peroxidase study, with a note on the fiber-of-passage problem. *The Journal of comparative neurology, 173*(1), 123-146. doi:10.1002/cne.901730107

Herkenham, M., & Nauta, W. J. (1979). Efferent connections of the habenular nuclei in the rat. *The Journal of comparative neurology, 187*(1), 19-47. doi:10.1002/cne.901870103

Herkenham, M., & Pert, C. B. (1982). Light Microscopic Localization of Brain Opiate Receptors - a General Autoradiographic Method Which Preserves Tissue Quality. *Journal of Neuroscience, 2*(8), 1129-1149.

Herrero, M. T., Insausti, R., & Gonzalo, L. M. (1991). Cortically projecting cells in the periaqueductal gray matter of the rat. A retrograde fluorescent tracer study. *Brain research, 543*(2), 201-212.

Hirschfeld, R. M. (2000). History and evolution of the monoamine hypothesis of depression. *J Clin Psychiatry, 61 Suppl 6*, 4-6.

Hirschfeld, R. M. (2001). The Comorbidity of Major Depression and Anxiety Disorders: Recognition and Management in Primary Care. *Prim Care Companion J Clin Psychiatry, 3*(6), 244-254.

Hirschfeld, R. M., Montgomery, S. A., Keller, M. B., Kasper, S., Schatzberg, A. F., Moller, H. J., . . . Bourgeois, M. (2000). Social functioning in depression: a review. *J Clin Psychiatry, 61*(4), 268-275.

Holmer, H. K., Rodman, J. E., Helmreich, D. L., & Parfitt, D. B. (2003). Differential effects of chronic escapable versus inescapable stress on male syrian hamster (Mesocricetus auratus) reproductive behavior. *Hormones and behavior, 43*(3), 381-387. doi:10.1016/s0018-506x(03)00009-6

Holstege, G. (1991a). Descending motor pathways and the spinal motor system: limbic and non-limbic components. *Prog Brain Res, 87*, 307-421.

Holstege, G. (1991b). Descending Pathways from the Periaqueductal Gray and Adjacent Areas. *Midbrain Periaqueductal Gray Matter, 213*, 239-265.

Holstege, G., & Subramanian, H. H. (2016). Two different motor systems are needed to generate human speech. *The Journal of comparative neurology, 524*(8), 1558-1577. doi:10.1002/cne.23898

Honrubia, M. A., Vilaró, M. T., Palacios, J. M., & Mengod, G. (2000). Distribution of the histamine H2 receptor in monkey brain and its mRNA localization in monkey and human brain. *Synapse*.

Hoover, W. B., & Vertes, R. P. (2007). Anatomical analysis of afferent projections to the medial prefrontal cortex in the rat. *Brain Struct Funct, 212*(2), 149-179. doi:10.1007/s00429-007-0150-4

Hoover, W. B., & Vertes, R. P. (2011). Projections of the medial orbital and ventral orbital cortex in the rat. *The Journal of comparative neurology, 519*(18), 3766-3801. doi:10.1002/cne.22733

Hope, B. T., Michael, G. J., Knigge, K. M., & Vincent, S. R. (1991). Neuronal Nadph Diaphorase Is a Nitric-Oxide Synthase. *Proceedings of the National Academy of Sciences of the United States of America, 88*(7), 2811-2814. doi:DOI 10.1073/pnas.88.7.2811

Hopkins, D. A., & Holstege, G. (1978). Amygdaloid projections to the mesencephalon, pons and medulla oblongata in the cat. *Experimental brain research, 32*, 529-547.

Hopkins, D. A., & Niessen, L. W. (1976). Substantia nigra projections to the reticular formation, superior colliculus and central gray in the rat, cat and monkey. *Neurosci Lett, 2*(5), 253-259.

Hosken, I. T., Sutton, S. W., Smith, C. M., & Gundlach, A. L. (2015). Relaxin-3 receptor (Rxfp3) gene knockout mice display reduced running wheel activity: implications for role of relaxin-3/RXFP3 signalling in sustained arousal. *Behavioural brain research, 278*, 167-175. doi:10.1016/j.bbr.2014.09.028

Hosobuchi, Y., Rossier, J., Bloom, F. E., & Guillemin, R. (1979). Stimulation of human periaqueductal gray for pain relief increases immunoreactive beta-endorphin in ventricular fluid. *Science, 203*(4377), 279-281.

Hsu, D. T., Sanford, B. J., Meyers, K. K., Love, T. M., Hazlett, K. E., Wang, H., . . . Zubieta, J. K. (2013). Response of the mu-opioid system to social rejection and acceptance. *Molecular psychiatry, 18*(11), 1211-1217. doi:10.1038/mp.2013.96

Hubbard, J. E., & Di Carlo, V. (1974). Fluorescence histochemistry of monoamine-containing cell bodies in the brain stem of the squirrel monkey (Saimiri sciureus). III. Serotonin-containing groups.

Humphreys, R. K., & Ruxton, G. D. (2018). A review of thanatosis (death feigning) as an anti-predator behaviour. *Behav Ecol Sociobiol, 72*(2), 22. doi:10.1007/s00265-017-2436-8

Hunsperger, R. (1956). Affektreaktionen auf elektrische Reizung im Hirnstamm der Katze. *Helv. physiol. pharmacol. Acta, 14*, 70-92.

Hurlemann, R., Wagner, M., Hawellek, B., Reich, H., Pieperhoff, P., Amunts, K., . . . Dolan, R. J. (2007). Amygdala control of emotion-induced forgetting and remembering: evidence from Urbach-Wiethe disease. *Neuropsychologia, 45*(5), 877-884. doi:10.1016/j.neuropsychologia.2006.08.027

Hurley, K. M., Herbert, H., Moga, M. M., & Saper, C. B. (1991). Efferent projections of the infralimbic cortex of the rat. *The Journal of comparative neurology, 308*(2), 249-276. doi:10.1002/cne.903080210

Iigaya, K., Horiuchi, J., McDowall, L. M., & Dampney, R. A. (2010). Topographical specificity of regulation of respiratory and renal sympathetic activity by the midbrain dorsolateral periaqueductal gray. *Am J Physiol Regul Integr Comp Physiol, 299*(3), R853-861. doi:10.1152/ajpregu.00249.2010

Insausti, R., Amaral, D. G., & Cowan, W. M. (1987). The entorhinal cortex of the monkey: III. Subcortical afferents. *The Journal of comparative neurology, 264*(3), 396-408. doi:10.1002/cne.902640307

Iwase, K., Takemura, M., Shimada, T., Wakisaka, S., Nokubi, T., & Shigenaga, Y. (1998). Ontogeny of NADPH-diaphorase in rat forebrain and midbrain. *Anat Embryol (Berl), 197*(3), 229-247.

Jansen, A. S., Farkas, E., Mac Sams, J., & Loewy, A. D. (1998). Local connections between the columns of the periaqueductal gray matter: a case for intrinsic neuromodulation.

Jasmin, L., Burkey, A. R., Granato, A., & Ohara, P. T. (2004). Rostral agranular insular cortex and pain areas of the central nervous system: a tract-tracing study in the rat. *The Journal of comparative neurology, 468*(3), 425-440. doi:10.1002/cne.10978

Jenck, F., Moreau, J. L., & Martin, J. R. (1995). Dorsal Periaqueductal Gray-Induced Aversion as a Simulation of Panic Anxiety - Elements of Face and Predictive-Validity. *Psychiatry Research, 57*(2), 181-191. doi:Doi 10.1016/0165-1781(95)02673-K

Jennes, L., Stumpf, W. E., & Kalivas, P. W. (1982). Neurotensin: topographical distribution in rat brain by immunohistochemistry. *The Journal of comparative neurology, 210*(3), 211-224. doi:10.1002/cne.902100302

Johnson, M. D., & Ma, P. M. (1993). Localization of NADPH diaphorase activity in monoaminergic neurons of the rat brain. *The Journal of comparative neurology, 332*(4), 391-406. doi:10.1002/cne.903320402

Jones, B. E., & Moore, R. Y. (1977). Ascending projections of the locus coeruleus in the rat. II. Autoradiographic study. *Brain research, 127*(1), 25-53.

Jones, B. E., & Yang, T. Z. (1985). The efferent projections from the reticular formation and the locus coeruleus studied by anterograde and retrograde axonal transport in the rat. *The Journal of comparative neurology, 242*(1), 56-92. doi:10.1002/cne.902420105

Jurgens, U., & Lu, C. L. (1992). Interactions between glutamate, GABA, acetylcholine and histamine in the periaqueductal gray's control of vocalization in the squirrel monkey.

Kaada, B. (1967). *Brain mechanisms related to aggressive behavior*. Paper presented at the UCLA Forum Med Sci.

Kaas, J. H. (2012). The evolution of neocortex in primates. *Prog Brain Res, 195*, 91-102. doi:10.1016/B978-0-444-53860-4.00005-2

Kakeyama, M., & Yamanouchi, K. (1993). Female sexual behaviors in male rats with dorsal raphe nucleus lesions: treatment with p-chlorophenylalanine. *Brain Res Bull, 30*(5-6), 705-709.

Karlstedt, K., Nissinen, M., Michelsen, K. A., & Panula, P. (2001). Multiple sites of L-histidine decarboxylase expression in mouse suggest novel developmental functions for histamine. *Dev Dyn, 221*(1), 81-91. doi:10.1002/dvdy.1127

Kataoka, K., Mizuno, N., & Frohman, L. A. (1979). Regional Distribution of Immunoreactive Neurotensin in Monkey Brain. *Brain Research Bulletin, 4*(1), 57-60. doi:Doi 10.1016/0361-9230(79)90058-3

Keay, K. A., & Bandler, R. (1993). Deep and superficial noxious stimulation increases Fos-like immunoreactivity in different regions of the midbrain periaqueductal grey of the rat. *Neurosci Lett, 154*(1-2), 23-26.

Keay, K. A., & Bandler, R. (2015). Periaqueductal Gray. 207-221. doi:10.1016/b978-0-12-374245-2.00010-3

Keay, K. A., Feil, K., Gordon, B. D., Herbert, H., & Bandler, R. (1997). Spinal afferents to functionally distinct periaqueductal gray columns in the rat: an anterograde and retrograde tracing study. *The Journal of comparative neurology, 385*(2), 207-229.

Kemp, I. R., & Kaada, B. R. (1975). The relation of hippocampal theta activity to arousal, attentive behaviour and somato-motor movements in unrestrained cats. *Brain research, 95*(2-3), 323-342.

Khachaturian, H., Lewis, M. E., & Watson, S. J. (1983). Enkephalin Systems in Diencephalon and Brain-Stem of the Rat. *Journal of Comparative Neurology, 220*(3), 310-320. doi:DOI 10.1002/cne.902200305

Kim, M. A., Lee, H. S., Lee, B. Y., & Waterhouse, B. D. (2004). Reciprocal connections between subdivisions of the dorsal raphe and the nuclear core of the locus coeruleus in the rat. *Brain research, 1026*(1), 56-67. doi:10.1016/j.brainres.2004.08.022

Kimura, H., McGeer, P. L., Peng, J. H., & McGeer, E. G. (1981). The central cholinergic system studied by choline acetyltransferase immunohistochemistry in the cat. *The Journal of comparative neurology, 200*(2), 151-201. doi:10.1002/cne.902000202

Kingsbury, M. A., Kelly, A. M., Schrock, S. E., & Goodson, J. L. (2011). Mammal-like organization of the avian midbrain central gray and a reappraisal of the intercollicular nucleus. *PloS one, 6*(6), e20720. doi:10.1371/journal.pone.0020720

Kirk, R. (2013). *Experimental Design: Procedures for the Behavioral Sciences*.

Kittelberger, J. M., & Bass, A. H. (2013). Vocal-motor and auditory connectivity of the midbrain periaqueductal gray in a teleost fish. *The Journal of comparative neurology, 521*(4), 791-812. doi:10.1002/cne.23202

Klein, D. F. (1993). False suffocation alarms, spontaneous panics, and related conditions - an integrative hypothesis. *Archives of General Psychiatry, 50*(4), 306-317.

Klein, M. O., Cruz Ade, M., Machado, F. C., Picolo, G., Canteras, N. S., & Felicio, L. F. (2014). Periaqueductal gray mu and kappa opioid receptors determine behavioral selection from maternal to predatory behavior in lactating rats. *Behavioural brain research, 274*, 62-72. doi:10.1016/j.bbr.2014.08.008

Koen, N., Fourie, J., Terburg, D., Stoop, R., Morgan, B., Stein, D. J., & van Honk, J. (2016). Translational neuroscience of basolateral amygdala lesions: Studies of Urbach-Wiethe disease. *J Neurosci Res, 94*(6), 504-512. doi:10.1002/jnr.23731

Kohler, C., & Steinbusch, H. (1982). Identification of serotonin and non-serotonin-containing neurons of the mid-brain raphe projecting to the entorhinal area and the hippocampal formation. A combined immunohistochemical and fluorescent retrograde tracing study in the rat brain. *Neuroscience, 7*(4), 951-975.

Kramer, J. M., Nolan, P. C., & Waldrop, T. G. (1999). In vitro responses of neurons in the periaqueductal gray to hypoxia and hypercapnia. *Brain research, 835*(2), 197-203.

Kramis, R. V., C.H.; Bland, B.H. (1975). Two Types of Hippocampal Rhythmical Slow Activity in Both the Rabbit and the Rat: Relations to Behavior and Effects of Atropine, Diethyl Ether, Urethane, and Pentobarbital.

Krettek, J. E., & Price, J. L. (1978). Amygdaloid projections to subcortical structures within the basal forebrain and brainstem in the rat and cat.

Kroes, R. A., Burgdorf, J., Otto, N. J., Panksepp, J., & Moskal, J. R. (2007). Social defeat, a paradigm of depression in rats that elicits 22-kHz vocalizations, preferentially activates the cholinergic signaling pathway in the periaqueductal gray. *Behavioural brain research, 182*(2), 290-300. doi:10.1016/j.bbr.2007.03.022

Krout, K. E., Jansen, A. S., & Loewy, A. D. (1998). Periaqueductal gray matter projection to the parabrachial nucleus in rat. *The Journal of comparative neurology, 401*(4), 437-454.

Krout, K. E., & Loewy, A. D. (2000). Periaqueductal gray matter projections to midline and intralaminar thalamic nuclei of the rat. *The Journal of comparative neurology, 424*(1), 111-141.

Kwiat, G. C., & Basbaum, A. I. (1990). Organization of tyrosine hydroxylase- and serotonin-immunoreactive brainstem neurons with axon collaterals to the periaqueductal gray and the spinal cord in the rat. *Brain research, 528*(1), 83-94.

Kyuhou, S., & Gemba, H. (1998). Two vocalization-related subregions in the midbrain periaqueductal gray of the guinea pig. *Neuroreport, 9*(7), 1607-1610.

Lalla, L., Rueda Orozco, P. E., Jurado-Parras, M. T., Brovelli, A., & Robbe, D. (2017). Local or Not Local: Investigating the Nature of Striatal Theta Oscillations in Behaving Rats. *eNeuro, 4*(5). doi:10.1523/ENEURO.0128-17.2017

Lamotte, C., Pert, C. B., & Snyder, S. H. (1976). Opiate receptor binding in primate spinal cord: distribution and changes after dorsal root section. *Brain research, 112*(2), 407-412.

Lawther, A. J., Clissold, M. L., Ma, S., Kent, S., Lowry, C. A., Gundlach, A. L., & Hale, M. W. (2015). Anxiogenic drug administration and elevated plus-maze exposure in rats activate populations of relaxin-3 neurons in the nucleus incertus and serotonergic neurons in the dorsal raphe nucleus. *Neuroscience, 303*, 270-284. doi:10.1016/j.neuroscience.2015.06.052

LeDoux, J. (2012). Rethinking the emotional brain. *Neuron, 73*(4), 653-676. doi:10.1016/j.neuron.2012.02.004

Lee, H. Y., Tae, W. S., Yoon, H. K., Lee, B. T., Paik, J. W., Son, K. R., . . . Ham, B. J. (2011). Demonstration of decreased gray matter concentration in the midbrain encompassing the dorsal raphe nucleus and the limbic subcortical regions in major depressive disorder: an optimized voxel-based morphometry study. *J Affect Disord, 133*(1-2), 128-136. doi:10.1016/j.jad.2011.04.006

Leger, L., Charnay, Y., Dubois, P. M., & Jouvet, M. (1986). Distribution of enkephalin-immunoreactive cell bodies in relation to serotonin-containing neurons in the raphe nuclei of the cat: immunohistochemical evidence for the coexistence of enkephalins and serotonin in certain cells. *Brain research, 362*(1), 63-73.

Leigh, P. N., Connick, J. H., & Stone, T. W. (1990). Distribution of NADPH-diaphorase positive cells in the rat brain. *Comp Biochem Physiol C, 97*(2), 259-264.

Leite Silveira, M. C., Zangrossi Jr, H., de Barros Viana, M., Silveira, R., & Graeff, F. G. (2001). Differential expression of Fos protein in the rat brain induced by performance of avoidance or escape in the elevated T-maze. *Behavioural brain research, 126*(1–2), 13-21. doi:http://dx.doi.org/10.1016/S0166-4328(01)00233-9

Leman, S., Dielenberg, R. A., & Carrive, P. (2003). Effect of dorsal periaqueductal gray lesion on cardiovascular and behavioural responses to contextual conditioned fear in rats. *Behavioural brain research, 143*(2), 169-176. doi:10.1016/s0166-4328(03)00033-0

Lever, C., Burton, S., & O'Keefe, J. (2006). Rearing on Hind Legs, Environmental Novelty, and the Hippocampal Formation. *Reviews in the Neurosciences, 17*(1-2). doi:10.1515/revneuro.2006.17.1-2.111

Levey, A. I., Kitt, C. A., Simonds, W. F., Price, D. L., & Brann, M. R. (1991). Identification and localization of muscarinic acetylcholine receptor proteins in brain with subtype-specific antibodies. *The Journal of neuroscience, 11*(10), 3218-3226.

Levine, E. S., & Jacobs, B. L. (1992). Neurochemical afferents controlling the activity of serotonergic neurons in the dorsal raphe nucleus: microiontophoretic studies in the awake cat. *The Journal of neuroscience, 12*(10), 4037-4044.

Li, S., & Kirouac, G. J. (2012). Sources of inputs to the anterior and posterior aspects of the paraventricular nucleus of the thalamus. *Brain Struct Funct, 217*(2), 257-273. doi:10.1007/s00429-011-0360-7

Li, Y., & Han, J. S. (1989). Cholecystokinin-octapeptide antagonizes morphine analgesia in periaqueductal gray of the rat. *Brain research, 480*(1-2), 105-110.

Li, Y. Q., Takada, M., & Mizuno, N. (1993). Collateral Projections of Single Neurons in the Periaqueductal Gray and Dorsal Raphe Nucleus to Both the Trigeminal Sensory Complex and Spinal-Cord in the Rat. *Neuroscience Letters, 153*(2), 153-156. doi:Doi 10.1016/0304-3940(93)90310-H

Li, Y. Q., Takada, M., Shinonaga, Y., & Mizuno, N. (1993). Direct projections from the midbrain periaqueductal gray and the dorsal raphe nucleus to the trigeminal sensory complex in the rat. *Neuroscience, 54*(2), 431-443.

Li, Y. Q., Zeng, S. L., Dong, Y. X., Rao, Z. R., & Shi, J. W. (1991). Serotonin-, substance P- and tyrosine hydroxylase-like immunoreactive neurons projecting from the periaqueductal gray to the ventromedial hypothalamic nucleus in the rat. *Neurosci Lett, 134*(1), 33-36.

Lim, L. W., Temel, Y., Sesia, T., Vlamings, R., Visser-Vandewalle, V., Steinbusch, H. W. M., & Blokland, A. (2008). Buspirone induced acute and chronic changes of neural activation in the periaqueductal gray of rats. *Neuroscience, 155*(1), 164-173.

Lindquist, K. A., Wager, T. D., Kober, H., Bliss-Moreau, E., & Barrett, L. F. (2012). The brain basis of emotion: a meta-analytic review. *Behav Brain Sci, 35*(3), 121-143. doi:10.1017/S0140525X11000446

Lino-de-Oliveira, C., Sales, A. J., Del Bel, E. A., Silveira, M. C., & Guimaraes, F. S. (2001). Effects of acute and chronic fluoxetine treatments on restraint stress-induced Fos expression. *Brain Res Bull, 55*(6), 747-754.

Liu, C., Eriste, E., Sutton, S., Chen, J., Roland, B., Kuei, C., . . . Lovenberg, T. W. (2003). Identification of relaxin-3/INSL7 as an endogenous ligand for the orphan G-protein-coupled receptor GPCR135. *The Journal of biological chemistry, 278*(50), 50754-50764. doi:10.1074/jbc.M308995200

Liu, H., Chandler, S., Beitz, A. J., Shipley, M. T., & Behbehani, M. M. (1994). Characterization of the effect of cholecystokinin (CCK) on neurons in the periaqueductal gray of the rat: Immunocytochemical and in vivo and in vitro electrophysiological studies. *Brain research, 642*, 83-94.

Liu, R. P., & Swenberg, M. L. (1988). Autoradiographic localization of substance P ligand binding sites and distribution of immunoreactive neurons in the periaqueductal gray of the rat. *Brain research, 475*(1), 73-79.

Ljungdahl, A., Hokfelt, T., & Nilsson, G. (1978). Distribution of substance P-like immunoreactivity in the central nervous system of the rat--I. Cell bodies and nerve terminals. *Neuroscience, 3*(10), 861-943.

Lonstein, J. S., & Stern, J. M. (1997a). Role of the midbrain periaqueductal gray in maternal nurturance and aggression: c-fos and electrolytic lesion studies in lactating rats. *The Journal of neuroscience, 17*(9), 3364-3378.

Lonstein, J. S., & Stern, J. M. (1997b). Somatosensory contributions to c-fos activation within the caudal periaqueductal gray of lactating rats: Effects of perioral, rooting, and suckling stimuli from pups. *Hormones and behavior, 32*(3), 155-166. doi:DOI 10.1006/hbeh.1997.1416

Lonstein, J. S., & Stern, J. M. (1998). Site and behavioral specificity of periaqueductal gray lesions on postpartum sexual, maternal, and aggressive behaviors in rats. *Brain research, 804*(1), 21-35.

Lopes da Silva, F. H., & Kamp, A. (1969). Hippocampal theta frequency shifts and operant behaviour. *Electroencephalogr Clin Neurophysiol, 26*(2), 133-143.

Loren, I., Alumets, J., Hakanson, R., & Sundler, F. (1979). Distribution of gastrin and CCK-like peptides in rat brain. An immunocytochemical study. *Histochemistry, 59*(4), 249-257.

Lovick, T. A. (2008). Pro-nociceptive action of cholecystokinin in the periaqueductal grey: a role in neuropathic and anxiety-induced hyperalgesic states. *Neuroscience and biobehavioral reviews, 32*(4), 852-862. doi:10.1016/j.neubiorev.2008.01.003

Lu, C. L., & Jurgens, U. (1993). Effects of chemical stimulation in the periaqueductal gray on vocalization in the squirrel monkey. *Brain Res Bull, 32*(2), 143-151.

Lu, J., Jhou, T. C., & Saper, C. B. (2006). Identification of wake-active dopaminergic neurons in the ventral periaqueductal gray matter. *The Journal of neuroscience, 26*(1), 193-202. doi:10.1523/JNEUROSCI.2244-05.2006

Lukkes, J., Vuong, S., Scholl, J., Oliver, H., & Forster, G. (2009). Corticotropin-Releasing Factor Receptor Antagonism within the Dorsal Raphe Nucleus Reduces Social Anxiety-Like Behavior after Early-Life Social Isolation. *J. Neurosci., 29*(32), 9955-9960. doi:10.1523/jneurosci.0854-09.2009

Lydiard, R. B., & Ballenger, J. C. (1987). Antidepressants in panic disorder and agoraphobia. *J Affect Disord, 13*(2), 153-168.

Lyon, M., Halpern, M., & Mintz, E. (1968). The significance of the mesencephalon for coordinated feeding behavior. *Acta Neurol Scand, 44*(3), 323-346.

Ma, S., Allocca, G., Ong-Palsson, E. K., Singleton, C. E., Hawkes, D., McDougall, S. J., . . . Gundlach, A. L. (2017). Nucleus incertus promotes cortical desynchronization and behavioral arousal. *Brain Struct Funct, 222*(1), 515-537. doi:10.1007/s00429-016-1230-0

Ma, S., Blasiak, A., Olucha-Bordonau, F. E., Verberne, A. J., & Gundlach, A. L. (2013). Heterogeneous responses of nucleus incertus neurons to corticotrophin-releasing factor and coherent activity with hippocampal theta rhythm in the rat. *The Journal of physiology, 591*(Pt 16), 3981-4001. doi:10.1113/jphysiol.2013.254300

Ma, S., Bonaventure, P., Ferraro, T., Shen, P. J., Burazin, T. C., Bathgate, R. A., . . . Gundlach, A. L. (2007). Relaxin-3 in GABA projection neurons of nucleus incertus suggests widespread influence on forebrain circuits via G-protein-coupled receptor-135 in the rat. *Neuroscience, 144*(1), 165-190. doi:10.1016/j.neuroscience.2006.08.072

Ma, S., Olucha-Bordonau, F. E., Hossain, M. A., Lin, F., Kuei, C., Liu, C., . . . Gundlach, A. L. (2009). Modulation of hippocampal theta oscillations and spatial memory by relaxin-3 neurons of the nucleus incertus. *Learning & memory, 16*(11), 730-742. doi:10.1101/lm.1438109

Ma, S., Roozendaal, B., Burazin, T. C., Tregear, G. W., McGaugh, J. L., & Gundlach, A. L. (2005). Relaxin receptor activation in the basolateral amygdala impairs memory

consolidation. *The European journal of neuroscience, 22*(8), 2117-2122. doi:10.1111/j.1460-9568.2005.04374.x

Ma, S., Sang, Q., Lanciego, J. L., & Gundlach, A. L. (2009). Localization of relaxin-3 in brain of Macaca fascicularis: identification of a nucleus incertus in primate. *The Journal of comparative neurology, 517*(6), 856-872. doi:10.1002/cne.22197

Mackie, G. O., Mills, C. E., & Singla, C. L. (1992). Giant Axons and Escape Swimming in Euplokamis dunlapae (Ctenophora: Cydippida). *Biol Bull, 182*(2), 248-256. doi:10.2307/1542118

Magierek, V., Ramos, P. L., da Silveira-Filho, N. G., Nogueira, R. L., & Landeira-Fernandez, J. (2003). Context fear conditioning inhibits panic-like behavior elicited by electrical stimulation of dorsal periaqueductal gray. *Neuroreport, 14*, 1641-1644.

Mai, J. K., Triepel, J., & Metz, J. (1987). Neurotensin in the human brain. *Neuroscience, 22*(2), 499-524.

Mansour, A., Fox, C. A., Thompson, R. C., Akil, H., & Watson, S. J. (1994). mu-Opioid receptor mRNA expression in the rat CNS: comparison to mu-receptor binding. *Brain research, 643*(1-2), 245-265.

Mansour, A., Khachaturian, H., Lewis, M. E., Akil, H., & Watson, S. J. (1987). Autoradiographic differentiation of mu, delta, and kappa opioid receptors in the rat forebrain and midbrain. *The Journal of neuroscience, 7*(8), 2445-2464.

Mantyh, P. W. (1982a). The ascending input to the midbrain periaqueductal gray of the primate. *The Journal of comparative neurology, 211*(1), 50-64. doi:10.1002/cne.902110106

Mantyh, P. W. (1982b). The midbrain periaqueductal gray in the rat, cat, and monkey: a Nissl, Weil, and Golgi analysis. *The Journal of comparative neurology, 204*(4), 349-363. doi:10.1002/cne.902040406

Mantyh, P. W. (1983). Connections of midbrain periaqueductal gray in the monkey .2. Descending efferent projections. *Journal of neurophysiology, 49*(3), 582-594.

Mantyh, P. W., Hunt, S. P., & Maggio, J. E. (1984). Substance P receptors: localization by light microscopic autoradiography in rat brain using [3H]SP as the radioligand.

Marchand, J. E., & Hagino, N. (1983). Afferents to the periaqueductal gray in the rat. A horseradish peroxidase study. *Neuroscience, 9*(1), 95-106.

Marcus, J. N., Aschkenasi, C. J., Lee, C. E., Chemelli, R. M., Saper, C. B., Yanagisawa, M., & Elmquist, J. K. (2001). Differential expression of orexin receptors 1 and 2 in the rat brain. *The Journal of comparative neurology, 435*(1), 6-25.

Markham, C. M., Blanchard, D. C., Canteras, N. S., Cuyno, C. D., & Blanchard, R. J. (2004). Modulation of predatory odor processing following lesions to the dorsal premammillary nucleus. *Neurosci Lett, 372*(1-2), 22-26. doi:10.1016/j.neulet.2004.09.006

Markowitsch, H. J., Calabrese, P., Wurker, M., Durwen, H. F., Kessler, J., Babinsky, R., . . . Gehlen, W. (1994). The amygdala's contribution to memory--a study on two patients with Urbach-Wiethe disease. *Neuroreport, 5*(11), 1349-1352.

Marson, L. (2004). Lesions of the periaqueductal gray block the medial preoptic area-induced activation of the urethrogenital reflex in male rats. *Neurosci Lett, 367*(3), 278-282. doi:10.1016/j.neulet.2004.06.026

Martin, G. F., Humbertson Jr., A. O., Laxson, L. C., Panneton, W., M., & Tschismadia, I. (1979). Spinal projections from the mesencephalic and pontine reticular formation in the north american opossum: A study using axonal transport techniques.

Martinez-Bellver, S., Cervera-Ferri, A., Martinez-Ricos, J., Ruiz-Torner, A., Luque-Garcia, A., Blasco-Serra, A., . . . Teruel-Marti, V. (2015). Regular theta-firing neurons in the nucleus incertus during sustained hippocampal activation. *The European journal of neuroscience, 41*(8), 1049-1067. doi:10.1111/ejn.12884

Mathew, R. J., & Weinman, M. L. (1982). Sexual dysfunctions in depression. *Arch Sex Behav, 11*(4), 323-328.

Matsuda, L. A., Bonner, T. I., & Lolait, S. J. (1993). Localization of cannabinoid receptor mRNA in rat brain. *The Journal of comparative neurology, 327*(4), 535-550. doi:10.1002/cne.903270406

McCarthy, M. M., Pfaff, D. W., & Schwartz-Giblin, S. (1991). Midbrain central gray GABAA receptor activation enhances, and blockade reduces, sexual behavior in the female rat. *Experimental brain research, 86*(1), 108-116.

McClung, C. A., & Nestler, E. J. (2003). Regulation of gene expression and cocaine reward by CREB and DeltaFosB. *Nature neuroscience, 6*(11), 1208-1215. doi:10.1038/nn1143

McFarland, W., Teitelbaum, H., & Hedges, E. (1975). Relationship between hippocampal theta activity and running speed in the rat. *Journal of Comparative and Physiological Psychology, 88*(1), 324.

McIntyre, D. C., Kelly, M. E., & Staines, W. A. (1996). Efferent projections of the anterior perirhinal cortex in the rat. *The Journal of comparative neurology, 369*(2), 302-318. doi:10.1002/(SICI)1096-9861(19960527)369:2<302::AID-CNE10>3.0.CO;2-J

McKenna, J. T., & Vertes, R. P. (2001). Collateral projections from the median raphe nucleus to the medial septum and hippocampus. *Brain Research Bulletin, 54*(6), 619-630.

McNally, G. P., Pigg, M., & Weidemann, G. (2004). Opioid receptors in the midbrain periaqueductal gray requlate extinction of pavlovian fear conditioning. *The Journal of neuroscience, 24*, 6912-6919.

McNaughton, N., & Corr, P. J. (2004). A two-dimensional neuropsychology of defense: fear/anxiety and defensive distance. *Neuroscience and biobehavioral reviews, 28*(3), 285-305. doi:10.1016/j.neubiorev.2004.03.005

McNaughton, N., DeYoung, C. G., & Corr, P. J. (2016). Approach/Avoidance. 25-49. doi:10.1016/b978-0-12-800935-2.00002-6

McNaughton, N., & Gray, J. A. (2000). Anxiolytic action on the behavioural inhibition system implies multiple types of arousal contribute to anxiety. *Journal of Affective Disorders, 61*, 161-196.

McNaughton, N., Kocsis, B., & Hajos, M. (2007). Elicited hippocampal theta rhythm: a screen for anxiolytic and procognitive drugs through changes in hippocampal function?

McNaughton, N., Kocsis, B., & Hajós, M. (2007). Elicited hippocampal theta rhythm: a screen for anxiolytic and procognitive drugs through changes in hippocampal function? *Behavioural Pharmacology, 18*(5-6), 329-346.

McNaughton, N., & Sedgwick, E. M. (1978). Reticular stimulation and hippocampal theta rhythm in rats: effects of drugs. *Neuroscience, 3*, 629-632.

Meibach, R. C., & Siegel, A. (1977). Efferent connections of the hippocampal formation in the rat. *Brain research, 124*(2), 197-224.

Meller, S. T., & Dennis, B. J. (1986). Afferent projections to the periaqueductal gray in the rabbit. *Neuroscience, 19*(3), 927-964.

Meller, S. T., & Dennis, B. J. (1991). Efferent projections of the periaqueductal gray in the rabbit. *Neuroscience, 40*(1), 191-216. doi:10.1016/0306-4522(91)90185-q

Mellman, T. A., & Uhde, T. W. (1989). Electroencephalographic sleep in panic disorder. A focus on sleep-related panic attacks. *Arch Gen Psychiatry, 46*(2), 178-184.

Merchenthaler, I., Vigh, S., Petrusz, P., & Schally, A. V. (1982). Immunocytochemical localization of corticotropin-releasing factor (CRF) in the rat brain. *Am J Anat, 165*(4), 385-396. doi:10.1002/aja.1001650404

Meyer, P. J., Morgan, M. M., Kozell, L. B., & Ingram, S. L. (2009). Contribution of dopamine receptors to periaqueductal gray-mediated antinociception. *Psychopharmacology (Berl), 204*(3), 531-540. doi:10.1007/s00213-009-1482-y

Mitchell, V. A., Kawahara, H., & Vaughan, C. W. (2009). Neurotensin inhibition of GABAergic transmission via mGluR-induced endocannabinoid signalling in rat periaqueductal grey. *The Journal of physiology, 587*(Pt 11), 2511-2520. doi:10.1113/jphysiol.2008.167429

Mitra, P. (2007). *Observed Brain Dynamics*: Oxford University Press.

Miyamoto, Y., Watanabe, Y., & Tanaka, M. (2008). Developmental expression and serotonergic regulation of relaxin 3/INSL7 in the nucleus incertus of rat brain. *Regul Pept, 145*(1-3), 54-59. doi:10.1016/j.regpep.2007.08.010

Moldrich, G., & Wenger, T. (2000). Localization of the CB1 cannabinoid receptor in the rat brain. An immunohistochemical study. *Peptides, 21*(11), 1735-1742.

Molino, A., & McIntyre, D. C. (1972). Another inexpensive headplug for the electrical recording and or stimulation of rats. *Physiology & Behavior, 9*(2), 273-275. doi:10.1016/0031-9384(72)90249-1

Mongeau, R., & Marsden, C. A. (1997). Effect of central and peripheral administrations of cholecystokinin-tetrapeptide on panic-like reactions induced by stimulation of the dorsal periaqueductal grey area in the rat. *Biological psychiatry, 42*(5), 335-344. doi:10.1016/S0006-3223(96)00407-6

Moore, R. Y., & Goldberg, J. M. (1966). Projections of the inferior colliculus in the monkey. *Exp Neurol, 14*(4), 429-438.

Morilak, D. A., Garlow, S. J., & Ciaranello, R. D. (1993). Immunocytochemical localization and description of neurons expressing serotonin2 receptors in the rat brain. *Neuroscience, 54*(3), 701-717.

Moskowitz, A. S., & Goodman, R. R. (1985). Autoradiographic distribution of mu1 and mu2 opioid binding in the mouse central nervous system. *Brain research, 360*(1-2), 117-129.

Moss, M. S., & Basbaum, A. I. (1983a). The fine structure of the caudal periaqueductal gray of the cat: morphology and synaptic organization of normal and immunoreactive enkephalin-labeled profiles. *Brain research, 289*(1-2), 27-43.

Moss, M. S., & Basbaum, A. I. (1983b). The peptidergic organization of the cat periaqueductal gray. II. The distribution of immunoreactive substance P and vasoactive intestinal polypeptide. *The Journal of neuroscience, 3*(7), 1437-1449.

Moss, M. S., Glazer, E. J., & Basbaum, A. I. (1983). The peptidergic organization of the cat periaqueductal gray. I. The distribution of immunoreactive enkephalin-containing neurons and terminals. *The Journal of neuroscience, 3*(3), 603-616.

Mota-Ortiz, S. R., Sukikara, M. H., Felicio, L. F., & Canteras, N. S. (2009). Afferent connections to the rostrolateral part of the periaqueductal gray: a critical region influencing the motivation drive to hunt and forage. *Neural Plast, 2009*, 612698. doi:10.1155/2009/612698

Motta, S. C., Carobrez, A. P., & Canteras, N. S. (2017). The periaqueductal gray and primal emotional processing critical to influence complex defensive responses, fear learning and reward seeking. *Neuroscience and biobehavioral reviews, 76*(Pt A), 39-47. doi:10.1016/j.neubiorev.2016.10.012

Motta, S. C., Goto, M., Gouveia, F. V., Baldo, M. V., Canteras, N. S., & Swanson, L. W. (2009). Dissecting the brain's fear system reveals the hypothalamus is critical for responding in subordinate conspecific intruders. *Proc Natl Acad Sci U S A, 106*(12), 4870-4875. doi:10.1073/pnas.0900939106

Moyse, E., Rostene, W., Vial, M., Leonard, K., Mazella, J., Kitabgi, P., . . . Beaudet, A. (1987). Distribution of neurotensin binding sites in rat brain: a light microscopic radioautographic study using monoiodo [125 I] Tyr 3-neurotensin. *Neuroscience, 22*(2), 525-536.

Muller, C. J., Quintino-Dos-Santos, J. W., Schimitel, F. G., Tufik, S., Beijamini, V., Canteras, N. S., & Schenberg, L. C. (2017). On the verge of a respiratory-type panic attack: Selective activations of rostrolateral and caudoventrolateral periaqueductal gray matter following short-lasting escape to a low dose of potassium cyanide. *Neuroscience, 348*, 228-240. doi:10.1016/j.neuroscience.2017.02.022

Munn, R. G., Tyree, S. M., McNaughton, N., & Bilkey, D. K. (2015). The frequency of hippocampal theta rhythm is modulated on a circadian period and is entrained by food

availability. *Frontiers in behavioral neuroscience, 9*, 61. doi:10.3389/fnbeh.2015.00061

Murakami, S., Okamura, H., Yanaihara, C., Yanaihara, N., & Ibata, Y. (1987). Immunocytochemical distribution of met-enkephalin-Arg6-Gly7-Leu8 in the rat lower brainstem. *The Journal of comparative neurology, 261*(2), 193-208. doi:10.1002/cne.902610203

Murphy, A. Z., & Hoffman, G. E. (2001). Distribution of gonadal steroid receptor-containing neurons in the preoptic-periaqueductal gray-brainstem pathway: a potential circuit for the initiation of male sexual behavior. *The Journal of comparative neurology, 438*(2), 191-212.

Myers, R. D. (1966). Injection of Solutions into Cerebral Tissue - Relation between Volume and Diffusion. *Physiology & Behavior, 1*(2), 171-&. doi:Doi 10.1016/0031-9384(66)90064-3

Nambu, T., Sakurai, T., Mizukami, K., Hosoya, Y., Yanagisawa, M., & Goto, K. (1999). Distribution of orexin neurons in the adult rat brain. *Brain research, 827*(1-2), 243-260.

Nash, J. R., Sargent, P. A., Rabiner, E. A., Hood, S. D., Argyropoulos, S. V., Potokar, J. P., . . . Nutt, D. J. (2008). Serotonin 5-HT1A receptor binding in people with panic disorder: positron emission tomography study. *Br J Psychiatry, 193*(3), 229-234. doi:10.1192/bjp.bp.107.041186

Nassel, D. R., & Vanden Broeck, J. (2016). Insulin/IGF signaling in Drosophila and other insects: factors that regulate production, release and post-release action of the insulin-like peptides. *Cell Mol Life Sci, 73*(2), 271-290. doi:10.1007/s00018-015-2063-3

Nategh, M., Nikseresht, S., Khodagholi, F., & Motamedi, F. (2015). Nucleus incertus inactivation impairs spatial learning and memory in rats. *Physiol Behav, 139*, 112-120. doi:10.1016/j.physbeh.2014.11.014

Nauta, W. J. (1958). Hippocampal projections and related neural pathways to the midbrain in the cat. *Brain, 81*(3), 319-340.

Neafsey, E. J., Hurley-Gius, K. M., & Arvanitis, D. (1986). The topographical organization of neurons in the rat medial frontal, insular and olfactory cortex projecting to the solitary nucleus, olfactory bulb, periaqueductal gray and superior colliculus. *Brain research, 377*(2), 261-270. doi:10.1016/0006-8993(86)90867-x

Neckers, L. M., Schwartz, J. P., Wyatt, R. J., & Speciale, S. G. (1979). Substance P afferents from the habenula innervate the dorsal raphe nucleus. *Experimental brain research, 37*(3), 619-623.

Neophytou, S. I., Graham, M., Williams, J., Aspley, S., Marsden, C. A., & Beckett, S. R. G. (2000). Strain differences to the effects of aversive frequency ultrasound on behaviour and brain topography of c-fos expression in the rat. *Brain research, 854*(1-2), 158-164.

Nestler, E. J., Barrot, M., & Self, D. W. (2001). DeltaFosB: a sustained molecular switch for addiction. *Proc Natl Acad Sci U S A, 98*(20), 11042-11046. doi:10.1073/pnas.191352698

Nicholas, A. P., Pieribone, V., & Hokfelt, T. (1993a). Distributions of mRNAs for alpha-2 adrenergic receptor subtypes in rat brain: an in situ hybridization study. *The Journal of comparative neurology, 328*(4), 575-594. doi:10.1002/cne.903280409

Nicholas, A. P., Pieribone, V. A., & Hokfelt, T. (1993b). Cellular localization of messenger RNA for beta-1 and beta-2 adrenergic receptors in rat brain: an in situ hybridization study. *Neuroscience, 56*(4), 1023-1039.

Nichols, D. S., Thorn, B. E., & Berntson, G. G. (1989). Opiate and Serotonergic Mechanisms of Stimulation-Produced Analgesia within the Periaqueductal Gray. *Brain Research Bulletin, 22*(4), 717-724. doi:Doi 10.1016/0361-9230(89)90091-9

Nissinen, M. J., & Panula, P. (1995). Developmental patterns of histamine-like immunoreactivity in the mouse. *Journal of Histochemistry & Cytochemistry, 43*(2), 211-227.

Nunez, A., Cervera-Ferri, A., Olucha-Bordonau, F., Ruiz-Torner, A., & Teruel, V. (2006). Nucleus incertus contribution to hippocampal theta rhythm generation. *The European journal of neuroscience, 23*(10), 2731-2738. doi:10.1111/j.1460-9568.2006.04797.x

O'Connell, L. A., & Hofmann, H. A. (2012). Evolution of a vertebrate social decision-making network. *Science, 336*(6085), 1154-1157. doi:10.1126/science.1218889

Ogawa, S., Kow, L. M., McCarthy, M. M., Pfaff, D. W., & Schwartz-Giblin, S. (1991). Midbrain PAG Control of Female Reproductive Behavior: In Vitro Electrophysiological Characterization of Actions of Lordosis-Relevant Substances. *Midbrain Periaqueductal Gray Matter*.

Olschowka, J. A., O'Donohue, T. L., Mueller, G. P., & Jacobowitz, D. M. (1982). The distribution of corticotropin releasing factor-like immunoreactive neurons in rat brain. *Peptides, 3*(6), 995-1015.

Olucha-Bordonau, F. E., Teruel, V., Barcia-Gonzalez, J., Ruiz-Torner, A., Valverde-Navarro, A. A., & Martinez-Soriano, F. (2003). Cytoarchitecture and efferent projections of the nucleus incertus of the rat. *The Journal of comparative neurology, 464*(1), 62-97. doi:10.1002/cne.10774

Onstott, D., Mayer, B., & Beitz, A. J. (1993). Nitric-Oxide Synthase Immunoreactive Neurons Anatomically Define a Longitudinal Dorsolateral Column within the Midbrain Periaqueductal Gray of the Rat - Analysis Using Laser Confocal Microscopy. *Brain research, 610*(2), 317-324. doi:Doi 10.1016/0006-8993(93)91416-P

Ottersen, O. P. (1981). Afferent connections to the amygdaloid complex of the rat with some observations in the cat. III. Afferents from the lower brain stem.

Palacios, J. M., Wamsley, J. K., & Kuhar, M. J. (1981). The distribution of histamine H1-receptors in the rat brain: an autoradiographic study. *Neuroscience, 6*(1), 15-37.

Palkovits, M., & Jacobowitz, D. M. (1974). Topographic atlas of catecholamine and acetylcholinesterase-containing neurons in the rat brain. II. Hindbrain (mesencephalon, rhombencephalon). *The Journal of comparative neurology, 157*(1), 29-42. doi:10.1002/cne.901570104

Pan, Z. Z., Grudt, T. J., & Williams, J. T. (1994). Alpha 1-adrenoceptors in rat dorsal raphe neurons: regulation of two potassium conductances. *The Journal of physiology, 478 Pt 3*, 437-447.

Panula, P., Pirvola, U., Auvinen, S., & Airaksinen, M. S. (1989). Histamine-immunoreactive nerve fibers in the rat brain. *Neuroscience, 28*(3), 585-610.

Pardo-Bellver, C., Cadiz-Moretti, B., Novejarque, A., Martinez-Garcia, F., & Lanuza, E. (2012). Differential efferent projections of the anterior, posteroventral, and posterodorsal subdivisions of the medial amygdala in mice. *Front Neuroanat, 6*, 33. doi:10.3389/fnana.2012.00033

Parker, S. W., & Feldman, S. M. (1967). Effect of mesencephalic lesions on feeding behavior in rats. *Exp Neurol, 17*(3), 313-326.

Pasquier, D. A., Anderson, C., Forbes, W. B., & Morgane, P. J. (1976). Horseradish peroxidase tracing of the lateral habenular-midbrain raphe nuclei connections in the rat. *Brain Res Bull, 1*(5), 443-451.

Pasquier, D. A., & Reinoso-Suarez, F. (1977). Differential efferent connections of the brain stem to the hippocampus in the cat. *Brain research, 120*(3), 540-548.

Pasquier, D. A., & Reinoso-Suarez, F. (1978). The topographic organization of hypothalamic and brain stem projections to the hippocampus. *Brain Res Bull, 3*(4), 373-389.

Pavlovic, Z. W., Cooper, M. L., & Bodnar, R. J. (1996). Opioid antagonists in the periaqueductal gray inhibit morphine and beta-endorphin analgesia elicited from the amygdala of rats. *Brain research, 741*(1-2), 13-26.

Paxinos, G., & Watson, C. (1998). *The Rat Brain in Stereotaxic Coordinates*: Academic Press.

Paxinos, G., & Watson, C. (2007). The Rat Brain in Stereotaxic Coordinates. In (6 ed.): Academic Press.

Paykel, E. S. (1977). Depression and appetite. *J Psychosom Res, 21*(5), 401-407.

Pazos, A., Cortes, R., & Palacios, J. M. (1985). Quantitative autoradiographic mapping of serotonin receptors in the rat brain. II. Serotonin-2 receptors. *Brain research, 346*(2), 231-249.

Peckys, D., & Landwehrmeyer, G. B. (1999). Expression of mu, kappa, and delta opioid receptor messenger RNA in the human CNS: a 33P in situ hybridization study. *Neuroscience, 88*(4), 1093-1135.

Pereira, C. W., Santos, F. N., Sanchez-Perez, A. M., Otero-Garcia, M., Marchioro, M., Ma, S., . . . Olucha-Bordonau, F. E. (2013). Electrolytic lesion of the nucleus incertus retards extinction of auditory conditioned fear. *Behavioural brain research, 247*, 201-210. doi:10.1016/j.bbr.2013.03.025

Petrovich, G. D., Risold, P. Y., & Swanson, L. W. (1996). Organization of projections from the basomedial nucleus of the amygdala: a PHAL study in the rat. *The Journal of comparative neurology, 374*(3), 387-420. doi:10.1002/(SICI)1096-9861(19961021)374:3<387::AID-CNE6>3.0.CO;2-Y

Peyron, C., Luppi, P. H., Fort, P., Rampon, C., & Jouvet, M. (1996). Lower brainstem catecholamine afferents to the rat dorsal raphe nucleus. *The Journal of comparative neurology, 364*(3), 402-413. doi:10.1002/(SICI)1096-9861(19960115)364:3<402::AID-CNE2>3.0.CO;2-8

Phillipson, O. T. (1979). Afferent projections to the ventral tegmental area of Tsai and interfascicular nucleus: a horseradish peroxidase study in the rat. *The Journal of comparative neurology, 187*(1), 117-143. doi:10.1002/cne.901870108

Pieribone, V. A., Nicholas, A. P., Dagerlind, A., & Hokfelt, T. (1994). Distribution of alpha 1 adrenoceptors in rat brain revealed by in situ hybridization experiments utilizing subtype-specific probes. *The Journal of neuroscience, 14*(7), 4252-4268.

Pillot, C., Heron, A., Cochois, V., Tardivel-Lacombe, J., Ligneau, X., Schwartz, J. C., & Arrang, J. M. (2002). A detailed mapping of the histamine H3 receptor and its gene transcripts in rat brain. *Neuroscience, 114*(1), 173-193. doi:10.1016/s0306-4522(02)00135-5

Pilyavskii, A. I., Maiskii, V. A., Hariri, N. I., Peker, G. O., & Bulgakova, N. V. (1996). Distribution and quantitative characterization of NADPH-diaphorase-reactive neurons in analgesic zones of the rat midbrain. *Neurophysiology, 28*(1), 27-35. doi:Doi 10.1007/Bf02252560

Pin, C., Jones, B., & Jouvet, M. (1969). Topographie des neurones monoaminergiques du tronc cérébral du Chat: étude par histofluorescence.

Poitras, D., & Parent, A. (1978). Atlas of the distribution of monoamine-containing nerve cell bodies in the brain stem of the cat. *The Journal of comparative neurology, 179*(4), 699-717. doi:10.1002/cne.901790402

Pollard, H., Moreau, J., Arrang, J. M., & Schwartz, J. C. (1993). A detailed autoradiographic mapping of histamine H3 receptors in rat brain areas. *Neuroscience, 52*(1), 169-189.

Pompeiano, M., Palacios, J. M., & Mengod, G. (1992). Distribution and cellular localization of mRNA coding for 5-HT1A receptor in the rat brain: correlation with receptor binding. *The Journal of neuroscience, 12*(2), 440-453.

Powell, E. W. (1963). Septal efferents revealed by axonal degeneration in the rat.

Price, J. L., & Amaral, D. G. (1981). An autoradiographic study of the projections of the central nucleus of the monkey amygdala. *The Journal of neuroscience, 1*(11), 1242-1259.

Quik, M., Polonskaya, Y., Gillespie, A., Jakowec, M., Lloyd, G. K., & Langston, J. W. (2000). Localization of nicotinic receptor subunit mRNAs in monkey brain by in situ hybridization. *The Journal of comparative neurology, 425*(1), 58-69.

Quintino-dos-Santos, J. W., Muller, C. J., Santos, A. M., Tufik, S., Rosa, C. A., & Schenberg, L. C. (2014). Long-lasting marked inhibition of periaqueductal gray-evoked defensive

behaviors in inescapably-shocked rats. *The European journal of neuroscience, 39*(2), 275-286. doi:10.1111/ejn.12410
Rainbow, T. C., Parsons, B., & Wolfe, B. B. (1984). Quantitative autoradiography of beta 1- and beta 2-adrenergic receptors in rat brain. *Proc Natl Acad Sci U S A, 81*(5), 1585-1589.
Rainville, P., Duncan, G. H., Price, D. D., Carrier, B., & Bushnell, C. (1997). Pain Affect Encoded in Human Anterior Cingulate But Not Somatosensory Cortex. *Science*.
Raisman, G., Cowan, W. M., & Powell, T. P. (1966). An experimental analysis of the efferent projection of the hippocampus. *Brain, 89*(1), 83-108.
Rampon, C., Luppi, P. H., Fort, P., Peyron, C., & Jouvet, M. (1996). Distribution of glycine-immunoreactive cell bodies and fibers in the rat brain. *Neuroscience, 75*(3), 737-755.
Redgrave, P., & Dean, P. (1991). Does the PAG Learn about Emergencies from the Superior Colliculus? *Midbrain Periaqueductal Gray Matter*.
Reep, R. L., & Winans, S. S. (1982). Efferent connections of dorsal and ventral agranular insular cortex in the hamster, Mesocricetus auratus. *Neuroscience, 7*(11), 2609-2635.
Reichling, D. B. (1991). Gabaergic Neuronal Circuitry in the Periaqueductal Gray-Matter. *Midbrain Periaqueductal Gray Matter, 213*, 329-344.
Reichling, D. B., & Basbaum, A. I. (1991). Collateralization of periaqueductal gray neurons to forebrain or diencephalon and to the medullary nucleus raphe magnus in the rat. *Neuroscience, 42*(1), 183-200.
Reiner, A., Brauth, S. E., & Karten, H. J. (1984). Evolution of the Amniote Basal Ganglia. *Trends in neurosciences, 7*(9), 320-325. doi:Doi 10.1016/S0166-2236(84)80080-6
Renno, W. M., Mullett, M. A., & Beitz, A. J. (1992). Systemic morphine reduces GABA release in the lateral but not the medial portion of the midbrain periaqueductal gray of the rat. *Brain research, 594*(2), 221-232. doi:http://dx.doi.org/10.1016/0006-8993(92)91129-3
Rhudy, J. L., & Meagher, M. W. (2000). Fear and anxiety: divergent effects on human pain thresholds. *Pain, 84*(1), 65-75.
Ricardo, J. A. (1981). Efferent connections of the subthalamic region in the rat. II. The zona incerta. *Brain research, 214*(1), 43-60.
Rinaman, L. (2010). Ascending projections from the caudal visceral nucleus of the solitary tract to brain regions involved in food intake and energy expenditure. *Brain research, 1350*, 18-34. doi:10.1016/j.brainres.2010.03.059
Rizvi, T. A., Ennis, M., Behbehani, M. M., & Shipley, M. T. (1991). Connections between the Central Nucleus of the Amygdala and the Midbrain Periaqueductal Gray - Topography and Reciprocity. *Journal of Comparative Neurology, 303*(1), 121-131. doi:DOI 10.1002/cne.903030111
Rizvi, T. A., Ennis, M., & Shipley, M. T. (1992). Reciprocal Connections between the Medial Preoptic Area and the Midbrain Periaqueductal Gray in Rat - a Wga-Hrp and Pha-L Study. *Journal of Comparative Neurology, 315*(1), 1-15. doi:DOI 10.1002/cne.903150102
Rodella, L., Rezzani, R., Agostini, C., & Bianchi, R. (1998). Induction of NADPH-diaphorase activity in the rat periaqueductal gray matter after nociceptive visceral stimulation. *Brain research, 793*(1-2), 333-336.
Roeling, T. A. P., Veening, J. G., Kruk, M. R., Peters, J. P. W., Vermelis, M. E. J., & Nieuwenhuys, R. (1994). Efferent connections of the hypothalamic "aggression area" in the rat. *Neuroscience, 59*, 1001-1024.
Roger, M., & Cadusseau, J. (1985). Afferents to the zona incerta in the rat: a combined retrograde and anterograde study. *The Journal of comparative neurology, 241*(4), 480-492. doi:10.1002/cne.902410407
Roncon, C. M., Almada, R. C., Maraschin, J. C., Audi, E. A., Zangrossi, H., Jr., Graeff, F. G., & Coimbra, N. C. (2015). Pharmacological evidence for the mediation of the panicolytic

effect of fluoxetine by dorsal periaqueductal gray matter mu-opioid receptors. *Neuropharmacology, 99*, 620-626. doi:10.1016/j.neuropharm.2015.08.037

Roncon, C. M., Biesdorf, C., Coimbra, N. C., Audi, E. A., Zangrossi, H., Jr., & Graeff, F. G. (2013). Cooperative regulation of anxiety and panic-related defensive behaviors in the rat periaqueductal grey matter by 5-HT1A and mu-receptors. *J Psychopharmacol, 27*(12), 1141-1148. doi:10.1177/0269881113485144

Roncon, C. M., Biesdorf, C., Santana, R. G., Zangrossi, H., Graeff, F. G., & Audi, E. A. (2012). The panicolytic-like effect of fluoxetine in the elevated T-maze is mediated by serotonin-induced activation of endogenous opioids in the dorsal periaqueductal grey. *Journal of Psychopharmacology, 26*(4), 525-531. doi:10.1177/0269881111434619

Room, P., & Groenewegen, H. J. (1986). Connections of the parahippocampal cortex in the cat. II. Subcortical afferents. *The Journal of comparative neurology, 251*(4), 451-473. doi:10.1002/cne.902510403

Rothman, R. B., Herkenham, M., Pert, C. B., Liang, T., & Cascieri, M. A. (1984). Visualization of rat brain receptors for the neuropeptide, substance P. *Brain research, 309*(1), 47-54.

Routtenberg, A. (1968). Hippocampal correlates of consummatory and observed behavior☆☆☆. *Physiology & Behavior, 3*(4), 533-535. doi:10.1016/0031-9384(68)90007-3

Ruan, M., Young, C. K., & McNaughton, N. (2017). Bi-Directional Theta Modulation between the Septo-Hippocampal System and the Mammillary Area in Free-Moving Rats. *Front Neural Circuits, 11*, 62. doi:10.3389/fncir.2017.00062

Ruiz-Torner, A., Olucha-Bordonau, F., Valverde-Navarro, A. A., & Martinez-Soriano, F. (2001). The chemical architecture of the rat's periaqueductal gray based on acetylcholinesterase histochemistry: a quantitative and qualitative study. *Journal of chemical neuroanatomy, 21*(4), 295-312.

Russo, A. S., Guimaraes, F. S., De Aguiar, J. C., & Graeff, F. G. (1993). Role of benzodiazepine receptors located in the dorsal periaqueductal grey of rats in anxiety. *Psychopharmacology (Berl), 110*(1-2), 198-202.

Ryan, P. J., Buchler, E., Shabanpoor, F., Hossain, M. A., Wade, J. D., Lawrence, A. J., & Gundlach, A. L. (2013). Central relaxin-3 receptor (RXFP3) activation decreases anxiety- and depressive-like behaviours in the rat. *Behavioural brain research, 244*, 142-151. doi:10.1016/j.bbr.2013.01.034

Sainsbury, R. S., Harris, J. L., & Rowland, G. L. (1987). Sensitization and hippocampal type 2 theta in the rat. *Physiol Behav, 41*(5), 489-493.

Sainsbury, R. S., Heynen, A., & Montoya, C. P. (1987). Behavioral correlates of hippocampal type 2 theta in the rat. *Physiol Behav, 39*(4), 513-519.

Sakuma, Y., & Pfaff, D. W. (1979a). Facilitation of female reproductive behavior from mesensephalic central gray in the rat. *Am J Physiol, 237*(5), R278-284.

Sakuma, Y., & Pfaff, D. W. (1979b). Mesencephalic mechanisms for integration of female reproductive behavior in the rat. *Am J Physiol, 237*(5), R285-290.

Sakurai, T. (2005). Roles of orexin/hypocretin in regulation of sleep/wakefulness and energy homeostasis. *Sleep Med Rev, 9*(4), 231-241. doi:10.1016/j.smrv.2004.07.007

Sakurai, T., Amemiya, A., Ishii, M., Matsuzaki, I., Chemelli, R. M., Tanaka, H., . . . Yanagisawa, M. (1998). Orexins and Orexin Receptors: A Family of Hypothalamic Neuropeptides and G Protein-Coupled Receptors that Regulate Feeding Behavior.

Salchner, P., & Singewald, N. (2002). Neuroanatomical substrates involved in the anxiogenic-like effect of acute fluoxetine treatment. *Neuropharmacology, 43*(8), 1238-1248. doi:10.1016/s0028-3908(02)00329-5

Salzberg, H. C., Lonstein, J. S., & Stern, J. M. (2002). GABA(A) receptor regulation of kyphotic nursing and female sexual behavior in the caudal ventrolateral periaqueductal gray of postpartum rats. *Neuroscience, 114*(3), 675-687.

Santos, N. R., Huston, J. P., & Brandao, M. L. (2000). Escape behavior under tonic inhibitory control of histamine H2-receptor mediated mechanisms in the midbrain tectum.

Saper, C. B. (1982). Convergence of autonomic and limbic connections in the insular cortex of the rat. *The Journal of comparative neurology, 210*(2), 163-173. doi:10.1002/cne.902100207

Saper, C. B., Swanson, L. W., & Cowan, W. M. (1978). The efferent connections of the anterior hypothalamic area of the rat, cat and monkey. *The Journal of comparative neurology, 182*(4), 575-599. doi:10.1002/cne.901820402

Sapolsky, R. M. (1998). Why zebras don't get ulcers: An updated guide to stress, stress-related diseases, and coping. .

Sar, M., Stumpf, W. E., Miller, R. J., Chang, K. J., & Cuatrecasas, P. (1978). Immunohistochemical localization of enkephalin in rat brain and spinal cord. *The Journal of comparative neurology, 182*(1), 17-37. doi:10.1002/cne.901820103

Schenberg, L. C., Capucho, L. B., Vatanabe, R. O., & Vargas, L. C. (2002). Acute effects of clomipramine and fluoxetine on dorsal periaqueductal grey-evoked unconditioned defensive behaviours of the rat. *Psychopharmacology (Berl), 159*(2), 138-144. doi:10.1007/s002130100883

Schimitel, F. G., de Almeida, G. M., Pitol, D. N., Armini, R. S., Tufik, S., & Schenberg, L. C. (2012). Evidence of a suffocation alarm system within the periaqueductal gray matter of the rat. *Neuroscience, 200*, 59-73. doi:10.1016/j.neuroscience.2011.10.032

Schreiner, L., & Kling, A. (1953). Behavioral changes following rhinencephalic injury in cat. *Journal of neurophysiology*.

Schroeder, B. E., Binzak, J. M., & Kelley, A. E. (2001). A common profile of prefrontal cortical activation following exposure to nicotine- or chocolate-associated contextual cues. *Neuroscience, 105*(3), 535-545.

Schulz, G. M., Varga, M., Jeffires, K., Ludlow, C. L., & Braun, A. R. (2005). Functional neuroanatomy of human vocalization: an H215O PET study. *Cerebral cortex, 15*(12), 1835-1847. doi:10.1093/cercor/bhi061

Scuvée-Moreau, J. J., & Dresse, A. E. (1979). Effect of various antidepressant drugs on the spontaneous firing rate of locu coeruleus and dorsal raphe neurons of the rat.

Segal, M. (1977). Afferents to the entorhinal cortex of the rat studied by the method of retrograde transport of horseradish peroxidase. *Exp Neurol, 57*(3), 750-765.

Segal, M., & Landis, S. (1974). Afferents to the hippocampus of the rat studied with the method of retrograde transport of horseradish peroxidase. *Brain research, 78*(1), 1-15.

Sesack, S. R., Deutch, A. Y., Roth, R. H., & Bunney, B. S. (1989). TOPOGRAPHICAL ORGANIZATION OF THE EFFERENT PROJECTIONS OF THE MEDIAL PREFRONTAL CORTEX IN THE RAT - AN ANTEROGRADE TRACT-TRACING STUDY WITH PHASEOLUS-VULGARIS LEUCOAGGLUTININ. *Journal of Comparative Neurology, 290*(2), 213-242. doi:10.1002/cne.902900205

Shabanpoor, F., Akhter Hossain, M., Ryan, P. J., Belgi, A., Layfield, S., Kocan, M., . . . Wade, J. D. (2012). Minimization of human relaxin-3 leading to high-affinity analogues with increased selectivity for relaxin-family peptide 3 receptor (RXFP3) over RXFP1. *J Med Chem, 55*(4), 1671-1681. doi:10.1021/jm201505p

Shammah-Lagnado, S. J., Negrao, N., Silva, B. A., & Ricardo, J. A. (1987). Afferent connections of the nuclei reticularis pontis oralis and caudalis: a horseradish peroxidase study in the rat. *Neuroscience, 20*(3), 961-989.

Sharif, N. A., & Hughes, J. (1989). Discrete Mapping of Brain-Mu and Delta-Opioid Receptors Using Selective Peptides - Quantitative Autoradiography, Species-Differences and Comparison with Kappa-Receptors. *Peptides, 10*(3), 499-522. doi:Doi 10.1016/0196-9781(89)90135-6

Shimada, S., Ishikawa, M., & Tanaka, C. (1976). Histochemical mapping of dopamine neurons and fiber pathways in dog mesencephalon. *The Journal of comparative neurology, 168*(4), 533-543. doi:10.1002/cne.901680406

Shimogawa, Y., Sakuma, Y., & Yamanouchi, K. (2015). Efferent and afferent connections of the ventromedial hypothalamic nucleus determined by neural tracer analysis: implications for lordosis regulation in female rats. *Neurosci Res, 91*, 19-33. doi:10.1016/j.neures.2014.10.016

Shipley, M. T., Ennis, M., Rizvi, T. A., & Behbehani, M. M. (1991). Topographical Specificity of Forebrain Inputs to the Midbrain Periaqueductal Gray - Evidence for Discrete Longitudinally Organized Input Columns. *Midbrain Periaqueductal Gray Matter, 213*, 417-448.

Shirhatti, V., Borthakur, A., & Ray, S. (2016). Effect of Reference Scheme on Power and Phase of the Local Field Potential. *Neural Comput, 28*(5), 882-913. doi:10.1162/NECO_a_00827

Short, K. R., & Maier, S. F. (1993). Stressor controllability, social interaction, and benzodiazepine systems. *Pharmacol Biochem Behav, 45*(4), 827-835.

Silvestrini, B. (1989). Trazodone: from the mental pain to the "dys-stress" hypothesis of depression. *Clin Neuropharmacol, 12 Suppl 1*, S4-10.

Simantov, R., Kuhar, M. J., Uhl, G. R., & Snyder, S. H. (1977). Opioid peptide enkephalin: immunohistochemical mapping in rat central nervous system. *Proc Natl Acad Sci U S A, 74*(5), 2167-2171.

Simerly, R. B., & Swanson, L. W. (1986). The organization of neural inputs to the medial preoptic nucleus of the rat. *The Journal of comparative neurology, 246*(3), 312-342. doi:10.1002/cne.902460304

Simerly, R. B., & Swanson, L. W. (1988). Projections of the medial preoptic nucleus: a Phaseolus vulgaris leucoagglutinin anterograde tract-tracing study in the rat. *The Journal of comparative neurology, 270*(2), 209-242. doi:10.1002/cne.902700205

Simon, H., Le Moal, M., & Calas, A. (1979). Efferents and afferents of the ventral tegmental-A10 region studied after local injection of [3H]leucine and horseradish peroxidase. *Brain research, 178*(1), 17-40.

Sirinathsinghji, D. J. (1985). Modulation of lordosis behaviour in the female rat by corticotropin releasing factor, beta-endorphin and gonadotropin releasing hormone in the mesencephalic central gray. *Brain research, 336*(1), 45-55.

Skoubis, P. D., Hradil, V., Chin, C. L., Luo, Y., Fox, G. B., & McGaraughty, S. (2006). Mapping brain activity following administration of a nicotinic acetylcholine receptor agonist, ABT-594, using functional magnetic resonance imaging in awake rats. *Neuroscience, 137*(2), 583-591. doi:10.1016/j.neuroscience.2005.08.072

Smit, F., Cuijpers, P., Oostenbrink, J., Batelaan, N., de Graaf, R., & Beekman, A. (2006). Costs of nine common mental disorders: implications for curative and preventive psychiatry. *J Ment Health Policy Econ, 9*(4), 193-200.

Smith, C. M., Hosken, I. T., Sutton, S. W., Lawrence, A. J., & Gundlach, A. L. (2012). Relaxin-3 null mutation mice display a circadian hypoactivity phenotype. *Genes, brain, and behavior, 11*(1), 94-104. doi:10.1111/j.1601-183X.2011.00730.x

Smith, C. M., Lawrence, A. J., Sutton, S. W., & Gundlach, A. L. (2009). Behavioral phenotyping of mixed background (129S5:B6) relaxin-3 knockout mice. *Annals of the New York Academy of Sciences, 1160*, 236-241. doi:10.1111/j.1749-6632.2009.03953.x

Smith, C. M., Ryan, P. J., Hosken, I. T., Ma, S., & Gundlach, A. L. (2011). Relaxin-3 systems in the brain--the first 10 years. *Journal of chemical neuroanatomy, 42*(4), 262-275. doi:10.1016/j.jchemneu.2011.05.013

Smith, C. M., Shen, P. J., Banerjee, A., Bonaventure, P., Ma, S., Bathgate, R. A., . . . Gundlach, A. L. (2010). Distribution of relaxin-3 and RXFP3 within arousal, stress, affective, and

cognitive circuits of mouse brain. *The Journal of comparative neurology, 518*(19), 4016-4045. doi:10.1002/cne.22442

Souza, R. R., & Carobrez, A. P. (2016). Acquisition and expression of fear memories are distinctly modulated along the dorsolateral periaqueductal gray axis of rats exposed to predator odor. *Behavioural brain research, 315*, 160-167. doi:10.1016/j.bbr.2016.08.021

Staiger, J. F., & Nurnberger, F. (1991). The Efferent Connections of the Lateral Septal Nucleus in the Guinea-Pig - Projections to the Diencephalon and Brain-Stem. *Cell and Tissue Research, 264*(3), 391-413. doi:Doi 10.1007/Bf00319031

Stamp, J. A., & Semba, K. (1995). Extent of colocalization of serotonin and GABA in the neurons of the rat raphe nuclei. *Brain research, 677*(1), 39-49.

Steeves, J. D., & Jordan, L. M. (1984). Autoradiographic demonstration of the projections from the mesencephalic locomotor region. *Brain research, 307*(1-2), 263-276.

Steinbusch, H. W. M. (1981). Distribution of serotonin-immunoreactivity in the central nervous system of the rat-cell bodies and terminals. *Neuroscience, 6*(4), 557-618.

Steinbusch, H. W. M. (2009). Distribution of Histaminergic Neurons and Fibers in Rat Brain. *Acta Oto-Laryngologica, 111*(sup479), 12-23. doi:10.3109/00016489109121144

Stiller, C. O., Gustafsson, H., Fried, K., & Brodin, E. (1997). Opioid-induced release of neurotensin in the periaqueductal gray matter of freely moving rats. *Brain research, 774*(1-2), 149-158.

Subramanian, H. H., Balnave, R. J., & Holstege, G. (2008). The midbrain periaqueductal gray control of respiration. *The Journal of neuroscience, 28*(47), 12274-12283. doi:10.1523/JNEUROSCI.4168-08.2008

Sudre, E. C., de Barros, M. R., Sudre, G. N., & Schenberg, L. C. (1993). Thresholds of electrically induced defence reaction of the rat: short- and long-term adaptation mechanisms. *Behavioural brain research, 58*(1-2), 141-154.

Sukikara, M. H., Mota-Ortiz, S. R., Baldo, M. V., Felicio, L. F., & Canteras, N. S. (2006). A role for the periaqueductal gray in switching adaptive behavioral responses. *The Journal of neuroscience, 26*(9), 2583-2589. doi:10.1523/JNEUROSCI.4279-05.2006

Swanson, L. W. (1988). Citation Classic - the Central Adrenergic System - an Immunofluorescence Study of the Location of Cell-Bodies and Their Efferent Connections in the Rat Utilizing Dopamine-Beta-Hydroxylase as a Marker. *Current Contents/Life Sciences*(46), 17-17.

Swanson, L. W. (1992). *Brain Maps: Structure of the Rat Brain*.

Swanson, L. W., & Cowan, W. M. (1977). An autoradiographic study of the organization of the efferent connections of the hippocampal formation in the rat. *The Journal of comparative neurology, 172*(1), 49-84. doi:10.1002/cne.901720104

Swanson, L. W., & Hartman, B. K. (1975). The central adrenergic system. An immunofluorescence study of the location of cell bodies and their efferent connections in the rat utilizing dopamine-beta-hydroxylase as a marker.

Swanson, L. W., Simmons, D. M., Whiting, P. J., & Lindstrom, J. (1987). Immunohistochemical localization of neuronal nicotinic receptors in the rodent central nervous system. *The Journal of neuroscience, 7*(10), 3334-3342.

Takagishi, M., & Chiba, T. (1991). Efferent projections of the infralimbic (area 25) region of the medial prefrontal cortex in the rat: an anterograde tracer PHA-L study. *Brain research, 566*(1-2), 26-39.

Takeuchi, Y., Kimura, H., & Sano, Y. (1982). Immunohistochemical demonstration of the distribution of serotonin neurons in the brainstem of the rat and cat. *Cell Tissue Res, 224*(2), 247-267.

Tamm, S. L. (2014). Cilia and the life of ctenophores. *Invertebrate Biology, 133*(1), 1-46. doi:10.1111/ivb.12042

Tanaka, M., Iijima, N., Miyamoto, Y., Fukusumi, S., Itoh, Y., Ozawa, H., & Ibata, Y. (2005). Neurons expressing relaxin 3/INSL 7 in the nucleus incertus respond to stress. *The European journal of neuroscience, 21*(6), 1659-1670. doi:10.1111/j.1460-9568.2005.03980.x

Taylor, K. M., Gfeller, E., & Snyder, S. H. (1972). Regional localization of histamine and histidine in the brain of the rhesus monkey. *Brain research, 41*(1), 171-179.

Terburg, D., Morgan, B. E., Montoya, E. R., Hooge, I. T., Thornton, H. B., Hariri, A. R., . . . van Honk, J. (2012). Hypervigilance for fear after basolateral amygdala damage in humans. *Transl Psychiatry, 2*, e115. doi:10.1038/tp.2012.46

Thoburn, K. K., Hough, L. B., Nalwalk, J. W., & Mischler, S. A. (1994). Histamine-induced modulation of nociceptive responses. *Pain, 58*(1), 29-37.

Thompson, R. H., Canteras, N. S., & Swanson, L. W. (1996). Organization of projections from the dorsomedial nucleus of the hypothalamus: a PHA-L study in the rat. *The Journal of comparative neurology, 376*(1), 143-173. doi:10.1002/(SICI)1096-9861(19961202)376:1<143::AID-CNE9>3.0.CO;2-3

Thompson, R. H., & Swanson, L. W. (1998). Organization of inputs to the dorsomedial nucleus of the hypothalamus: a reexamination with Fluorogold and PHAL in the rat. *Brain Res Brain Res Rev, 27*(2), 89-118.

Thompson, R. K. R., Foltin, R. W., Boylan, R. J., Sweet, A., Graves, C. A., & Lowitz, C. E. (1981). Tonic Immobility in Japanese Quail Can Reduce the Probability of Sustained Attack by Cats. *Animal Learning & Behavior, 9*(1), 145-149. doi:Doi 10.3758/Bf03212037

Tolle, T. R., Berthele, A., Zieglgansberger, W., Seeburg, P. H., & Wisden, W. (1993). The differential expression of 16 NMDA and non-NMDA receptor subunits in the rat spinal cord and in periaqueductal gray. *The Journal of neuroscience, 13*(12), 5009-5028.

Traiffort, E., Pollard, H., Moreau, J., Ruat, M., Schwartz, J. C., Martinez-Mir, M. I., & Palacios, J. M. (1992). Pharmacological characterization and autoradiographic localization of histamine H2 receptors in human brain identified with [125I]iodoaminopotentidine. *J Neurochem, 59*(1), 290-299.

Tryon, V. L., & Mizumori, S. J. Y. (2018). A Novel Role for the Periaqueductal Gray in Consummatory Behavior. *Frontiers in behavioral neuroscience, 12*. doi:10.3389/fnbeh.2018.00178

Tsou, K., Brown, S., Sanudo-Pena, M. C., Mackie, K., & Walker, J. M. (1998). Immunohistochemical distribution of cannabinoid CB1 receptors in the rat central nervous system. *Neuroscience, 83*(2), 393-411.

Uhl, G. R., Goodman, R. R., Kuhar, M. J., Childers, S. R., & Snyder, S. H. (1979). Immunohistochemical mapping of enkephalin containing cell bodies, fibers and nerve terminals in the brain stem of the rat. *Brain research, 166*(1), 75-94.

Ungerstedt, U. (1971). Stereotaxic mapping of the monoamine pathways in the rat brain. *Acta Physiol Scand Suppl, 367*, 1-48.

Unguez, G. A., & Schneider, J. S. (1988). Dopaminergic dorsal raphe neurons in cats and monkeys are sensitive to the toxic effects of MPTP. *Neurosci Lett, 94*(1-2), 218-223.

Unterwald, E. M., Knapp, C., & Zukin, R. S. (1991). Neuroanatomical localization of kappa 1 and kappa 2 opioid receptors in rat and guinea pig brain. *Brain research, 562*(1), 57-65.

Uphouse, L., Caldarola-Pastuszka, M., & Droge, M. (1992). 8-OH-DPAT in the midbrain central gray inhibits lordosis behavior. *Pharmacol Biochem Behav, 43*(3), 833-838.

Van Bockstaele, E. J., Aston-Jones, G., Pieribone, V. A., Ennis, M., & Shipley, M. T. (1991). Subregions of the periaqueductal gray topographically innervate the rostral ventral medulla in the rat. *The Journal of comparative neurology, 309*(3), 305-327. doi:10.1002/cne.903090303

van Groen, T., & Wyss, J. M. (1990). Extrinsic projections from area CA1 of the rat hippocampus: olfactory, cortical, subcortical, and bilateral hippocampal formation

projections. *The Journal of comparative neurology, 302*(3), 515-528. doi:10.1002/cne.903020308

Vanbockstaele, E. J., Biswas, A., & Pickel, V. M. (1993). Topography of Serotonin Neurons in the Dorsal Raphe Nucleus That Send Axon Collaterals to the Rat Prefrontal Cortex and Nucleus-Accumbens. *Brain research, 624*(1-2), 188-198. doi:Doi 10.1016/0006-8993(93)90077-Z

Vanderhorst, V. G., Terasawa, E., Ralston, H. J., 3rd, & Holstege, G. (2000). Monosynaptic projections from the lateral periaqueductal gray to the nucleus retroambiguus in the rhesus monkey: implications for vocalization and reproductive behavior. *The Journal of comparative neurology, 424*(2), 251-268.

Vanderveldt, A., Oliveira, L., & Green, L. (2016). Delay discounting: Pigeon, rat, human--does it matter? *J Exp Psychol Anim Learn Cogn, 42*(2), 141-162. doi:10.1037/xan0000097

Vasconcelos, M., Stein, D. J., & de Almeida, R. M. (2015). Social defeat protocol and relevant biomarkers, implications for stress response physiology, drug abuse, mood disorders and individual stress vulnerability: a systematic review of the last decade. *Trends Psychiatry Psychother, 37*(2), 51-66. doi:10.1590/2237-6089-2014-0034

Vaughan, C. W., Bandler, R., & Christie, M. J. (1996). Differential responses of lateral and ventrolateral rat periaqueductal grey neurones to noradrenaline in vitro. *The Journal of physiology, 490 (Pt 2)*, 373-381.

Vaughan, C. W., Ingram, S. L., Connor, M. A., & Christie, M. J. (1997). How opioids inhibit GABA-mediated neurotransmission. *Nature, 390*(6660), 611-614. doi:Doi 10.1038/37610

Veening, J., Buma, P., Ter Horst, G. J., Roeling, T. A. P., Luiten, P. G. M., & Nieuwenhuys, R. (1991). Hypothalamic projections to the PAG in the rat: Topographical, immuno-electronmicroscopical and function aspects. In A. Depaulis & R. Bandler (Eds.), *Midbrain Periaqueductal Gray Matter* (pp. 387-415). New York: Plenum Press.

Versteeg, D. H., Van Der Gugten, J., De Jong, W., & Palkovits, M. (1976). Regional concentrations of noradrenaline and dopamine in rat brain. *Brain research, 113*(3), 563-574.

Vertes, R. P. (1981). An analysis of ascending brain stem systems involved in hippocampal synchronization and desynchronization. *Journal of neurophysiology, 46*(5), 1140-1159.

Vertes, R. P. (1991). A PHA-L analysis of ascending projections of the dorsal raphe nucleus in the rat. *The Journal of comparative neurology, 313*(4), 643-668. doi:10.1002/cne.903130409

Vertes, R. P. (1992). PHA-L analysis of projections from the supramammillary nucleus in the rat. *The Journal of comparative neurology, 326*(4), 595-622. doi:10.1002/cne.903260408

Vertes, R. P. (2006). Interactions among the medial prefrontal cortex, hippocampus and midline thalamus in emotional and cognitive processing in the rat. *Neuroscience, 142*(1), 1-20. doi:10.1016/j.neuroscience.2006.06.027

Vertes, R. P., & Crane, A. M. (1996). Descending projections of the posterior nucleus of the hypothalamus: Phaseolus vulgaris leucoagglutinin analysis in the rat. *The Journal of comparative neurology, 374*, 607-631.

Vertes, R. P., Fortin, W. J., & Crane, A. M. (1999). Projections of the median raphe nucleus in the rat. *Journal of Comparative Neurology, 407*(4), 555-582.

Vianna, D. M. L., Graeff, F. G., Landeira-Fernandez, J., & Brandao, M. L. (2001). Lesion of the ventral periaqueductal gray reduces conditioned fear but does not change freezing induced by stimulation of the dorsal periaqueductal gray. *Learning & memory, 8*(3), 164-169. doi:10.1101/lm.36101

Vidal-Gonzalez, I., Vidal-Gonzalez, B., Rauch, S. L., & Quirk, G. J. (2006). Microstimulation reveals opposing influences of prelimbic and infralimbic cortex on the expression of conditioned fear. *Learning & memory, 13*(6), 728-733. doi:10.1101/lm.306106

Viellard, J., Baldo, M. V., & Canteras, N. S. (2016). Testing conditions in shock-based contextual fear conditioning influence both the behavioral responses and the activation of circuits potentially involved in contextual avoidance. *Behavioural brain research, 315*, 123-129. doi:10.1016/j.bbr.2016.08.033

Vincent, S. R., & Kimura, H. (1992). Histochemical mapping of nitric oxide synthase in the rat brain. *Neuroscience, 46*(4), 755-784.

Vinck, M., van Wingerden, M., Womelsdorf, T., Fries, P., & Pennartz, C. M. (2010). The pairwise phase consistency: a bias-free measure of rhythmic neuronal synchronization. *Neuroimage, 51*(1), 112-122. doi:10.1016/j.neuroimage.2010.01.073

Vizuete, M. L., Traiffort, E., Bouthenet, M. L., Ruat, M., Souil, E., Tardivel-Lacombe, J., & Schwartz, J. C. (1997). Detailed mapping of the histamine H2 receptor and its gene transcripts in guinea-pig brain. *Neuroscience, 80*(2), 321-343.

Waksman, G., Hamel, E., Fournie-Zaluski, M. C., & Roques, B. P. (1986). Autoradiographic comparison of the distribution of the neutral endopeptidase "enkephalinase" and of mu and delta opioid receptors in rat brain. *Proc Natl Acad Sci U S A, 83*(5), 1523-1527.

Wamsley, J. K., Lewis, M. S., Young, W. S., & Kuhar, M. J. (1981). Autoradiographic localization of muscarinic cholinergic receptors in rat brainstem. *The Journal of neuroscience, 1*(2), 176-191.

Wanaka, A., Kiyama, H., Murakami, T., Matsumoto, M., Kamada, T., Malbon, C. C., & Tohyama, M. (1989). Immunocytochemical localization of beta-adrenergic receptors in the rat brain. *Brain research, 485*(1), 125-140.

Ward, N. G., Bloom, V. L., Dworkin, S., Fawcett, J., Narasimhachari, N., & Friedel, R. O. (1982). Psychobiological markers in coexisting pain and depression: toward a unified theory. *J Clin Psychiatry, 43*(8 Pt 2), 32-41.

Waselus, M., Galvez, J. P., Valentino, R. J., & Van Bockstaele, E. J. (2006). Differential projections of dorsal raphe nucleus neurons to the lateral septum and striatum. *Journal of chemical neuroanatomy, 31*(4), 233-242. doi:10.1016/j.jchemneu.2006.01.007

Watanabe, T., Taguchi, Y., Shiosaka, S., Tanaka, J., Kubota, H., Terano, Y., . . . Wada, H. (1984). Distribution of the histaminergic neuron system in the central nervous system of rats; a fluorescent immunohistochemical analysis with histidine decarboxylase as a marker. *Brain research, 295*(1), 13-25.

Waterhouse, B. D., Border, B., Wahl, L., & Mihailoff, G. A. (1993). Topographic organization of rat locus coeruleus and dorsal raphe nuclei: distribution of cells projecting to visual system structures. *The Journal of comparative neurology, 336*(3), 345-361. doi:10.1002/cne.903360304

Weber, E., & Barchas, J. D. (1983). Immunohistochemical distribution of dynorphin B in rat brain: relation to dynorphin A and alpha-neo-endorphin systems. *Proc Natl Acad Sci U S A, 80*(4), 1125-1129.

Weber, E., Roth, K. A., & Barchas, J. D. (1982). Immunohistochemical distribution of alpha-neo-endorphin/dynorphin neuronal systems in rat brain: evidence for colocalization. *Proc Natl Acad Sci U S A, 79*(9), 3062-3066.

Weiner, D. M., Levey, A. I., Sunahara, R. K., Niznik, H. B., O'Dowd, B. F., Seeman, P., & Brann, M. R. (1991). D1 and D2 dopamine receptor mRNA in rat brain. *Proc Natl Acad Sci U S A, 88*(5), 1859-1863.

Wiberg, M., & Blomqvist, A. (1984). The Spinomesencephalic Tract in the Cat - Its Cells of Origin and Termination Pattern as Demonstrated by the Intraaxonal Transport Method. *Brain research, 291*(1), 1-18. doi:Doi 10.1016/0006-8993(84)90645-0

Wiesenfeld-Hallin, Z., de Arauja Lucas, G., Alster, P., Xu, X. J., & Hokfelt, T. (1999). Cholecystokinin/opioid interactions. *Brain research, 848*(1-2), 78-89.

Wilkinson, G., Balestrieri, M., Ruggeri, M., & Bellantuono, C. (2009). Meta-analysis of double-blind placebo-controlled trials of antidepressants and benzodiazepines for

patients with panic disorders. *Psychological medicine, 21*(04), 991. doi:10.1017/s0033291700029986

Willner, P. (1984). The validity of animal models of depression. *Psychopharmacology (Berl), 83*(1), 1-16.

Witter, M. P., & Groenewegen, H. J. (1986a). Connections of the parahippocampal cortex in the cat. III. Cortical and thalamic efferents. *The Journal of comparative neurology, 252*(1), 1-31. doi:10.1002/cne.902520102

Witter, M. P., & Groenewegen, H. J. (1986b). Connections of the parahippocampal cortex in the cat. IV. Subcortical efferents. *The Journal of comparative neurology, 252*(1), 51-77. doi:10.1002/cne.902520104

Wyss, J. M., & Sripanidkulchai, K. (1984). The topography of the mesencephalic and pontine projections from the cingulate cortex of the rat. *Brain research, 293*(1), 1-15.

Wyss, J. M., Swanson, L. W., & Cowan, W. M. (1979). A study of subcortical afferents to the hippocampal formation in the rat. *Neuroscience, 4*(4), 463-476.

Yamamoto, T., Nozaki-Taguchi, N., & Chiba, T. (2002). Analgesic effect of intrathecally administered orexin-A in the rat formalin test and in the rat hot plate test. *Br J Pharmacol, 137*(2), 170-176. doi:10.1038/sj.bjp.0704851

Yamashita, P. S., Spiacci, A., Jr., Hassel, J. E., Jr., Lowry, C. A., & Zangrossi, H., Jr. (2017). Disinhibition of the rat prelimbic cortex promotes serotonergic activation of the dorsal raphe nucleus and panicolytic-like behavioral effects. *J Psychopharmacol, 31*(6), 704-714. doi:10.1177/0269881116684334

Yokoyama, C., Okamura, H., Nakajima, T., Taguchi, J., & Ibata, Y. (1994). Autoradiographic distribution of [3H]YM-09151-2, a high-affinity and selective antagonist ligand for the dopamine D2 receptor group, in the rat brain and spinal cord. *The Journal of comparative neurology, 344*(1), 121-136. doi:10.1002/cne.903440109

Young, C. K., & Eggermont, J. J. (2009). Coupling of mesoscopic brain oscillations: recent advances in analytical and theoretical perspectives. *Prog Neurobiol, 89*(1), 61-78. doi:10.1016/j.pneurobio.2009.06.002

Young, C. K., Ruan, M., & McNaughton, N. (2017). A Critical Assessment of Directed Connectivity Estimates with Artificially Imposed Causality in the Supramammillary-Septo-Hippocampal Circuit. *Front Syst Neurosci, 11*, 72. doi:10.3389/fnsys.2017.00072

Zangrossi, H., Jr., & Graeff, F. G. (2014). Serotonin in anxiety and panic: contributions of the elevated T-maze. *Neuroscience and biobehavioral reviews, 46 Pt 3*, 397-406. doi:10.1016/j.neubiorev.2014.03.007

Zanoveli, J. M., Netto, C. F., Guimaraes, F. S., & Zangrossi, H., Jr. (2004). Systemic and intra-dorsal periaqueductal gray injections of cholecystokinin sulfated octapeptide (CCK-8s) induce a panic-like response in rats submitted to the elevated T-maze. *Peptides, 25*(11), 1935-1941. doi:10.1016/j.peptides.2004.06.016

Zanoveli, J. M., Nogueira, R. L., & Zangrossi, H., Jr. (2007). Enhanced reactivity of 5-HT1A receptors in the rat dorsal periaqueductal gray matter after chronic treatment with fluoxetine and sertraline: evidence from the elevated T-maze. *Neuropharmacology, 52*(4), 1188-1195. doi:10.1016/j.neuropharm.2007.01.001

Zanoveli, J. M., Pobbe, R. L., de Bortoli, V. C., Carvalho, M. C., Brandao, M. L., & Zangrossi, H., Jr. (2010). Facilitation of 5-HT1A-mediated neurotransmission in dorsal periaqueductal grey matter accounts for the panicolytic-like effect of chronic fluoxetine. *Int J Neuropsychopharmacol, 13*(8), 1079-1088. doi:10.1017/S146114570999099X

Zarbin, M. A., Wamsley, J. K., & Kuhar, M. J. (1981). Glycine receptor: light microscopic autoradiographic localization with [3H]strychnine. *The Journal of neuroscience, 1*(5), 532-547.

Zhang, C., Chua, B. E., Yang, A., Shabanpoor, F., Hossain, M. A., Wade, J. D., . . . Gundlach, A. L. (2015). Central relaxin-3 receptor (RXFP3) activation reduces elevated, but not

basal, anxiety-like behaviour in C57BL/6J mice. *Behavioural brain research, 292*, 125-132. doi:10.1016/j.bbr.2015.06.010

Zhang, S. P., Bandler, R., & Carrive, P. (1990). Flight and Immobility Evoked by Excitatory Amino-Acid Microinjection within Distinct Parts of the Subtentorial Midbrain Periaqueductal Gray of the Cat. *Brain research, 520*(1-2), 73-82. doi:Doi 10.1016/0006-8993(90)91692-A

Zhang, W., Hayward, L. F., & Davenport, P. W. (2007). Respiratory responses elicited by rostral versus caudal dorsal periaqueductal gray stimulation in rats. *Auton Neurosci, 134*(1-2), 45-54. doi:10.1016/j.autneu.2007.02.003

Zubieta, J. K., & Frey, K. A. (1993). Autoradiographic mapping of M3 muscarinic receptors in the rat brain. *J Pharmacol Exp Ther, 264*(1), 415-422.

7. Postscript

This section contains figures that are cited in Chapter 5. The numbering is sequential with the figures included in the chapter.

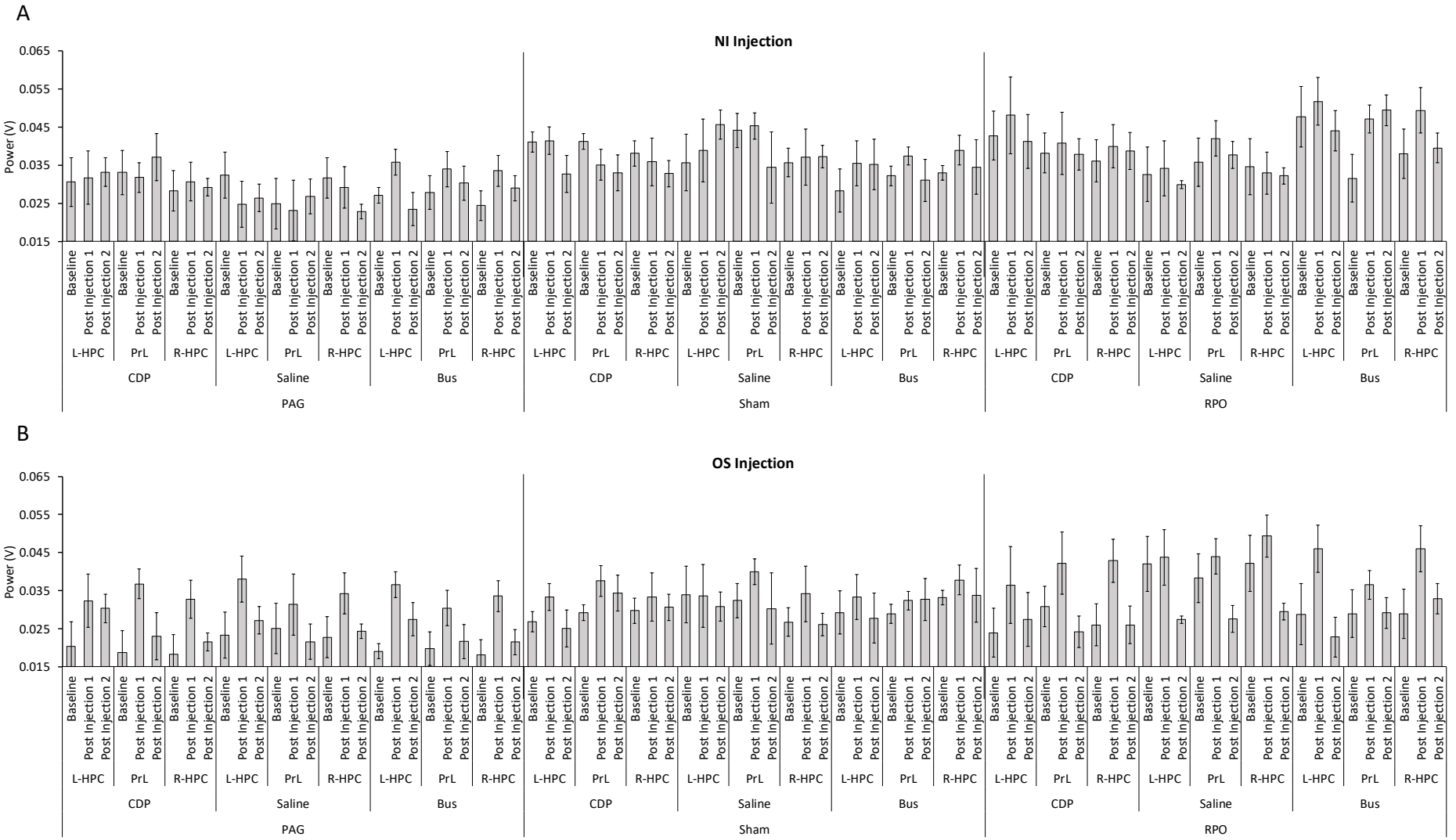

Figure P7.1. The effect of CDP and buspirone over LFP power in the hippocampus and PrL during PAG, sham and RPO stimulations over three time periods. Panel A: NI injected animals (N=3). Panel B: OS injected animals (N=3).

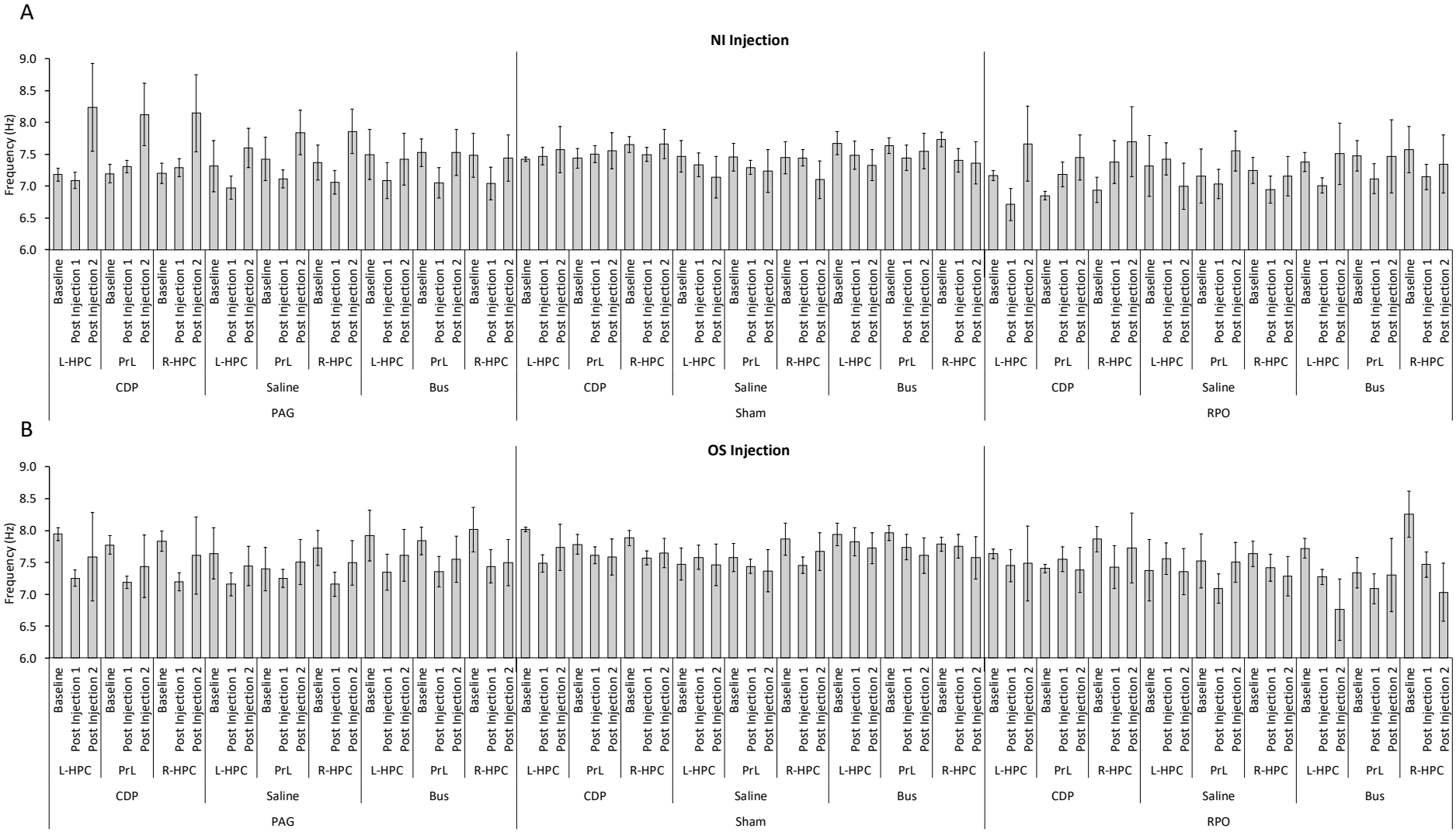

Figure P7.2. The effect of CDP and buspirone over LFP frequency in the hippocampus and PrL during PAG, sham and RPO stimulations over three time periods. Panel A: NI injected animals (N=3). Panel B: OS injected animals (N=3).

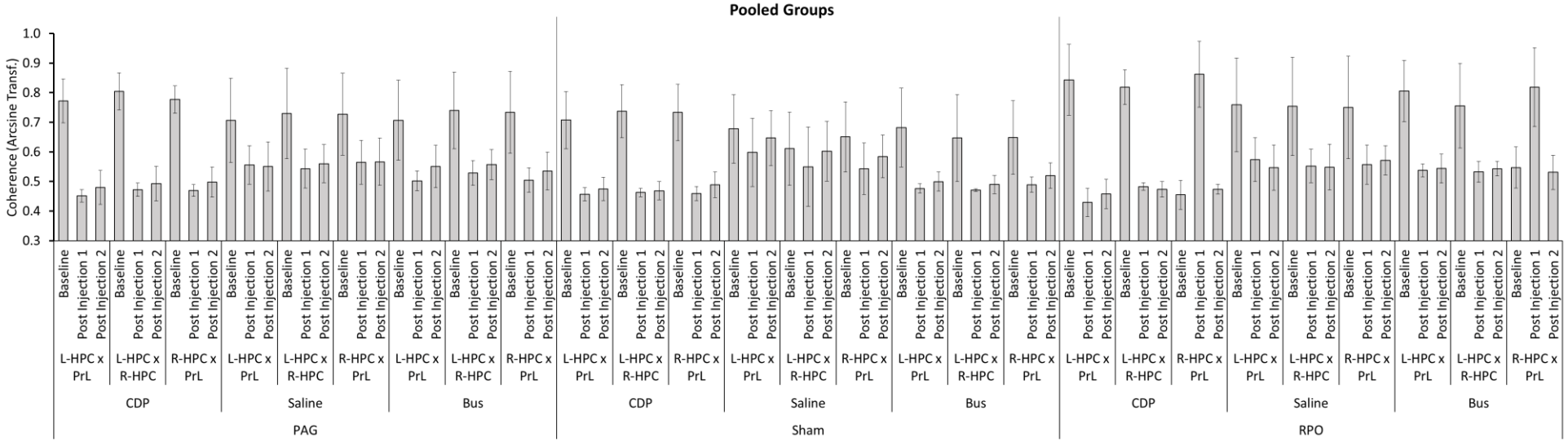

Figure P7.3. The effect of CDP and buspirone over theta coherence in the hippocampus and PrL during PAG, sham and RPO stimulations over three time periods. This figure shows the pooled data from the two groups (N=6).

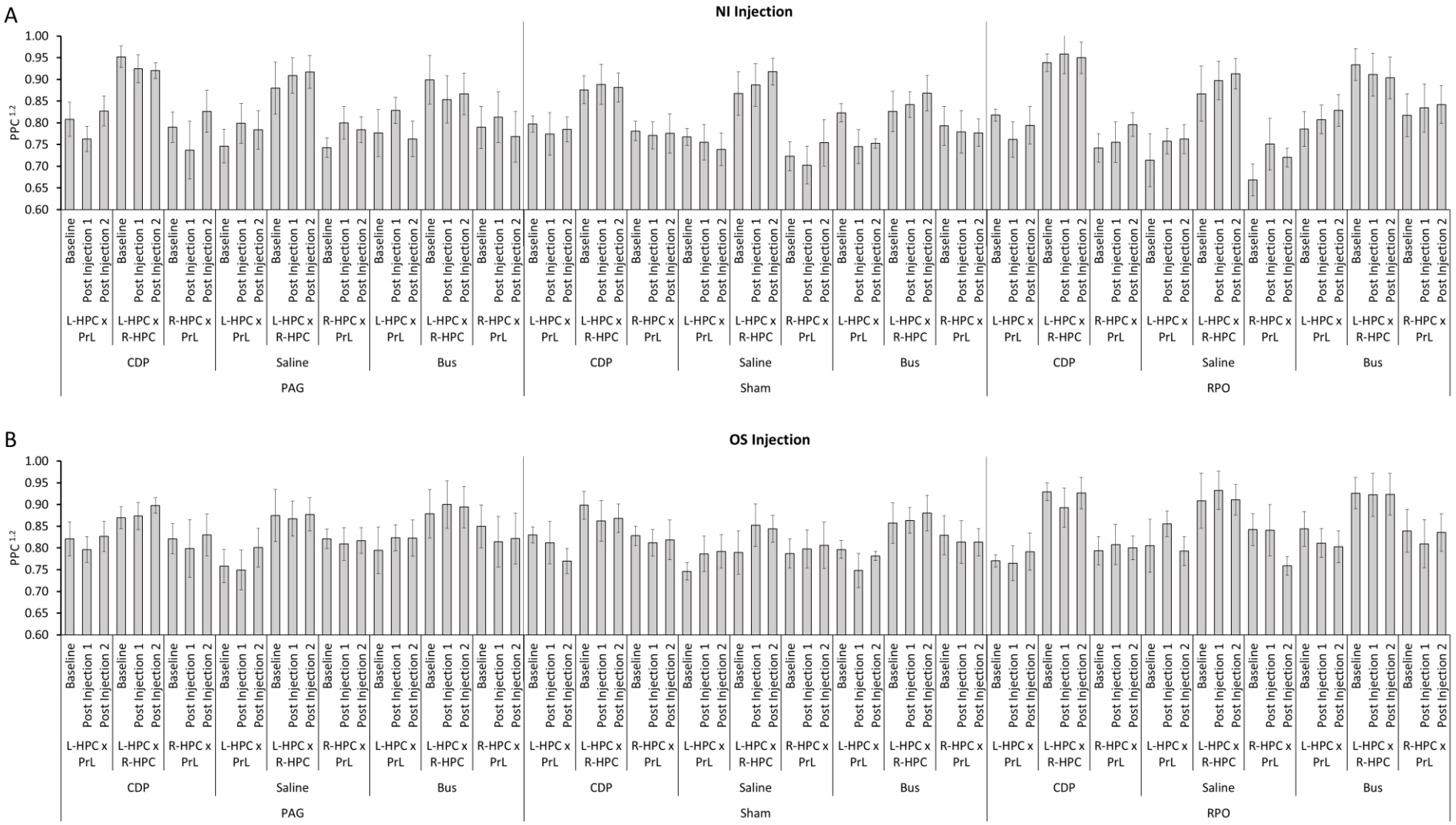

Figure P7.4. The effect of CDP and buspirone over PPC in the hippocampus and PrL during PAG, sham and RPO stimulations over three time periods. Panel A: NI injected animals (N=3). Panel B: OS injected animals (N=3).

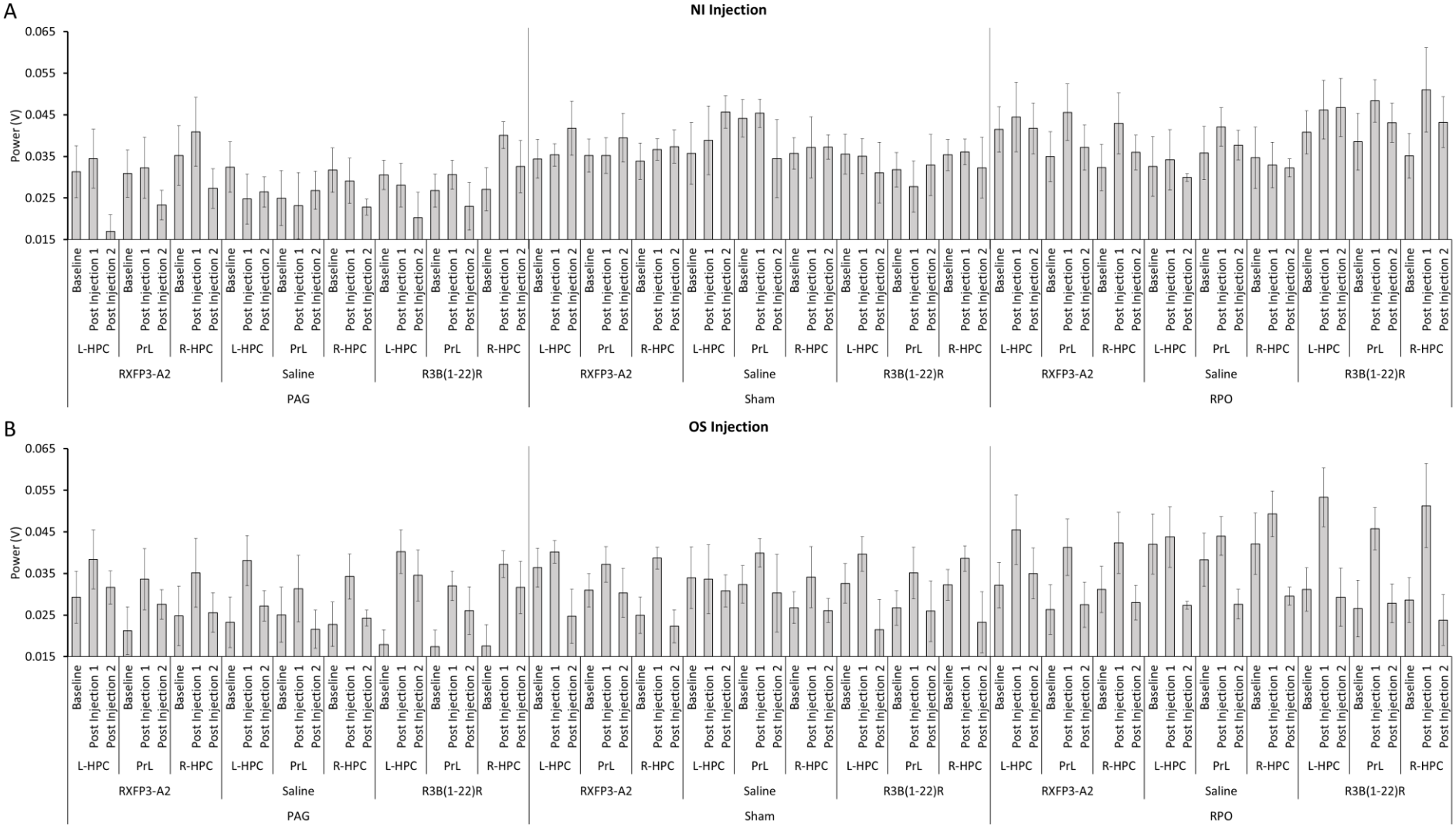

Figure P7.5. The effect of RXFP3-A2 and R3B(1-22)R over LFP power in the hippocampus and PrL during PAG, sham and RPO stimulations over three time periods. Panel A: NI injected animals (N=3). Panel B: OS injected animals (N=3).

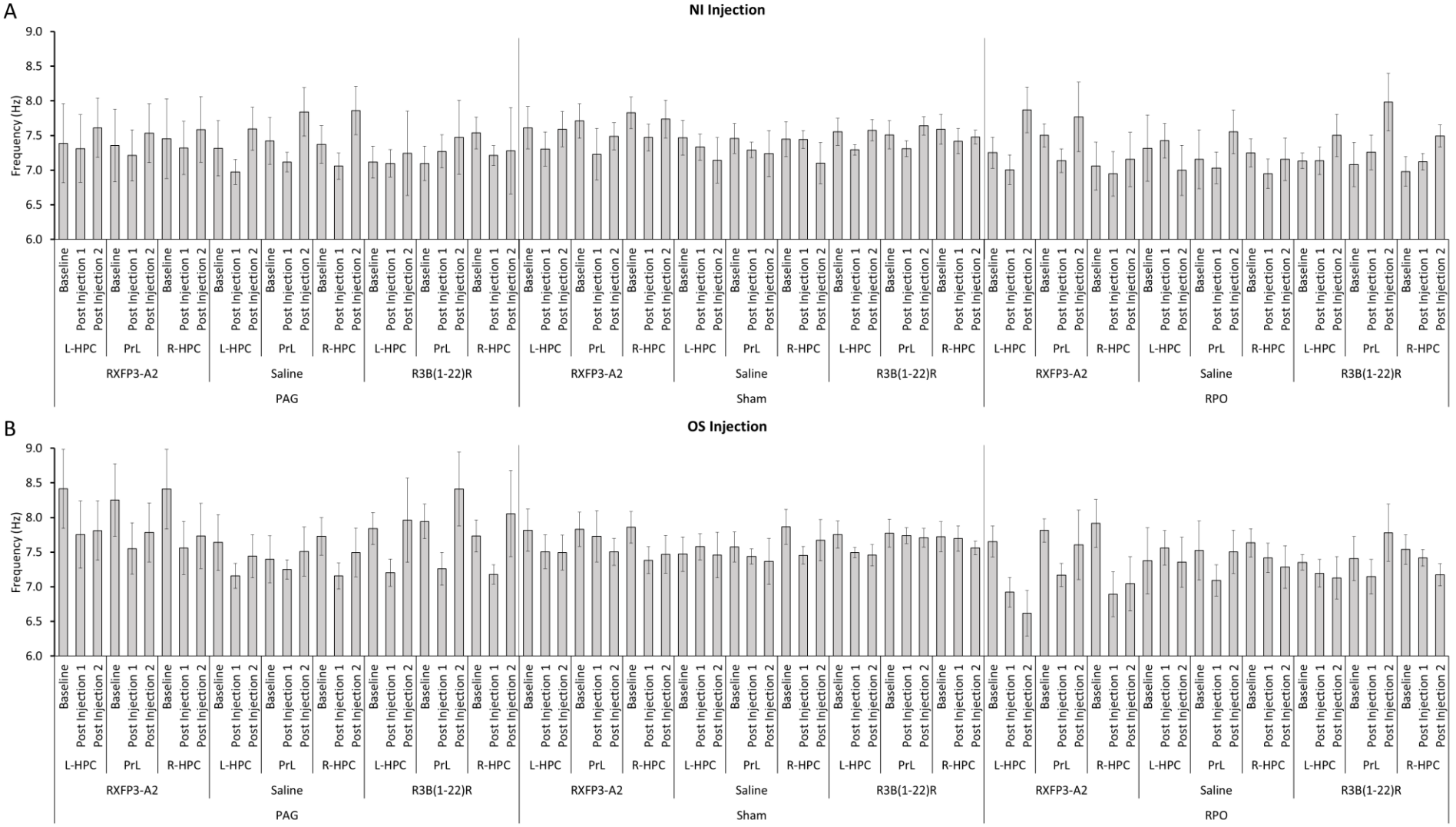

Figure P7.6. The effect of RXFP3-A2 and R3B(1-22)R over LFP frequency in the hippocampus and PrL during PAG, sham and RPO stimulations over three time periods. Panel A: NI injected animals (N=3). Panel B: OS injected animals (N=3).

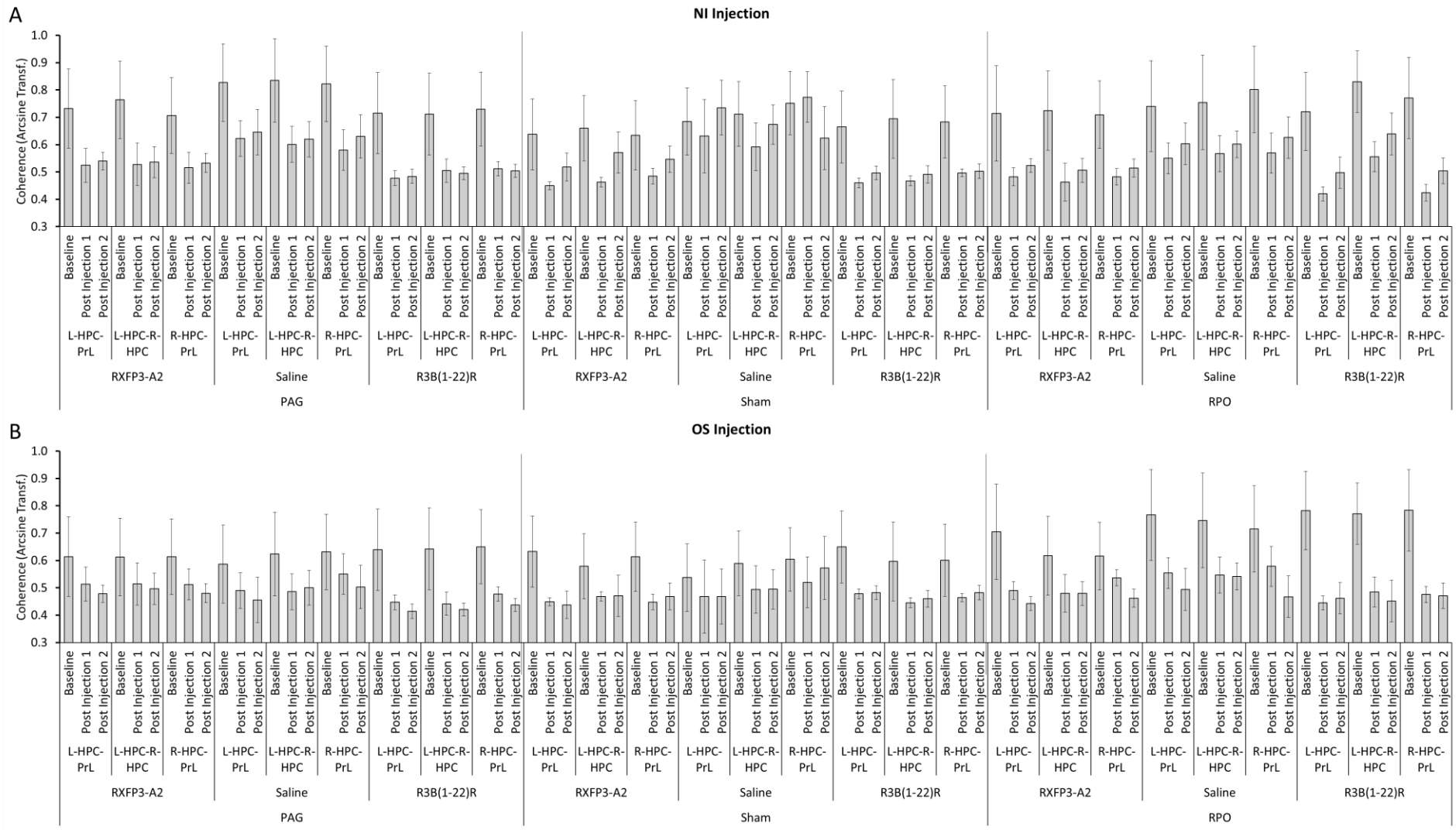

Figure P7.7. The effect of RXFP3-A2 and R3B(1-22)R over theta coherence in the hippocampus and PrL during PAG, sham and RPO stimulations over three time periods. Panel A: NI injected animals (N=3). Panel B: OS injected animals (N=3).

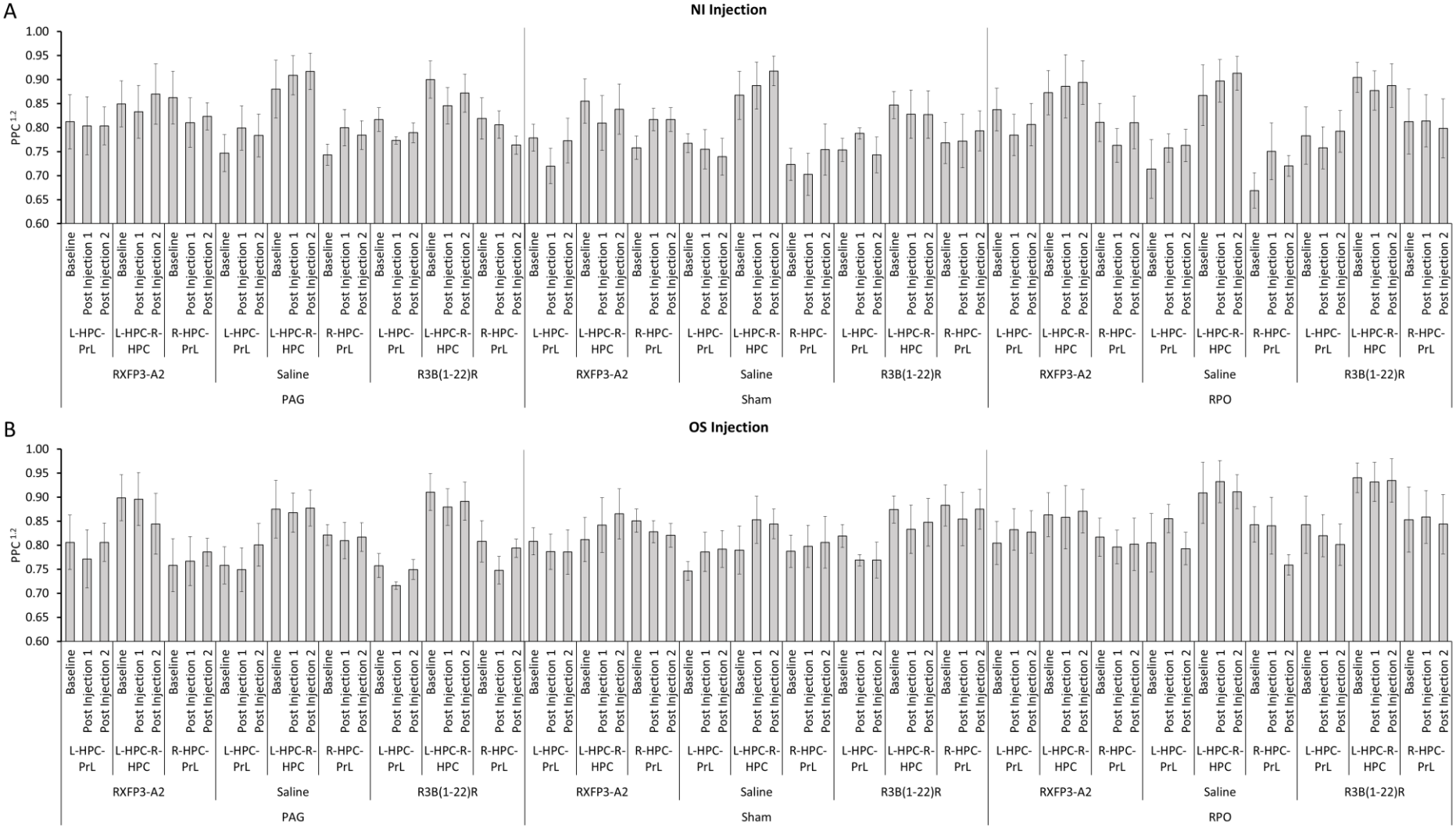

Figure P7.8. The effect of RXFP3-A2 and R3B(1-22)R over PPC in the hippocampus and PrL during PAG, sham and RPO stimulations over three time periods. Panel A: NI injected animals (N=3). Panel B: OS injected animals (N=3).

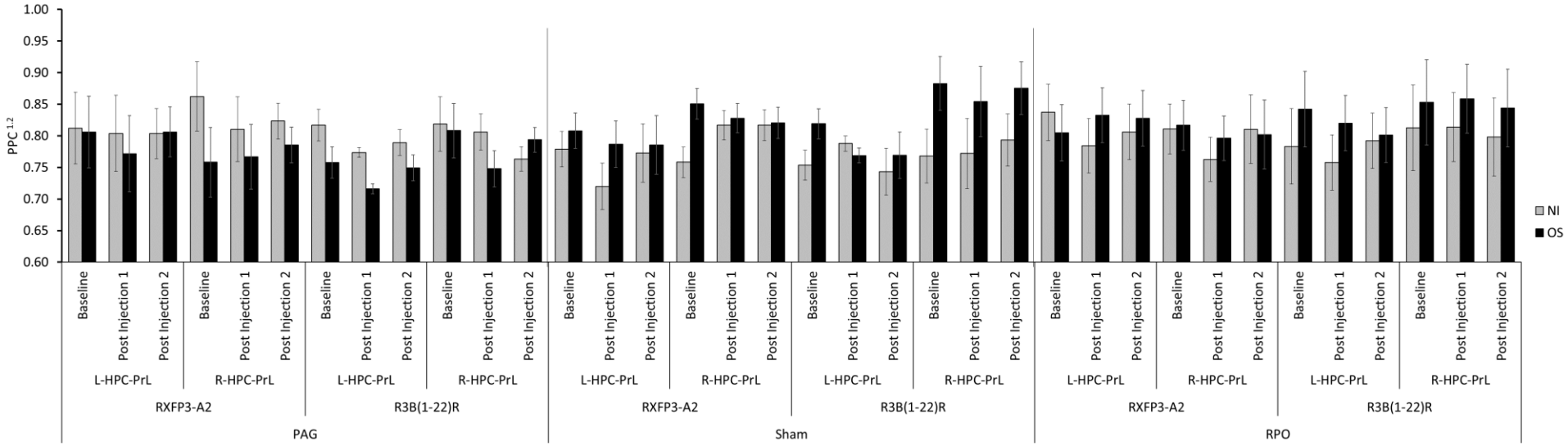

Figure P7.9. A comparison of the effects of RXFP3-A2 and R2B(1-22)R in the NI (N=3) and OS (N=3) groups under PAG, Sham and RPO stimulations, capturing the two significant trends (linear, linear, linear, quadratic and quadratic, linear, linear, quadratic).